



UCGE Reports

Number 20370

Department of Geomatics Engineering

Proposed LOS Fast TTFF Signal Design for IRNSS

by

Vyasaraj Guru Rao

January 2013



UNIVERSITY OF CALGARY

Proposed LOS Fast TTF Signal Design for IRNSS

by

Vyasaraj Guru Rao

A THESIS

SUBMITTED TO THE FACULTY OF GRADUATE STUDIES
IN PARTIAL FULFILMENT OF THE REQUIREMENTS FOR THE
DEGREE OF DOCTOR OF PHILOSOPHY

DEPARTMENT OF GEOMATICS ENGINEERING

CALGARY, ALBERTA

January, 2013

© Vyasaraj Guru Rao, 2013

Abstract

Amongst GNSS receiver design criteria such as accuracy, sensitivity, channels etc., Time To First Fix (TTFF) is an important criterion, which defines how fast a navigation solution is available to the user since receiver power on. TTFF is defined as the time that a receiver takes to acquire and track a minimum of four satellites and extract the necessary information (ephemeris - primary parameter) from the demodulated navigation data bits. In the past decade, there has been a constant demand from the user community to optimize TTFF specifications. For example, for E911 use, Global Navigation Satellite System (GNSS) receivers integrated as a part of mobile handsets obtain assistance from a base station (terrestrial link) to enhance the TTFF. However, this link may not be always guaranteed. In addition, for military handheld equipment, to depend on a terrestrial link may not be practical. Thus, it becomes critical to optimize the TTFF parameter of a GNSS receiver from the satellites directly.

This research work focuses primarily on improving the TTFF parameter of a GNSS receiver. As highlighted earlier, the TTFF depends on both receiver algorithms (to acquire and track a minimum of four satellites) and navigation data structure (to collect ephemeris as fast as possible from the satellites tracked). The former is receiver specific whereas the latter depends on the satellites. Since the upcoming Indian Regional Navigation Satellite System (IRNSS) is in its preliminary design stage, there is a large potential for improvement of the TTFF parameter without having to compromise on any other mission objectives. Towards this goal, several new signal design strategies have been proposed and analyzed. Though the upcoming IRNSS is considered as the target platform herein, the results can be extended to any emerging GNSS constellation.

The research activities performed are categorized based on the service (civilian or restricted) and frequencies supported (single or dual). As a first objective, a signal design for single frequency system and a reference Navigation (NAV) data structure is developed. Subsequently, three new methods are proposed with an emphasis on minimizing TTFF in single frequency mode of receiver operation. Subsequently, three new methods are proposed with an emphasis on minimizing the TTFF in the single frequency mode of receiver operation. As a second objective, three new signal designs are proposed based on diversities of code and carrier. Third, a signal design for civilian and restricted services optimized for TTFF is proposed based on new cross correlation techniques. Lastly, third frequency of operation for IRNSS and thus a hot start are proposed. The results from the proposed methods are best till date.

Using the relevant theory, these proposed methods are experimentally established and verified through testing and associated results. The research experiments make use of a reference hardware simulator and new software is developed to generate the proposed signals. To demonstrate the achievable benefits under each scheme, algorithms and new receiver software is written. Post integrated test results of each scheme are encouraging and will assist Line of Sight (LOS) TTFF performance drastically. In addition, this research presents some propositions that have drastic cost reductions. Finally, these results lead to recommendations on further research in the area of LOS TTFF.

Preface

The thesis includes contents such as figures, tables and texts, which have been published in conference papers or as part of pending patents. The listing is as follows:

1. Cross Correlation Detection And Time To First Fix Optimization Primary Inventor: **Vyasaraj Guru Rao**, 2011, Patent application initiated
2. Navigation Data Configuration For Optimal Time To First Fix Primary Inventor: **Vyasaraj Guru Rao**, 2011, Patent application initiated
3. **Rao, V. G** and G. Lachapelle (2012) Will IRNSS solve the LOS TTFF problem? Coordinates magazine December 2012 issue
4. **Rao, V. G** and G. Lachapelle (2012) Proposed Third Frequency of Operation for IRNSS and its Advantages. Accepted for publication in the proceedings of NAVCOM -2012, Pearl Jubilee International Conference, Navigation & Communication, 4 pages
5. **Rao, V. G** and G. Lachapelle (2012) New Method of Cross Correlation Detection in IRNSS and Civil Aviation Receivers. Accepted for publication in the proceedings of NAVCOM - 2012, Pearl Jubilee International Conference, Navigation & Communication, 5 pages
6. **Rao, V. G** and G. Lachapelle (2012) Proposed Single Frequency Signal Design for optimal TTFF in IRNSS. Accepted for publication in the proceedings of NAVCOM -2012, Pearl Jubilee International Conference, Navigation & Communication, 6 pages
7. **Rao, V. G** and G. Lachapelle (2012) Proposed Dual Frequency Signal Design for Optimal TTFF in IRNSS. Accepted for publication in the proceedings of NAVCOM -2012, Pearl Jubilee International Conference, Navigation & Communication, 4 pages

8. **Rao, V.G**, G. Lachapelle and S. B. Pappu (2012) Proposed NAV Data Signal Design for Optimal TTFF in a Single Frequency IRNSS Receiver. Proceedings of GNSS12 (Nashville, TN, 18-21 Sep), The Institute of Navigation, 12 pages
9. **Rao, V. G**, G. Lachapelle and S. B. Pappu (2011) Proposed Code and Carrier Dimension Dependent Signal Design for Optimal TTFF in IRNSS. GNSS Signals 2011 Workshop, ENAC, Toulouse, 8-9 December, 12 pages
10. **Rao, V. G**, G. Lachapelle and M.A.A. Sashidharan (2011) Proposed LOS Signal Design for IRNSS to Reduce TTFF in a Single Frequency Receiver. GNSS Signals 2011 Workshop, ENAC, Toulouse, 8-9 December, 12 pages
11. Navigation Data Generation and Data Transmission For Optimal Time To First Fix;
Primary Inventor: **Vyasaraj Guru Rao**, 2011, Patent application filed
12. Satellite Navigation System For Optimal Time To First Fix Using Code And Carrier Diversity; Primary Inventor: **Vyasaraj Guru Rao**, 2011, Patent application filed
13. **Rao V. G**, Lachapelle and V. Kumar S B (2011) Analysis of IRNSS over Indian Subcontinent. Proceedings of International Technical Meeting, Institute of Navigation, San Diego, 24-26 January, 13 pages

The above listed papers/pending patents were generated by the author during the course of this research. The first author would like to thank his supervisor and the other co-authors for their feedback. Consent has been sought and obtained from the co-authors and the proceedings forum for usage of the above material as a part of this thesis.

Acknowledgements

Foremost, I would like to thank my Supervisor, Prof. Gérard Lachapelle for his constant support, partial funding of my doctoral research and effective guidance towards the set goals. His diligence towards completion of tasks and meticulous follow-up has made a tremendous impact on my research. The only regret is that I was not able to beat him to running the stairs to the third floor once during my course work or go on a trek with him. Thank your SIR for all your support. My sincere thanks to the management of M/s Accord Software & Systems Pvt Ltd India for partially sponsoring my doctoral studies. My special thanks to Mr. J M Sunderesan, CEO Accord Software & Systems for triggering me to pursue doctoral studies. In addition, it would be most appropriate to revere Dr. Jayanta Kumar Ray for following up with me on my doctoral study plans for almost three years and keeping me on my toes. Able supervision of Mr. Rakesh Nayak, Mr. S Muralikrishna, Mr. S Purushotham, Mr. P S Bhat, Mr. Shashidhar, Mr. Varadaraj and finally with Dr Jayanta Kumar Ray at Accord spread across fourteen years, has had a significant influence on me. This has helped me immensely during my research work. Thank you all.

I would like to thank Prof. Kyle O' Keefe and Prof. John Nielsen for accepting to be on my research supervisory committee and provide inputs on research progress.

It would be most appropriate to thank all my dear friends "The GANG" especially Balaji Rangaswamy and Dr. Sai Prakash Gudlapalli, who were instrumental in shaping my initial academic days, else probably would have been lost to the game of cricket!!!

I would like to thank Dr. Shashank Satyanarayana, Dr. Pratibha Anantharamu, Anup Dhittal, Srinivas Bhaskar and all my other friends in PLAN group at University of Calgary who made the student life very memorable. In addition, special thanks to my fellow colleagues Sashidharan MAA and Sumadhva Pappu for their assistance extended throughout the research.

The last two years my thought process has only been TTFF, TTFF & TTFF. This would not have been possible without the understanding and support of my dear wife Deepika and son Sudhanvaa. A heartfelt THANKS TO BOTH OF YOU.

Last but not the least, I would like to thank Almighty to have provided me with this wonderful opportunity to learn from experts in the field at University of Calgary, meet and interact with Who's Who of GNSS (during ION GNSS conferences), thoroughly enjoy the journey of my Doctoral studies and tour North America with my family!!!!

Poojyaya Raghavendraya Satya Dharma

Rathayacha |

Bhajataam Kalpavrukshaya Namataam Kamadhenave

Dedicated to my Parents

&

Accord Software & Systems

Thank you for what I am today

Table of Contents

Abstract.....	ii
Preface.....	iv
Acknowledgements.....	vi
Table of Contents.....	ix
List of Tables.....	xv
List of Figures.....	xviii
List of Abbreviations.....	xxv
List of Symbols.....	xxviii
CHAPTER ONE: INTRODUCTION AND OVERVIEW.....	1
1.1 Background.....	3
1.2 Literature review.....	5
1.2.1 Characterization.....	5
1.2.1.1 Limitations.....	6
1.2.2 Navigation data structures.....	6
1.2.2.1 Limitations.....	7
1.2.3 Receiver architectures.....	7
1.2.3.1 Limitations.....	8
1.2.4 Cross Correlation Detection (CCD).....	9
1.2.4.1 Limitations.....	9
1.2.5 Multi frequency GNSS systems.....	10
1.2.5.1 Limitations.....	10
1.3 Objectives and contributions.....	11
1.4 Thesis outline.....	13
CHAPTER TWO: RECEIVER NUANCES AND NEED FOR FAST TTFF.....	16
2.1 System components - IRNSS.....	17
2.1.1 Space segment.....	18
2.1.2 Control segment.....	20
2.1.3 Receiver segment.....	21
2.2 Receiver operations – Analog Signal Processing (ASP).....	23
2.2.1 Antenna.....	23
2.2.2 RF down conversion.....	25
2.3 Receiver Operations – Baseband Processing Unit (BPU).....	26
2.3.1 Architecture.....	27
2.3.2 Navigation Signal Processing (NSP).....	27
2.3.2.1 Sampling clock generation.....	28
2.3.2.2 Acquisition.....	28
2.3.2.3 Tracking.....	32
2.3.3 Navigation Data and System Time Formulation (NDSTF).....	33
2.3.4 Measurement Formulation and Corrections (MFC).....	35
2.3.5 Satellite State Vector Computation (SSVC).....	37
2.3.6 User Position Estimation (UPE) and 1 PPS generation.....	37

2.3.7 External Interface	38
2.4 GNSS receiver categorization	38
2.4.1 Sensitivity	38
2.4.2 Accuracy	40
2.4.3 Reliability	40
2.4.4 Dynamics	41
2.4.5 TTFF	41
2.5 Fast TTFF – without external assistance	42
2.5.1 Cold Start	42
2.5.2 Warm start	43
2.5.3 Hot Start	44
2.5.4 Snap Start	44
2.6 Fast TTFF - Assisted GPS (AGPS)	45
2.6.1 Ephemeris assistance	45
2.6.2 Absolute mode	45
2.6.3 Measurement engine	45
2.6.4 Extended ephemeris	46
2.7 TTFF characterisation	46
2.7.1 Test apparatus	46
2.7.2 Procedure	47
2.7.3 Analysis	50
2.8 Need for fast TTFF in critical applications	50
2.8.1 Example 1: Underwater launch	51
2.8.2 Example 2: Aircraft launch	52
2.9 Summary	54

CHAPTER THREE: SINGLE FREQUENCY SIGNAL DESIGN FOR TTFF IN IRNSS

56

3.1 Overview of GNSS NAV data structures	57
3.1.1 GLONASS L1	57
3.1.2 GPS L5	57
3.1.3 GALILEO E1	59
3.1.4 QZSS	60
3.2 Limitations of existing GNSS NAV data	60
3.2.1 Primary data	60
3.2.2 Secondary data	62
3.3 NAV data signal design derivation	63
3.3.1 Subframe structure	64
3.3.2 Ephemeris parameters	67
3.3.3 Secondary data	69
3.3.4 Four Subframe Architecture (FSA)	71
3.3.5 Three Subframe Normal (TSN)	74
3.3.6 Three Subframe Fixed (TSF)	77
3.4 Signal simulation methodology	80
3.4.1 Software	80

3.4.2 Hardware.....	82
3.5 Receiver design.....	83
3.5.1 Hardware.....	84
3.5.2 Software.....	84
3.5.3 Analysis of the proposed signal (implementation merits) w.r.t TTFF.....	89
3.5.3.1 Interleaving.....	89
3.5.3.2 Tail bits.....	90
3.5.3.3 Synchronization pattern.....	91
3.6 Test methodology and performance analysis.....	92
3.6.1 Procedure.....	93
3.6.2 GPS L1 NAV data in IRNSS.....	94
3.6.3 FSA.....	94
3.6.4 TSN architecture.....	95
3.6.5 TSF.....	96
3.7 Summary.....	97
CHAPTER FOUR: DIVERSITY BASED SIGNAL DESIGN FOR TTFF IN IRNSS.....	99
4.1 Overview of dual frequency processing.....	100
4.1.1 Civilian signal.....	101
4.1.1.1 Acquisition.....	101
4.1.1.2 Tracking.....	102
4.1.1.3 Measurements.....	102
4.1.1.4 Navigation solution.....	102
4.1.2 Restricted signals.....	103
4.1.2.1 Needs and benefits.....	104
4.1.2.2 SPS assisted acquisition.....	105
4.1.2.3 Direct acquisition.....	106
4.1.3 TTFF characterization.....	106
4.1.3.1 Civilian signal.....	106
4.1.3.2 Restricted signals.....	107
4.2 Limitations in existing dual frequency GNSS w.r.t TTFF.....	108
4.2.1 Civilian signal.....	109
4.2.2 Restricted signal.....	110
4.3 Diversity based NAV data signal design derivation.....	114
4.3.1 Assumptions on IRNSS NAV data.....	114
4.3.2 Code diversity.....	116
4.3.3 Carrier diversity.....	119
4.3.4 Hybrid.....	120
4.4 Signal simulation.....	121
4.4.1 Architecture.....	121
4.4.2 Code diversity.....	122
4.4.3 Hybrid method.....	123
4.4.4 Modifications for TSN.....	124
4.5 Receiver software design.....	126
4.5.1 Code diversity.....	127

4.5.2 Hybrid scheme	130
4.6 Test methodology and performance analysis.....	131
4.6.1 Procedure	131
4.6.2 Code diversity	131
4.6.3 Carrier diversity	132
4.6.4 Hybrid scheme	133
4.7 Summary.....	133
CHAPTER FIVE: CROSS CORRELATION DETECTION AND NAV DATA SIGNAL DESIGN FOR OPTIMAL TTFF IN IRNSS	135
5.1 Need for secondary data.....	136
5.1.1 Visibility	136
5.1.2 Code phase and Doppler estimation	137
5.1.3 Predictive Receiver Autonomous Integrity Monitoring (PRAIM)	137
5.1.4 Cross correlation	138
5.2 Cross correlation detection overview and the proposed methods.....	139
5.2.1 Range differencing.....	141
5.2.2 Experimental analysis	142
5.2.3 Limitations	143
5.2.4 Proposed cross correlation methods.....	145
5.2.4.1 CCD-NAV	145
5.2.4.2 CCD-SVID.....	146
5.3 Combinational design for optimal TTFF	148
5.3.1 Combined mode 1	149
5.3.2 Combined mode 2	150
5.3.3 Optimal civilian mode (OCM).....	153
5.3.4 Optimal restricted mode (ORM).....	156
5.4 Components of test apparatus	158
5.4.1 Signal generation	159
5.4.2 Receiver algorithm design	160
5.5 Test methodology and performance analysis.....	161
5.5.1 Cross correlation	161
5.5.2 TTFF	164
5.6 Summary.....	165
CHAPTER SIX: THIRD FREQUENCY AND REAL TIME HOT/SNAP START OF GNSS/IRNSS 166	
6.1 Overview of multi-frequency GNSS system	167
6.1.1 Existing/proposed GNSS systems.....	167
6.1.2 SBAS.....	169
6.1.3 System level challenges	170
6.1.3.1 Interoperability.....	170
6.1.3.2 Backward compatibility	171
6.1.3.3 Frequency Filing.....	171
6.2 Indian navigation systems.....	171

6.2.1 GAGAN	171
6.2.2 IRNSS	173
6.2.3 Optimization	175
6.3 Proposed third frequency in IRNSS.....	176
6.3.1 Availability and accuracy	178
6.3.1.1 IRNSS on GAGAN.....	178
6.3.1.2 GAGAN on IRNSS GEO.....	182
6.3.1.3 IRNSS with GAGAN GEO	182
6.3.2 Implementation issues.....	183
6.3.3 Interoperability.....	184
6.3.4 Expandability	184
6.3.5 Advantages.....	185
6.3.5.1 SBAS & high dynamics	186
6.3.5.2 Satellite count.....	186
6.3.5.3 Control segment	187
6.3.5.4 Third frequency on IRNSS	187
6.4 Proposed fast start of GNSS using IRNSS	188
6.4.1 Real-time hot start of GNSS	188
6.5 Test Methodology.....	189
6.5.1 Signal generation	189
6.5.2 Receiver algorithm design	191
6.5.3 Test Apparatus	193
6.5.4 Method	194
6.5.5 Mapping test apparatus to proposed IRNSS	195
6.6 Analysis.....	196
6.7 Real time snap start architectures in IRNSS.....	199
6.7.1 ORM method based fast TTFF	199
6.7.2 Time from L1 channel of IRNSS.....	199
6.8 Summary.....	200
CHAPTER SEVEN: CONCLUSIONS AND RECOMMENDATIONS	202
7.1 Conclusions.....	202
7.1.1 Single frequency signal design	202
7.1.2 Diversity based signal design.....	203
7.1.3 Optimized signal design.....	204
7.1.4 Triple frequency IRNSS system	205
7.2 Recommendations.....	206
REFERENCES	209
APPENDIX A: NAV DATA STRUCTURE FOR FOUR SUBFRAME.....	216
A.1. Primary navigation parameters	216
A.2. Secondary navigation parameters	218
APPENDIX B: NAV DATA STRUCTURE FOR THREE SUBFRAME NORMAL ...	223

APPENDIX C: NAV DATA STRUCTURE FOR THREE-SUBFRAME FIXED ARCHITECTURE	225
APPENDIX D: PDOP VARIATION WITH A SATELLITE EXCLUSION IN TSF METHOD	226
APPENDIX E: ALGORITHM FOR THREE-SUBFRAME ARCHITECTURE	228
E.1. Code Diversity.....	228
E.1.1. Half Data Block Collection (HDBC)	228
E.1.2. Full Data Block Collection (FDBC)	230
E.1.3. Rearrangement	231
E.2. Carrier Diversity/Hybrid	232
E.2.1. HDBC.....	233
E.2.2. FDBC	235
E.2.3. Rearrangement	235
E.3. Summary	236
APPENDIX F: NAV DATA SIGNAL DESIGN FOR HOT START OF GNSS	238
APPENDIX G: PERFORMANCE WITH THE THIRD GEO AT 90°E AND 100°E ...	240

List of Tables

Table 2-1: Distribution of receiver components leading to TTFF.....	50
Table 2-2: Potential future components of a datasheet with the TTFF parameter spelt out with service and frequency of operation supported.	54
Table 3-1: Table summarizing the maximum time required to collect primary and secondary NAV data in GPS/GLONASS L1, GALIEO E1 and GPS L5 post bit synchronization.....	62
Table 3-2: Sample IRNSS and GPS L1 ephemeris parameters and their bit definitions.....	69
Table 3-3: Sample message type definitions to be transmitted as a part of the fourth subframe in IRNSS.	71
Table 3-4: Data straddling with alternate page arrangement for global coverage and optimal T_{sec} in IRNSS.....	73
Table 3-5: Proposed message types with their periodicities as a part of third subframe in TSN architecture.....	76
Table 3-6: Signal specifications characteristics used in the simulation of the proposed IRNSS signals.	83
Table 3-7: Summary of ephemeris collection time in various proposed methods of IRNSS with bit-synchronization on the first bit of a subframe.....	97
Table 3-8: Comparison of primary and secondary parameters performance in proposed methods.	97
Table 3-9: Summary of the proposed methods in comparison with GPS L1 C/A.....	98
Table 4-1: Representative datasheet of a receiver w.r.t TTFFs in IRNSS single frequency mode of operation.	99
Table 4-2: Summary of the achievable TTFF and secondary data collection in civilian dual frequency of operation for various combinations of existing operational systems, post bit synchronization.	110
Table 4-3: List of assumptions with which the signals are derived in diversity mode for IRNSS.	114
Table 4-4: Summary of proposed methods compared to GPS L1/L2 (30 s) for civilian applications.	134
Table 4-5: Summary of proposed methods compared to GPS L1/L2 (36 s) for restricted applications.	134

Table 5-1: Representative datasheet of a receiver w.r.t TTFFs in single/dual frequency modes of receiver operation of IRNSS.....	135
Table 5-2: Summary of NAV data signal design in combined mode 1 of IRNSS.	150
Table 5-3: OCM of NAV data signal design in IRNSS.....	156
Table 5-4: Summary of ORM of NAV data signal design in IRNSS.....	158
Table 6-1: Assumptions towards the engineering optimization proposition.	176
Table 6-2: Summary of the IRNSS and GAGAN locations considered for simulations.....	178
Table 6-3: Assumed power levels onboard proposed IRNSS+GAGAN configuration.	183
Table 6-4: Assumptions made towards transmitting L1 signal on geosynchronous satellites of IRNSS.	184
Table 6-5: Methodology to accomplish real time hot start of GNSS using the geosynchronous satellites of IRNSS.....	188
Table 6-6: Mapping of test apparatus to the system segments of IRNSS.....	195
Table 7-1: Potential IRNSS receiver datasheet w.r.t TTFF in open sky conditions using proposed signals (post bit synchronization).....	206
Table 7-2: Possible future activities to enhance the TTFF performance.....	207
Table A1: Subframe ID description of IRNSS signals in four-subframe architecture.	216
Table A2: Subframe-1 parameter list for proposed IRNSS signals.....	217
Table A3: Subframe-2 parameters list as a part of proposed IRNSS signals.	218
Table A4: Message ID description for proposed IRNSS secondary messages.	219
Table A5: Almanac-Iono / Message Type 1 field descriptions.	220
Table A6: Almanac- UTC/ Message type 2 field descriptions.	221
Table A7: User defined message types to be transmitted as a part of subframe 4.	222
Table B1: Subframe ID description of IRNSS signals in TSN.....	223

Table B2: UTC-Iono Message / Message Type 3 field descriptions.	224
Table C1: Subframe ID definitions for TSF structure.	225
Table E1: Received 1800 symbols in HDBC-case 1.	229
Table E2: Received 1800 symbols in HDBC-case 2.	229
Table E3: Received 1800 symbols in HDBC-case 3.	230
Table E4: Received 1800 symbols in HDBC-case 4.	230
Table E5: Received 1800 symbols in FDBC.	231
Table E6: Contents of three buffers.	231
Table E7: Received 1800 symbols in HDBC-case 1.	233
Table E8: Received 1800 symbols in HDBC-case 2.	233
Table E9: Received 1800 symbols in HDBC-case 3.	234
Table E10: Received 1800 symbols in HDBC-case 4.	235
Table E11: Received 1800 symbols.	235
Table E12: Content of three buffers.	236
Table F1: NAV data structure proposed for transmission on the third frequency of IRNSS geosynchronous satellites.	238

List of Figures

Figure 1-1: Positioning in deep forests without aid to terrestrial link.	4
Figure 1-2: Summary of chapters and their contents.	15
Figure 2-1: Representative datasheet of a GNSS receiver depicting performance, physical, electrical and environmental specifications.	17
Figure 2-2: Overview of IRNSS system components.	18
Figure 2-3: IRNSS constellation depicting three GEO and four GSO satellites.	19
Figure 2-4: IRNSS availability illustrating satellite distribution and specifically the assured visibility over the Indian subcontinent.	20
Figure 2-5: Functional blocks of a typical GNSS receiver from antenna to navigation output.	23
Figure 2-6: Block schematic of RF down conversion process to generate IF signal.	26
Figure 2-7: Block schematic of baseband processing unit from analog IF to receiver position computation.	26
Figure 2-8: Acquisition correlator.	30
Figure 2-9: Bit synchronization scheme depicting the construction of moving correlation sets for estimating the bit boundaries.	31
Figure 2-10: Tracking correlator and measurement generator.	32
Figure 2-11: GPS L1 C/A NAV data structure depicting frames, words, bit and their duration. ..	34
Figure 2-12: IRNSS system time formulation based on the HOW word and bits collected in the receiver.	35
Figure 2-13: Summary of signal flow within a receiver from IF to position computation encompassing all functional components.	39
Figure 2-14: Summary of receiver categories highlighting the specific features necessary for each segment.	42
Figure 2-15: Receiver start modes with the available estimates at power-on and their achievable TTFF.	44
Figure 2-16: TTFF characterization test apparatus highlighting the boot-time captured on DSO.	47

Figure 2-17: GUI illustrating the status of the receiver health and depicting various receiver components leading to TTFF.	49
Figure 2-18: TTFF characterisation timing diagram capturing receiver’s underlying time components and parallel drawn with AGPS mode of operation.	49
Figure 2-19: GNSS receiver onboard a vehicle launched from a submarine with touch down timing from surface of water.	52
Figure 2-20: Event sequence from vehicle emergence from submarine to touchdown.	53
Figure 2-21: GNSS receiver onboard a vehicle released from underneath an aircraft with touchdown time from release.	54
Figure 3-1: NAV data signal design of GLONASS L1 depicting frames and its constituents, strings and bit definitions.	58
Figure 3-2: NAV data signal design of a) GPS L5 b) GALILEO E1 with message types/pages, its constituents and bit definitions.	59
Figure 3-3: Signal design of almanac transmission in GPS L1 across satellites.	63
Figure 3-4: Proposed IRNSS NAV data structuring detailing its constituents.	66
Figure 3-5: Simulation software flow to deduce the IRNSS Keplerian parameters as a part of each satellite’s ephemeris.	68
Figure 3-6: Proposed data straddling technique of almanac transmission across satellites in IRNSS.	70
Figure 3-7: Proposed almanac and textual message transmission to enhance T_{sec} in IRNSS.	71
Figure 3-8: Proposed IRNSS NAV data signal design with four subframes data streaming.	72
Figure 3-9: Proposed IRNSS NAV data signal design with TSN architecture.	75
Figure 3-10: Proposed NAV data with transmission in TSN architecture to enhance T_{eph} and T_{sec} in IRNSS.	76
Figure 3-11: Proposed NAV data architecture with TSF transmission to enhance T_{eph} and T_{sec} in IRNSS.	78
Figure 3-12: PDOP variation over Indian subcontinent with all satellites and exclusion of GEO-1.	79
Figure 3-13: a) Test-rig used for proposed IRNSS signal generation b) hardware-software interaction diagram illustrating the signal flow.	81

Figure 3-14: Flow diagram of the signal simulation software to generate the proposed IRNSS signals.	82
Figure 3-15: Triple RF GPS GLONASS (a) receiver hardware (b) hardware software signal flow.	84
Figure 3-16: High level software flow within GPSGL receiver showing various modules, changes required and the proposed new module.	85
Figure 3-17: Conventional data collection method and its limitations w.r.t TTFF.	86
Figure 3-18: Proposed data grouping technique to enhance TTFF with initial bit synchronization occurring in the middle of a subframe.....	87
Figure 3-19: New software flow diagram for the proposed IRNSS signals.	88
Figure 3-20: Data symbols populated in rows and columns and a scenario where partial interleaved symbols are collected in a receiver.	90
Figure 3-21: Subframe processing from a TTFF perspective (a) without tail bits and (b) with tail bits.....	91
Figure 3-22: Flowchart for subframe synchronization with synch pattern encoded and its overhead.....	92
Figure 3-23: Test apparatus for the validation of the proposed IRNSS signals.....	93
Figure 3-24: Altitude plot illustrating time required to collect ephemeris and almanac in FSA of IRNSS post bit synchronization.	95
Figure 3-25: Altitude plot illustrating time required to collect ephemeris and almanac in TSN architecture of IRNSS post bit synchronization.....	96
Figure 3-26: Altitude plot illustrating time required to collect ephemeris and almanac in TSF architecture of IRNSS post bit synchronization.....	96
Figure 4-1: Signals transmitted from GPS/GLONASS satellites.	100
Figure 4-2: Design augmentations necessary to adapt a single frequency receiver for optimal processing of dual frequency signals and leverage advantages.	103
Figure 4-3: Illustration of P-code acquisition based on HOW assistance from SPS.....	106
Figure 4-4: NAV data streaming on GPS L1 C/A, L5 and L2C and their transmission periods.	109
Figure 4-5: Bubble diagram depicting the region where a) restricted and civilian signals are ineffective b) civilian signal is ineffective c) operable region.....	113

Figure 4-6: Summary of diversity based signal processing and its limitations w.r.t TTFF.....	114
Figure 4-7: Assumption on IRNSS ranging codes and NAV data across frequencies/service...	116
Figure 4-8: NAV data bits sourcing from subframe array on either service of IRNSS.....	117
Figure 4-9: Signal design based on code diversity a) similar to GPS L1 b) direct reversal scheme c) optimal transmission method as applied to FSA in IRNSS.	118
Figure 4-10: Signal design based on carrier diversity of SPS in IRNSS as applied to FSA.	119
Figure 4-11: Signal design based on hybrid method in IRNSS as applied to FSA of NAV data streaming	120
Figure 4-12: Signal simulation software design to generate the proposed diversity based IRNSS signals.	121
Figure 4-13: IRNSS NAV data signal generation to optimize TTFF based on code diversity. .	122
Figure 4-14: Carrier and hybrid methods of NAV data signal generation in IRNSS with a FSA.	124
Figure 4-15: Architecture-1 with the NAV data bits are grouped into sets of four and straddled.....	125
Figure 4-16: Architecture-2 with NAV data symbols grouped into sets of four and straddled..	125
Figure 4-17: Top level details of the triple RF GPSGL receiver used for validation of the diversity results.	126
Figure 4-18: The software flowchart illustrating the proposed three diversity schemes for IRNSS.	128
Figure 4-19: Timing diagram of NAV data collection with FSA in single frequency mode of IRNSS receiver operation.	129
Figure 4-20: Timing diagram of code diversity based on NAV data collection with FSA in IRNSS.	129
Figure 4-21: Timing diagram of carrier and hybrid method of NAV data collection with FSA in IRNSS.	130
Figure 4-22: Altitude plot summarizing the improvements in proposed diverse methods for IRNSS.	132
Figure 5-1: Use of almanac in various receiver applications.....	136

Figure 5-2: A typical scenario of cross correlation in outdoor application.	140
Figure 5-3: Existing cross correlation detection method based on range differencing in civil aviation GPS L1 C/A receivers.	141
Figure 5-4: a). Test apparatus used to demonstrate cross correlation effects and detection based on existing methods b) the GGVISION snap-shot depicting the cross correlated channels.	143
Figure 5-5: Proposed cross correlation methods based on NAV data processing in IRNSS.	147
Figure 5-6: NAV data signal design in combined mode 1 of IRNSS.	149
Figure 5-7: NAV data signal design in combined mode 2 of operation in IRNSS.	151
Figure 5-8: Proposed TSF method of NAV data transmission on L5 path of restricted service of IRNSS in combined mode 2 (sequencing of MT3 changed w.r.t Figure 3-11 and assuming it to be supported on S1 to resolve DOP).	152
Figure 5-9: Timing diagram illustrating the transmission slots of various messages in either frequencies of the SPS/RES service in IRNSS OCM method of NAV data design.	154
Figure 5-10: OCM of NAV data signal design in IRNSS.	155
Figure 5-11: ORM of NAV data signal design in IRNSS.	157
Figure 5-12: Signal generation methodology to derive the proposed OCM signals in IRNSS. .	159
Figure 5-13: Signal generation methodology to derive the proposed ORM signals in IRNSS. .	160
Figure 5-14: High level receiver design to derive the benefits of OCM and ORM of NAV data signal design in IRNSS.	161
Figure 5-15: Time taken to detect cross correlation with various methods a) range differencing as in GPS L1, b) proposed NAV data processing, c) proposed satellite id method.	163
Figure 5-16: Altitude plot illustrating the TTFF performance with the OCM/ORM method of NAV data signal design.	164
Figure 6-1: Existing and proposed GNSS systems and their frequencies/minimum assured power levels (IRNSS power levels assumed).	168
Figure 6-2: Control and space segment architectures of a) GAGAN b) IRNSS.	174
Figure 6-3: GAGAN (GEO-3 position assumed) and IRNSS geostationary satellites.	175

Figure 6-4: Satellite availability with current IRNSS and proposed IRNSS constellation.....	180
Figure 6-5: PDOP with current IRNSS and proposed IRNSS constellation.	181
Figure 6-6: Availability and PDOP with IRNSS and GAGAN.....	182
Figure 6-7: Proposed integrated IRNSS+GAGAN architecture.....	187
Figure 6-8: Methodology to generate the proposed L1 signals onboard channels of IRNSS geosynchronous satellites.....	190
Figure 6-9: Receiver architecture to achieve HOT start of GPS/GLONASS in real time using the third frequency on geosynchronous satellites.	192
Figure 6-10: Block schematic detailing the test apparatus used for the simulation.....	194
Figure 6-11: a). Test apparatus used to simulate GNSS Hot start performance with IRNSS b) rear panel connects of the simulator c) various subsystems used as a part of test setup.	196
Figure 6-12: Fast TTFF test results for IRNSS and GPS in Hot start mode of operation.	197
Figure 6-13: Time taken to transmit NAV data of GPS satellites on geosynchronous satellites.....	198
Figure 6-14: Summary of chapter contribution.	200
Figure 7-1: Summary of contributions/conclusions of the research.	203
Figure A1: Subframe data structure for primary navigation parameters.....	216
Figure A2: Subframe data structure for message transmission in subframe 4 of IRNSS.....	219
Figure D1: Variation in PDOP considering the GEO-2 and GEO-3 exclusion in IRNSS.	226
Figure D2: Variation in PDOP considering the GSO-1 and GSO-2 exclusion in IRNSS.....	227
Figure D3: Variation in PDOP considering the GSO-3 and GSO-4 exclusion in IRNSS.....	227
Figure E1: Proposed three-subframe data structure carrier diversity or hybrid architecture in IRNSS.	232

Figure E2: Initial bit synchronization and data reconstruction mechanism.....	237
Figure G1: Visibility plots for the third GEO at 90°E and 100°E.	240
Figure G2: PDOP plots for the third GEO at 90°E and 100°E.	241

List of Abbreviations

Abbreviations	Description
ADC	Analog to Digital Converter
AGPS	Assisted GPS
AIV	All In View
ALM	Almanac
ASP	Analog Signal Processing
ASIC	Application Specific Integrated Circuit
BOC	Binary Offset Carrier
BPF	Band Pass Filter
BPSK	Binary Phase Shift Keying
BPU	Baseband Processing Unit
CAN	Controller Area Network
CCD	Cross Correlation Detection
CDMA	Code Division Multiple Access
CLL	Carrier Lock Loop
CRC	Cyclic Redundancy Check
CSR	Cambridge Silicon Radio
C/A	Coarse / Acquisition
dB	Decibel
DDC	Direct Down Conversion
DEM	Data Extraction Module
DGNSS	Differential GNSS
DLL	Delay Lock Loop
DoD	Department of Defense
DOP	Dilution Of Precision
DSP	Digital Signal Processing
DSO	Digital Storage Oscilloscope
EGNOS	European Geostationary Navigation Overlay Service
FDBC	Full Data Block Collection
FDE	Fault Detection and Exclusion
FDMA	Frequency Division Multiple Access
FEC	Forward Error Correction
FFT	Fast Fourier Transform
FLL	Frequency Lock Loop
FMS	Flight Management System
FPGA	Field Programmable Gate Array
FSA	Four Subframe Architecture
GAGAN	GPS aided Geo Augmented Navigation
GEO	Geo-stationary Orbit
GLONASS	Global Navigation Satellite System
GNSS	Global Navigation Satellite System
GPS	Global Positioning System
GPSGL	GPS GLONASS

GSO	Geosynchronous Orbit
HDBC	Half Data Block Collection
HOW	Hand Over Word
Hz	Hertz
ICAO	International Civil Aviation Organization
ICD	Interface Control Document
IF	Intermediate Frequency
INS	Inertial Navigation System
IODC	Issue of Data Clock
IODE	Issue of Data Ephemeris
IRIMS	IRNSS Range Integrity Monitoring Stations
IRNSS	Indian Regional Navigation Satellite System
ISRO	Indian Space Research Organization
LNA	Low Noise Amplifier
LOS	Line of Sight
LSB	Least Significant Bit
MATLAB	Matrix Laboratory
MFC	Measurement Formulation and Corrections
MIL	Military
MIPS	Million Instructions Per Second
MSAS	Multi-functional Satellite Augmentation System
MSB	Most Significant Bit
MSGID	Message Identification Number
MT	Message Type
NAV	Navigation
NF	Noise Figure
NSP	Navigation Signal Processing
OCM	Optimal Civilian Mode
ORM	Optimal Restricted Mode
PDOP	Position Dilution of Precision
PLL	Phase Lock Loop
PPS	Pulse Per Second
PRAIM	Predictive Receiver Autonomous Integrity Monitoring
PRN	Pseudo Random Number
PS	Precision Service
QZSS	Quazi Zenith Satellite System
RAIM	Receiver Autonomous Integrity Monitoring
RES	Restricted Service
RF	Radio Frequency
RHCP	Right Hand Circular Polarization
RTC	Real Time Clock
RTCM	Radio Technical Commission for Maritime applications
SBAS	Satellite Based Augmentation System
SDBM	Satellite Data Base Manager
SF	Subframe

SFID	Subframe Identification
SiS	Signal in Space
SNR	Signal to Noise Ratio
SPMG	Signal Processing and Measurements Generation
SPS	Standard Positioning Service
SSVC	Satellite State Vector Computation
SSW	Search Synch Word
SV	Satellite Vehicle
SVID	Satellite Vehicle Identification
SYNC	Synchronization
TLM	Telemetry
TOW	Time Of Week
TSF	Three Subframe Fixed
TSN	Three Subframe Normal
TTFB	Time To First Fix
UD	User Defined
UHF	Ultra High Frequency
UPE	User Position Estimation
UPEM	User Position Estimation Module
URA	User Range Accuracy
USB	Universal Serial Bus
UTC	Universal Time Coordinated
WAAS	Wide Area Augmentation System
WN	Week Number

List of Symbols

Symbol	Definition
\sqrt{A}	Square root of semi major axis ($m^{1/2}$)
B	Signal bandwidth [Hz]
c	PRN code
C/No	Carrier to Noise Ratio (dB-Hz)
d	Navigation data bits
f_c	Carrier frequency [Hz]
f_D	Doppler frequency [Hz]
f	Sampling frequency [Hz]
N_0	Thermal noise power spectral density
F	Noise factor of the system
C_t	Transmitted carrier power [dBW]
C	Received carrier power [dBm]
I	In-phase component
k	Boltzmann constant
NAVDATA	Navigation data
NAV_{pri}	Navigation data bits primary
SFID	Subframe ID
NAV_{sec}	Navigation data bits secondary
SF_{n-enc}	Encoded nth subframe data
Q	Quadrature phase component
π	Pi
e	Orbital Eccentricity
Ω_0	Longitude of ascending node of the orbit plane at reference time (radians)
I_0	Inclination Angle of the orbit plane at reference time (radians)
ω	Argument of perigee
Ω_{dot}	Rate of right ascension
M_0	Mean Anomaly at reference time (radians)
T_A	Antenna Noise Temperature [$^{\circ}$ Kelvin]
T_s	Sampling period [s]
T_b	Data bit period [s]
τ	Time delay [s]
T_c	Coherent integration time [s]
T	Total integration time [s]
T_{pri}	Time required to collect primary NAV data parameters [s]
$T_{TFF_{opt}}$	Optimal TTF [s]
$T_{eph-GPS}$	Ephemeris collection time in GPS [s]
$T_{eph3I-N}$	Ephemeris collection time in IRNSS Three subframe Normal data structure [s]
$T_{eph3I-F}$	Ephemeris collection time in Three subframe Fixed data structure [s]
$T_{Ion-GPS}$	Ionosphere collection time in GPS [s]

$T_{\text{Ion3I-F}}$	Time taken to collect Ionosphere correction terms in Three subframe fixed data structure of IRNSS [s]
$T_{\text{Ion3I-N}}$	Time taken to collect Ionosphere correction terms in Three subframe Normal data structure of IRNSS [s]
T_{sec}	Time required to collect secondary NAV data [s]
T_{eph}	Time required to collect ephemeris [s]
T_{alm}	Time required to collection complete almanac [s]
T_{utcion}	Time required to collect UTC Ionosphere terms [s]
T_{mt}	Time required to collect complete textual messages [s]
T_{b}	Time to boot a system [s]
T_{a}	Time required to acquire a satellite [s]
T_{bs}	Time required to achieve bit synchronization [s]
T_{posc}	Time to output position with ionosphere error correction [s]
$T\text{TFF}_{\text{opt}}$	Optimal Time To First Fix [s]
α	Ionosphere correction co-efficient
β	Ionosphere correction co-efficient
ω_{m_l5}	Angular frequency of L5 carrier [radians]
ω_{m_s1}	Angular frequency of S1 carrier [radians]

Chapter One: INTRODUCTION AND OVERVIEW

The GPS was designed and developed in the late seventies by the US Department of Defense (DoD) based on Code Division Multiple Access (CDMA) technology (Dixon 2004). The primary objective of this system was to provide the US military with a high degree of navigation accuracy. As an offshoot of this development, civilian receivers based on Coarse / Acquisition (C/A) signal transmitted from GPS was developed. This dual use enabled civilian users worldwide to obtain position and timing solutions with comparable degree of reliability and accuracy to that of receivers based on restricted signals (IS-GPS-200E 2010). In a parallel development, the GLONASS system from Russia evolved. The European Union (Galileo) and China (Compass) are also in the process of having their own GNSS (Galileo 2008). India is planning to have a regional positioning system, namely IRNSS (Kibe & Gowrishankar 2008). With these proposed GNSSs, multi-constellation fully operational systems are becoming a reality.

The existing GPS initially supported dual and single frequencies on restricted and civilian signals respectively (IS-GPS-200E 2010). The resounding successes of civilian L1 C/A on GPS and a persistent demand for a second frequency resulted in GPS L2C. This signal is also targeted to indoor applications where sensitivity demands are very high (Fontana et al 2001). The aviation community is another main GPS beneficiary (EGNOS TRAN 2003) which demands a dedicated signal in the protected L5 band. This led to the third signal emerging in the L5 band for GPS, primarily for civil aviation (Erlandson et al 2004). As a part of GPS modernization, the L1C signal with enhanced capabilities and interoperable with other L1 GNSS systems are proposed (Stewardship Project 2004).

Unlike GPS, GLONASS is a Frequency Division Multiple Access (FDMA) system (GLONASS-ICD, 1998) which also has widespread use. Over the years, limitations in the FDMA technique for precise navigation applications have been reported. One specific application is surveying, where carrier phase ambiguity resolution plays a vital role and is an involved process with FDMA (Petovello 2010). In addition, the interoperable navigation accuracies achievable with other GNSS are reduced due to limitations in FDMA. To overcome this, administrators have proposed CDMA GLONASS with the first test signal currently being available on one of the GLONASS K satellite (Ipatov & Shebshayevich 2010).

The user receivers developed based on the above signals can be categorized as high dynamic, civil aviation, handheld users, indoor, survey grade etc. (Kaplan & Hegarty 2006). The categorization is primarily based on the diverse applications supported by the user equipment. At present, receiver manufacturers have developed user equipment that can operate in any or combination of L1, L2, L5 frequencies supporting GPS, GLONASS, and GALILEO systems with as many as 200+ channels (for example, (Triumph 2012)).

The large number of receivers which are in use pose a major challenge for signal design modifications or the inclusion of new signals due to the following reasons: First, constraints due to conflicting user requirements. For example, indoor applications demand a signal which assists higher sensitivity (for example, longer data bit duration) that conflicts with a design for fast TTFF (for example, higher data rate). Second, a limitation of an existing signal is that it cannot be changed abruptly or stopped all together (for example, increase in the number of bits representing week number in GPS SPS L1 C/A). Third, a new signal should not affect performance adversely and should enable seamless co-existence with existing operational systems (for example, GPS L5 w.r.t to its predecessors L1, L2C) (Stewardship Project 2004).

Given these issues, during signal design care is to be exercised to systematically address the needs of different user groups and improve upon an existing limitation.

However, for upcoming new systems like IRNSS or CDMA GLONASS, there exists an opportunity to use the learning from the legacy operational GNSS systems and explore new signal design methods to optimize certain receiver specifications (for example, jamming margins, sensitivity improvements, spoofing, multipath or TTFF).

1.1 Background

Given the widespread use of GNSS receivers, the need for accurate, reliable and *fast* positioning is now of major importance (Hein et al 2010). During the late eighties and early nineties, a receiver powered on without any assistance (primary or secondary data, approximate user position or time), provided a navigation solution within about 10 minutes (Melbourne et al 1993). Subsequently, it dropped to 3 minutes early in the last decade (PocketGPSWorld 2012), which currently has reached around 30-32 s for the existing operational GNSS systems (SkyTraQ 2012). The improvements are attributed to progress in signal processing methods (Pany 2011) and catalyzed by the tremendous growth witnessed in the semiconductor technology (Jansen 2012).

The past decade has witnessed the evolution of several integrated applications based on GNSS technology (Li 2005). This was intended to improve a limitation of the other sensors or assist the GNSS receiver itself thereby providing the user with an optimal system level solution. Inertial Navigation System (INS) integration (Salychev et al 2000) is an example for the former and AGPS (Van Diggelen 2009) for the latter. With AGPS technology, the receivers are able to obtain the required data assistance on a terrestrial link and thereby reduce the TTFF (Assisted

GPS 2010). This has paved the way for using the GNSS receivers as an aid in many life critical scenarios such as E911 (Greene 2006). *However, the availability of the link is not always guaranteed as shown in Figure 1-1. In addition, the user needs to pay for this service as well.*

The major promoters of most GNSS programs are often military organizations (for example, GPS and GLONASS). The defense applications usually have needs like high dynamics, high maneuverability and fast TTFF (Dynerics 2010). Not much of data is available on the restricted signals of either GPS or GLONASS in open source. However, based on the datasheets of the GPS receiver manufacturers supporting restricted signals, TTFF is comparable to that of civilian users, namely 30-32 s without assistance (CommSync II 2010). Extending the AGPS (Figure 1-1) concept to critical applications (for example, portable receivers based on restricted signal for soldiers in deserts, forests, mountains, etc.) *is not practical or economically viable.*



Figure 1-1: Positioning in deep forests without aid to terrestrial link.

To overcome the above real world problems and to achieve an enhanced TTFF directly from the satellites, new methods need to be explored, which is the scope of this research. In pursuit of

lower TTFF values, other benefits (for example, accuracy, power required to transmit the signal, jamming margins, etc.) achieved in the existing operational GNSS should not be compromised. One potential system where TTFF improvements can be explored is the IRNSS.

1.2 Literature review

Based on initial studies and the broad level limitations cited above, TTFF emerged as a strong candidate for research. An in-depth study was conducted on the methods employed in the receivers till date, which encompass novel approaches proposed by industry and academia.

With an emphasis on understanding the basic tenets of TTFF and to explore the limitations and drawbacks in the existing methods, a literature survey was carried out. The collated data is grouped and analysed under the following headings:

Characterization, Navigation (NAV) data structures, Receiver architectures, Cross correlation detection and finally, Multiple frequency GNSS system. The following paragraphs give a brief overview of each category, emphasizing its limitation and conclude with a potential research prospect.

1.2.1 Characterization

The industry and researchers have proposed methods to reduce the TTFF of a GNSS receiver, which can be grouped and categorized as signal processing and data aiding (Van Diggelen 2009). In signal processing, the characterization component is the time required to acquire a satellite – the acquisition time. Acquisition of a CDMA signal is a two dimensional search process – in ranging code (for example, 10-bit C/A code on GPS L1) and Doppler (Misra & Enge 2001). Typically for static applications, the Doppler (from satellite motion) search range is of the order of ± 5 KHz. However, for high dynamic applications (satellite + user motion), this will be of the

order of ± 50 KHz ((Bao & Tsui 2004), (Kaplan & Hegarty 2006)). For optimal TTFF performance, signal acquisition time needs to be minimal.

W.r.t data aiding, the receiver operations can be categorized into various start modes namely: Cold, Warm, Hot and Snap. Each of these modes is differentiated based on the assistance with which the receiver is powered on. Accordingly, the TTFF achieved in each mode is different (Rao et al 2011) . Thus, the global parameter used to characterize performance in data aiding is TTFF.

1.2.1.1 Limitations

To date, the existing characterization has globally established the limits w.r.t signal processing and data aiding. However, not many papers have experimentally established various timing components in the receiver leading to positioning in detail from a TTFF perspective (Hein, et al., 2010). In addition, no work till date has addressed the *TTFF characterization of dual frequency civilian or restricted receivers* explicitly. This provides an opportunity to characterize TTFF performance and carry out research on the derived components.

1.2.2 Navigation data structures

As mentioned earlier, the data transmitted from the satellites can be grouped into primary and secondary parameters. The primary parameters are mainly responsible for the user position computation. Across the existing and proposed GNSS systems, this grouping is differentiated based on NAV data structure adopted in a particular system. A close examination of the GPS L1 ICD reveals that several data fields are dummies, with a subframe structure being the mode of NAV data structuring (IS-GPS-200E 2010). Recent developments in GPS L2C and L5 have optimized the NAV data design relative to that of GPS L1 (ICD-GPS-705 2002). Similarly,

GLONASS adopts a technique of string transmission (GLONASS-ICD 1998). Like GPS, GALILEO has three frequencies, dedicated to civilian users and has absorbed the concepts of GPS and GLONASS (for example, E1 and F1 page respectively, (Galileo 2008)). Typically, the data transmission rate is 50 Hz across most systems, which limits its collection within the receiver.

1.2.2.1 Limitations

Though several NAV data structures have been devised recently, none have directly focused on optimizing the TTFF. GPS L5, which adopts messaging architecture, does not really reduce the TTFF or L2C with a 25 Hz data rate. Till date, there is no literature that describes the derivation of an optimal NAV data structure for the TTFF. In addition, as a part of data integrity, several implementation concepts such as interleaving, Forward Error Correction (FEC) encoding, usage of Tail and Synchronization bits as part of NAV data have been described and used in the existing and proposed GNSS system (Vucetic & Yuan 2010). The implications of these parameters from a TTFF point of view have not been theoretically described till date. The above listing provides a strong case to carry out related research, to establish clearly the inherent nuances, design and test optimal NAV data signal structures.

1.2.3 Receiver architectures

The first generation of GNSS receivers developed in the early eighties were based on slower processors (Parkinson & Spilker 1996). The size was large (for example, TI 4100, (Magnavox-WM101 2012)) as compared to modern day integrated chip solutions (for example, (GR-10 2012)). During the early days of the GPS program, realizing parallel channel architecture meant a linear increase in the dimensions of the receiver. With this limitation, it was restricted to a

fewer channels, which resulted in a longer time to acquire and track a particular satellite. The result was delayed fix, which then was not a critical requirement.

The advent of Digital Signal Processors (DSP) revolutionized signal processing capabilities with large on-the-chip memory space and processing power (MIPS – Million Instructions per second - (Analog Devices 2012)). This enabled parallel channels to be processed concurrently. The receivers completely realized on DSP (for example, (Phoenix 2012)) reduced the TTFF to around 180 s.

Further with the advent of Field Programmable Gate Arrays (FPGA), the processing resources were shared between DSP and FPGA (for example, (Xilinx 2012)). With this architecture, a dedicated channel was available for each satellite. This minimized the time required to program the visible satellites onto respective channels and thus a TTFF of 48 s became a reality (for example, (Navika 2012)).

In the last 6 to 8 years, the trend has shifted towards realization of a single chip solution, which encompasses the complete receiver. The overall receiver size has drastically reduced to 5 mm X 5 mm X 1.2 mm (for example, (GR-10 2012)). Typically, the architecture followed is a parallel massive correlator (for example, dedicated correlator for each chip of 10-bit C/A of GPS, 1023 in all) which enables fast acquisition of the visible satellites and takes a maximum of 32 s to obtain the position.

1.2.3.1 Limitations

Work till date has assessed the performance of receivers from a TTFF perspective. Not much literature is available that explores TTFF's underlying limitations or have proposed techniques to optimize the TTFF of a LOS single frequency receiver. Further, there are only a few

contributions which take advantage of frequency (Galileo 2008) and none on code diversities. In addition, for restricted signals, no work (w.r.t TTF optimization) is available in the open literature either for single or dual frequencies of receiver operations. For the reasons cited, this research aims at developing signal design methods to provide optimal TTF directly from the satellites for dual frequency civilian and restricted users without increasing data rate or power.

1.2.4 Cross Correlation Detection (CCD)

GPS, GALILEO or the proposed IRNSS and GLONASS employ CDMA technology. The satellite signals are on the same frequency but differentiated based by the unique ranging code assigned to each satellite. This differentiation is achieved based on the cross correlation properties of the ranging codes (Dixon 2004). For GPS L1 C/A, the practically achievable cross correlation margin is around 22 dB (Parkinson & Spilker 1996). For a pair of C/A ranging codes, if the differential power exceeds this margin (typical), cross correlation occurs. With this, the user will not be able to differentiate a weak signal from a strong one, resulting in misleading information.

1.2.4.1 Limitations

The problem of cross correlation is more prevalent for indoor than for outdoor applications (Balaei & Akos 2011). Several techniques based on signal processing methods have been presented to overcome this phenomenon. However, an inherent assumption made in the formulation of the techniques prevents it from being used generally (Glennon & Dempster 2005). In civil aviation where integrity is of paramount importance, cross correlation detection requires a fool proof method and warrants the use of a specific technique at the data level (DO-229D 2006). The above technique, which depends on secondary parameters (IS-GPS-200E 2010),

delays the detection. Hence, there exists an opportunity to design and test new techniques to detect cross correlation.

1.2.5 Multi frequency GNSS systems

When the GPS program was conceptualized, one of the objectives was to guarantee accuracy to US DoD and its allied forces using dual frequency of operation. Till 2006, GPS was available only on L1 (with NAV data) for the civilian users (Ray et al 2006). With the passage of time and inroads made by GPS, civilian receivers have now gained access to the new L2C and L5 signals. In addition, GALILEO also beams signals on three frequencies for civilians (Galileo 2008). One of the biggest challenges during the signal design is the interoperability (independent and dual existence of two systems) issue across GNSS systems. When a new frequency or a modulation technique on an existing system is proposed, the system designers should demonstrate its ill effects, if any. In addition, the frequency filing to allotment process is lengthy (Kibe & Gowrishankar 2008). Following these procedures, it is proposed to transmit IRNSS signals in the L5 and S1 frequency bands (Kibe & Gowrishankar 2008).

1.2.5.1 Limitations

At present, there is no open source document available highlighting the reasons for selecting L5 and S1 frequencies for IRNSS. In addition, there is no literature available which has explored the potential third frequency of operation in IRNSS. For a regional coverage, IRNSS has all the satellites in geostationary orbits (Kibe & Gowrishankar 2008). In addition to IRNSS, Indian space based navigation has SBAS in GPS Aided Geo Augmented Navigation (GAGAN), which is also in geostationary orbits with footprints over the Indian subcontinent (Ganeshan 2012). GAGAN is similar to Wide Area Augmentation System (WAAS), operates in the L1 band. There

is no literature available which explores the possibility of having GAGAN on IRNSS or IRNSS on GAGAN. This provides an ideal platform to explore a possibility, propose and demonstrate the usage of the third frequency with minimal interoperability or frequency filing issues. Another objective is to extend this research and derive an algorithm for hot/snap start of GNSS/IRNSS receivers using IRNSS over the Indian subcontinent.

1.3 Objectives and contributions

Based on the signal design of existing GNSS and the TTFFs in LOS usage, this research will explore methods to optimize TTFF specification in IRNSS. The target platform will be single/dual frequency civilian/restricted IRNSS users. The main contributions are as follows:

1. **Need for Fast TTFF in real world applications:** As mentioned earlier, some real world applications require the TTFF to be very short if GNSS is to be effectively used. With two examples, the need for fast TTFF is theoretically established and explained in detail for an LOS user.
2. **Single frequency signal design:** An *optimal method of obtaining the TTFF within a maximum of 12 s* (from tracking the satellites) is presented. In addition, an optimal architecture to obtain the entire NAV data from the satellite system is presented. Towards this, TTFF is first formulated and its underlying components are deduced. Through proper derivation, the optimal TTFF in a single frequency receiver is established and the signal structure deduced. A hardware simulator with newly developed software is used to generate the proposed signal. A receiver developed based on the new signal is integrated with the simulator to test and demonstrate the improvements claimed.

3. **Dual Service / Frequency based signal design:** Using the results obtained from the above objective, three new signal design algorithms are proposed: *two exclusively* for restricted signals and *one* for civilian users. The proposed signals are derived and results established experimentally. It is shown that the *TTFB in cold start is reduced to 9 s* post signal tracking.
4. **New methods of cross correlation detection:** The cross-correlation method proposed in WAAS DO-229 (2006) standard is experimentally evaluated. The limitation of this method for the existing GNSS systems is described. *Two new schemes of cross correlation detection* are proposed, which flag an alert before the measurements are used for the navigation solution within the receiver. The proposed methods are experimentally demonstrated and *shown to detect cross correlation instantaneously without any assistance*.
5. **Optimized dual frequency signal design:** Following the results of contribution 3 & 4, four new optimal signal structure architectures are proposed for different usage criteria. From an optimized TTFB perspective, *6 and 9 s TTFB (post tracking) for civilian and restricted users respectively are demonstrated. The result is commensurate with HOT start of GPS and is achieved without any receiver aiding*.
6. **Proposed new IRNSS constellation:** A new constellation (location of IRNSS satellites) for increased availability is proposed. The results are encouraging with *significant* improvement in IRNSS availability compared to existing constellation.
7. **Proposed third frequency of operation for IRNSS:** This research *proposes an engineering synergy between IRNSS and GAGAN* and in turn establishes the third

frequency of operation for IRNSS. By this method, the satellite usage can be optimized and results in a *drastic reduction of operational costs*.

8. **HOT Start of GNSS using IRNSS:** This research proposes a method of achieving real time HOT start of existing GNSS using the proposed third frequency of operation in IRNSS. The scheme of operation is theoretically derived and the experimental results demonstrate a TTF of *6 - 8 s for existing GNSS* in real time with IRNSS. Using this method, TTF as obtained in AGPS (with ephemeris assistance mode) is achieved without aiding from any network.

1.4 Thesis outline

A brief overview of the remaining chapters (seven in all) is as follows:

Chapter Two covers the fundamental theoretical aspects specific to this research: With a representative data sheet of a receiver and necessary assumptions, the IRNSS system components are explained broadly. Following this, a high level explanation of the signal transmitted from a typical GNSS satellite is presented. Further, the signal flow from the receiver antenna to position computation is explained in detail for a single frequency of operation. Subsequently, a brief overview of different categories of GNSS receivers is presented. With an experimental setup, TTF formulation is derived and its relevance to the receiver architecture is explained in detail. Following this, various receiver start modes and achievable TTF are elaborated. Finally, with two real world examples, the need for fast TTF directly from the satellite is presented.

Chapter Three presents the signal design for single frequency of operation: A brief theory of the existing operational and proposed GNSS data structures is presented highlighting its

limitations w.r.t TTFF. Following this, the derivation of the proposed NAV data structure is presented and used as a reference throughout this research. Subsequently, four new methods of NAV data signal design are proposed. The simulator used as a reference throughout the research is described in detail from both hardware and software perspectives. To validate the proposed methods, the new receiver software is developed, whose main functionalities are described. Finally, the merits of the proposed signal are presented with test results compared with the existing GPS L1.

Chapter Four provides the proposed signal design for dual frequency of receiver operation: A brief theory of the dual frequency civilian and restricted signal processing is presented emphasising its drawbacks w.r.t TTFF. Following this, three new methods of signal transmission for dual frequency/service is derived for IRNSS. To demonstrate the performance improvement, the methodology to generate the proposed signals is described. The new receiver software to demonstrate the efficacy of the proposed signals is explained. The test results achieved are presented with relevant explanations.

Chapter Five is entirely dedicated to cross correlation detection and optimal signal design of IRNSS restricted and civilian users' w.r.t TTFF: The basic impediment for an optimal TTFF is explained in detail. To overcome this, two new methods of cross-correlation detection based on the proposed signal is derived. As a fall out, four new configurations of NAV data transmission are proposed for IRNSS. The experimental setup to demonstrate the cross-correlation detection and TTFF improvements are explained. The receiver software used to achieve these results is elaborated in detail. Finally, the test methodology and results achieved are presented and analysed.

Chapter Six proposes a third frequency for IRNSS and presents real time HOT start method of a GNSS using IRNSS: To begin with, a brief theory of the proposed IRNSS and GAGAN is presented at the system level. Following this, three engineering propositions are theoretically designed. First, the possibility of accommodating GAGAN onboard IRNSS is detailed. Alternatively, augmenting GAGAN with IRNSS frequencies is elaborated. Considering the latter approach, a method of achieving Real time HOT start of GNSS is derived. The test setup to demonstrate the third frequency of operation and real time HOT start of GPS is thoroughly discussed. The test apparatus to accomplish the above scheme is described in detail. Finally, the test methodology and results obtained are presented and analysed.

Chapter Seven summarizes the results from this research and discusses possible future activities.

The summary of the chapters and their broad level objectives are shown in Figure 1-2.

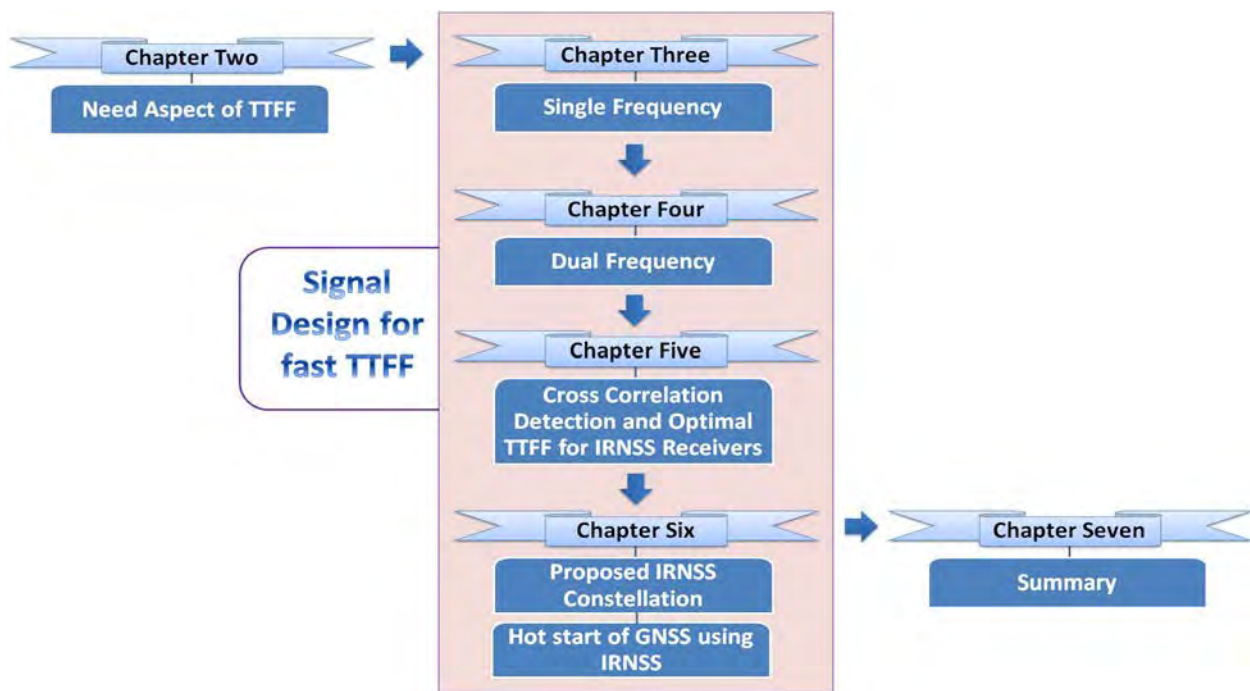


Figure 1-2: Summary of chapters and their contents.

Chapter Two: RECEIVER NUANCES AND NEED FOR FAST TTFF

At a top level, this chapter explains the receiver operations leading to positioning, the methods employed to achieve a fast TTFF with assistance and finally establishes the need for fast TTFF from LOS signal directly. First, a brief explanation of a representative receiver datasheet is presented. Following this, the sub-system components, which constitute any GNSS, are presented with emphasis on IRNSS. The relevant theory starting from the satellite signal through meeting the specifications of the datasheet is explained in detail. Subsequently, various receiver categories are explained in the context of receiver theory. Further, TTFF is pictorially defined with the receiver signal flow. The receiver start modes and the achievable TTFF are explained in detail, with emphasis on AGPS technology. Following this, an experimental setup to formulate the TTFF measure is established and the results are presented. With two real world examples, the existing limitations and needs for fast TTFF are presented for restricted applications. To conclude, a potential futuristic component in a receiver's datasheet w.r.t TTFF is presented and provides pointers to the ensuing chapters.

Figure 2-1 shows a top level receiver data sheet with the parameters collated from various receiver manufacturers. The specifications are broadly grouped under the following headings: Performance, Physical/Electrical and Environmental. The last two categories are more specific to receiver hardware. The performance parameters which are relevant to this research are explained in detail in the following sections. The user equipment performance commensurate with the representative datasheet is guaranteed only with the synergetic existence and contribution from space and control segments. These all together effectively constitute a GNSS system (Misra & Enge 2001). The following section touches upon these components at a high level.

Performance Characteristics			
• Number of channels	: 216		
• Signals supported	: GPS-L1, L2C, L5 GLONASS-L1, L2 Galileo-E1, E5 SBAS		
• Position update rate	: 50 Hz		
• Time To First Fix	: < 36 s (Cold Start), 6-8 s (Hot Start), 2-3 s (Snap Start)		
• Signal dynamics	Low	Medium	High
• Velocity (m/s)	: 515	1000	12000
• Acceleration (g)	: 4	10	50
• Jerk (g/s)	: 1	4	10
• Position accuracy (m) (1 σ)	: 0.01	1	5
• Velocity accuracy (m/s) (1 σ)	: 0.001	0.005	0.1
• Timing solution (1 σ)	: 1 PPS, 15 ns		
• Signal re-acquisition time	: 1 s		
• Support to DGNS	: Available		
• Noise figure	: 1.5 dB		
• Multipath rejection in Antenna	: Available		
• Interference rejection	: Available		
• Support for RAIM, FDE	: Available		
• Sensitivity	: -160 dBm		
• Multiple RF support	: Available		

Physical and Electrical Specifications	Environmental Specification
• Dimension	: 60 mm x 100 mm x 9.1 mm
• Weight	: 37 g
• Input power supply	: +3.3 VDC, 1.3 A
• Antenna LNA power output	: 5 VDC, 100 mA
• Interfaces supported	: RS-232, CAN, USB
	• Temperature
	: -40°C to +85°C
	• Humidity
	: 95 %
	• Vibration
	: 7.7 g
	• Shock
	: 25 g
	• Bump
	: 40 g

Figure 2-1: Representative datasheet of a GNSS receiver depicting performance, physical, electrical and environmental specifications.

2.1 System components - IRNSS

Figure 2-2 depicts the three components of an IRNSS system namely: Space, Control and User segment. The space segment consists of satellites which form the core of any GNSS system. The upkeep and maintenance of the space segment is performed by the control segment. Signals from satellites are acquired, tracked and processed by the receiver to provide the user navigation solution. The following section briefly explains these components.

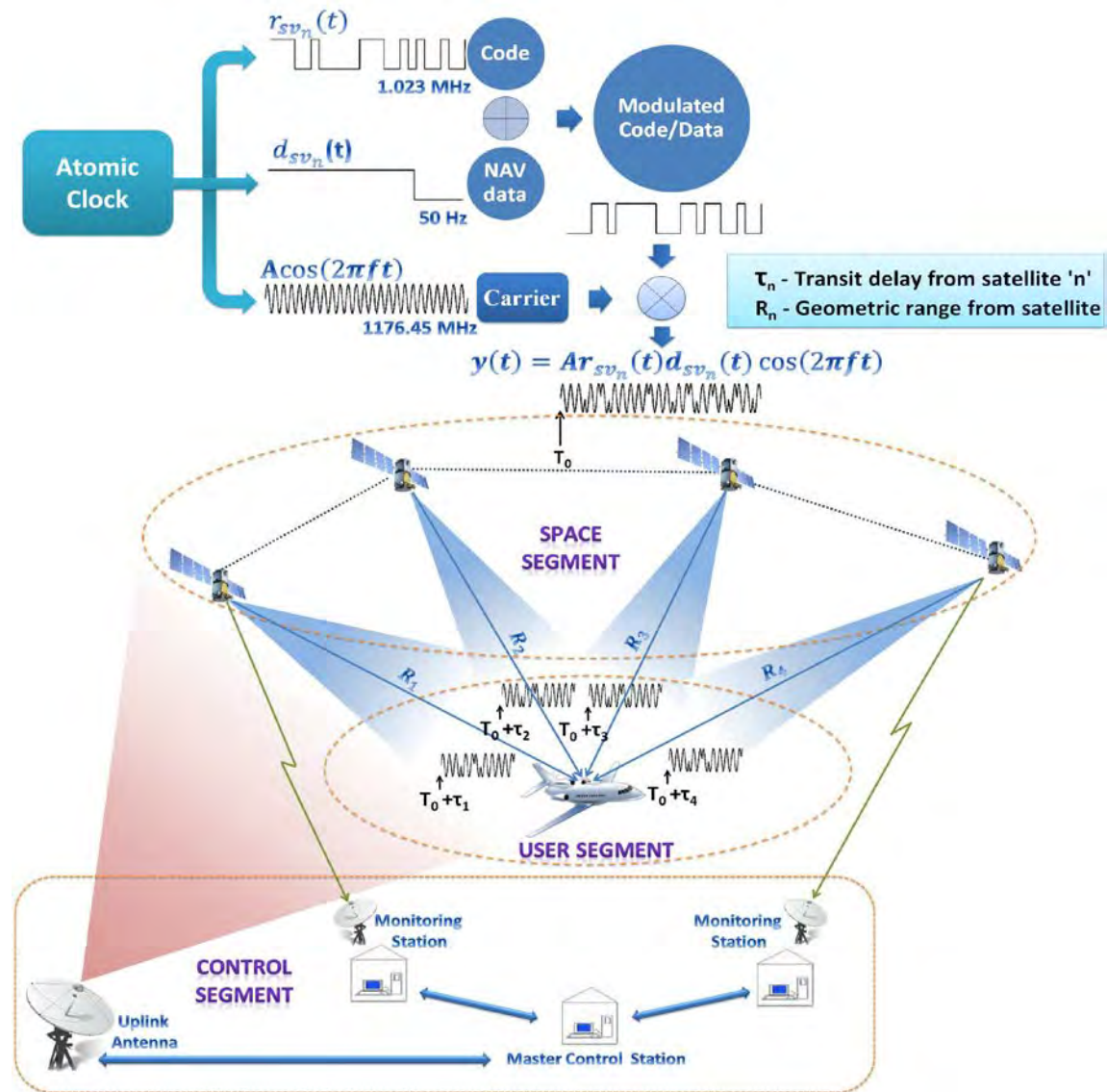


Figure 2-2: Overview of IRNSS system components.

2.1.1 Space segment

The space segment can be broadly categorized based on its contribution as: System and Sub-system. System level traits include availability, accuracy, reliability and integrity (Ryan & Lachapelle 1999). However, the Sub-system mainly focusses on satellite specific features. Based on the available open source literature on IRNSS, the availability and subsystem parameters are explained with necessary assumptions.

Availability is defined as the period of time a system is usable or alternatively is the ability of the system to provide solutions over a specified region (O'Keefe 2001). The satellite distribution topology for IRNSS is as shown in Figure 2-3 (Bhaskaranarayana 2008). The availability as illustrated in Figure 2-4 assures visibility to a user from all the seven satellites over the Indian subcontinent.

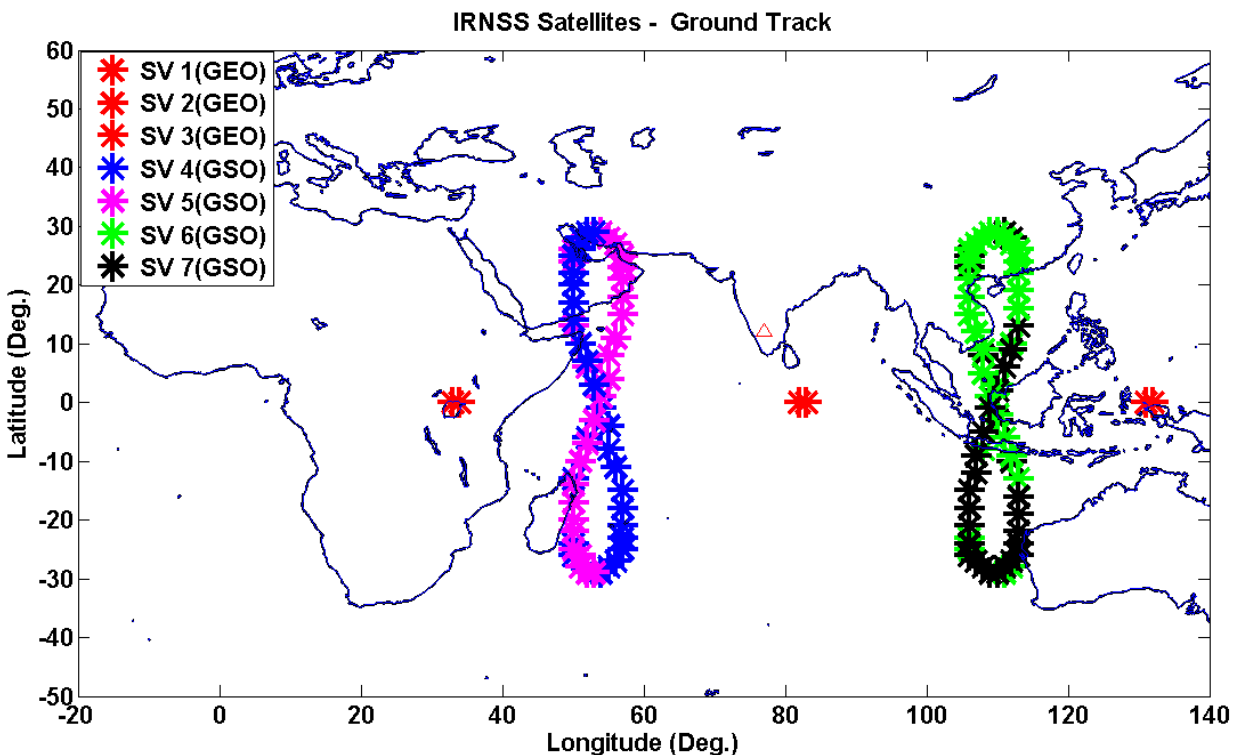


Figure 2-3: IRNSS constellation depicting three GEO and four GSO satellites.

The main sub-system feature is the operational frequencies supported by the GNSS, which for IRNSS are L5 (1176.45 MHz) and S1 (2492.028 MHz) bands. Though the Interface Control Document (ICD) of IRNSS has not been released, at a top level, the system is expected to support Binary Phase Shift Keying (BPSK) and Binary Offset Carrier (BOC) modulations, with the former accessible to civilians (Kibe & Gowrishankar 2008). For ease of explanation and depiction, the characteristics of GPS L1 C/A ranging code and data are assumed on L5 of

IRNSS, with BPSK modulation. The composite signal is generated by the onboard satellite hardware with the reference derived from a standard atomic clock.

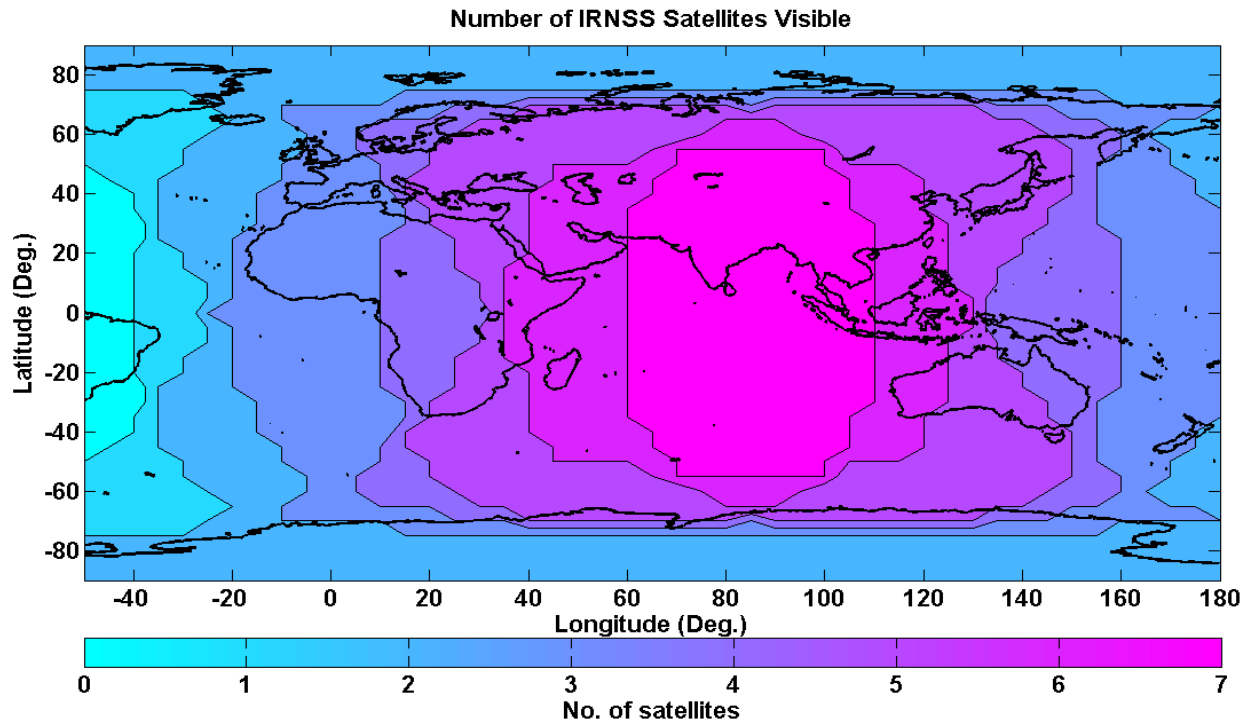


Figure 2-4: IRNSS availability illustrating satellite distribution and specifically the assured svisibility over the Indian subcontinent.

2.1.2 Control segment

The operation and maintenance of satellites post deployment is performed by the control segment. At a high level, the functions of the control segment can be grouped into two sets: first, continuously track and monitor the satellite signal – monitoring stations. Second, provide NAV data to the onboard satellite hardware to generate the composite RF signal – master control station (Parkinson & Spilker 1996).

The monitoring stations are equipped with sophisticated receivers, which are positioned at surveyed locations (Kaplan & Hegarty 2006). These stations are geographically distributed to receive and process the satellite signal. The key components generated from signal processing

are measurements (accurate estimate of range to a satellite and time information) and signal quality information (integrity of ranging code, carrier and data from satellite), which are relayed to the master control station (Gerein et al 2007).

Master control station also generates measurements based on a highly stable atomic clock, which is used as a reference for the system (IRNSS) time. With its measurements and the data collated from several monitoring stations, the master control station processes the data using a complex batch processing algorithm (typically) and generates the necessary NAV data of each satellite (Parkinson & Spilker 1996). The main constituents of this data are the ephemeris and the secondary parameters. Ephemeris primarily contains the orbital information of the satellite and the clock parameters. Specifically, the latter component ensures the synchronization of the satellite clock with the standard atomic source maintaining the system time at the master control station. In addition, master control station tracks the system time offset from UTC and also transmits this information as a part of secondary NAV data (IS-GPS-200E 2010).

2.1.3 Receiver segment

System level symbiotic interaction between the space and the control segment ensures in user receiving the IRNSS signal. The signal emerging from the IRNSS satellite can be modelled as (Kaplan & Hegarty 2006)

$$r(t) = Ac(t)d(t) \cos(2\pi f_c t) \quad (2-1)$$

where

A – Carrier power of the transmitted signal

$c(t)$ – Ranging code, chipped at 1.023 MHz

$d(t)$ – Navigation data transmitted at 50 Hz, generated by the control segment.

f_c – Signal transmission frequency 1176.45 MHz, BPSK signal

At a top level, the receiver needs to solve three unknowns in position - latitude, longitude and altitude and receiver time, based on the measurements performed on the signal (Eq. (2-1)). The signal transmission from each satellite is synchronous as shown in Figure 2-2 (Lachapelle 2010). Typically, the measurements within a receiver are generated from a relatively inferior grade oscillator (for example, TCXO/crystal type to minimize the cost) in comparison with the onboard atomic clock (Van Diggelen 2009). To facilitate position estimation, measurements need to be synchronous to the satellite clocks, which necessitate the estimation of the local clock misalignment (Bao & Tsui 2004). With this as the fourth unknown, the position and time solution mandates measurements to a minimum of four satellites for the user position solution.

Following this brief overview of the GNSS system components, the next section explains the receiver operations from the antenna to user navigation solution computation. The terms, concepts and parameters presented are used extensively in this thesis later. In addition, the explanation parallels the performance characteristics of the representative datasheet. To process the signal originating from the satellite (Eq. (2-1)) and compute the user position, a typical receiver's internal blocks are shown in Figure 2-5. The functional groups are distinguished broadly as Analog Signal Processing (ASP) and Baseband Processing Unit (BPU). With present day technologies, these functions are realized in a single Application Specific Integrated Circuit (ASIC). However, for a better appreciation of the signal flow, a block schematic of ASP and BPU (realized with FPGA and DSP) are presented with the necessary assumptions made. The explanation in the following sections is as follows: an introduction to necessary theoretical concepts followed by commensurate generic receiver implementation available from open source to gain a better understanding of operations leading to the TTFF.

2.2 Receiver operations – Analog Signal Processing (ASP)

ASP mainly constitutes antenna and Radio Frequency (RF) down conversion. The main objective of this section is to translate the received weak (-130 dBm, typical) Ultra High Frequency (UHF) analog signal to a digital Intermediate Frequency (IF) and thus facilitate operation in the baseband section (Kennedy 1999)

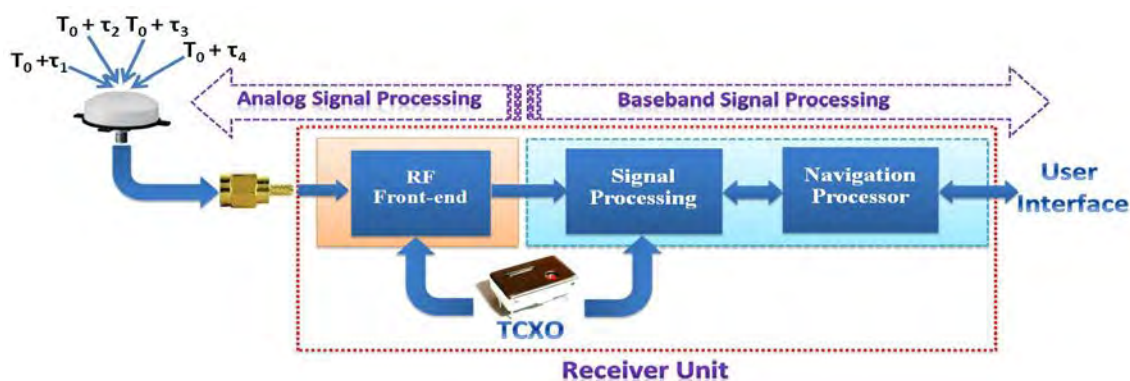


Figure 2-5: Functional blocks of a typical GNSS receiver from antenna to navigation output.

2.2.1 Antenna

The incoming signal is of Right Hand Circular Polarization (RHCP) (IS-GPS-200E 2010), the first element is per force an RHCP antenna with a beam-width (signal capture range) adequate to source satellites from zenith to 5° elevation (Kaplan & Hegarty 2006). Typically, two antenna topologies are in practice: Passive and Active (Kennedy 1999). The passive antenna requires that the processing section be very close to the physical antenna. An example is a handheld GNSS receiver. Practically, many applications require the receiver unit to be at a certain distance from the antenna. The cable inter-connecting antenna to the receiver introduces attenuation to the signal. To compensate for this, a Low Noise Amplifier (LNA) of appropriate gain is used closest to the antenna. The power feed to the LNA is provided from the receiver, which makes the configuration active (Woodcock & Girard 2008).

To protect the receivers from unwanted interference, most antennas have a Band Pass Filter (BPF) following the LNA (Ray & Cannon 2000). This component allows the intended signal and attenuates interfering components outside the desired band ensuring subsequent stages to operate linearly.

Finally, the satellites are spatially distributed and are at different elevations w.r.t to the user antenna. Typically, an antenna has maximum attenuation for the horizon satellites to suppress ground reflected multipath (Ray et al 1998), which is often high for low elevation satellites.

Two important formulations are introduced in this section: Noise power and Noise Figure. The noise power originates from galactic radiations detected by the antenna, which is characterized by an effective noise temperature. The output noise power from an antenna is given as (Bao & Tsui 2004),

$$N_A = k T_A B \quad (2-2)$$

Where k is the Boltzmann constant ($1.3806504 \times 10^{-23}$ J/K), T_A is the antenna noise temperature and B is the signal bandwidth (Satyanarayana 2011). The signals received from satellites are buried within this noise and Eq. (2-2) is used as a reference during detection of signal.

The Noise Figure (NF) in effect characterizes the sensitivity of the receiver, which is the lowest signal level that can be detected for extraction of information (Jasper 2010), which is determined by LNA, the first active component in RF down conversion (Kennedy 1999). Care is exercised during the design stage to select an appropriate LNA with adequate gain and low NF to effectively interface the signal to the receiver unit for RF down conversion (Kaplan & Hegarty 2006).

2.2.2 RF down conversion

The signal from antenna is connected to the receiver unit with a suitable (for example, low loss) RF cable as shown in Figure 2-6. The signal can be represented as (Borio 2008),

$$r[t] = \sum_{i=1}^L A_i \mathbb{C}_i[t - \tau_{i,0}^a] d_i[t - \tau_{i,0}^a] \cos[2\pi(f_{IF} + f_{d,0}^i)t + \phi_{i,0}] + \eta[t] \quad (2-3)$$

where, A_i is the amplitude of the i^{th} satellite carrier signal, $\mathbb{C}_i[n]$ is the PRN code of the i^{th} satellite, $\tau_{i,0}^a$ is the delay introduced by the communication channel, $d_i(t)$ is the navigation data of the i^{th} satellite, f_{IF} is the intermediate frequency, $f_{d,0}^i$ is the Doppler frequency affecting the i^{th} satellite carrier signal, $\phi_{i,0}$ is the initial phase of the i^{th} satellite carrier signal, $\eta[t]$ is the noise in the received signal and L is the number of available satellites from M satellites of the constellation. In case of IRNSS, L is equal to M over the Indian subcontinent (Rao et al 2011).

The signal can be down converted directly or by adopting the conventional heterodyne principle to extract information. The Direct Down Conversion (DDC) requires Analog to Digital Converter (ADC) to operate at UHF and provide adequate gains for the BPU. Though this approach has been demonstrated, it has not been a preferred option in GNSS receivers due to practical issues in realizing ADCs at high frequencies (Bao & Tsui 2004).

The general heterodyne down conversion scheme used as a part of a GNSS receiver is as shown in Figure 2-6 (Haykin 2001). Typically, the first component is the biasing circuit, which provides the requisite power to the LNA embed in the antenna. In addition, this module also performs the antenna open/short circuit detection (Arknava 2008). Following this, the first down conversion is performed using a suitable RF mixer. At the output of mixer, two converted signals are generated: Upper Side Band (USB) and Lower Side Band (LSB). With an appropriate filter, the

LSB is filtered and subsequently amplified (Haykin 2001). The resultant signal is subjected to the next stage of down conversion to generate the analog IF signal. Typically, the gain introduced by filtering and further amplification is of the order of 100 dB (Kaplan & Hegarty 2006). Further, it is ensured that this signal power level straddles within the dynamic range (difference of detectable (high-low) signal) of ADC - the first component in the BPU (Halamek et al 2001).

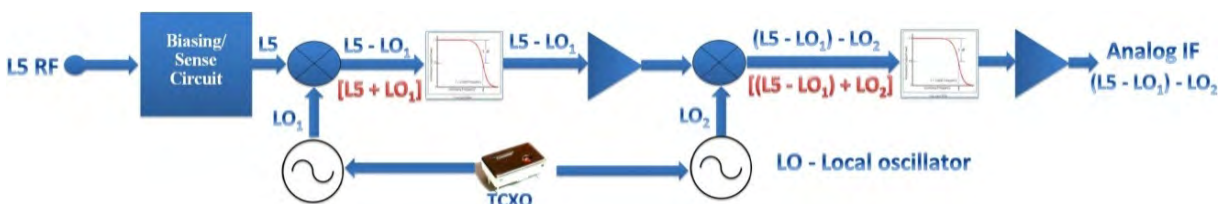


Figure 2-6: Block schematic of RF down conversion process to generate IF signal.

2.3 Receiver Operations – Baseband Processing Unit (BPU)

The main objective of the BPU is to synthesize the Analog IF and generate the user navigation solution. A high level block diagram of BPU depicting the various functions is shown in Figure 2-7 (open source data grouped and summarized based on the tasks necessary to estimate user position (thus TTFF) in a typical GNSS receiver).

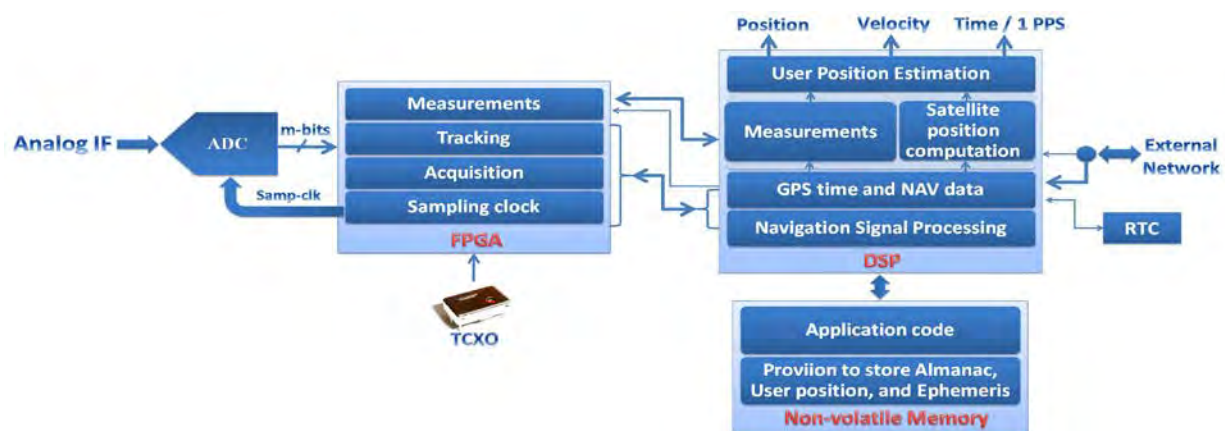


Figure 2-7: Block schematic of baseband processing unit from analog IF to receiver position computation.

The operations of BPU are closely linked between DSP and FPGA. The grouping of the tasks of BPU is based on the operations performed on the signal which are as follows: Architecture, Navigation Signal Processing, Navigation Data and System Time Formulation, Measurement Formulation and Corrections, Satellite State Vector Computation, User Position Estimation & 1PPS Generation and External Interface ((Parkinson & Spilker 1996), (Kaplan & Hegarty 2006), (Misra & Enge 2001)). To begin with, a brief explanation on the architecture is presented. Subsequently, other modules are elaborated with main emphasis on the signal flow leading to the position computation.

2.3.1 Architecture

The application code (program) of the FPGA and DSP resides in a non-volatile memory as shown in Figure 2-7. With power on, the program contents are transferred to DSP and FPGA (XILINX 2010). In addition, ephemeris, almanac, last estimated user position (from previous power-on) and Real Time Clock (RTC) (internal assistance), if available, are read by DSP (Martin-Yug 2009). These activities post power-on are termed as boot-phase and the time associated with them as boot-time of the receiver (Hein et al 2010). Following this, FPGA and DSP are in a state to communicate and exchange the information for effective baseband processing.

2.3.2 Navigation Signal Processing (NSP)

The main objective of NSP is to detect the presence of satellite signals and generate the NAV data bits for further processing (Kay 1998). Towards this, the module performs the following tasks: Sampling clock generation, Acquisition, Data-bit synchronization and Tracking (Shivaramaiah 2004).

2.3.2.1 Sampling clock generation

Based on the analog IF, appropriate sampling clock (f_s) satisfying the Nyquist rate (Haykin 2001) is generated by the FPGA, which is fed to the ADC. The source clock for FPGA is derived from the same TXCO (thus enabling the fourth measurement to map unambiguously to this common reference), which is used for RF down conversion process (Kaplan & Hegarty 2006). The digitized samples are read by FPGA for further processing. Based on the processing capabilities of FPGA (for example, memory slices) and application needs (for example, jamming) the numbers of digitized bits used are determined (Deshpande & Cannon 2004).

2.3.2.2 Acquisition

The signal at the output of ADC is given by (Borio 2008)

$$r[n] = \sum_{i=1}^L A_i C_i [n - \tau_{i,0}] d_i [n - \tau_{i,0}] \cos[2\pi F_{D,0}^i n + \phi_{i,0}] + \eta[n] \quad (2-4)$$

where, $\tau_{0,i}$ is the delay introduced by the communication channel

$$\tau_{0,i} = \tau_{i,0}^a / T_s . \quad (2-5)$$

$F_{D,0}^i$ is the Doppler frequency affecting the i^{th} satellite carrier signal and

$$F_{D,0}^i = (f_{IF} + f_{d,0}^i) T_s . \quad (2-6)$$

$\eta[n]$ is the sampled version of the noise.

The objective of the acquisition process is to extract and obtain the coarse estimate of the code phase (C_i) and Doppler (f_D) of a satellite. Based on the FPGA and DSP resources, the number of processing channels is deduced, whereby the detection process is performed in a dedicated manner (Pany 2011). If the number of channels available for processing (L) is less than M (for

example, a 12 channel GPS receiver with a 32 satellite constellation), the visible satellites are searched sequentially (assuming without any assistance), which increases the acquisition time. However, with the current Application Specific Integrated Circuits (ASIC) technologies, L , of the order of 216 channels, is easily handled concurrently, enabling processing of parallel channels (for example, across frequencies/GNSS systems (Triumph 2012)).

The acquisition is a two dimensional search process in code and Doppler. Typically, a matched filter or a correlator is employed for detecting the signals as shown in Figure 2-8 (Kay 1998). In a hardware correlator (realized in a FPGA / ASIC), any channel can be programmed with a Pseudo Random Number (PRN) of a satellite from a GNSS constellation (Shivaramaiah 2004). With a 10-bit C/A code as in GPS, search in code dimension occurs for all possible chip-shifts from 1 to 1023. The chip is programmed by DSP to FPGA. For each chip, the Doppler is generated in FPGA (f_D) employing a Numerically Controlled Oscillator (NCO) depending on the required search range which is a function of satellite, user dynamics and the local clock drift. The correlation values generated corresponding to each chip shift are integrated and processed to obtain precise code and Doppler information of a visible satellite. The acquisition is declared successful when the correlation value constantly exceeds a threshold (Eq. (2-2)), which is a function of noise variance (Borio 2008).

The estimation of the noise variance is the first task performed post booting. To determine this, a code (not used as a part of M satellites of a GNSS constellation) from the same family of (C_i) is programmed in one of the acquisition correlator channel. The correlation values for the entire chip shifts are obtained to estimate the variance which is given by (Borio & Lachapelle 2009).

$$\sigma_n^2 = \frac{1}{2N} \sum_{i=0}^{N-1} I^2 + Q^2$$

(2-7)

where I and Q are in-phase and quadrature correlator outputs (Figure 2-8) corresponding to a sample and N is the code length.

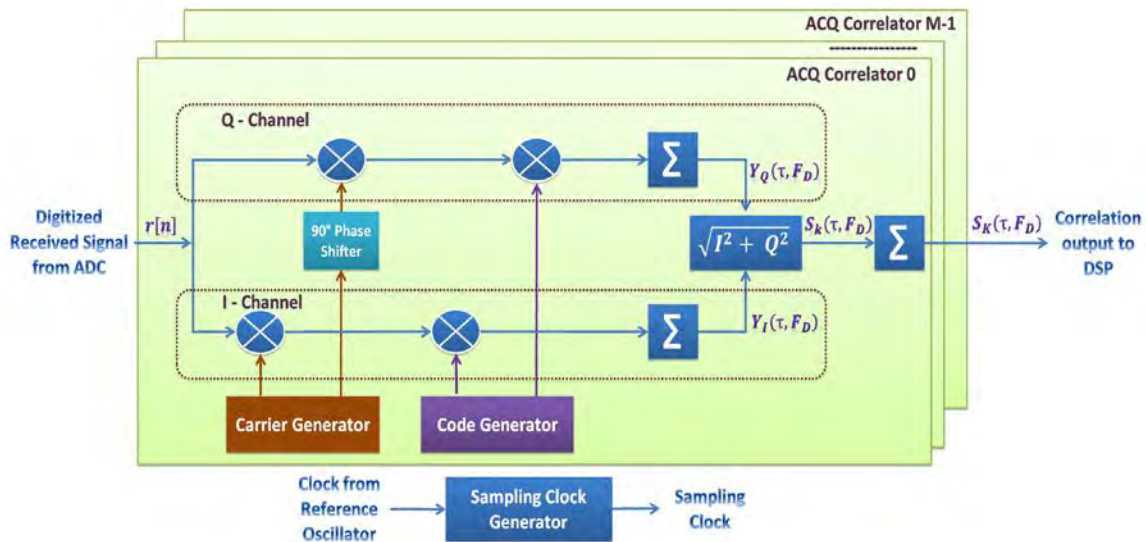


Figure 2-8: Acquisition correlator.

The fictitious code ensures that the output of correlator are zero mean and Gaussian. Following the noise floor computation on each acquisition channel, a distinct PRN is programmed and searched for all possible chip shifts. The correlation values are integrated for a suitable duration in DSP (based on sensitivity requirements) to enhance the achievable Signal to Noise Ratio (SNR) and thereby improve the probability of detection (Borio 2010). On the resulting samples, typically a Fast Fourier Transform (FFT) operation is performed to detect the presence of a signal (Lyons 2004). With the signal, a distinct peak is observed at the output of the FFT. The FFT bin corresponding to this peak provides the coarse estimate of Doppler for the chip shift programmed in FPGA. With this, DSP confirms signal acquisition.

The following points arising from the acquisition process are worth mentioning: The NAV data is eliminated during the squaring operation (Eq. (2-7)) as shown in Figure 2-8. Integration of these samples is generally termed as non-coherent (Borio 2008), which ensures f_D is filtered and processed to obtain the Doppler. This phenomenon is known as Carrier Wipe off. The signal is however buried in noise. With correlation (specific code), the processing gain achieved alleviates the signal above noise (Eq. (2-2)) and removes the modulated code. This process is known as Code Wipe off (Kaplan & Hegarty 2006).

The next step is the identification of the data bit boundary, which is performed as shown in Figure 2-9. The correlation values (Eq. (2-7)) obtained are grouped into sets. Each set is an integration of 20 consecutive correlator (1 ms) outputs and stored as a moving window as shown in Figure 2-9. Twenty such sets are generated and profiled for the maximum value, which correspond to that set integrated for the complete data bit duration.

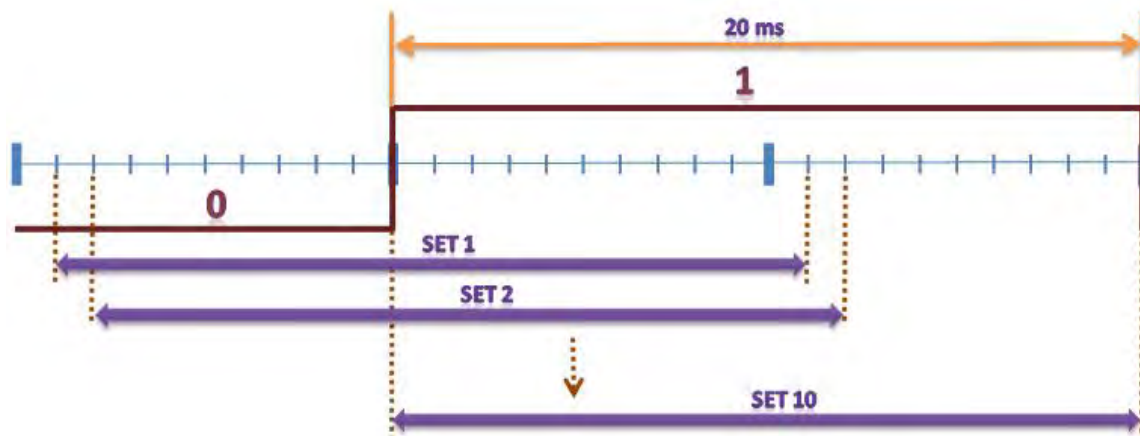


Figure 2-9: Bit synchronization scheme depicting the construction of moving correlation sets for estimating the bit boundaries.

With this as a reference, the bit-synchronization is declared by DSP. This process assumes a bit transition in the recent 20 sets of integrated data.

2.3.2.3 Tracking

Following acquisition, the next step is to track the signal finely, sustain and demodulate the data. The acquisition estimates (post bit synchronization) are taken as a reference, programmed to the carrier and code generators in the tracking arm of the correlator in FPGA, as shown in Figure 2-10.

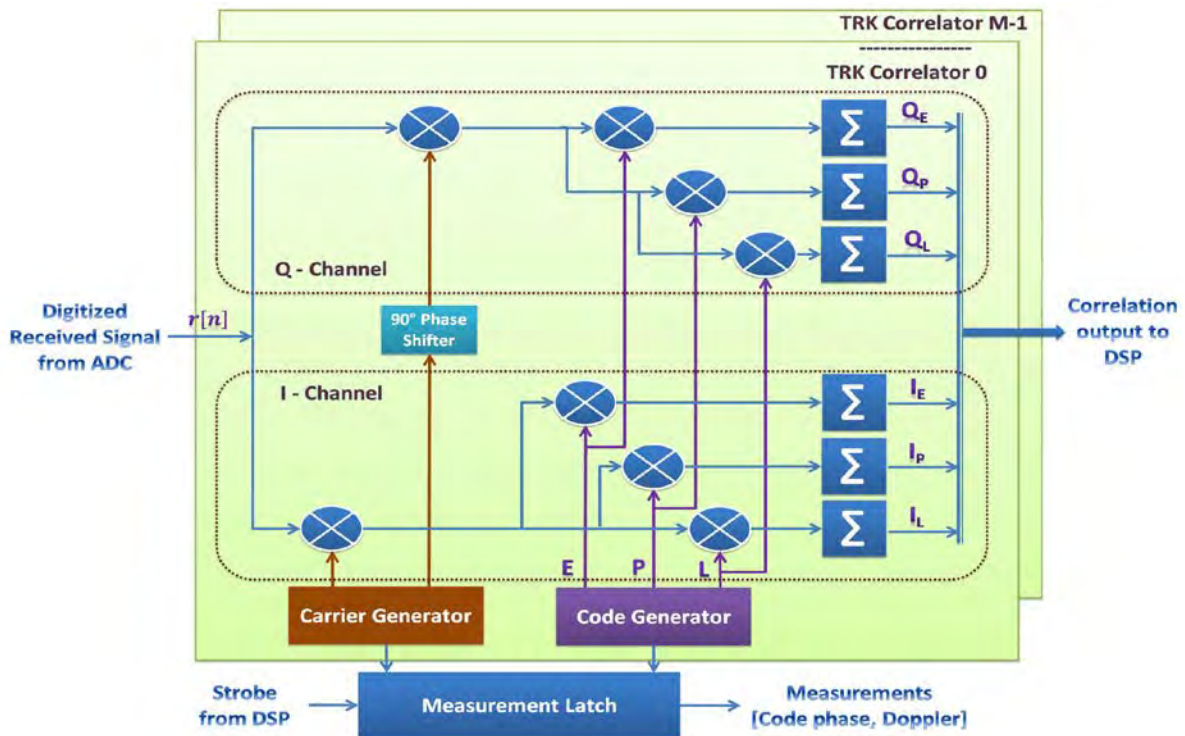


Figure 2-10: Tracking correlator and measurement generator.

The initial part of the tracking is similar to acquisition, where the carrier-wipe off occurs. The carrier stripped signal is correlated with local versions of code - early, prompt, and late (Kaplan & Hegarty 2006). Typically, the early and late are separated by a phase of one chip and the phase separation between prompt and early/late is a half chip period. A code generator and an NCO are used to generate the PRN code and Doppler respectively. Subsequently, a shift register is used to generate the shifted version of all three codes. The integrated in-phase and the quadrature

correlation samples corresponding to early, late and prompt are output to DSP for further processing, typically at 1 ms (Shivaramaiah 2004).

The samples read by the DSP perform (typically) the following functions:

- First, the correlation values for each tracking arm are processed periodically and integrated. In addition, the estimate of bit boundaries is maintained.
- Second, at bit boundaries, Delay Lock Loop (DLL) and Carrier Lock Loop (CLL) (Phase or Frequency Lock Loop (PLL / FLL)) are invoked to ensure continuous track in code and Doppler domain. The loop order and bandwidth are selected based on the input signal dynamics {for example, to accommodate signal variations due to velocity, acceleration and jerk of (user + satellite)} (Parkinson & Spilker 1996).
- Third, the discriminators outputs generated in DLL and CLL are fed back to FPGA as corrections to track the dynamics of the incoming signal.
- Fourth, coherent integration (correlation values integrated for NAV data bit duration) ensures optimal noise rejection and accumulated (typically one second) values of these samples generate the Carrier to Noise (C/No) estimate of a particular channel (Borio 2010).
- Finally, the estimates (code and Doppler) of channels for reacquisition (temporary signal blockage) are maintained for each tracked channel. With these estimates, the code and Doppler are programmed and the signal is reacquired immediately.

2.3.3 Navigation Data and System Time Formulation (NDSTF)

The data bits generated from the tracking process are grouped based on the ICD of the GNSS system. Having assumed GPS like data on IRNSS, the L1 C/A NAV data of GPS is presented to emphasize the formulation of the system time. The NAV data is grouped into five sets referred as

sub-frames as shown in Figure 2-11. The first three subframes constitute of ephemeris data and the last two are dedicated to the almanac (secondary data).

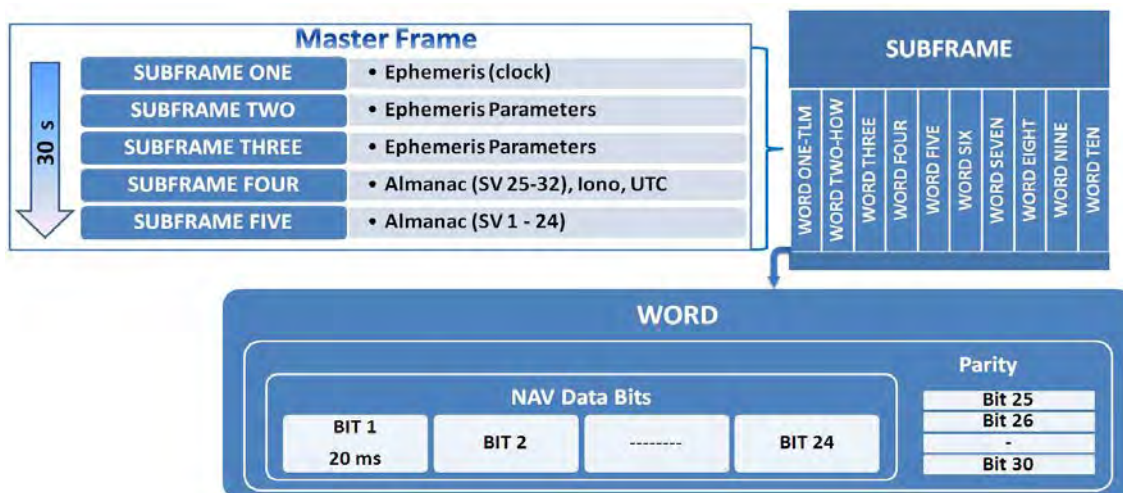


Figure 2-11: GPS L1 C/A NAV data structure depicting frames, words, bit and their duration.

As a part of the ephemeris, clock corrections and Keplerian parameters corresponding to the satellite orbit are transmitted. The almanac page contains the coarse Keplerian parameters, UTC and Ionosphere correction terms. Each subframe consists of 300 NAV data bits, grouped in 10-30 bit words. Each word has 24 NAV data and 6 parity bits, respectively. With a data-rate of 50 Hz, each subframe takes 6 s, which translates to 30 s to collect all the five subframes (IS-GPS-200E 2010).

With the data bits grouped as 300 bits, subframe synchronization (which ensures data of a frame is available), is attempted. This is performed based on some standard checks (IS-GPS-200E 2010) on all the tracking and bit-synched channels. With continuous lock for 36 s (worst case when the bit-synch occurs on the second word of a subframe and the data up to the start of the next subframe is discarded), the entire master frame information is available and thus the NAV data is formulated (Rao et al 2011).

The system time is typically computed only once for a power-on in a receiver and further incremented periodically. Post subframe synchronization of the first bit-synched channel (typically), the Hand Over Word (HOW), which is a part of the NAV data containing the system time, is extracted. The system time (of the constellation) corresponds to the first bit of the next subframe. To this, the time commensurate to bits collected post subframe synchronization within the receiver is added to generate the channel time (specifically maintained for each channel/satellite). The IRNSS satellites are in geosynchronous orbit at 36000 km altitude. The time corresponding to this range added (typically) to the channel time of the first tracked and subframe synched satellite (for example, in a scenario as depicted in Figure 2-12), provides the system time at receiver (Misra & Enge 2001) and is given by,

$$SystemTime_{@Rx} = \{[Time\ in\ HOW] + (32 * 20) + 120\ ms\} \quad (2-8)$$

Figure 2-12 shows a clear illustration of system time formulation in a receiver.

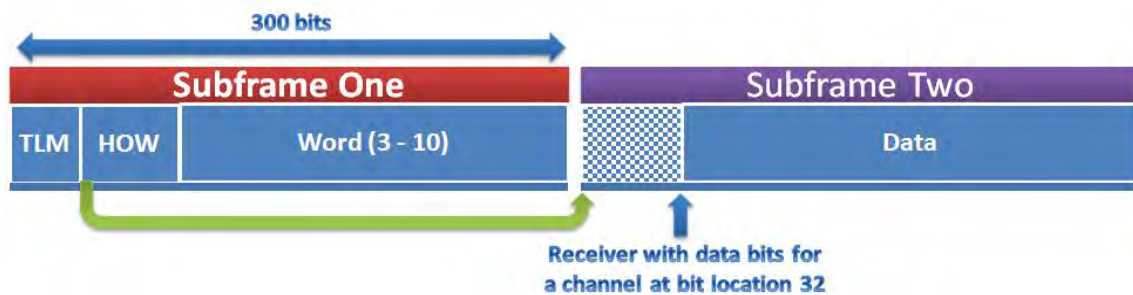


Figure 2-12: IRNSS system time formulation based on the HOW word and bits collected in the receiver.

2.3.4 Measurement Formulation and Corrections (MFC)

The next task is to estimate the measurements of each tracked satellite in the code and Doppler dimension. The code measurement results in a pseudorange and the Doppler in a deltarange. The pseudorange is estimated as follows: the channel time estimated periodically for each subframe

synched channel provides a measurement at the milli-second level. To achieve synchronization across channels, the measurements are all latched (strobe) at a common reference and the corresponding system time (SolutionTime) is noted as well (Vijaykumar & Rao 2007). Corresponding to this, for all tracked channels, the code-generator values in the measurement block (Figure 2-10) of FPGA is latched (specifically code phase) and added to the channel time, which results in measurement up to nano-second for a channel. Subsequently, the pseudorange for a channel is estimated as

$$Pseudorange = [SolutionTime - ChannelTime] * C \quad (2-9)$$

The Doppler corresponding to strobe instant from the carrier generator results in a deltarange given by (Misra & Enge 2001)

$$Deltarange = Doppler * \left[\frac{C}{L5} \right] \quad (2-10)$$

The pseudorange is formulated on the signal which has traversed through the Ionosphere and Troposphere. This introduces different delay for each satellite, which needs to be estimated and corrected. For a single frequency user, as a part of the NAV data, the model terms for Ionosphere are transmitted (IS-GPS-200E 2010). In addition, there exist several models such as Saastamoinen, Black, EGNOS, etc, for Troposphere (Parkinson & Spilker 1996). Post application of the delay estimated by the above mentioned models, the corrected pseudoranges are used for position estimation (Vimala et al 2000). In addition, Differential GNSS (DGNSS) networks transmit pseudorange corrections as a lumped parameter, region wise (Ray & Kalligudd 2001). These corrections, if available, are applied to measurements resulting in relatively accurate position solution.

2.3.5 *Satellite State Vector Computation (SSVC)*

Satellite positions and velocities for each tracked channel are estimated using ephemeris data. Following standard equations (IS-GPS-200E 2010), the satellite position is computed for the time (accounting the transit delay) given by (Kaplan & Hegarty 2006),

$$t = \{[SolutionTime] - [Pseudorange]\} \quad (2-11)$$

Similarly, the satellite velocity is estimated as (Rao et al 2006)

$$Satvel(t) = SatPos(t + 0.5) - SatPos(t - 0.5) \quad (2-12)$$

2.3.6 *User Position Estimation (UPE) and 1 PPS generation*

Based on the measurements and satellite state vectors, the user position solution is estimated using either a Least squares or Kalman filter technique (Petovello 2010). The highlights of the user solution are as follows:

- The position solution results in a clock bias (C_b) estimation, which arises due to the initial offset and assumed range uncertainty across satellites (for example, 120 ms). This estimate, applied to the system time, results in an accurate time estimate available within the receiver synchronous to satellites (Lachapelle 2010) commensurate with the *solution time*.
- The measurements are performed based on TCXO, with relatively inferior drift characteristics compared to the onboard satellite clock. To ensure that the system time is maintained with that of the satellites, the clock drift (C_d) obtained as a part of receiver velocity estimation is applied to the system time periodically (Kaplan & Hegarty 2006) and is given as

$$SystemTime = SystemTime_{@Rx} + C_b + C_d \quad (2-13)$$

For timing applications, receiver outputs 1 Pulse Per Second (PPS), which are a train of pulses accurate w.r.t to system time (2-13). To achieve this within a receiver, a high resolution counter in FPGA is initialized to generate a pulse every second corresponding to the second boundary of the system time.

2.3.7 External Interface

Finally, as part of the receiver hardware interface, peripherals such as RS232, Universal Synchronous Bus (USB) etc. exists to communicate the internal data to the user. In addition, data from the external world such as Differential GNSS correction (DGNSS) or AGPS assistance is sourced through this port (for example, (CSR 2011)). A summary of the signal flow within a receiver is shown in Figure 2-13.

Having established the receiver operations and addressed the performance characteristics commensurate with the datasheet (Figure 2-1), the following section highlights specific receiver categories (GNSS) and associated technologies.

2.4 GNSS receiver categorization

Receivers are generally grouped based on the application they cater to, which in turn determines certain specifications. Based on the requirement, the architecture is suitably customized at various stages of the receiver. At the top-level, receivers are categorized as: Sensitivity, Accuracy, Reliability, Dynamics and TTFF. The following sections detail the top-level architectural changes necessary to meet the specific user requirement.

2.4.1 Sensitivity

High sensitivity receivers are typically used indoors where the signals are severely attenuated and impair the detection process. In such scenarios, obtaining position is more important than accuracy. To maximise the signal detection probability, the SNR needs to be improved

drastically (Kay 1998). This is accomplished by increasing signal integration duration which is bounded by the data bit period. To extend it further, the data is either predicted or obtained externally. By this process, sensitivities of the order of -163 dBm have been demonstrated (Satyanarayana et al 2011).

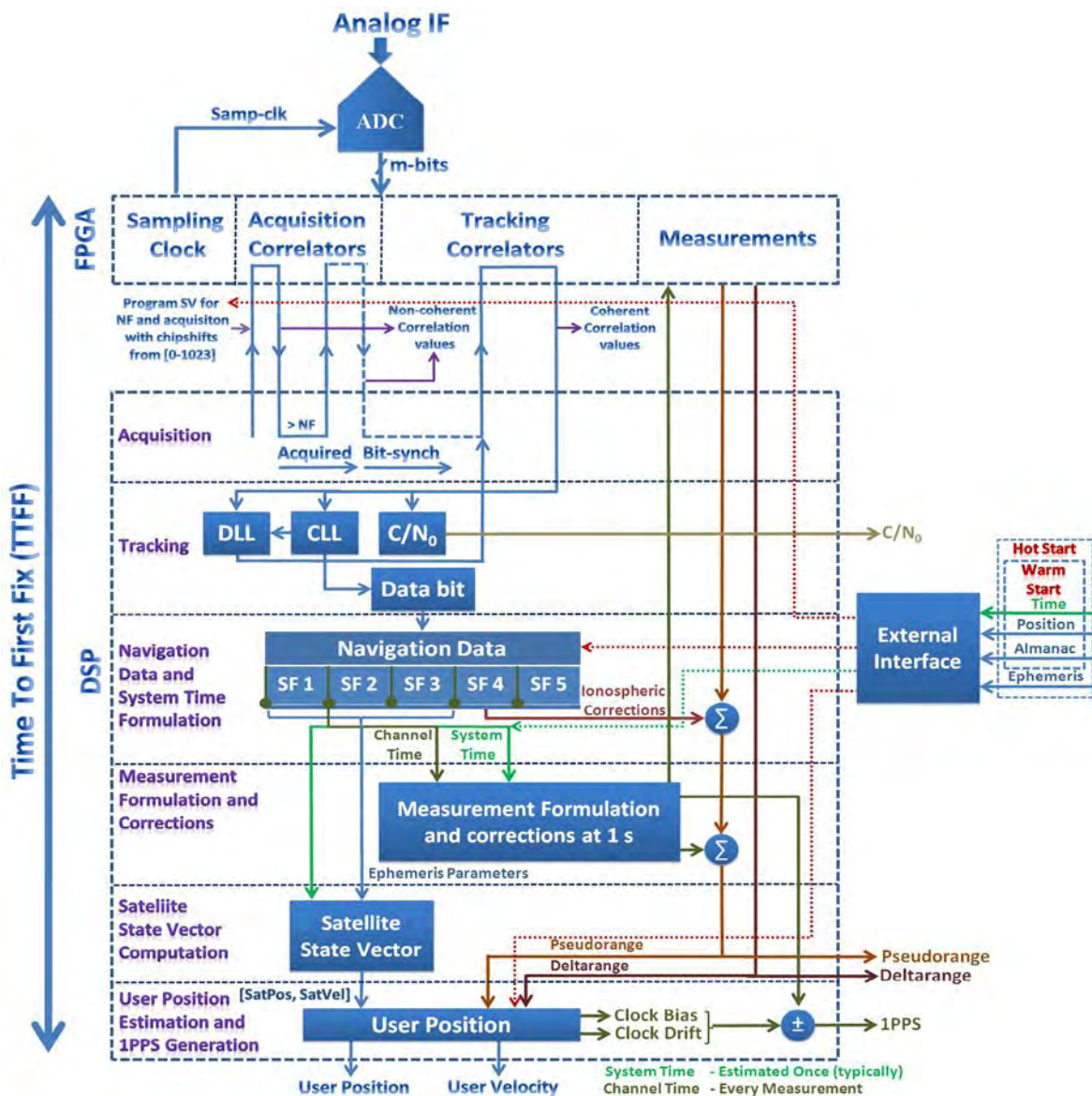


Figure 2-13: Summary of signal flow within a receiver from IF to position computation encompassing all functional components.

To achieve this feature, the algorithms in DSP are modified. In addition, through the interface unit, data assistance from the external world is received. Further, to improve upon acquisition time, massive correlator architectures are employed (Van Diggelen 2009) in FPGA.

2.4.2 Accuracy

Survey grade and Reference station receivers fall under the category of high accuracy receivers. The main objective of this class of receivers is to generate high accuracy measurements and navigation solutions. The receivers are exposed to open sky conditions and generally located with relatively minimal multipath and interference conditions. In addition, the antennas are placed at survey locations (Gerein et al 2007).

To accomplish the above mentioned requirements, the BPU is modified both in FPGA and DSP. The accuracies of the measurements from the FPGA need be an order of magnitude higher than those of a general receiver (for example, receivers used in automobile applications). Typically, this is accomplished using technologies such as Narrow Correlator (Fontana et al 2001). Further, to minimize multipath, advanced multipath mitigation schemes are employed in DSP (Ray et al 2000). In addition, Signal Quality Monitoring (SQM) is performed on the received signal in DSP to provide anomaly alarms in the received signal, if any (Jakab 2001). With these augmentations, the measurements are generated from the SPMG unit.

2.4.3 Reliability

Though this requirement is necessary for all user equipment, the need for high reliability is critical in aviation grade receivers. Such receivers demand that the outputs be highly reliable (Ray et al 2006). In addition, the aviation grade receivers necessarily need to apply the SBAS (for example, the integrity and correction information) as a part of its measurements (Nayak & Ray 2008). Further, this class of receivers must employ Receiver Autonomous Integrity

Monitoring (RAIM), which performs Fault (in measurements) Detection and Exclusion (FDE). This is integrated with the navigation solution algorithm in DSP. Based on statistical properties of the measurements, this algorithm ensures that the user receives integrated position solution always (Ray & Nayak 2008).

2.4.4 Dynamics

For most restricted and space applications, the receivers typically experience signal dynamics of the order of ± 8 km/s, 25 g, 10 g/s velocity, acceleration and jerk respectively. In addition, the vehicle on which the receiver is mounted may experience severe attitude maneuvers (Kopp 1996).

To meet such challenging environments, signal search range is extended to accommodate relatively high Doppler of ± 50 KHz with higher order tracking loops (for example, third order FLL) (Bao & Tsui 2004). Further, such receivers support multiple RF front-ends to source the data from several antennas and process the data independently (Rao et al 2006). This necessitates multiple ASPs as a part of the receiver and is processed by a single SPMG.

2.4.5 TTFF

A GNSS user whose primary objective is to obtain the navigation solution would require it immediately from power-on. The need for fast TTFF is a major specification of handheld and restricted applications.

To accomplish this requirement, augmentations both in FPGA and DSP are carried out. TTFF of the order of 2-3 s is achieved with data assistance from external network through the interface unit (Fastraxgps 2012). Figure 2-14 summarizes various receiver categories. The following section explains in detail the various methods practised in industry to enhance TTFF in assistance mode of receiver operation.

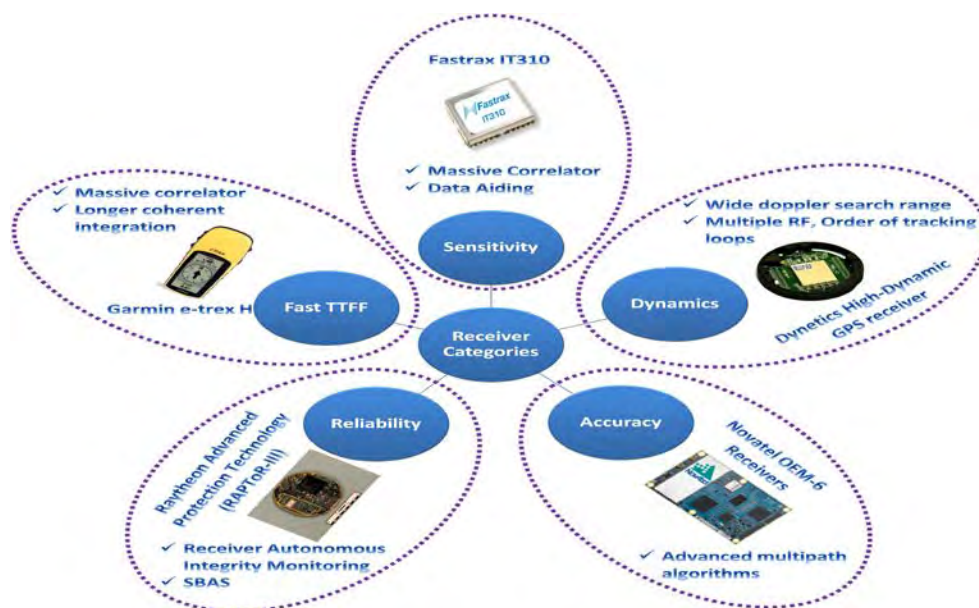


Figure 2-14: Summary of receiver categories highlighting the specific features necessary for each segment.

2.5 Fast TTF – without external assistance

As mentioned in the previous sections position computation involves receiver acquiring signals from a minimum of four satellites, establish bit synchronization, generate measurements and demodulate NAV data. The time associated to accomplish these tasks effectively determines TTF. Further, based on the inputs available at power-on, a receiver is categorized into four different modes - Cold, Warm, Hot and Snap. The following paragraph explains each mode of receiver operation and its achievable TTF.

2.5.1 Cold Start

In this mode of operation, a receiver has no prior inputs (assistance) available (for example, receiver powered-on for the first time and thus no data in its non-volatile memory. Alternatively, no link to external network either). With power-on, the receiver needs to search for satellites available. Subsequently, the system time estimation, measurements to four satellites and NAV

data collection are performed. For GPS L1, this process typically takes 34 to 36 s assuming the initial search is based on fast signal acquisition techniques (Van Diggelen 2009).

2.5.2 Warm start

Receivers in this mode have access to satellites' almanac, approximate user position and time as shown in Figure 2-15. They are either supplied externally or maintained internally in the receiver. In the internal configuration case, the time at the last power cycle is maintained and estimated typically in RTC. Similarly, user position and almanac are maintained in non-volatile memory.

The advantages of these parameters are twofold: First, the receiver will be able to compute the list of visible satellites and restrict the signal detection to those fewer satellites that are above the horizon (for example, visible L GPS satellites out of possible 32). Second, with the almanac and time (RTC), the receiver will be able to compute approximate satellite position; with such an approximate user position, the geometric range can be established. With time and range, the approximate code phase is determined, which reduces the search range from $[1 \ 1023]$ to $\pm n$ chips (for example, from 1-1023 reduces to ± 25 chips depending on the accuracy of time, user position and age of almanac). From satellite positions, velocities and in turn the Doppler are established (Eq. (2-10) and Eq. (2-12)). This ensures the search range of ± 5 KHz effectively drop to around ± 125 Hz (typically, one bin of FFT) (Van Diggelen 2009).

This results in a reduced search range in the code and Doppler domain, which enhances acquisition time. Subsequently, the remaining operations leading to TTFF is similar to cold start mode and takes 32 s.

2.5.3 Hot Start

In addition to the warm start estimates, with a valid ephemeris (for example, in GPS L1, the ephemeris is valid for 4 hours from upload time) at power-on, TTFF reduces to 6-8 s and this mode of operation is termed as Hot start (Kaplan & Hegarty 2006). With ephemeris, the only parameter that needs to be established is the system time. Typically, this mode is adopted in most automotive grade receivers.

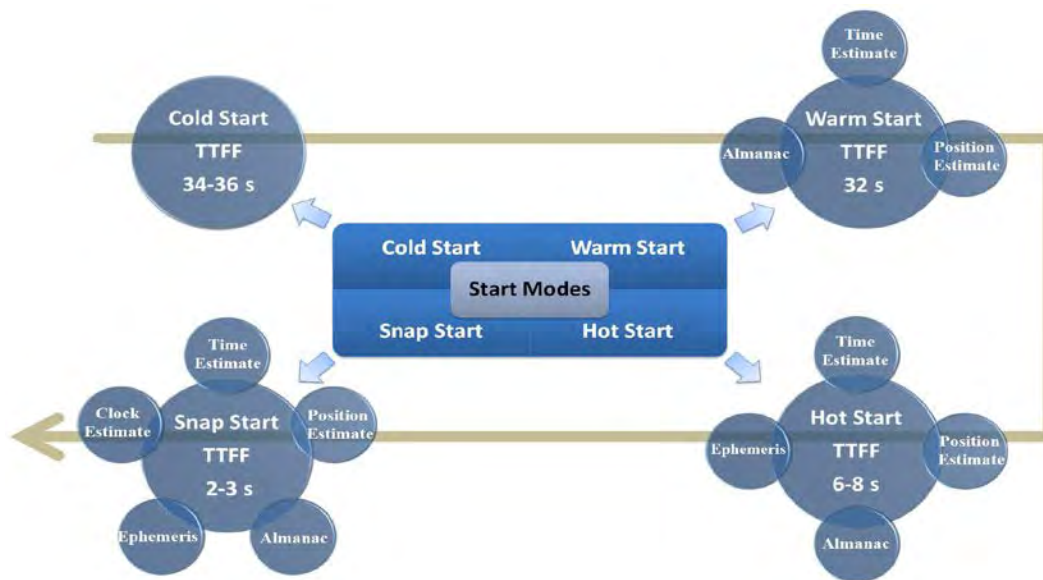


Figure 2-15: Receiver start modes with the available estimates at power-on and their achievable TTFF.

2.5.4 Snap Start

The last mode of receiver operation is the Snap start where, in addition to hot start parameters, the receiver clock is also estimated internally. The advantage with this approach is further reduction of system time estimation. With bit synchronization established on four satellites, TTFF is achieved instantaneously. This mode assumes that the receiver was powered on recently (Van Diggelen 2009).

2.6 Fast TTFF - Assisted GPS (AGPS)

The various start modes assumed receivers have the necessary information stored as a part of its internal memory or assisted from external network, the former being receiver specific, the latter being addressed by AGPS. AGPS works on the principle of client server architecture (with its server time referenced to GPS), with the receiver (handset) operated as client. Based on the levels of service offered, AGPS can be categorized as: Ephemeris Assistance, Absolute, Measurement Engine and Extended Ephemeris (Assisted GPS 2010). The following section briefly touches upon these options.

2.6.1 Ephemeris assistance

This method of AGPS assistance is similar to the hot start mode of operation. With a link to the server, the receiver will be able to obtain approximate position (for example, within a cell of the network), time and latest ephemeris. Subsequently, the receiver operations are similar to hot start with an achieved TTFF of the order of 6-8 s.

2.6.2 Absolute mode

This mode assumes the receiver to have a constant link with the server, synchronize to the network (enabling precise time transfer) and thus be able to predict the code and the Doppler search ranges precisely. This is similar to the Snap start mode of receiver, which is able to provide the TTFF in 2-3 s. However, the load on the server is higher in comparison with the ephemeris assistance mode (Van Diggelen 2009).

2.6.3 Measurement engine

A major hardware challenge for handheld devices is power consumption. In order to minimize this, AGPS supports a measurement only mode of operation in the receiver. The receiver only needs to obtain the measurements (pseudoranges and delta-pseudoranges) and transmit them to

the server, which calculates the navigation solution. The power consumption, although optimized (reduced processing), puts a large computational burden on the server. The TTFF achievable is similar to that for the absolute mode of operation with the position computed at the server.

2.6.4 Extended ephemeris

An inherent limitation in the above methods is the ephemeris data, which is updated periodically with the handset. To minimize this, extended ephemeris in the AGPS mode of operation is supported. The required data to propagate ephemeris is communicated onto the receiver. Using this data and its corresponding algorithm (CSR 2011), satellite positions are estimated and used directly in navigation solution. With this, the receiver is able to achieve a TTFF similar to that in ephemeris assistance mode (with time alone estimated from satellite). The advantage is that the transaction with the network is greatly reduced (for example, extended ephemeris parameters obtained once can be used to estimate satellite positions for 7-14 days). However, the drawback with this method is accuracy decrease with the age of the extended ephemeris parameters.

2.7 TTFF characterisation

With the details of receiver start modes, the next step is to experimentally understand the TTFF from power-on and quantify various parameters underlying it. Towards this, the experimental setup shown in Figure 2-16 is employed (Rao et al 2011).

2.7.1 Test apparatus

The apparatus consisted of a GPS-GLONASS receiver from Accord Software & Systems Pvt Ltd, which was used as a platform to profile various receiver parameters. The receiver supports 32 GPS and 14 GLONASS channels. In addition, it supports three RF front-ends separately. This receiver along with a graphical user interface (GGVISION) is used as a tool to profile the status of various channels and has a provision to log the data. This platform is used as a reference on

which the developed receiver software is tested in this thesis. The receiver does not have the provision of storing or estimating any parameters from previous power-on or hardware to support external data. Specifically, the receiver operates in cold start mode of operation. The explanation presented is for GPS, which is equally applicable to GLONASS.

2.7.2 Procedure

The receiver's one RF port (two others terminated) was connected to a GPS GLONASS antenna, placed in a surveyed location under open sky. A Digital Storage Oscilloscope (DSO) is connected to the boot-pin of the Digital Signal Processor (DSP) to profile the application boot time (post power on) as shown in Figure 2-16. The communication latency is the time required to transact the parameters to the console. This is based on the baud-rate at which the receiver (configured) outputs the data (Figure 2-17). Once configured, latency remains the same for each data transacted with the console. With power-on, the boot-time with this receiver was around 240 ms.

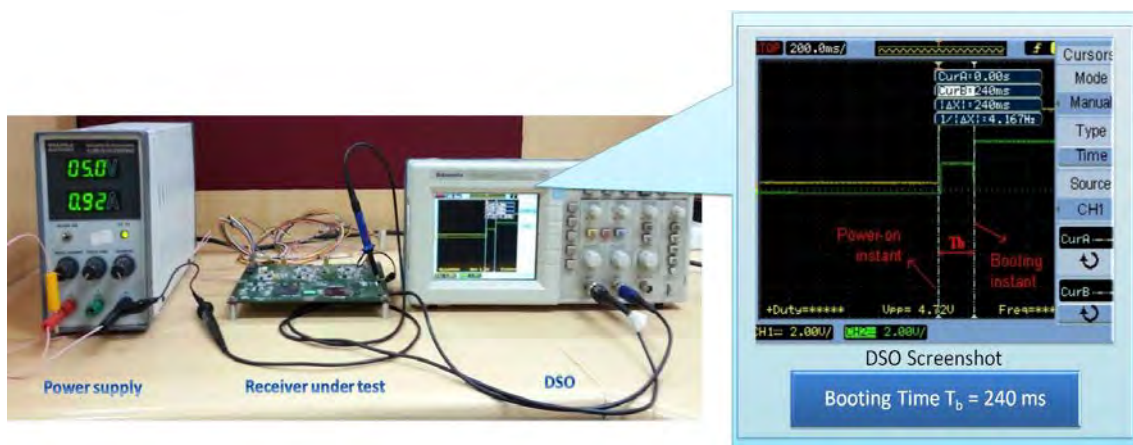


Figure 2-16: TTFF characterization test apparatus highlighting the boot-time captured on DSO.

Generalizing this component, let,

T_b be the time taken to boot the receiver application (2-14)

Subsequent to booting, the receiver is programmed with 32 GPS and 14 GLONASS satellites to respective channels for further processing. The satellites visible at the receiver antenna take between 2 to 8 s for signal acquisition (non-massive correlator architecture). Generalizing this component, let

T_a be the time taken to acquire the visible satellites (2-15)

Subsequent to acquisition, each channel took a finite time for bit-synchronization. This was around 800 ms. Generalizing this component, let

T_{bs} be the time required for bit-synchronization (2-16)

The next activity on each of the bit-synched channel is the collection of NAV data, specifically the ephemeris. This took anywhere between 18 and 30 s for GPS. Let,

T_{eph} be the time required to collect ephemeris. (2-17)

Finally, from the NAV data extracted and the measurements formulated (on a minimum of four satellites), the user position was computed. Using Eq. (2-14) through Eq. (2-17), the TTFF for any LOS receiver is given by

$$TTFF = T_b + T_a + T_{bs} + T_{eph}. \quad (2-18)$$

Subsequently, for each tracked channel, the almanac is collected, which took 12.5 minutes from the instant of the first tracked channel. Generalizing this component, let

T_{alm} be the time taken to collect almanac (2-19)

Following the almanac collection, the receiver applies the ionosphere correction to the pseudoranges to improve accuracy. Accounting for this correction, the overall time required to output position with the ionosphere correction is given by

$$T_{posc} = T_b + T_a + T_{bs} + T_{eph} + T_{alm} \quad (2-20)$$

Based on 50 trials, the above timing components are profiled and tabulated in Table 2-1. Figure 2-18 summarizes the various timing components of a generic receiver.

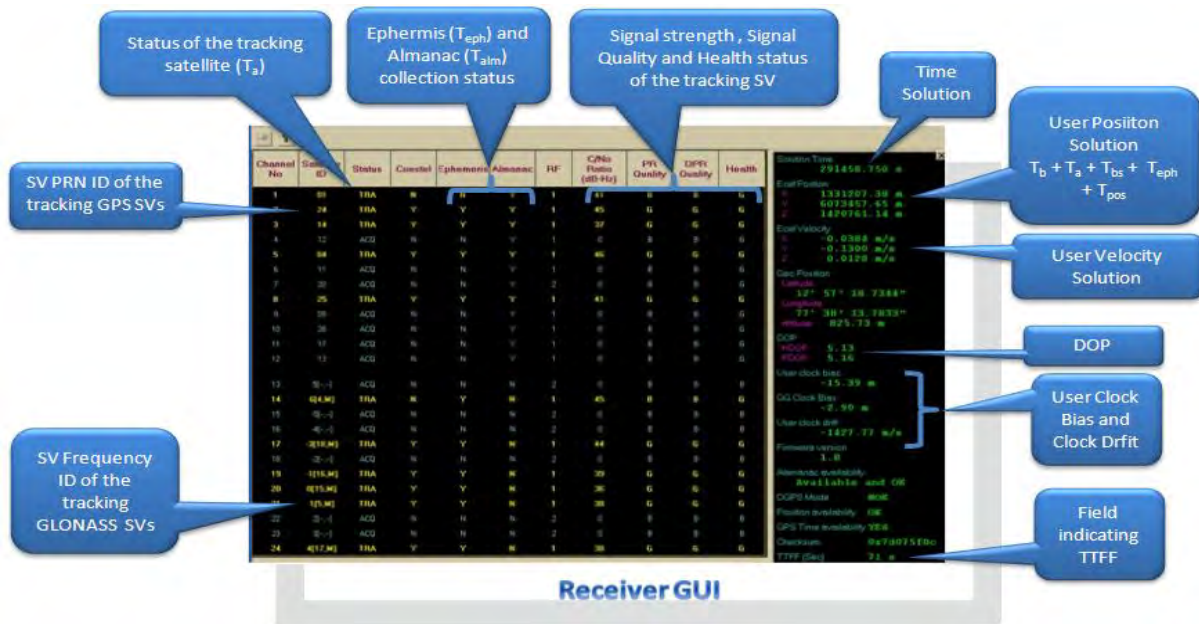


Figure 2-17: GUI illustrating the status of the receiver health and depicting various receiver components leading to TTFF.

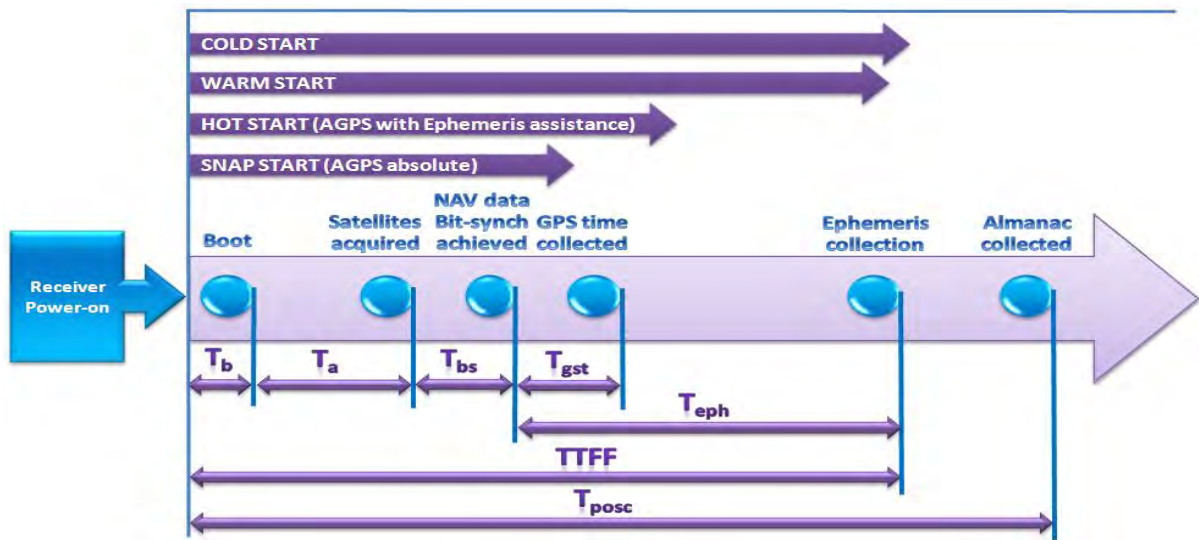


Figure 2-18: TTFF characterisation timing diagram capturing receiver’s underlying time components and parallel drawn with AGPS mode of operation.

2.7.3 Analysis

For an IRNSS user in the Indian subcontinent, the satellites would always be visible. Extending the results of the previous section and assuming a user receiver with massive correlator architecture, acquisition and bit synchronization of the signal occurs approximately in 1 - 2 s ($T_a + T_{bs}$) for all the channels. It is evident from Table 2-1 that the major component underlying the TTFF for an open sky user is T_{eph} which needs to be reduced to achieve fast TTFF, which is the scope of this research (Rao et al 2011). Since T_{eph} dictates the TTFF, throughout this research T_{eph} and TTFF are used interchangeably.

Table 2-1: Distribution of receiver components leading to TTFF.

Parameter	Description [s]	Time taken (%)
T_b	Booting time [0.250]	1
T_a	Acquisition time [1.5]*	4.5
T_{bs}	Time for Bit-synch [0.5]	1.5
T_{eph}	Ephemeris collection time [30]	93

* Assuming fast acquisition techniques

2.8 Need for fast TTFF in critical applications

The start modes and AGPS provide means of achieving a fast TTFF with the assumption of the receiver having the necessary data within or sourced from an external network respectively. Figure 1-1 showed an example for civilian usage where the above assumptions may not be necessarily valid.

Extending this, an attempt is made to establish the need for fast TTFF in critical applications, which is based on restricted signals supported on both L1 and L2 of GPS and GLONASS. Not much literature is available in open source w.r.t to ICD of these signals. In addition, there is no documentary evidence describing the sequence of operation or assumptions with which a restricted signal receiver operates from power-on leading to TTFF.

The datasheets of receiver manufacturers supporting restricted signals are the sole means to access related TTFF performance. In addition, receivers which support restricted and civil signals have the TTFF listed in datasheets as a single number rather than an independent listing (for example, civilian/military single/dual frequency) (CommSync II 2010). Assuming this number represents the best achievable TTFF for All In View (AIV) architecture, restricted signal cold starts are at most comparable to civilian ones. In addition, restricted receivers support dual frequency of operation (P(Y) is available on GPS L1 and L2). The following section describes two examples from *open source highlighting the TTFF assuming a cold start mode of operation*. The various events assumed in the examples are only from an analysis and illustration perspective and not specific to any particular application.

2.8.1 Example 1: Underwater launch

The Figure 2-19 illustrates an example of a possible use of a GNSS receiver in a critical application (Launching in Underwater 2012). The theoretical analysis performed assumes the overall duration of the mission to be 200 s. With lift off, the vehicle requires finite time to emerge from the submarine and reach the water surface; this time is assumed to be 15 s. During this phase, signal acquisition is not possible due to severe attenuation and multipath (Veggeberg 2010). Further, assistance from another receiver in the submarine is not possible either. Subsequently, the vehicle is exposed to open sky. Receiver dependence on an external network is not practical for this application. Hence, the TTFF achieved in the absolute cold start mode of receiver operation results in a position within 32 – 36 s (from receiver datasheets supporting restricted signals in cold start mode). With a mission time of 200 s, significant portion (25%) of the application is without GNSS.

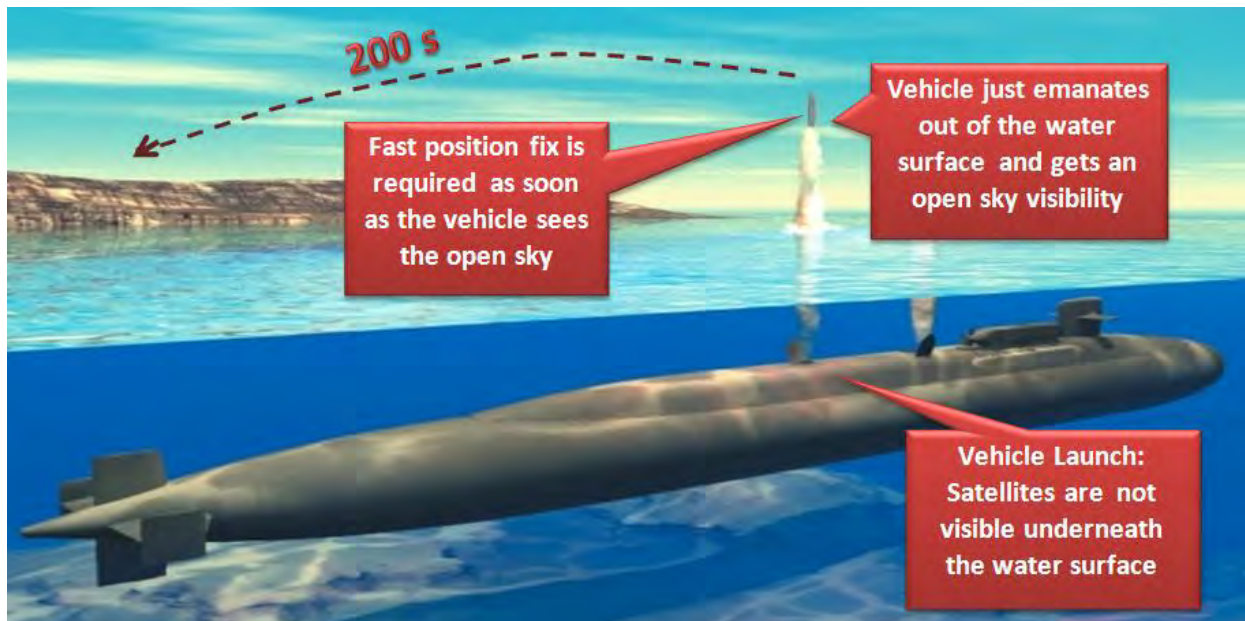


Figure 2-19: GNSS receiver onboard a vehicle launched from a submarine with touch down timing from surface of water.

Typically, such applications have system level navigation outputs derived from GNSS and Inertial Navigation system (INS) with appropriate filtering techniques (Licata 2000). Initially with the absence of GNSS, navigation is solely based on INS, which accumulates error over time. This translates to relatively inferior navigation accuracies. With a navigation solution from GNSS, the filter takes a finite time for convergence (due to error build up in INS), which further delays the system level (GNSS+INS) solution (Salychev et al 2000). Figure 2-20 provides the detailed timing diagram corresponding to this application emphasizing the duration of the GNSS absence w.r.t mission time.

2.8.2 Example 2: Aircraft launch

The second example analysed is the application shown in Figure 2-21 where the vehicle is released from underneath an aircraft (Predator Drone 2012). Assuming mission duration of 50 s, obtaining position from GNSS is a tough proposition with the cold start mode of receiver

operation. Typically, such applications can obtain assistance from an onboard GNSS receiver (Kopp 1996). With this assistance, the receiver enters into the hot start mode of operation with a TTFF available within 6 – 8 s from release. However, in cases where this assistance is not practical, the application may have to depend only on INS for navigation (for example, cold start TTFF comparable to mission time), resulting in relatively degraded accuracies.

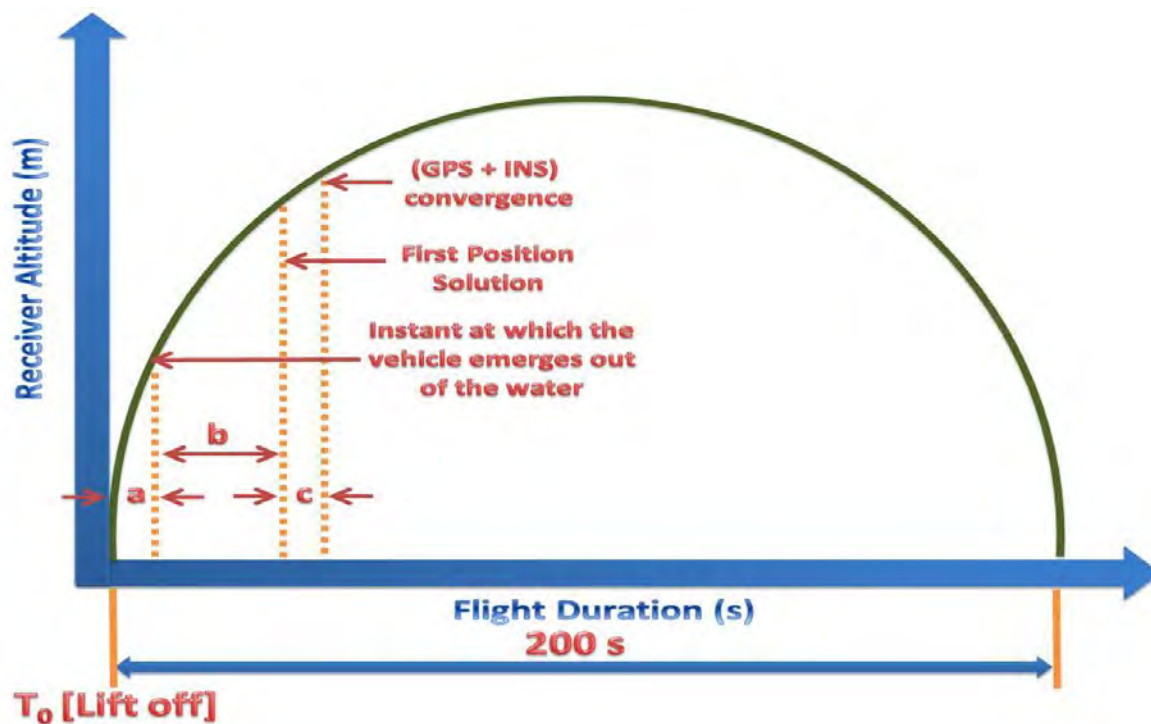


Figure 2-20: Event sequence from vehicle emergence from submarine to touchdown.

With these examples and Figure 1-1, the need for fast TTFF directly from the satellite signals without any assistance from a network or stored parameters within the receiver is established. With this as the goal of the research, Table 2-2 presents pointers which may potentially become a datasheet parameter w.r.t TTFF in future. The ensuing chapters answer each of these questions.



Figure 2-21: GNSS receiver onboard a vehicle released from underneath an aircraft with touchdown time from release.

Table 2-2: Potential future components of a datasheet with the TTFF parameter spelt out with service and frequency of operation supported.

Service Frequency	TTFF (IRNSS)		Hot Start of GNSS using IRNSS (s)
	Civilian (s)	Restricted (s)	
Single	?	?	?
Dual	?	?	

2.9 Summary

In this chapter, the signal travel from the control segment to space and then to users and resulting in position computation was presented. A representative data sheet explained the various performance parameters which constitute a typical GNSS receiver. A brief overview of the IRNSS space segment and the availability achievable over the Indian subcontinent was

presented. The main features of a control segment were presented. Based on generic receiver architecture, the signal flow from the receiver antenna to user position computation was described. Various receiver categories with emphasis on technology and applications were highlighted. Different receiver start modes with achievable TTFF values were presented. The major component underlying the TTFF was highlighted. The AGPS concept and its achievable TTFF were discussed. With a GPS GLONASS receiver, various parameters contributing to TTFF were characterized. Using two real world examples, the limitations of start modes/AGPS and the need for fast TTFF signal design were presented. In the following chapters, various signal design methods are proposed for different user scenarios (frequency/service supported) to overcome the limitations presented in this chapter.

Chapter Three: SINGLE FREQUENCY SIGNAL DESIGN FOR TTFF IN IRNSS

Semiconductor technology has revolutionized GNSS receiver architectures and thus an All In View (AIV) signal reception across GNSS is now reality. Though multiple frequencies are supported by existing operational GNSS systems, some applications are based on the usage of single frequency due to constraining factors of size, power and cost on the receiver design. In addition, some applications enter into sleep (powered-down) mode post navigation solution estimation to optimize the system level power requirements (for example, handheld receivers). Further, as mentioned in the previous chapter, mission critical applications require TTFF within minimal time from power-on/ antenna being exposed to open sky. These constraining factors necessitate a satellite signal that is optimal from a TTFF perspective. This research primarily focuses on proposing a signal design for single frequency IRNSS where TTFF achievable from satellite is minimized.

To begin, a brief overview of the existing GNSS and the proposed modernized signals are presented emphasizing their limitations w.r.t. TTFF. Subsequently, derivation of the signal design for a single frequency IRNSS is presented, with four new transmission techniques are proposed. Following this, high level details of the simulator, which is used as a part of this and the following chapters, to generate the proposed signals, are elaborated in detail. Later, newly developed receiver algorithms commensurate with the proposed signal to demonstrate the derivable benefits are explained in detail. Finally, using a detailed analysis of the test results, the merits of the proposed signal are detailed comparing with GPS L1.

3.1 Overview of GNSS NAV data structures

Prior to the signal design, the existing signals (operational) and emerging systems are presented. The fully operational global systems – GPS and GLONASS L1 are explained first. With not much information available on COMPASS at this time, representative signals from the emerging systems GPS L5 and GALILEO E1 are presented. Quazi Zenith Satellite System (QZSS), a regional system from Japan is briefly touched upon. The main emphasis is to highlight the limitations and formulate a basis for the proposed new signal design.

3.1.1 GLONASS L1

In GLONASS L1, the entire NAV data is grouped into 15 strings of 100 bits each. The first four strings constitute the clock and the satellite ephemeris as shown in Figure 3-1. String five contains non-immediate information. Following this are the 10 strings carrying the almanac information of 5 satellites. Totally, 15 strings constitute a frame and 5 frames make a super frame.

Each string contains 200 NAV data symbols (encoded data bits) and is transmitted in 2 s. Specifically, each string has 170 bits of NAV symbols (the Modulo-2 addition of 50 Hz navigation data and 100 Hz auxiliary meander sequence (bi-binary code)) and 30 bits of time mark. The time mark (shortened pseudo random sequence) consists of 30 bits, clocked at 100 Hz (GLONASS-ICD 1998). With this arrangement, to collect the entire NAV data (for example, 24 almanac pages), a satellite needs to be tracked continuously for 2.5 minutes.

3.1.2 GPS L5

As a part of GPS modernization, the L5 signal has been designed with a new scheme of NAV data transmission as shown in Figure 3-2a), which are “message type” at defined rates. Each message is identified based on a message-id. The NAV data transmitted is similar to GPS L1

(explained in Chapter Two), with the first two messages predominantly constituting ephemeris and clock parameters. Unlike GPS L1, the UTC and Ionosphere correction terms are de-coupled from the almanac and are transmitted as a part of a third message separately (ICD-GPS-705 2002). A fourth message is dedicated for the satellite almanac transmission and the fifth contains textual messages, a new feature to enhance user operations.

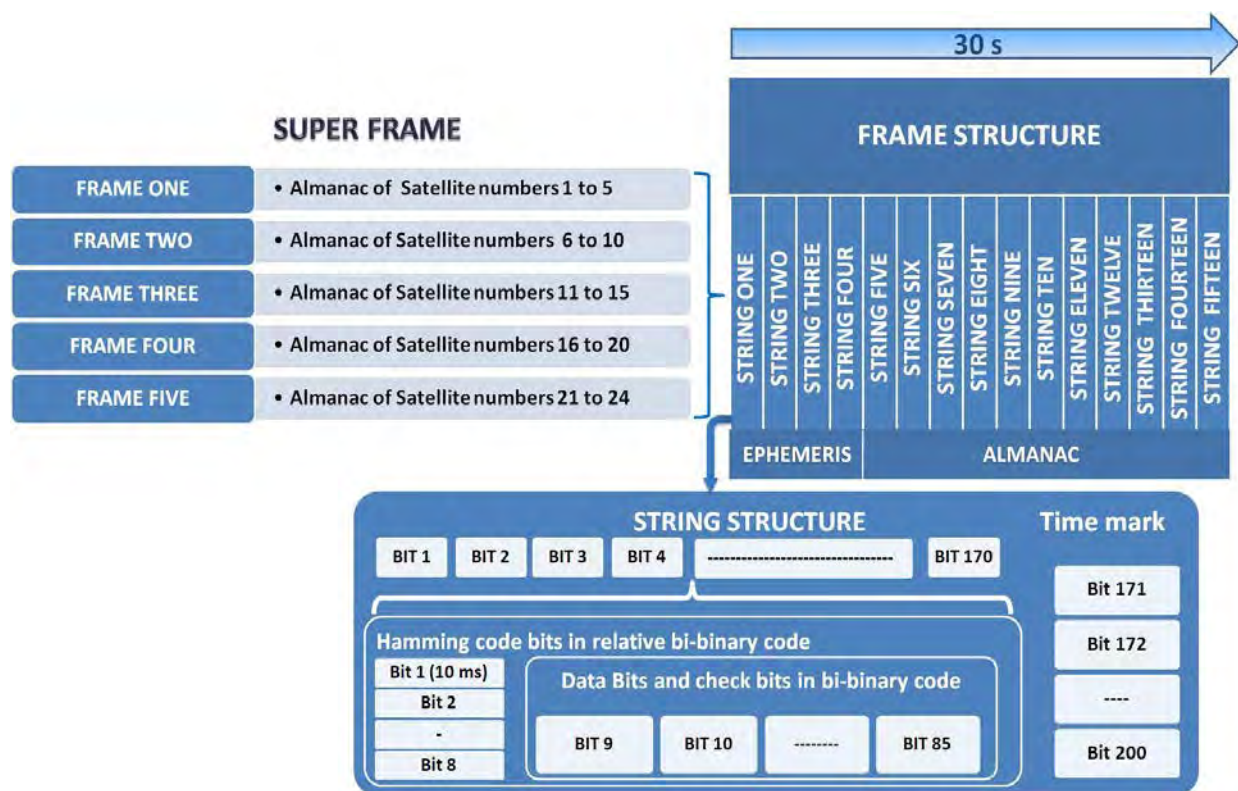


Figure 3-1: NAV data signal design of GLONASS L1 depicting frames and its constituents, strings and bit definitions.

GPS L5 has a 24 bit Cyclic Redundancy Check (CRC) for 239 bits of effective NAV data and encoded using a rate $\frac{1}{2}$ 7-bit Viterbi algorithm (ICD-GPS-705 2002). The effective symbols are transmitted at 100 sps. With this messaging arrangement, transmitting the entire NAV data including the secondary parameters of all satellites takes approximately 10 minutes.

3.1.3 GALILEO E1

A high level NAV data format of GALILEO (Galileo 2008) is shown in Figure 3-2b), which has sub-frame architecture as in GPS L1 termed as pages. Each frame consists of five pages, with Page 1 and 5 primarily containing secondary parameters. Pages 2 to 4 are dedicated to primary ephemeris parameters. Twelve such frames constitute a master frame.

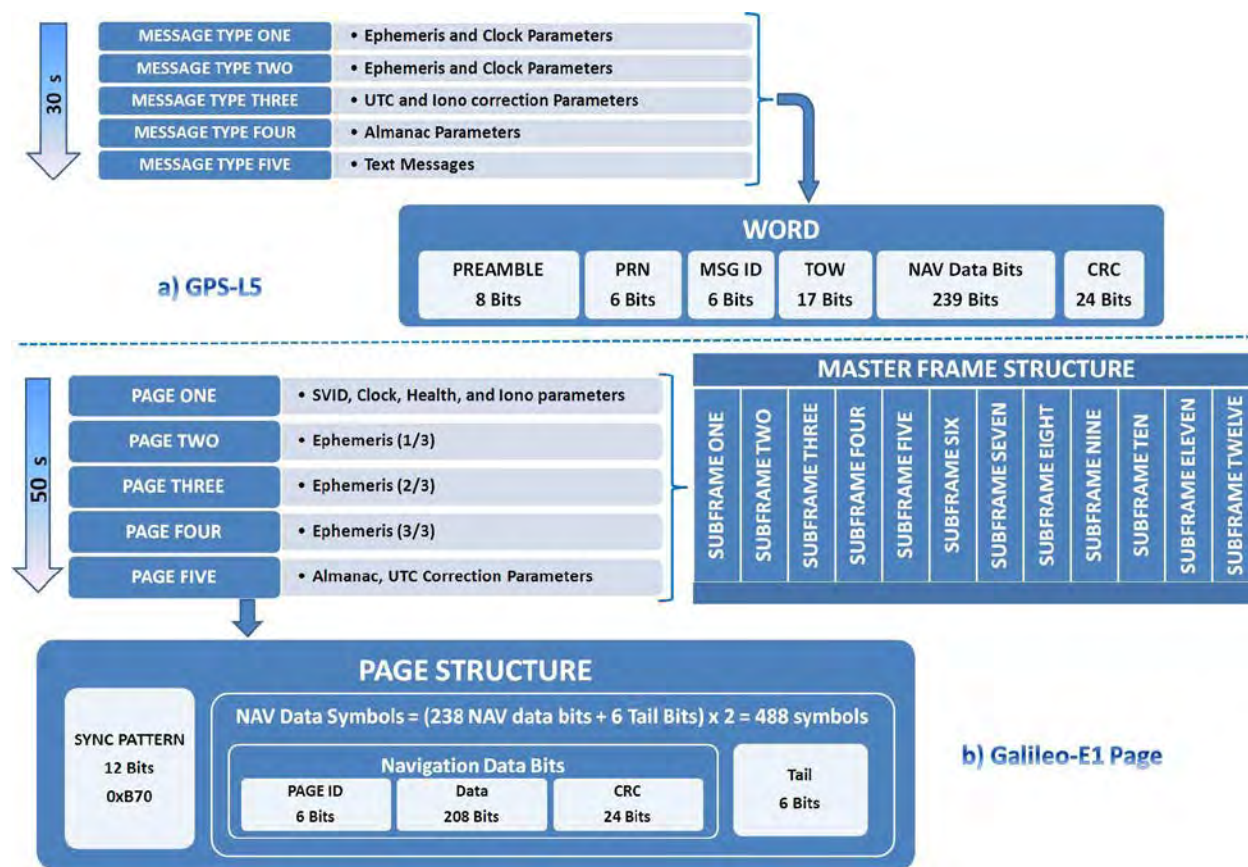


Figure 3-2: NAV data signal design of a) GPS L5 b) GALILEO E1 with message types/pages, its constituents and bit definitions.

Each page contains 208 NAV data bits with a page id. With a 24-bit CRC algorithm, these data bits are encoded employing a rate $\frac{1}{2}$ 7-bit Viterbi algorithm as shown in Figure 3-2b). Unlike GPS L5, tail bits (resets decoder at the end of each frame) are added to the NAV data before encoding and symbols are interleaved (symbols scrambled to overcome burst errors). Post

interleaving, each page is appended with a synch pattern (enables identification (start) of each frame) of 12 bits to make a NAV data packet of 500 symbols. The symbols are clocked at 50 Hz, with an effective data rate of 25 Hz. The synch pattern along with the tail bits enable synchronization and data decoding respectively.

3.1.4 QZSS

Quazi Zenith Navigation Satellite System (QZSS) is an initiative from Japan to augment the GPS over its territorial footprint and slightly beyond. This system is expected to have 3 geostationary satellites (currently one operational) and transmit data similar to the GPS L1 C/A with an objective of improving regional availability (Glennon 2011). Unlike IRNSS, QZSS is a regional augmentation system than an independent navigation system.

3.2 Limitations of existing GNSS NAV data

With the NAV data overview and the TTFB characterisation of GPS L1 (previous chapter), this section presents the limitations under two data types: primary and secondary. The primary type affects the TTFB of a receiver, while the secondary affects the effective usability within the receiver (for example, ionosphere/UTC page collection determines the application of the corrections on pseudorange measurements).

3.2.1 Primary data

As detailed in the previous chapter, to minimize TTFB, the time associated with the primary data reception needs to be minimal, which is linked to the overall frame architecture. The following paragraph presents the limitations of GPS/GLONASS L1, GPS L5 and GALILEO E1 and provides pointers from a new signal design perspective.

- GPS L1:

The major drawback in this scheme is for every 24 bits, 6 parity bits are transmitted (Figure 2-11). This constrains the effective primary transmission and thus delays the TTFF. In each sub-frame, there exist some words and bits that necessarily need to be transmitted (for example, Telemetry (TLM), Hand Over Word (HOW), sub-frame id) which is an overhead from TTFF perspective. Following a detailed analysis of GPS L1 ICD, several spare or reserved fields which carry no information are transmitted as a part of the primary parameters, which further delays the data collection process.

- GLONASS L1:

Time information is broadcasted once in 30 s as a part of string one, which delays TTFF. In addition, it effectively delays the hot start (which solely depends on time from satellite) capability in GLONASS. For a single frequency L1 user, the ionosphere correction parameters are not broadcasted as a part of NAV data, which affects position accuracy.

- Galileo E1:

With interleaving, subframe synchronization can be invoked only after a complete data frame has been collected. If bit-synchronization occurs in the middle of a subframe, interleaving delays (explained later) the TTFF.

- In GPS L5:

The encoded data does not contain tail bits. From a decoding perspective, the initial time required to build the history of the encoder for effective data demodulation delays (explained later) the TTFF. Unlike GALILEO, the frame synch pattern (preamble) associated with each message is encoded, which does not assist the initial decoding process.

Table 3-1 summarizes the time required to collect the primary parameters from existing and emerging GNSS where T_{iono_utc} is the time required to transmit the ionosphere and the UTC page and T_{mt} is for collecting the textual message.

Table 3-1: Table summarizing the maximum time required to collect primary and secondary NAV data in GPS/GLONASS L1, GALIEO E1 and GPS L5 post bit synchronization.

Parameter	GPS-L1 (s)	GLONASS L1 (s)	GALILEO E1 (s)	GPS L5 (s)
T_{eph} / T_{TFF}	30	30	50	24
T_{alm}	750	150	600	576
T_{iono_utc}	750	150*	50	96
T_{mt}	-	-	-	As required ⁺

* UTC only

+ Per satellite

3.2.2 Secondary data

The main constituents of this data are almanac, UTC, Ionosphere correction terms and Textual data. The UTC and Ionosphere terms are grouped along with the almanac in GPS L1. This effectively delays the application of ionosphere corrections until all almanac/health pages are collected (the health page, which indicates the validity of ionosphere terms, is transmitted separately). However, this has been circumvented effectively in GPS L5 and GALILEO E1. Nevertheless, the transmission methodology adopted for almanac and the textual messages delay the collection process (for example, GPS L5 and GALILEO E1), which is explained below considering GPS L1 C/A:

The almanac is transmitted in two sub-frames in GPS L1. All the satellites transmit the same information as part of their subframe 4 and 5. The sub-frames 4 and 5 transmit almanac data for all the 25 pages with each page containing the almanac data of a particular satellite as described in Figure 3-3 (IS-GPS-200E 2010). This effectively delays the transmission process, which takes

12.5 minutes to transmit the almanac data in GPS L1. Similar transmission schemes exist in GPS L5 / GALILEO E1 w.r.t almanac and in addition, textual messages of L5 as depicted in Table 3-1.

With the enumerated limitations w.r.t primary/secondary data transmission in the existing GNSS and with IRNSS being a regional system, optimal signal designs are presented in the following section. As an additional *input/design constraint and to the extent possible, the proposed system shall be extendable globally.*

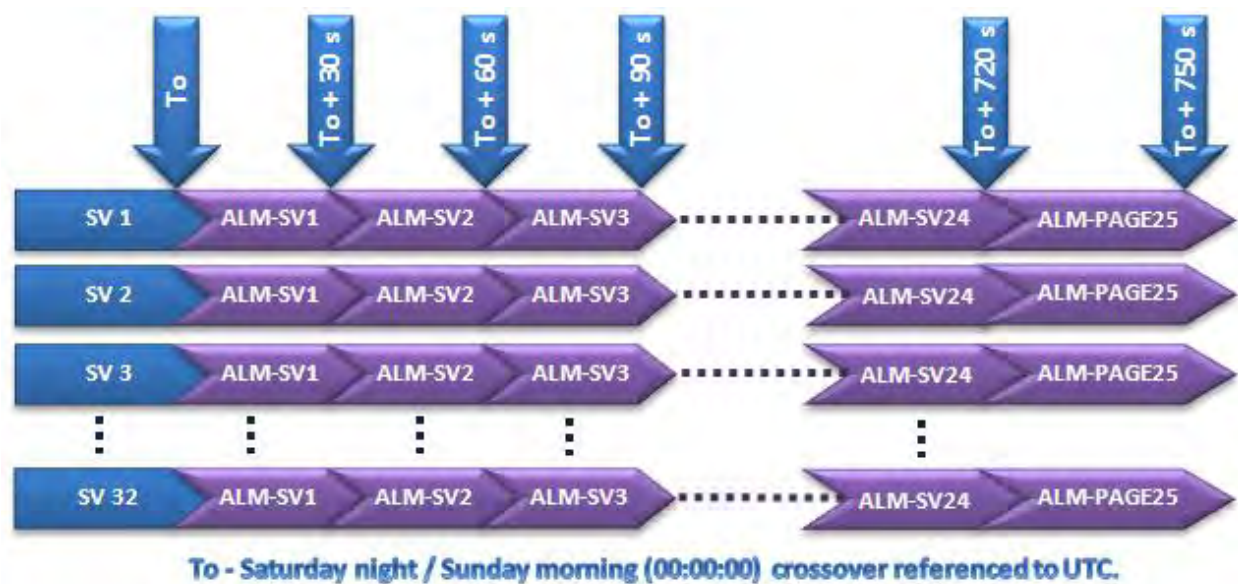


Figure 3-3: Signal design of almanac transmission in GPS L1 across satellites.

3.3 NAV data signal design derivation

With a goal of reducing T_{eph} , the main constraint in achieving the LOS TTFF, the objective is to develop an optimal NAV data transmission which reduces T_{eph} relatively. As a first step, a subframe structure for the proposed signal needs to be developed. With GPS L1 C/A as reference, the following are considered as design inputs /constraints:

- First, not to compromise with any of the major existing data fields present in the GPS L1.

- Second, is the selection of an appropriate integrity algorithm for the NAV data bits with minimal overheads.
- Finally, group the data bits into the four/three/two sub-frames.

3.3.1 Subframe structure

NAV data can be grouped as

$$NAVDATA = \{NAV_{pri} + NAV_{sec}\} \quad (3-1)$$

where,

NAV_{pri} is the primary navigation data

NAV_{sec} is the secondary navigation data, which includes almanac, UTC corrections, ionosphere corrections (Iono), differential corrections and text messages. Alternatively, Eq. (3-1) can be written as,

$$NAVDATA = \{Ephemeris + \{Almanac + UTC + Diff_{corr} + MessageTypes\}\} \quad (3-2)$$

Transmitting the entire NAVDATA in one single packet delays the collection of primary parameters (for example, transmitting the almanac/textual messages of all satellites as one set) which effectively retards TTFF. In addition, few bit errors effectively make the entire data packet unusable. With this as a design input, NAVDATA is structured as subframes (SF) with the following grouping:

SF₁ = Ephemeris1;

SF₂ = Ephemeris2;

SF₃ = Almanac;

SF₄ = Secondary data. (3-3)

In order to identify each subframe, unique identifiers are required to differentiate. A two bit field is exclusively apportioned as a part of NAV data. Generalizing,

$$SF_{n_data} = SFID + NAVDATA_n \quad (3-4)$$

As explained in the previous chapter, the above packet needs to be uniquely identified w.r.t the IRNSS system time, Time of Week (TOW). Adding this component Eq. (3-4) is re-written as

$$SF_{n_data} = TOW + SFID + NAVDATA_n \quad (3-5)$$

To enable identification (id) of each satellite, a dedicated PRN id is embedded as part of the NAV data. With only seven satellites in the proposed IRNSS constellation, a 3-bit field is adequate to represent each satellite. With an intention to support possible futuristic global extension, 5 bits (32 satellites) are dedicated. With this, Eq. (3-5) results in

$$SF_{n_data} = \{TOW + SFID + SVID + NAVDATA_n\} \quad (3-6)$$

As mentioned in the previous section, the NAV data needs to be protected from burst errors. To circumvent this, two integrity methods at the data level are adopted. First, a 24-bit CRC word is added to the data for integrity check (which ensures the correctness of the received data). The algorithm used in GALILEO (Galileo 2008), which detects single bit and burst errors, is considered

$$SF_{n_data} = \{TOW + SFID + SVID + NAVDATA_n\} + Integrity. \quad (3-7)$$

Additionally, the entire packet is encoded with a rate $\frac{1}{2}$ 7-bit Viterbi algorithm. To optimize decoding (explained later) with a constraint length of seven, six tail bits (Galileo 2008) are added to Eq. (3-7) to yield

$$SF_{n_data} = \{\{TOW + SFID + SVID + NAVDATA_n\} + Integrity\} + Tail. \quad (3-8)$$

To facilitate faster subframe synchronization, a “Sync” pattern is introduced at the beginning of each subframe (for example, contents between two synch words ensure encoded data of a frame and thus easier decoding in the receiver), without encoding, as

$$SF_{n_data} = Sync + \left\{ \left\{ \left\{ TOW + SFID + SVID + NAVDATA_n \right\} + Integrity \right\} + Tail \right\}. \quad (3-9)$$

Alternatively, Eq. (3-9) can be written as

$$SF_n = Sync + Nav_Data_Bits. \quad (3-10)$$

Assuming 6 s to transmit a subframe, the TOW effectively increments at this rate. In order to represent the total number of seconds in a week (604800 s), 17 bits are required. Further apportioning 12 sync symbols and at 100 sps, Eq. (3-10) post encoding reduces to

$$SF_{n-enc} = Sync + Nav_{Data_sym} \quad (3-11)$$

From Eq. (3-11) the effective NAV data symbols reduce to 480 or 240 bits prior to encoding. The resulting structure is shown in Figure 3-4, which is transmitted without interleaving.

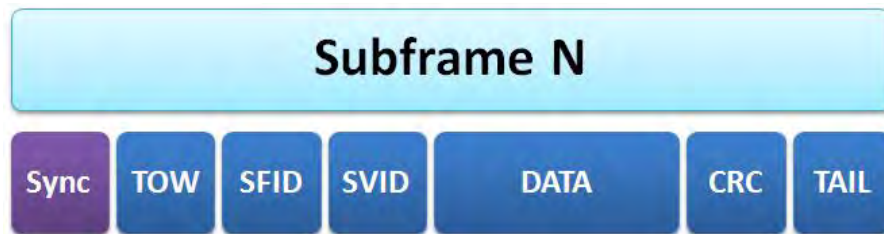


Figure 3-4: Proposed IRNSS NAV data structuring detailing its constituents.

This structure is used as a reference throughout the research work. Following this, the next objective is to construct the contents of Eq. (3-3). Towards this, ephemeris parameters are first deduced in the next section.

3.3.2 *Ephemeris parameters*

The proposed IRNSS constellation will have satellites distributed in geostationary and geosynchronous orbits (Rao et al 2011). It will be the first GNSS system where all the satellites are in geostationary orbits and used for independent positioning. The SBASs (Wide Area Augmentation System (WAAS), European Geostationary Navigation Overlay System (EGNOS), Multi-functional Satellite Augmentation System (MSAS) & GAGAN have the satellites in geostationary orbits and transmit its ephemeris as absolute state vectors (DO-229D 2006). As of now, the ICD of IRNSS is not available in the public domain and thus as a first objective the format of ephemeris transmission needs to be established.

Two possibilities are available: First to transmit as Keplerian parameters similar to GPS L1 or as absolute state vectors (for example, GLONASS L1). The latter proposition requires frequent ephemeris uploads to ensure orbital errors are minimal (for example, in GLONASS L1 ephemeris updates occur every 30 minutes (GLONASS-ICD 1998)). This research assumes Keplerian parameters as part of the NAV data (ephemeris) of IRNSS with the following section explains the simulation method to generate ephemeris and its adequacy to represent IRNSS orbit. The software simulation modules used for estimating the IRNSS satellite position computation with the Keplerian parameters is shown in Figure 3-5. The simulation methodology is as follows:

- First, the almanac file of IRNSS in Yuma file format (Rao et al 2011) is loaded to the MATLAB simulation algorithm.
- With an arbitrary system time, the simulation is initiated with T_{OA} – Time of almanac (as read from Yuma File) extrapolated to the system time.

- For every 2 hour interval (ephemeris update similar to GPS L1), Keplerian parameters (ephemeris) are generated for all the seven satellites based on the equations specified in the GPS ICD (2010).
- Based on the above ephemeris, the satellite positions are computed for 24 hours at 15 minute intervals.
- The computed satellite positions are plotted to form the ground track of the IRNSS satellites. The results are similar to Figure 2-3.
- Based on this result, it is deduced that the GPS L1 bit definitions (number of bits as shown in Table 3-2) are adequate to define the geostationary orbit of IRNSS. A sample value of the Keplerian parameters obtained from IRNSS is listed in Table 3-2.

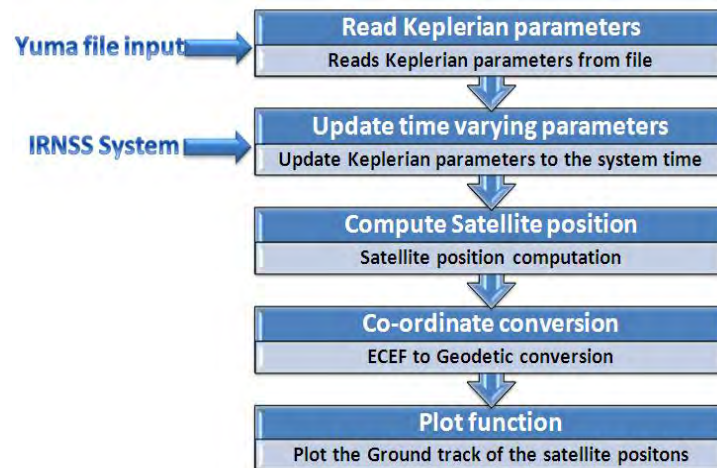


Figure 3-5: Simulation software flow to deduce the IRNSS Keplerian parameters as a part of each satellite’s ephemeris.

With the *ephemeris in Keplerian format* as reference, the following paragraph derives the NAV data structuring with an objective to reduce the time required to collect primary and secondary parameters and establishes the limits of achievable TTF in a single frequency of operation.

Towards this, four new techniques are proposed - one method to obtain secondary parameters faster and three to enhance TTFF.

Table 3-2: Sample IRNSS and GPS L1 ephemeris parameters and their bit definitions.

Parameter	Description	IRNSS (GEO-1)	GPS (SV-1)	No of bits
e	Eccentricity	$3e-4$	$0.4286766052e-003$	32
\sqrt{A}	Square root of semi major axis ($m^{1/2}$)	$6.493392256e+003$	5153.623535	32
Ω_0	Longitude of ascending node of the orbit plane at reference time (radians)	-2.08788513933950	$0.2649778414E+001$	32
I_0	Inclination Angle of the orbit plane at reference time (radians)	$1.74535456369656e-004$	0.9605440151	32
ω	Argument of perigee (radians)	$1.60138794496997e+000$	1.405611388	32
Ω_{dot}	Rate of right ascension(radians/s)	0	$-0.7691748964e-008$	24
M_0	Mean Anomaly at reference time (radians)	1.07111912116828	0.1592475041	32

3.3.3 Secondary data

In the case of IRNSS, seven almanac pages need to be transmitted as part of the third sub-frame. Adopting an almanac transmission similar to GPS for IRNSS, it takes 192 s (Figure 3-3, with seven almanac pages/UTC-ION-health page) to completely transmit the information of all satellites. With visibility assured to all the satellites, a unique signal design of data straddling across satellites is proposed as shown in Figure 3-6 and Figure 3-7 to reduce the secondary data transmission time. With a new almanac upload, each satellite is initialized with the almanac of different PRN. Based on the number of satellites in the constellation, in a cyclic fashion each

satellite transmits a different almanac. With this arrangement, the entire almanac of IRNSS is transmitted within a single subframe period (across satellites). In addition, the almanac contents are staggered with the Ionosphere and UTC terms. This ensures these parameters are transmitted at least once every 24 s. From a single satellite perspective, the entire data is transmitted within 168 s as shown in Figure 3-6.

The above concept is extended to textual messages, which is slotted in the fourth subframe. Textual messages contain constellation specific information, which is broadcast at pre-defined time intervals. These messages typically are differential corrections of each satellite (for example, some messages of SBAS applicable to IRNSS) or any other data relevant to the user community. Each message is identified by a unique id and transmitted by the satellite. The message sequences can be varied within the fourth subframe as shown in Figure 3-7.

These methods effectively reduce the time required to collect secondary NAV data (T_{sec}). A sample message type summary and its corresponding rates are as shown in the Table 3-3.

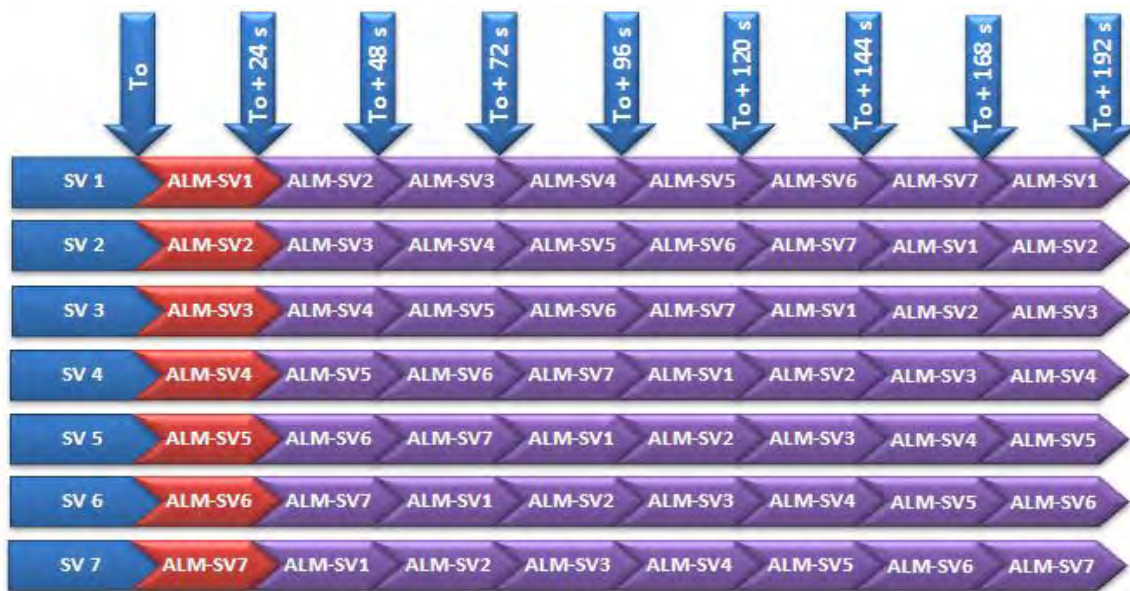


Figure 3-6: Proposed data straddling technique of almanac transmission across satellites in IRNSS.



Figure 3-7: Proposed almanac and textual message transmission to enhance T_{sec} in IRNSS.

Table 3-3: Sample message type definitions to be transmitted as a part of the fourth subframe in IRNSS.

Message Type	Description	Rate
00	Reserved	Not Applicable
02 – 63	Any User Defined Data	Once in 24 s

3.3.4 Four Subframe Architecture (FSA)

With the NAV data structure, ephemeris and secondary data streaming, the first proposed architecture of NAV data with four subframes is shown in Figure 3-8 (Rao et al 2012). The merit of this design is the primary data transmitted within 24 s from each satellite. In addition, the entire secondary data of the constellation is available within 24 s across satellites as shown in Figure 3-6 and Figure 3-7. From an analysis stand point, two points are noteworthy w.r.t data straddling across satellites: First, with IRNSS satellites always visible over the Indian

subcontinent, the almanac as a part of the NAV data is redundant. However, to support the global extension of IRNSS, the almanac is included as a part of NAV data.

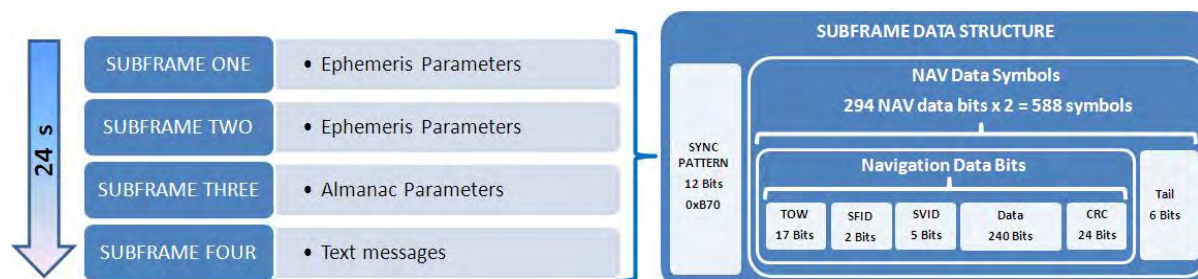


Figure 3-8: Proposed IRNSS NAV data signal design with four subframes data streaming.

Second, extending data straddling as a part of the existing global navigation systems reduces its secondary data transmission time but is not optimal as in IRNSS (regional). This is explained as follows: Assume IRNSS to have 32 satellites as a part of global coverage and eight or more satellites assured to be visible over the Indian subcontinent. Further, assume that the data is transmitted as shown in Figure 3-7. For the first eight satellites, transmission happens faster. Subsequently, though the data is straddled, only one new almanac is collected in the receiver from the visible tracking satellites (every 24 s). To overcome this scenario, the data straddling is alternated with almanac pages from the different sets as shown in Table 3-4 to ensure that the almanac of all satellites is collected faster. The satellites within each set are *cyclically rotated* (every 24 s) as well. With this arrangement, reduction in almanac collection time is directly proportional to the number of satellites tracked. For example, with eight visible satellites and by adopting the streaming method shown in Table 3-4, the data is effectively collected within 144 s in the receiver (for any arbitrary set of satellites tracked), a significant improvement as compared to 750 s for GPS L1. As shown in Table 3-4, at $T_0 + 210$ s, the contents of the sets are changed w.r.t the initial values of $T_0 + 18$ s. This ensures that each satellite would have transmitted the

data of all other satellites, which still take 750 s as earlier. However, a distinct advantage of this scheme is that the user would have received the entire data from all satellites much earlier.

Table 3-4: Data straddling with alternate page arrangement for global coverage and optimal T_{sec} in IRNSS.

Time (s)	SV [Channels in a receiver]			
	[1, 2, 3, ... 8]	[9, 10, 11,... 16]	[17, 18, 19, ... 24]	[25, 26, 27, ... 32]
$T_0 + 18$	Set 1	Set 2	Set 3	Set 4
$T_0 + 42$	Set 4	Set 1	Set 2	Set 3
$T_0 + 66$	Set 3	Set 4	Set 1	Set 2
$T_0 + 90$	Set 2	Set 3	Set 4	Set 1
$T_0 + 114$	Set 1	Set 2	Set 3	Set 4
$T_0 + 138$	Set 4	Set 1	Set 2	Set 3
$T_0 + 162$	Set 3	Set 4	Set 1	Set 2
$T_0 + 186$	Set 2	Set 3	Set 4	Set 1
Set 1 is [1, 2, 3, 4, 5, 6, 7, 8] Set 2 is [9, 10, 11, 12, 13, 14, 15, 16] Set 3 is [17, 18, 19, 20, 21, 22, 23, 24] Set 4 is [25, 26, 27, 28, 29, 30, 31, 32]				
$T_0 + 210$	Set 1	Set 2	Set 3	Set 4
$T_0 + 234$	Set 4	Set 1	Set 2	Set 3
$T_0 + 258$	Set 3	Set 4	Set 1	Set 2
$T_0 + 282$	Set 2	Set 3	Set 4	Set 1
$T_0 + 296$	Set 1	Set 2	Set 3	Set 4
$T_0 + 320$	Set 4	Set 1	Set 2	Set 3
$T_0 + 344$	Set 3	Set 4	Set 1	Set 2
$T_0 + 368$	Set 2	Set 3	Set 4	Set 1
Set 1 is [2, 3, 4, 5, 6, 7, 8, 1] Set 2 is [10, 11, 12, 13, 14, 15, 16, 9] Set 3 is [18, 19, 20, 21, 22, 23, 24, 17] Set 4 is [26, 27, 28, 29, 30, 31, 32, 25]				
:	:	:	:	:

Restricting the case to a single frequency regional system and a seven-channel receiver, FSA results in an overall improvement of 20% in T_{eph} and 85% in T_{sec} as compared to GPS L1.

3.3.5 Three Subframe Normal (TSN)

With the reference NAV data structure, the next objective is to reduce the T_{eph} further in a single frequency mode of operation without *increasing satellite data rate or power*. From a signal transmission perspective, the optimal TTFF with “n” visible satellites (Eq. (3-11)), can be written as

$$TTFF_{opt} = \min_t \sum_n \sum_j SF_{j-enc} \quad (3-12)$$

Eq. (3-12) is defined as the minimal time required to transmit the satellite data for “n” satellites with “j” subframes to achieve optimal TTFF.

Using Eq. (3-1) Eq. (3-12) can be decomposed as

$$TTFF_{opt} = \min_t \sum_n \sum_j SF_{j-pri} + \min_t \sum_n \sum_j SF_{j-sec} \quad (3-13)$$

where SF_{n-pri} and SF_{n-sec} are the subframe symbols associated with primary and secondary parameters respectively. From Eq. (3-13), to achieve an optimal TTFF, the NAV data parameters need to be transmitted faster or the number of primary NAV data parameters reduced. An increased data rate (reduced data bit period) necessitates more signal transmission power (Parkinson & Spilker 1996) to ensure Power Spectral Densities (PSD) and thus accuracies commensurate to the existing system (for example, in the case of GPS L1: for a C/N_0 of 42 dB-Hz, the code phase measurement accuracy is 10 cm. (DO-229D 2006)), which is a costly proposition onboard satellites. From the previous section on simulation, the optimal ephemeris data for IRNSS orbits was deduced, which negates the other possibility.

Alternatively, analyzing Eq. (3-13), the TTFF is enhanced by increasing the periodicity of the primary parameters, which is achieved by reducing the rate of secondary parameter transmission.

Adopting the latter approach, Eq. (3-13) is re-written as

$$TTFF_{opt} = \min_t \sum_n \sum_j SF_{j-pri} + \left\{ \min_t \sum_n \sum_j SF_{j-sec} \right\}_{constrained} \quad (3-14)$$

A method of achieving Eq. (3-14) is by staggering the subframe 3 and 4 and transmitting them alternatively as subframe 3. Subframes 1 and 2 are retained as in the four subframe method. This effectively reduces to a three subframe architecture as shown in Figure 3-9.

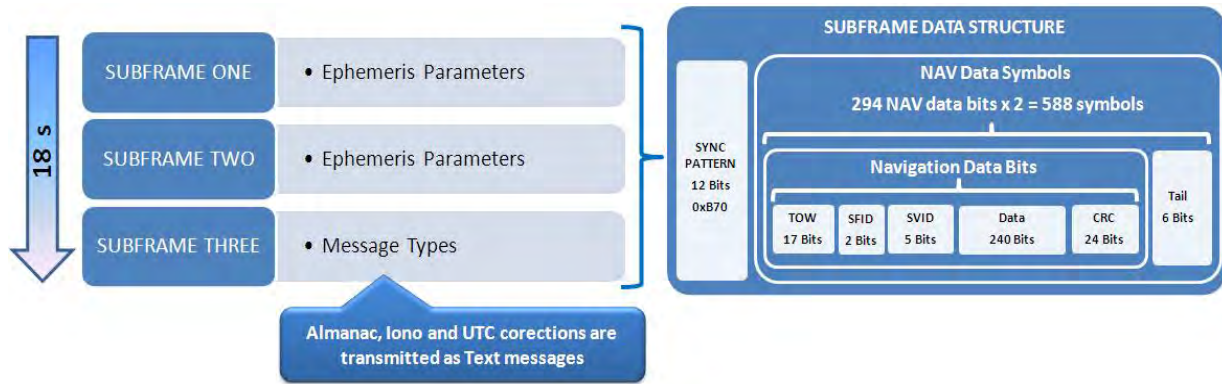


Figure 3-9: Proposed IRNSS NAV data signal design with TSN architecture.

Effectively, in the TSN architecture, the first two subframes are dedicated to the ephemeris and clock parameters. However, the almanac is grouped along with the textual messages and transmitted alternatively in the third subframe as shown in Figure 3-10. Another constraint is to ensure that the UTC and Ionosphere correction terms are transmitted in subframe 3 always, which ensures these parameters are transmitted every 18 s. This is done as follows: The subframe 3 transmission completes every $((T_0 + 18) * N)$ s, where N takes values from 1 to 33600 s (604800 (Seconds in a week)/18 s). For odd values of n, almanac pages are transmitted and for even values, textual messages are transmitted. The UTC and Ionosphere terms are grouped and transmitted along with the almanac pages. Of these pages, three carry UTC and four ionosphere terms, as shown in Figure 3-10.

Similarly, for even values of "N", the UTC and Ionosphere terms are grouped in one message (Table 3-5) and transmitted in one of the satellites. For either values of "N", pages are straddled in time to ensure that each satellite transmits the data independently.

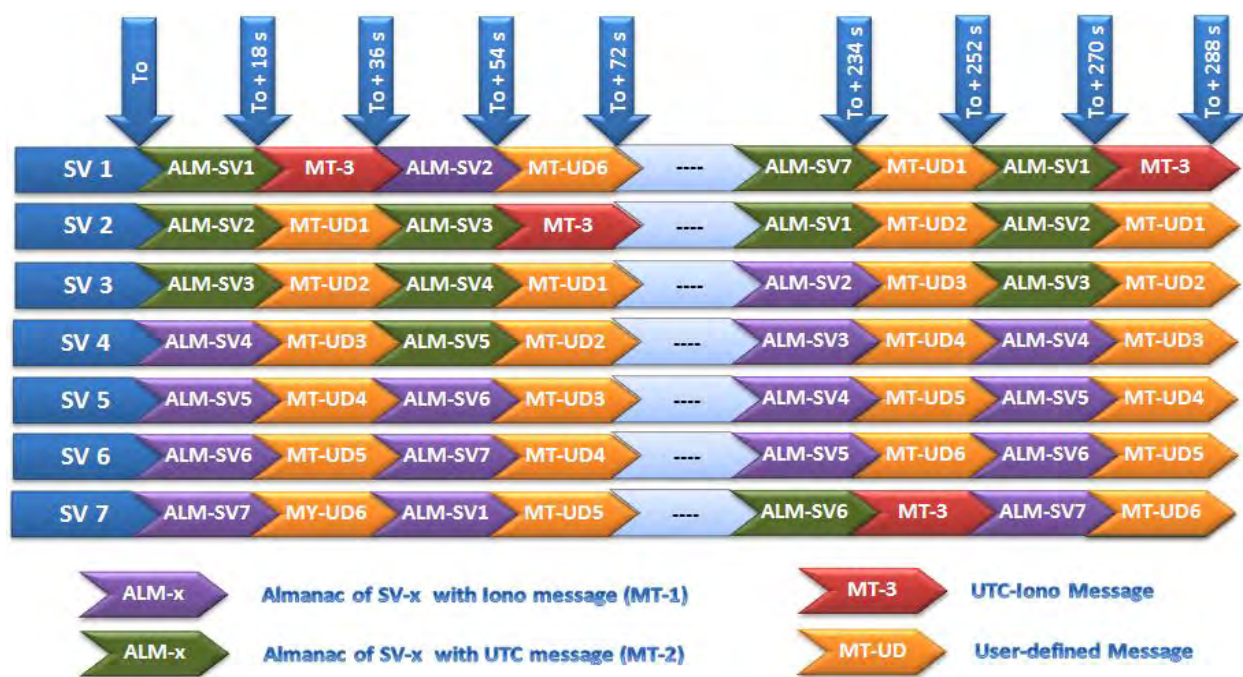


Figure 3-10: Proposed NAV data with transmission in TSN architecture to enhance T_{eph} and T_{sec} in IRNSS.

Table 3-5: Proposed message types with their periodicities as a part of third subframe in TSN architecture.

Message Type	Description	Satellite Id	Rate (s)
00	Reserved	--	---
01	Almanac-IONO	In all satellites staggered	$(T_0 + 18) * N^+$, where $N = 1, 3 \dots 33599$
02	Almanac-UTC	In all satellites staggered	$(T_0 + 18) * N$, where $N = 1, 3 \dots 33599$
03	Iono-UTC	One satellite, staggered	$(T_0 + 18) * N$, where $N = 2, 4 \dots 33600$
04 – 63	Any User Data	satellites, staggered (cyclic)	$(T_0 + 18) * N$, where $N = 2, 4 \dots 33600$

⁺ - Time at completion of 3rd subframe

The primary parameters are transmitted within 18 s (worst case) as opposed to 24 s in four subframes, which is an advantage with this approach. This effectively translates to a 40% reduction in T_{eph} as compared to GPS or GLONASS L1. The only limitation with this scheme is that the almanac transmission (and textual messages) occurs every 36 s as opposed to 24 s in 4 subframe architecture. From a regional perspective this compromise is generally acceptable. A sample timing diagram is shown in Figure 3-10.

Finally, assuming a global extension of IRNSS, the three subframe architecture is still valid. It can be shown with this arrangement that T_{eph} is 18 s and T_{sec} is commensurate with the architecture shown in Table 3-4 for a global scenario (for example with eight satellites tracked, it is 288 s), which is still better considering the existing and proposed GNSS constellations w.r.t primary and secondary NAV data collection together.

3.3.6 *Three Subframe Fixed (TSF)*

The final objective is to establish the theoretically achievable TTF limit (from transmission perspective) in a single frequency of operation for IRNSS. An assumption made here is that the UTC and Ionosphere terms are only transmitted as a part of secondary NAV data as in GPS L1. With this input and extending the previous derivation, this section deduces the optimal NAV data structure.

The argument that the almanac is redundant for IRNSS once applied to Eq.(3-14) reduces it to

$$TTF_{opt} = \min_t \sum_n \sum_j SF_{j-pri} + \min_t \sum_n \sum_j SF_{j-sec} \quad \text{fixed,constrained} \quad (3-15)$$

To use Eq. (3-15) from a system perspective, UTC and Ionosphere parameters are transmitted as a part of a subframe 3, staggered satellite wise – fixed slots. The details of the scheme are as follows: The first two subframes transmit ephemeris and clock parameters of satellites as in a

TSN method. Following this, the third subframe data of one of the satellite transmits UTC and Ionosphere terms, which appear once in 18 s from the constellation, as shown in Figure 3-11.



Figure 3-11: Proposed NAV data architecture with TSF transmission to enhance T_{eph} and T_{sec} in IRNSS.

One additional design consideration is the change in the subframe slotting following UTC and Ionosphere transmission. For example, for SV1 after $T_0 + 18$ s, instead of transmitting subframe 2 for SV1 commensurate with the other satellites, subframe 1 is transmitted. This ensures that the maximum time required to collect ephemeris (from the satellite) is restricted to 18 s. The merit of this scheme is T_{eph} reduces to 12 s with Ionosphere and UTC parameters transmitted periodically every 18 s. The TSF is as shown in Figure 3-11. One limitation with this approach is for 6 s (for

example, $T_0 + 12$ to $T_0 + 18$,) ephemeris from six satellites, as opposed to all seven, is available (Figure 3-11).

For 6 s (till $T_0 + 30$ s), the Position Dilution of Precision (PDOP – measure of satellite geometry (Petovello 2010)) will be relatively high as shown in Figure 3-12. The PDOP variation as a function of a single satellite dropped (7 satellites in all, 3 geostationary and 4 geosynchronous) is analyzed over the Indian subcontinent. The maximum PDOP is observed with the exclusion of GEO-1 as shown in Figure 3-12 (Appendix E illustrates the PDOP variation for the other excluded satellites). It is very clear that even with 6 satellites the PDOP is relatively good for most of the Indian subcontinent.

With TSF NAV data streaming, *the theoretically best possible TTF* is achieved for any GNSS system and in addition, the requisite secondary parameters are collected in minimal time.

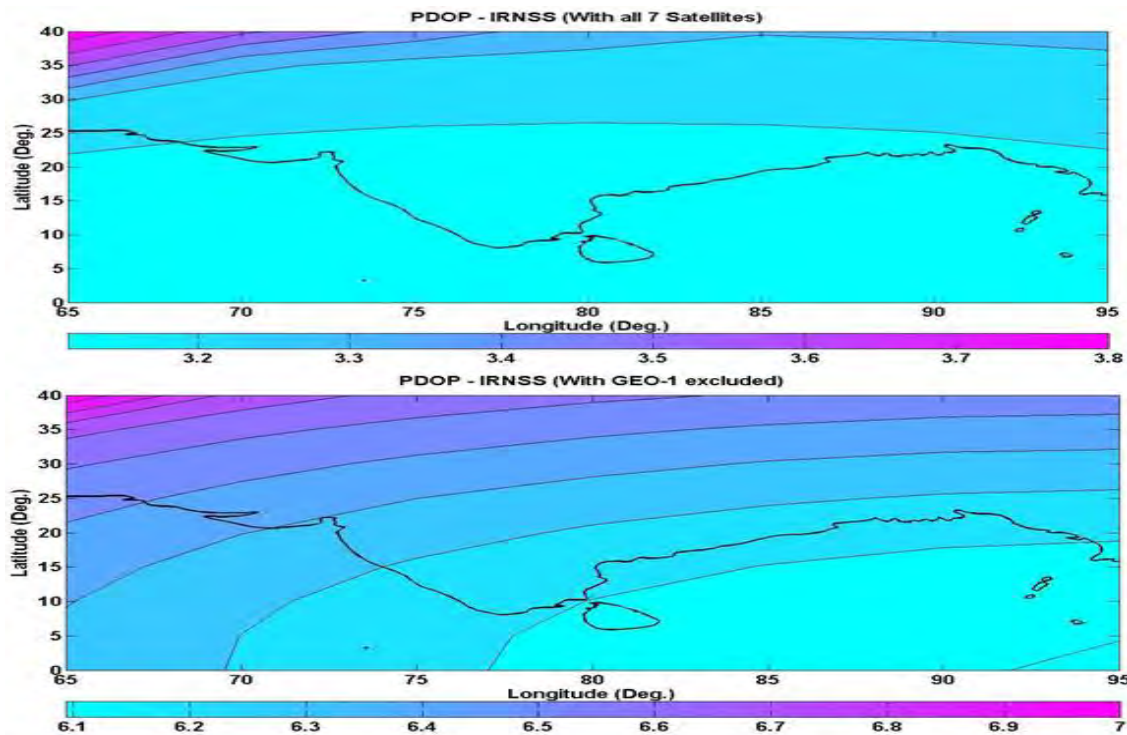


Figure 3-12: PDOP variation over Indian subcontinent with all satellites and exclusion of GEO-1.

Further, assuming global extension of IRNSS, the scheme is still valid w.r.t TTFB which is explained as follows: With M satellites in IRNSS global constellation, a single frequency receiver is assumed to have M parallel channels. This ensures a dedicated channel for each satellite and obviates the need for visibility (thus almanac) computation and reduces the signal search time. With this arrangement, T_{eph} is effectively reduced to 12 s, and the UTC and Ionosphere terms are collected in 18 s. In addition, the PDOP issue highlighted above with 7 satellites disappears in a global scenario with an assumption of a minimum of 8 or more satellite available. Finally, the UTC and Ionosphere terms need to be straddled in multiple satellites to ensure users across the globe obtain it from at least one satellite. The following section provides details of the signal simulation methodology for all the proposed techniques.

3.4 Signal simulation methodology

To generate the proposed signals, a test-rig from Accord Software & Systems is taken as the reference hardware platform. This section highlights the top-level hardware schematic and the software flow within the test rig, which is used as a reference platform throughout this research. The software modules specifically written for generating the proposed signals are elaborated in detail. The RF signal generation can be categorized into two components namely: signal simulation software and signal generation hardware, as shown in Figure 3-13. The signal flow is better understood with explanation of the software first, which generates the required data for the hardware platform to emulate the proposed signal.

3.4.1 Software

At a top level to generate an RF signal, the following three parameters are required: almanac, user position and the system time (Rao et al 2011). With this, the visible satellites list is

generated and signals commensurate to the user position are generated. Figure 3-13 b) shows the top-level flow of the simulation software where a real-time communication between the console (laptop) and the hardware platform exists. As shown in Figure 3-13 a), the signal simulation software runs on a console where the measurement data and the proposed NAV data bits are generated for all the visible satellites every 100 ms.

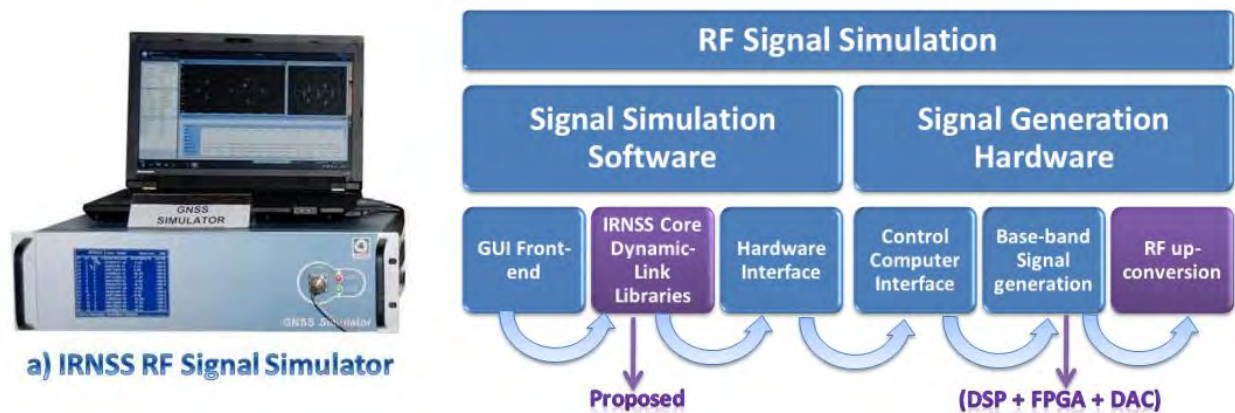


Figure 3-13: a) Test-rig used for proposed IRNSS signal generation b) hardware-software interaction diagram illustrating the signal flow.

The main constituents of measurements are pseudorange and delta-range. To ensure the fidelity of signal generation, the data generated on the console is transacted at 12 Mb/s to the hardware platform. Figure 3-14 shows the top-level flow of the simulation software. Apart from the code phase and Doppler measurements, the proposed NAV data in FSA, TSN and TSF are generated as independent version in correspondence with the bit definitions tabulated in Appendix A, Appendix B and Appendix C, respectively. In addition, the secondary data transmission schemes proposed in Figure 3-6 and Figure 3-7 are used as a reference for data modulation.

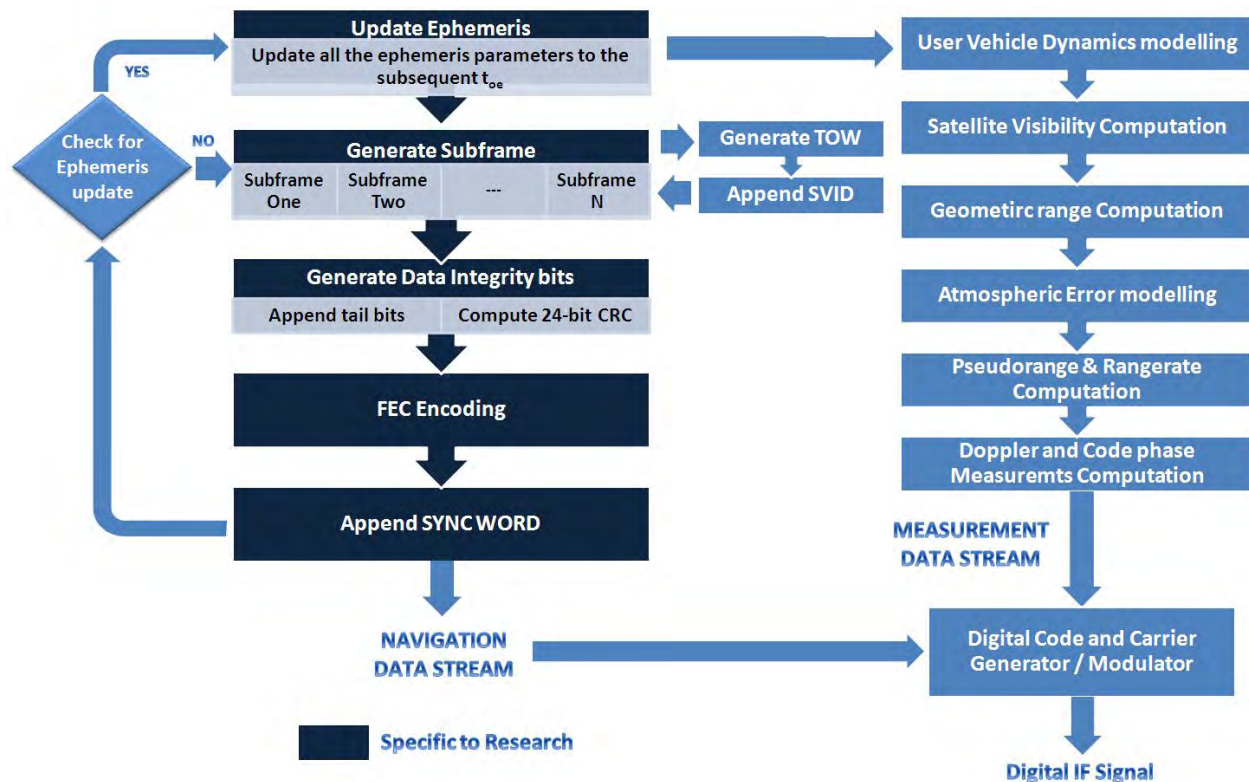


Figure 3-14: Flow diagram of the signal simulation software to generate the proposed IRNSS signals.

3.4.2 Hardware

The objective of this module is to generate RF signals commensurate with the data (measurements and NAV data bits) received from the console. The main components of the hardware platform are FPGA and DSP. The data received from the console by DSP is routed to appropriate channels, where operations dedicated to a specific satellite occur. The resources available in DSP are adequate to handle 45 satellite signals. For IRNSS, each satellite is slotted in a dedicated channel. The operations performed in each channel are as follows: The measurements received from the console are digital data words for a given epoch. Commensurate with this, the signals in the code and carrier dimension for a satellite are estimated in the signal generation hardware. If the previous instant values are available, the difference between the

estimated and the previous instant values is computed. This value is written to the corresponding channel in FPGA (Figure 3-13), where the actual signal generation occurs. The FPGA maintains code generators and Numerically Controlled Oscillators (NCO) dedicated for each channel. These are initialized with values every 100 ms from the DSP. To this, the NAV data signal is modulated to generate the composite IF signal. This IF is subsequently translated to obtain the IRNSS L5 and S1 signals (Eq. (2-1)). The characteristics of the RF signals are given in Table 3-6.

Table 3-6: Signal specifications characteristics used in the simulation of the proposed IRNSS signals.

Navigation Data Specifications	Encoding Scheme: Convolution Encoding, rate $\frac{1}{2}$
	Constraint length: 7
	Generator Polynomial: G1-171o; G2-133o
	Symbol rate: 100 sps
	NAV data bit definitions: Appendix A, Appendix B & Appendix C
Ranging Code Specifications	GPS L1 C/A (1 – 7)
	1023 chips
	1.023 MHz chipping rate
Carrier Specifications	Carrier frequency: L5 – 1176.45 MHz
	2 MHz Bandwidth
	BPSK Modulation
	-157 dBW

3.5 Receiver design

To demonstrate performance improvements, a 78 channel triple RF GPS GLONASS (GPSGL) receiver developed at Accord Software & Systems, as shown in Figure 3-15a), is used as a reference platform to implement the software based on the above proposed signals.

3.5.1 Hardware

The IRNSS RF signal generated at 1176.45 MHz (only L5 is considered for this research) is fed to the RF port of the receiver. Since the receiver has the capability to accept GPS and GLONASS, a mixer and filter combination is used to translate the L5 IRNSS signal to the GPS L1 band. This signal is subsequently down converted, digitized and input to the correlator implemented in FPGA. The correlation values from the FPGA are taken as input to the DSP where further processing such as acquisition, tracking, and data bit demodulation leading to position computation is performed. The signal flow within the receiver is as depicted in Figure 3-15b).

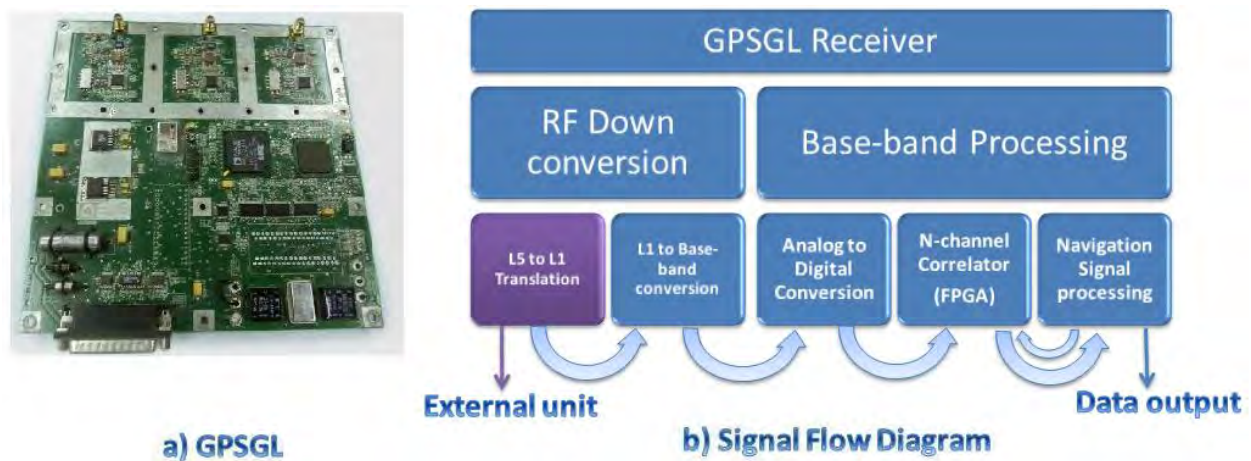


Figure 3-15: Triple RF GPS GLONASS (a) receiver hardware (b) hardware software signal flow.

3.5.2 Software

Figure 3-16 shows a top-level bubble diagram depicting various software modules of the GPSGL receiver, whose functions are commensurate with the theory presented in the previous chapter.

For this research, the modules in blue require minimal modification, if any. The modules in red are rewritten in accordance with the proposed NAV data signal design and mainly resides

(implemented) in DSP. The output on serial link in RS232 format is given to the laptop, where GGVISION is plugged (Figure 2-17). The data logged is used to measure the relative performance of the new scheme with that of the GPS L1. With the GPSGL software shown in Figure 3-16 as a reference, the following paragraphs explain the algorithms specifically implemented to achieve the results in receiver for the proposed signals:

- The data bits from the tracking module are grouped to form 600 symbols commensurate with Figure 3-4. As a first step, the synch pattern is searched in these 600 symbols.
- Following its successful match, the ensuing data symbols are collected and stored.

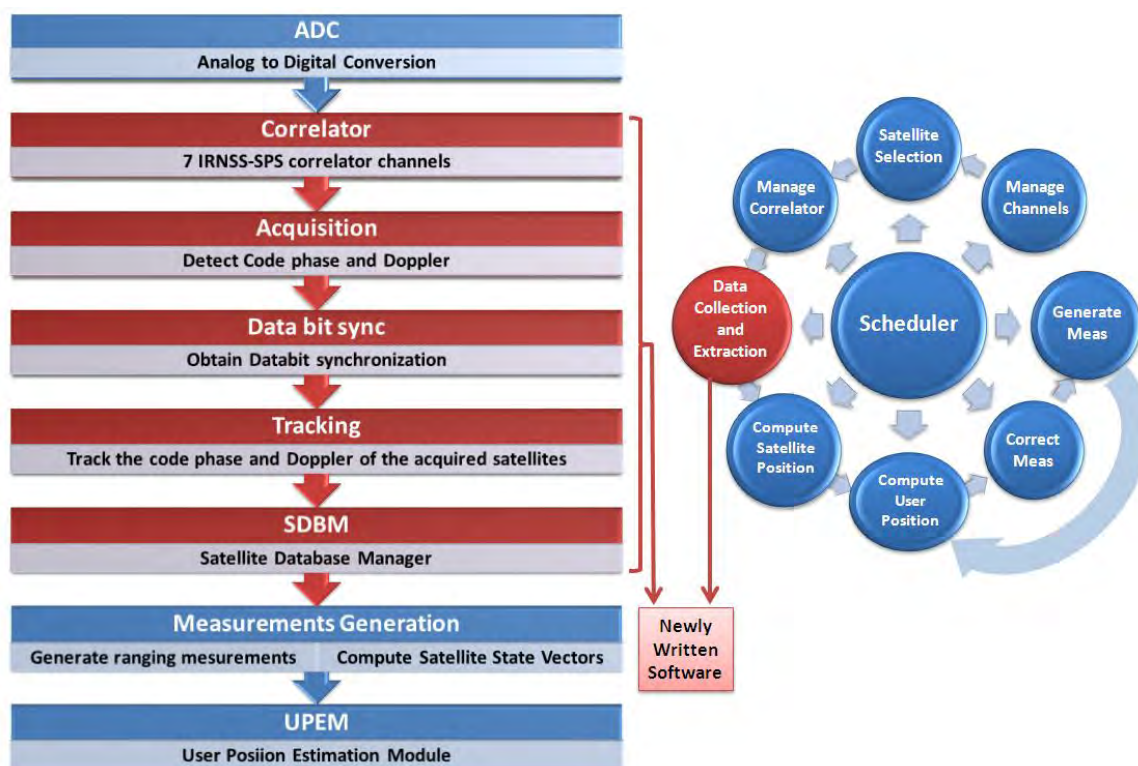


Figure 3-16: High level software flow within GPSGL receiver showing various modules, changes required and the proposed new module.

- With 588 symbols, the Viterbi decoder is invoked to generate the NAV data bits. Subsequently, CRC is computed on the resultant NAV data bits (Figure 3-19).

- Amongst other integrity tests, the differences of subframe id and TOW across consecutive subframe equal to one and six seconds respectively are checked. With these conditions met, subframe synch is declared.
- Based on the subframe id, the data is updated to primary or secondary NAV data buffers.
- Following data collection from all the subframes, ephemeris and almanac collection is declared for a particular satellite. With data from four satellites, the position estimation is performed.

The data bit-synchronization for a channel may occur anywhere in a subframe. From an implementation stand point, it is ideal if the processing started with the synch pattern and subsequently extracts the bits following it as shown in Figure 3-17.

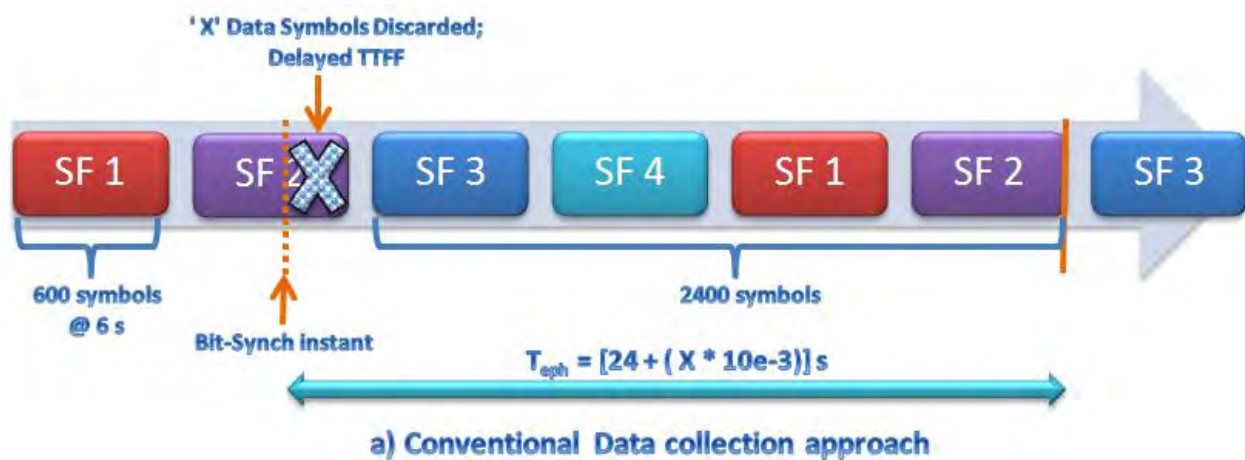


Figure 3-17: Conventional data collection method and its limitations w.r.t TTFF.

However, this delays the NAV data collection (T_{eph}) and in turn TTFF. As an example, assume bit synchronization on the 10th data symbol of subframe-2 after synch pattern. In order to collect ephemeris frames completely, we need to collect SF3, SF4, SF1 and SF2, which amounts to 24 s. In addition, the initial data (5.78 s ((588 – 10) * 10 ms)) post bit-synchronization and prior to

synch pattern (of SF3) delays the TTFF. To counter this, the following scheme where the data bits collected prior to the synch pattern are used for optimizing TTFF is explained:

The data symbols collected before the subframe sync are stored in the receiver. Subframe 1 and 2 repeat every 24 s with only the TOW being different (assuming no new ephemeris upload in between) an internal memory, with a count (initial count) of number of symbols collected. The next three (N+1, N+2 & N+3) subframes are processed as explained earlier and shown in blue in Figure 3-18.

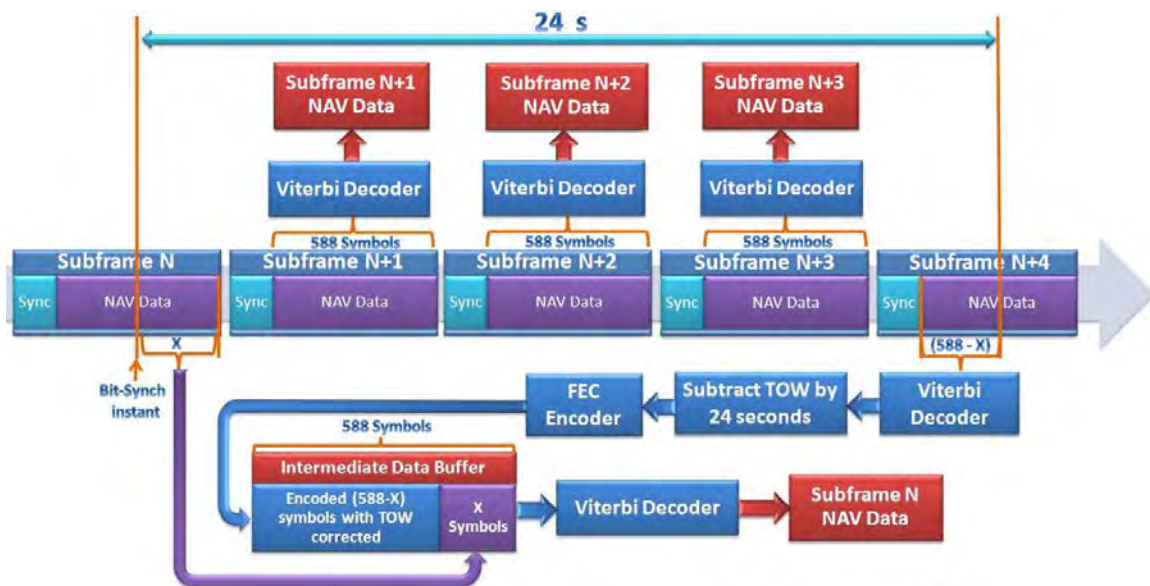


Figure 3-18: Proposed data grouping technique to enhance TTFF with initial bit synchronization occurring in the middle of a subframe.

However, for N+4, only (588-initial count) symbols are collected. To complete the sequence of 588 bits for this partial data, the immediate symbols prior to the synch pattern of (N+4) are extracted, appended to this (588-initial count) and subjected to Viterbi decoding to obtain the data bits. From this, the data bits corresponding to (588-initial count) are extracted which contains the TOW and other bits. With the knowledge that this frame is received 24 s after the partial data, the TOW is subtracted by 24 s, the resulting data bits are encoded and finally

appended with the partial data to form a complete frame. Subsequently, the encoding is performed on this partial data and appended to the initial symbols of subframe N. With this, the data recovery happens within 24 s as opposed to worst case duration of 30 s. This technique typically is applied initially when the satellite enters tracking (purple part of Figure 3-19). Subsequent to data collection, the data extraction follows the synch pattern.

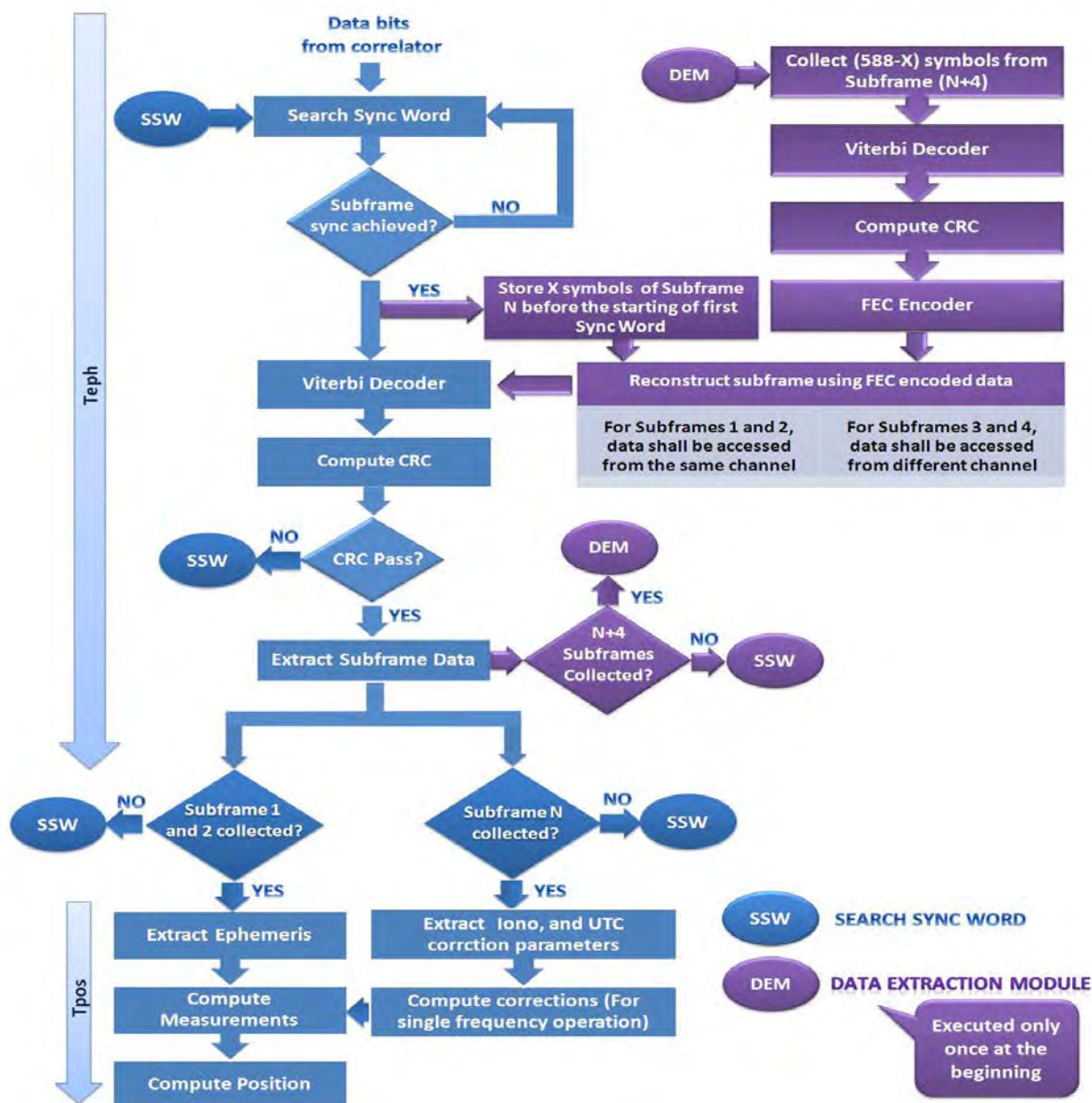


Figure 3-19: New software flow diagram for the proposed IRNSS signals.

Extending the above technique to the proposed secondary data transmission, the system data is collected from all the visible satellites simultaneously. The satellites which are programmed in dedicated channels post subframe synchronization collect the straddled data. From an implementation perspective, the (588-initial count) data of a channel is appended with the partial data collected from the previous channel (secondary data straddled across satellites in time). This arises due to satellite data straddling for the secondary NAV data. With all seven satellites, the data collected from subframe 3 and 4 results in an entire NAV data from IRNSS.

To test and demonstrate the improvements, four versions of software are implemented: (1) to compare the performance with GPS L1, the existing GPSGL software is modified for a seven-satellite GPS configuration, (2) a seven-channel IRNSS receiver with a proposed FSA (3) a seven-channel IRNSS receiver with a TSN architecture and finally (4) TSF NAV data streaming.

3.5.3 Analysis of the proposed signal (implementation merits) w.r.t TTFF

The proposed NAV data structure (Figure 3-8 & Figure 3-9) for IRNSS w.r.t data integrity has the following characteristics: without data interleaving, the presence of tail bits and synchronization bits are not encoded. Though some of these features are inherited from GPS L5 & GALILEO E1, the following section explains its uniqueness from a TTFF perspective:

3.5.3.1 Interleaving

With bit-synchronization in the middle of a subframe, the data grouping across subframes ensures complete data extraction within 24 s (Figure 3-18). However, with data interleaving this scheme is not applicable and necessitates the entire subframe to be collected, which slows down the TTFF as in GALILEO E1. This limitation stems from the de-interleaving, which is

performed prior to Viterbi decoding. This inherent problem associated with interleaving increases data latency as explained in Figure 3-20.

With the entire data symbols, interleaving is performed as 84 rows and 7 columns (for example, (Galileo 2008)), encoded and finally transmitted from the satellite. At the receiver, reverse operation of de-interleaving, decoding and CRC computation are performed. However, bit synchronization in the middle of a subframe as shown in Figure 3-20 affects the de-interleaving operation (due to a change in data (TOW) across subframes). This nulls the advantage of Figure 3-18 and affects the TTFF. To optimize the TTFF, interleaving is not adopted as in SBAS or GPS L5 ((DO-229D 2006), (ICD-GPS-705 2002)).



Figure 3-20: Data symbols populated in rows and columns and a scenario where partial interleaved symbols are collected in a receiver.

3.5.3.2 Tail bits

Eq. (3-8) can be reasoned with and without tail bits as shown in Figure 3-21. The tail bits consist of six zero-value bits (with 7-bit constraining) enabling completion of the FEC encoding of each subframe. Though these bits are an overhead from a transmission perspective, they bring the decoder to initial state at the end of each subframe. With this, the data collected after sync

pattern are easily decoded. With this scheme, the data grouping technique (Figure 3-18) is possible. Without tail bits, the Viterbi decoder has to initially build history (reset of the decoder is not possible), following which decoding will be successful. This overhead on bits collected prior to the sync pattern coupled with the errors due to initial unknown state of the decoder (till history of the decoder is established) delays the TTFF.

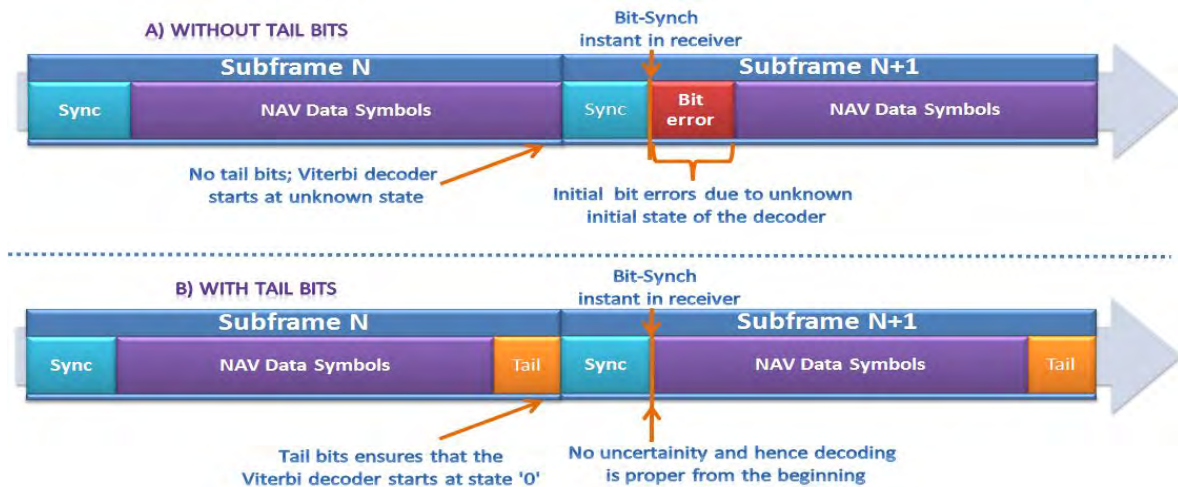


Figure 3-21: Subframe processing from a TTFF perspective (a) without tail bits and (b) with tail bits.

3.5.3.3 Synchronization pattern

As per Eq. (3-9), synchronization pattern is adopted for each subframe. The design problem is whether or not these bits need to be encoded. The data grouping technique (Figure 3-18) works effectively under the assumption of synch pattern not being encoded. However, if the synch pattern is encoded, the first operation after collection of 600 symbols is its decoding. If the initial bit synchronization occurs in the middle of a subframe, synch pattern may not be successfully detected until the decoder builds some history. This necessitates Viterbi decoding to be *invoked multiple times* till the decoder builds history after which the synch pattern is detected. Figure

3-22 shows the methodology to decode with synch pattern encoded. It takes relatively *higher computation resources* to extract the NAV data bits compared synch pattern without encoding.

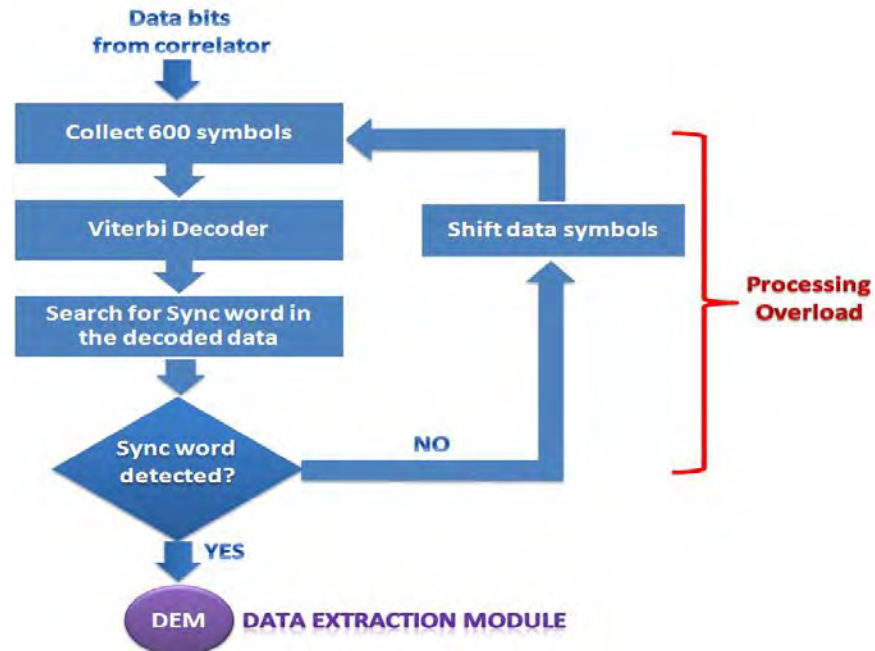


Figure 3-22: Flowchart for subframe synchronization with synch pattern encoded and its overhead.

3.6 Test methodology and performance analysis

The signal generator and receiver described in the previous sections are used to test the proposed signals. Figure 3-23 shows the test set-up used to demonstrate the performance improvements. Corresponding to the receiver software versions, four independent simulation suites are created as follows:

- IRNSS with NAV data as in GPS L1. This is used as a reference to compare the performance of the proposed signals.
- FSA
- TSN
- TSF

In addition, the secondary data commensurate with GPS L1 on seven satellites for first (Appendix A) and as per the proposed configuration for the rest (Figure 3-7, Figure 3-10, Figure 3-11) of the simulations are implemented.

3.6.1 Procedure

The signal from the simulator is input to the receiver through an LNA. The signal settings of the simulator are in lines with Table 3-6. The receiver output is connected to a console with the GGVISION to log and profile the receiver performance as shown in Figure 3-23. The primary objective is to demonstrate the benefits achievable from the proposed signal w.r.t T_{eph} and T_{sec} specifications in IRNSS.

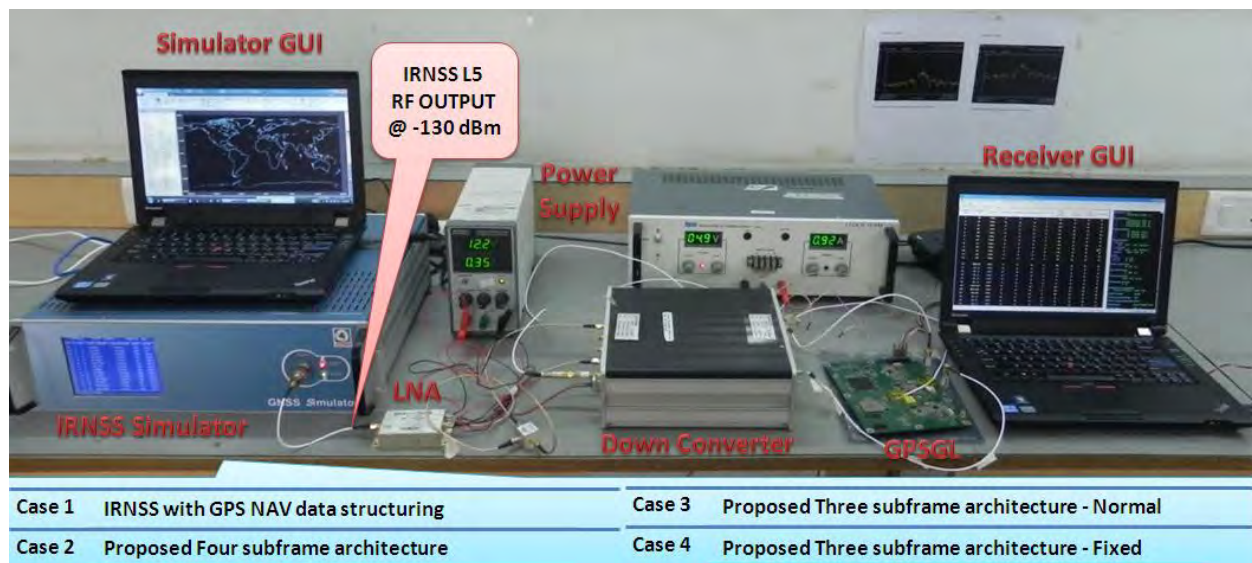


Figure 3-23: Test apparatus for the validation of the proposed IRNSS signals.

To measure the performance of T_{eph} - a satellite specific parameter, dedicated counters are maintained and initialized post bit-synchronization. From an analysis point of view, the maximum T_{eph} is profiled. Similarly, T_{alm} - a receiver global parameter indicates the availability of almanac from all the satellites. With bit-synch of all the satellites, a counter is initialised to profile the time taken to collect almanac. In addition, to illustrate performance improvement, the

simulator is enabled with an Ionosphere error based on the Klobochur model and all other errors are disabled. The time to collect and apply Ionosphere corrections leading to accurate position is profiled with the receiver's altitude plot.

The experiments in each scenario are carried about 50 times to ensure all possibilities w.r.t the initial lock occurring on different subframe id are captured. In addition, the receiver is operated in the cold start mode of operation.

3.6.2 GPS L1 NAV data in IRNSS

The simulator and receiver combination are tested in seven satellite configurations with GPS L1 NAV data. From the logged T_{eph} and T_{alm} data, the worst case results are 30 s and 192 s, respectively. The T_{eph} is attributed to an initial lock on the 4th subframe. T_{alm} is attributed to the collection of seven almanacs and one UTC-IONO/Health (validity of almanac) page. These results are used as a reference to compare the results of the proposed approaches.

3.6.3 FSA

The simulator-receiver combination is tested with FSA data streaming. The T_{eph} measure as a function of subframe synchronization achieved on various subframes (id) is shown in Figure 3-24. The worst-case TTFF measure corresponds to a lock of initial subframe with the fourth sub-frame as shown in Figure 3-24. The overall improvement is attributed to the reduced T_{eph} , which effectively translates to a 20% improvement in TTFF for a single frequency user. This is the best result to date, compared with existing operational GNSS systems.

The analysis of T_{alm} is as follows: with position estimation, receiver initially had errors attributed to the simulated ionosphere component. Subsequent to collection of ionosphere correction terms, the error is estimated and the navigation solutions resulted in improved accuracy. Figure 3-24

illustrates the altitude plot obtained with GPS L1 and from four subframe NAV data streaming of IRNSS.

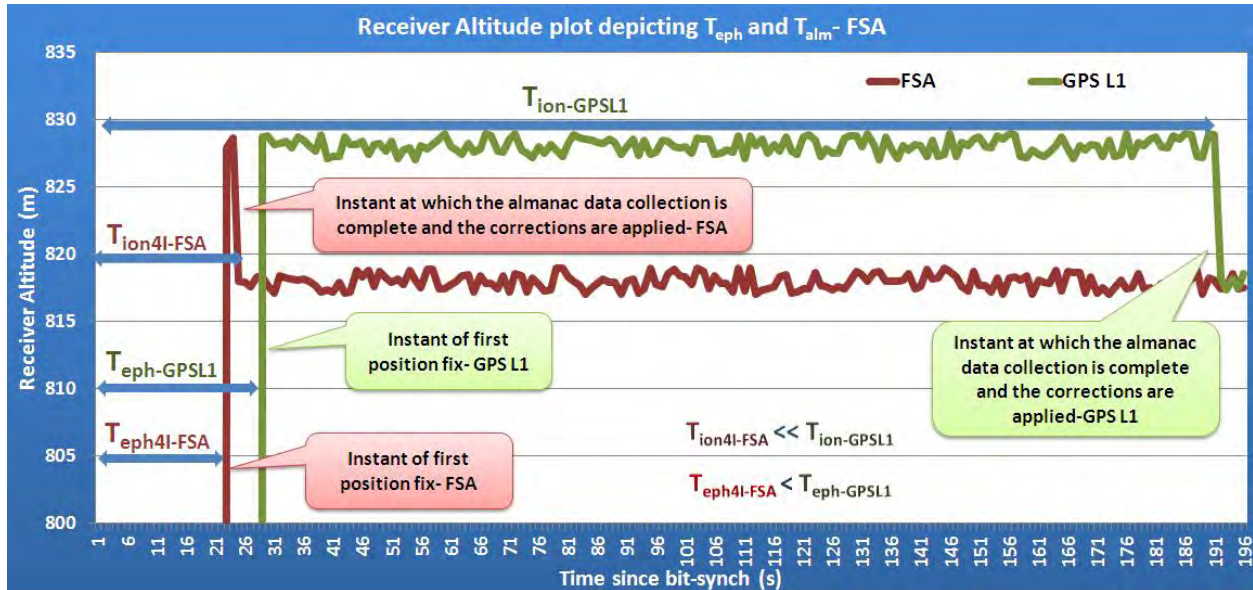


Figure 3-24: Altitude plot illustrating time required to collect ephemeris and almanac in FSA of IRNSS post bit synchronization.

It is observed with the proposed scheme that an *87% improvement in collection time and application of ionosphere corrections* occur, as compared to corresponding GPS L1 results.

3.6.4 TSN architecture

The signal generator and the receiver were modified for TSN data streaming and tested. Figure 3-25 shows the altitude plot of the receiver, which captures the reduction of ephemeris collection time, application of ionosphere corrections and almanac collection time and contrast with GPS L1.

It is clear from Figure 3-25 that the worst case TTFB performance has improved by 12 s w.r.t GPS L1. In addition, Ionosphere corrections are applied within 18 s, a 6 s improvement compared to four-subframe streaming. However, the almanac collection is delayed by 12 s compared to the four-subframe method.

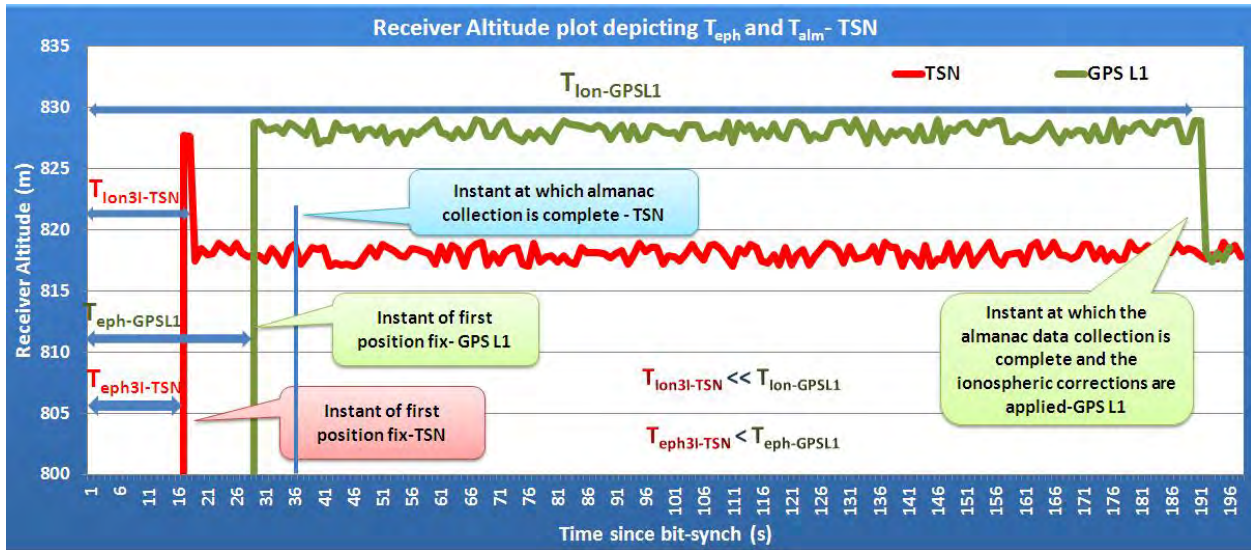


Figure 3-25: Altitude plot illustrating time required to collect ephemeris and almanac in TSN architecture of IRNSS post bit synchronization.

3.6.5 TSF

Finally, the simulator and the receiver are configured for three subframe fixed NAV data streaming. Figure 3-26 shows a 60% improvement in TTFF performance as compared to GPS L1.

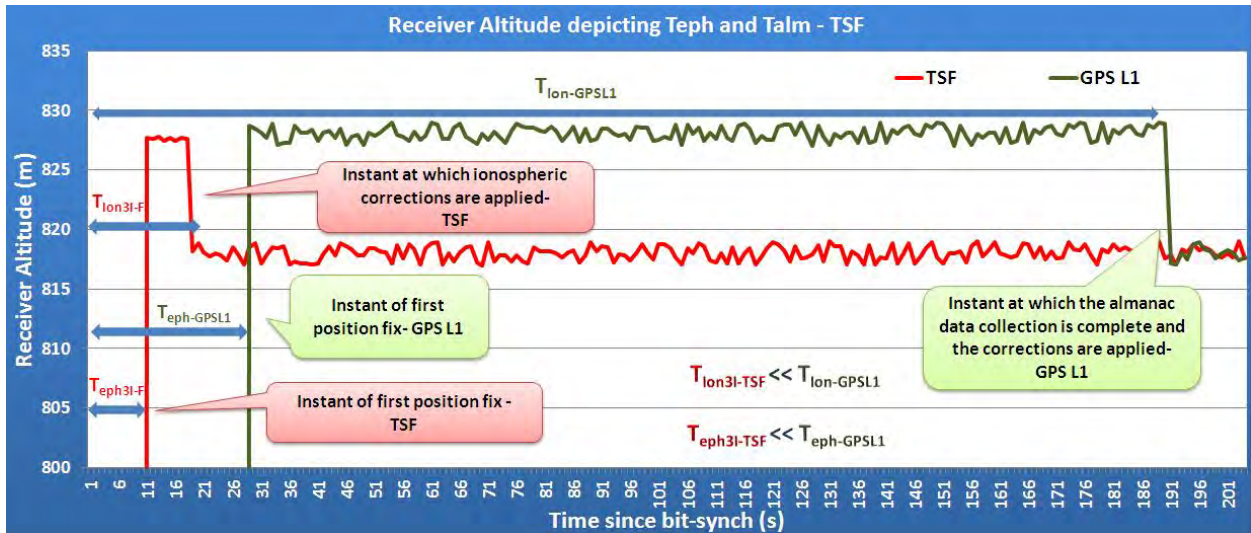


Figure 3-26: Altitude plot illustrating time required to collect ephemeris and almanac in TSF architecture of IRNSS post bit synchronization.

At the same time, the UTC and Ionosphere correction terms are collected within 18 s, similar to TSN method. For a single frequency GNSS system, this is the best TTFF result achieved to date. Table 3-7 gives the time taken to obtain the primary parameters as a function of subframe id whereas

Table 3-8 provides the summary of the results for the three methods of NAV data streaming and compares the results with GPS L1.

Table 3-7: Summary of ephemeris collection time in various proposed methods of IRNSS with bit-synchronization on the first bit of a subframe.

Subframe ID at Subframe Synch	Ephemeris Collection Time (T_{eph}) [s]			
	FSA	TSN	TSF	GPS Five Subframe Architecture
1	12	12	12	18
2	24	18	12	30
3	24	18	12	30
4	18	-	-	30
5	-	-	-	24

Table 3-8: Comparison of primary and secondary parameters performance in proposed methods.

Parameter	GPS-L1 (s)	FSA (s)	TSN (s)	TSF (s)
$T_{eph} / TTFF$	30	24	18	12
T_{alm}	192	24	36	-
$T_{iono-utc}$	192	24	18	18
T_{mt}	-	24	36	-

3.7 Summary

In this chapter, the NAV data structures of various GNSS constellations were presented. The limitations in achieving a short TTFF and time required to collect secondary parameters were highlighted. Following this, with necessary assumptions a proposed NAV data structure (subframe) was derived. Subsequently, a new method of data streaming for the secondary parameters was proposed for IRNSS. Further, three new methods specifically w.r.t NAV data

transmission for IRNSS were derived with a discussion of the effect of a global extension of IRNSS. Towards this, new software for signal generation and receiver commensurate with the proposed signal design were implemented. Experimentally, with simulator and receiver hardware, the results were established. It was shown that these proposed methods enhanced primary and secondary NAV data transmission. Thus, TTFF specifications and parallels were drawn with the existing system. Table 3-9 summarizes the proposed signals w.r.t primary and secondary data collection, and possible global extension.

Table 3-9: Summary of the proposed methods in comparison with GPS L1 C/A.

Parameter	FSA	TSN	TSF
Assumption	None	None	Secondary parameters are restricted to UTC and Ionosphere terms only
$T_{\text{eph}}/TTFF$	20% improvement	40% improvement	60% improvement
T_{alm}	87% improvement	82% improvement	Not Applicable
Global Extension of IRNSS	Possible	Possible	Possible

It is clear from Table 3-9 that the TTFF and the time required to collect the secondary parameters based on the proposed signals are best till date in a single frequency mode of receiver's operation. The following chapter explores methods for signal transmission assuming receiver operating in diverse modes (dual frequency/service).

Chapter Four: DIVERSITY BASED SIGNAL DESIGN FOR TTFF IN IRNSS

With the results from the previous chapter, the partially populated TTFF representative datasheet for a single frequency IRNSS receiver (with 7 channels) is as shown in Table 4-1. Assuming civilian ranging codes on both frequencies of IRNSS, 14 channels are essential for dual frequency of operation. Hence, additional 14 channels are required to augment restricted signals. Thus to operate concurrently in both services and frequencies, 28 channels are required. With proposed single frequency NAV data structures as reference and assuming receivers operating in dual frequency/service, this chapter focuses on evolving NAV data signal transmission methods. Specifically, the research focuses on NAV data signal design based on diversities of code and carrier components of the signal in order to improve the TTFF performance of civilian and restricted receivers.

Table 4-1: Representative datasheet of a receiver w.r.t TTFFs in IRNSS single frequency mode of operation.

Service Frequency	TTFF (IRNSS)		Hot Start of GNSS using IRNSS (s)
	Civilian (s)	Restricted (s)	
Single	12* / 18	?	?
Dual	?	?	?

* No Almanac / Secondary data

First, top level signal processing in a dual frequency receiver is presented for civilian and restricted signals. Following this, the existing signals are characterized (TTFF) in dual frequency mode of receiver operation on both services elaborating in detail their limitations w.r.t to TTFF. Next, with necessary assumptions, three new methods based on diversities of code or/and carrier, NAV data signal transmission are derived. The proposed methods are applied to four subframe

methods of NAV data architecture (established in previous chapter) to establish the achievable TTFF results. Following this, the signal simulation methodology and the commensurate receiver design are explained in detail. With test methodology and results, analysis of the achieved results and its benefits w.r.t TTFF are elaborated and compared with GPS L1/L2 civilian and restricted signals.

4.1 Overview of dual frequency processing

The single frequency receiver operation presented in Chapter Two is generic and applicable to any GNSS signal. However, with the second and additional frequencies (for example, L2C, L5, L1C in GPS) (Figure 4-1), necessary augmentations need to be applied to various sections of the receiver (Figure 2-13) to optimize and leverage the benefits. In addition, with the restricted signals (P and M codes on L1/L2), additional implementation aspects need to be addressed in the receiver design.

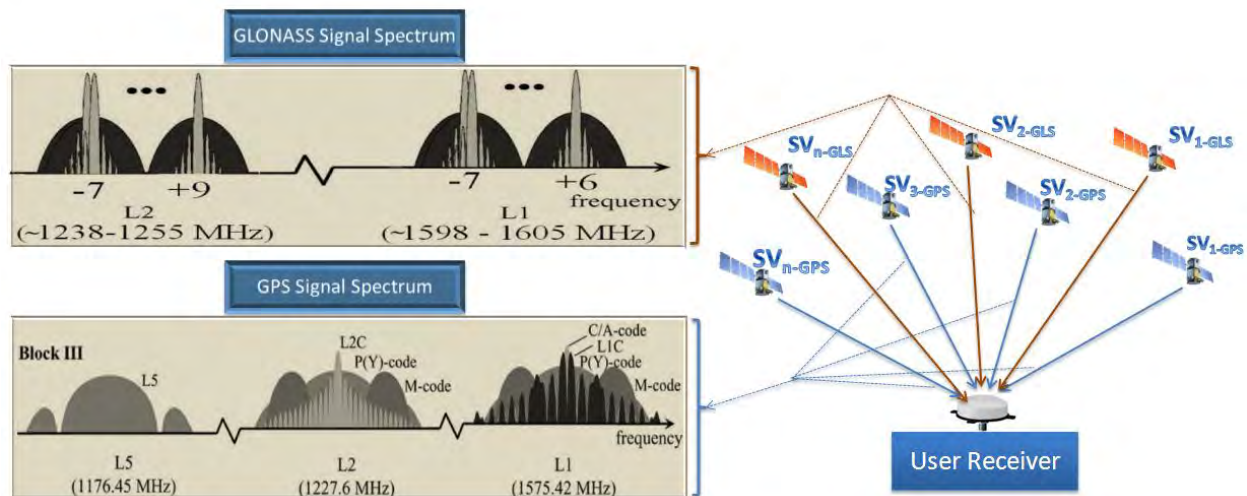


Figure 4-1: Signals transmitted from GPS/GLONASS satellites.

This section explains the receiver operations capturing the above mentioned points in dual frequency mode of operation w.r.t civilian signals. Further, with the available open source

information on restricted signal processing, the necessary architectural modifications are presented. The main objective of this explanation is to highlight the limitations in existing signals from a dual frequency and service point of view w.r.t TTFF.

4.1.1 Civilian signal

The composite signal from a GPS satellite to a user antenna is as shown in Figure 4-1. The standalone receiver operations on the individual frequencies L1/L2C (considered for explanation) are similar to those explained in Chapter Two. However, from a dual frequency perspective, modifications need to be applied in the following stages of the receiver: acquisition, tracking, measurements and navigation, as explained in the following paragraphs.

4.1.1.1 Acquisition

From a user perspective, the signal received at the antenna will have nearly the same Doppler (except for the ionosphere component and the relative delay (L1/L2C) in the satellite hardware (for example, the group delay variation across frequencies)). The civilian ranging codes on L1 and L2C are different. *Since signals originate from the same satellite*, (typically) the receiver detects one frequency and, with the estimates (Doppler & code phase), establishes a direct lock on the second frequency (Borio 2008). With the input that the Doppler measurements are nearly the same, an optimal technique needs to be evolved to estimate the code phase of the second frequency. To accomplish this, a relation between the ranging codes is established for each code shift and stored in the BPU's (explained in Chapter Two) memory of the receiver. This technique effectively optimizes the resource requirements (acquisition part of BPU) and further reduces the acquisition time of the second frequency (due to longer code length on second). To accomplish

these, the changes as indicated in the Figure 4-2a) are generally employed in dual frequency receiver architectures on the second frequency path.

4.1.1.2 Tracking

Following acquisition commensurate with the Signal in Space (SiS) characteristics, data-bit detection and tracking are performed resulting in NAV data bits from the second frequency. Based on the data integrity algorithm (for example, CRC or parity), data grouping is performed to obtain the primary and secondary NAV data from each frequency path of the satellite. With the system time, measurements and satellite state vector computations are performed.

4.1.1.3 Measurements

The major error contribution in a single frequency measurement is the ionosphere, which is estimated based on the correction terms transmitted as a part of the NAV data. With second frequency and thus measurements, direct estimation of the ionosphere delay is possible resulting in relatively accurate measurements (Ray & Cannon 2000). To accomplish this, the changes as shown in Figure 4-2b) are employed in a dual frequency receiver.

4.1.1.4 Navigation solution

With the measurements available from the L1 and L2 paths, independent positioning is possible. In addition, corrected measurements (in combined mode) are used to obtain relatively accurate navigation solution. The advantage of this solution is any residual error due to the ionosphere model in single frequency is eliminated (Parkinson & Spilker 1996). To accomplish this, the changes shown in Figure 4-2c) are performed.

The above explanation is equally applicable for the additional frequencies when added in the receiver (for example, L5 or L1C and across GNSS systems GALILEO E1/F1 or GLONASS L1/L2 or IRNSS L5/S1).

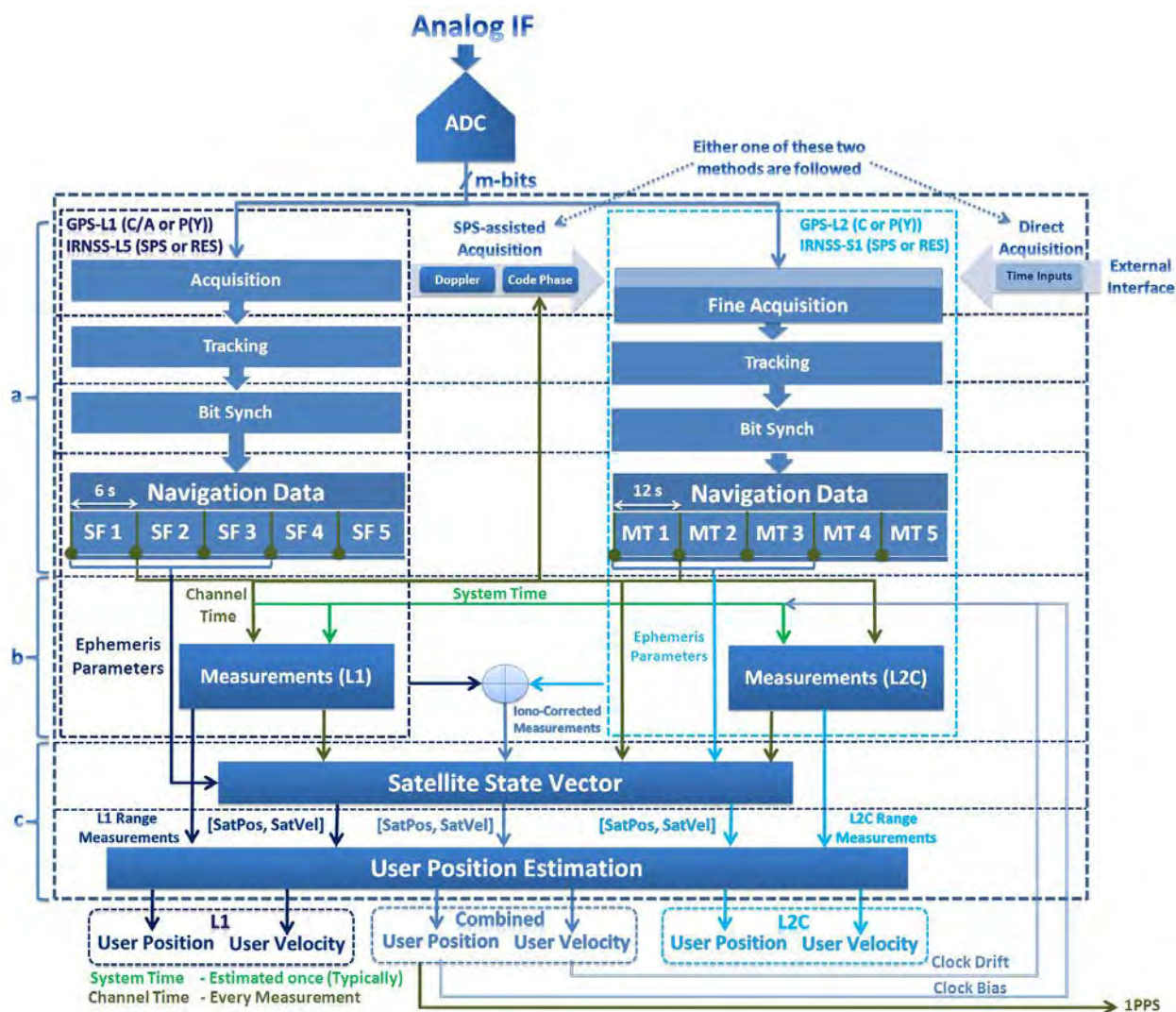


Figure 4-2: Design augmentations necessary to adapt a single frequency receiver for optimal processing of dual frequency signals and leverage advantages.

4.1.2 Restricted signals

With the signal design (w.r.t TTFB) for IRNSS restricted signals being one of the research objectives, this section introduces some concepts specific to restricted signal processing (as

available from open source) w.r.t GPS and GLONASS. First, the need and the salient features of restricted signals are presented.

4.1.2.1 Needs and benefits

When the signal design of GPS was formulated, major requirements of specific users were relatively high anti-jam margins, counter measures against spoofing and accuracies better than civilian users. The first requirement is attributed to the intentional jamming prevalent during militarily perturbed times. The second arises due to the intentional radiation of GNSS like fake signal to mislead users (Nielsen et al 2011). Finally, the results obtained during the initial trials of the GPS concept with civilian code demonstrated 20 m (1 sigma) positioning accuracy. This mandated the accuracies achievable from restricted signals to be better than that of civilian signals (Parkinson & Spilker 1996).

The L1 C/A signal is 10 bit long, clocked at 1.023 MHz and modulated with 50 Hz data. The signal at the user antenna is buried in noise, which is detected post correlation. The correlation introduces a Processing Gain (PG) that for the C/A signal is given by (Doberstein 2012)

$$PG = 10 \log (2 \text{ MHz} / 100 \text{ Hz}) \approx 43 \text{ dB.} \quad (4-1)$$

The P-code of GPS is one week long and clocked at 10.23 MHz. This signal is further modulated by a classified Y-Code to generate P(Y) code, which is accessible only to authorized users (GPS ICD 2010). Further, the code is modulated with NAV data (50 Hz) to generate the composite signal. Applying Eq. (4-1), the processing gain of P(Y) code is 53 dB, which results in an additional 10 dB jamming margin compared to the civilian signal and thus satisfying the first criterion of restricted signals.

To spoof a signal, its characteristics w.r.t code, data and carrier need to be known (Tippenhauer et al 2011). As mentioned, the P(Y) code is encrypted and its information is not available in the public domain. Thus, the second requirement from a signal design perspective is implicitly achieved by P(Y) code.

Finally, with dual frequencies and chipping rate of 10.23 MHz, restricted receivers are able to achieve ionosphere delay estimation and inherent robustness w.r.t multipath (due to the high chipping rate). This contributes to improved measurements and thus, better navigation solutions (Van Dierendonck 1994).

The concepts explained under dual frequency civilian signal processing are equally applicable to the restricted signals. However, the long code sets an inherent design constraint (for SPS, the ranging codes are short and in comparison, acquired easily) on its acquisition, which is explained in the following section.

4.1.2.2 SPS assisted acquisition

P(Y) code being one week long, acquisition is a computationally intensive operation. To counter this, receivers are assisted with an estimate of time corresponding to which the receiver generates the local code replica (E, P and L) and attempts to detect the signal. A chipping rate of 10.23 MHz (about 100 ns signal dwell time in a chip which repeats after one week) requires that the time information be precise barring which the search time will be large or detection may not be possible. In addition, this precise time estimate may not be always available and in some cases it may not be practical to feed-in either (for example, Figure 1-1). To obviate this, GPS restricted receivers first track the SPS signal and obtain the time information from the HOW. With this as a pointer to a memory in BPU containing the pointer to the P(Y) polynomial coefficients (Figure

4-3), enables signal acquisition (Kaplan & Hegarty 2006). This eliminates any dependency on external time input or its correctness (for example, manual entry in handheld mode). This technique is termed *SPS assisted acquisition* of restricted signals.

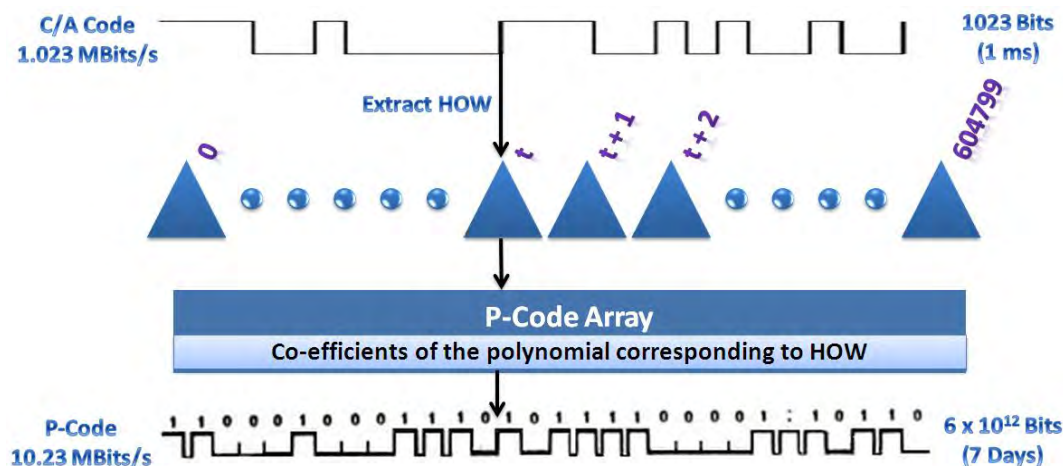


Figure 4-3: Illustration of P-code acquisition based on HOW assistance from SPS.

4.1.2.3 Direct acquisition

An alternate approach is to directly acquire the code assuming it to be relatively short as in the GLONASS high precision signal, which is 6.566 s (Rosbach 2000). This code is acquired with a technique similar to that explained in Chapter Two. However, the complexity of the correlator design is enormous (detailed later) without any assistance from the civilian signal.

4.1.3 TTF characterization

Following the above explanation, the next step is to characterize these signals from a TTF perspective.

4.1.3.1 Civilian signal

As derived and explained in Chapter Two, the TTF from GPS L1 SPS (neglecting the boot and with an implicit assumption of summation on “n” visible satellites) is given by

$$TTFF_{l1_sps} = T_{a-l1} + T_{bs_l1} + T_{eph_l1} + T_{pos_l1} \quad (4-2)$$

With acquisition estimates from L1 and its known relation to L2, the achievable TTFF from the L2 signal is given by

$$TTFF_{l2_sps_al1} = T_{bs_l2} + T_{eph_l2} + T_{pos_l2} \quad (4-3)$$

where $TTFF_{l2_sps_al1}$ is the TTFF on the L2 SPS signal assisted from L1. With the input that TTFF is dictated by T_{eph} , neglecting other terms (for example, assuming massive correlator on one frequency), the optimal TTFF in dual frequency mode of receiver operation is given by

$$TTFF_{opt_sps_dual} = \min(T_{eph_l1}, T_{eph_l2}). \quad (4-4)$$

Generalizing Eq. (4-4), the optimal TTFF in the dual frequency mode of receiver operation is given by

$$TTFF_{opt_f1_f2} = \min(T_{eph_f1}, T_{eph_f2}). \quad (4-5)$$

The following inferences based on the NAV data/rate in dual frequency of operation can be deduced from Eq.(4-5):

- First, if the data rate and the contents are similar, the achievable TTFF remains the same as in the single frequency civilian mode of operation (Eq.(2-18))
- Second, if the data rates are different with the data being the same, the TTFF corresponding to the maximum data rate results in the best TTFF.
- Finally, if data and rate are different, the one that transmits T_{eph} faster has the minimum TTFF.

4.1.3.2 Restricted signals

Applying the concepts explained for the acquisition of restricted signals, the TTFF from a single frequency restricted signal with SPS assistance is given by

$$TTFF_{l1_res_sps_aid} = T_{(a-sps)l1} + T_{bs_l1} + T_{HOW_l1} + T_{(a-res)l1} + T_{bs_res_l1} + T_{eph_l1} + T_{pos_l1} \quad (4-6)$$

where $TTFF_{l1_res_sps_aid}$ is the TTFF of the restricted signal with aiding from SPS. $T_{(a-sps)l1}$, T_{bs_l1} and T_{HOW_l1} are the acquisition time, bit-synchronization and the time required to achieve the subframe synchronization of SPS L1 respectively. $T_{(a-res)l1}$ is the fine acquisition performed from the estimates of its SPS L1 channel, specifically from the HOW word as explained in Figure 4-3. The remaining terms are as explained in Chapter Two for the civilian L1 signal Eq. (2-18). Thus the TTFF of a single frequency restricted signal with assistance from SPS is an extension of results obtained in Chapter Three, which when generalized is given by

$$TTFF_{res_sps_aid} = TTFF_{sps} + T_{HOW}. \quad (4-7)$$

The L2 restricted signal on GPS has the provision to transmit the data (Kaplan & Hegarty 2006). During transmission, the TTFF derivable from L2 is given by Eq. (4-6) as

$$TTFF_{res_sps_aid_l2} = T_{bs_res_l2} + T_{eph_l2} + T_{pos_l2} \quad (4-8)$$

Similarly, in the direct mode of restricted signal acquisition (for example, in GLONASS), the TTFF characterization follows (Eq.(2-18)) as

$$TTFF_{res_direct_l1} = T_b + T_{a-p(y)} + T_{bs_res} + T_{eph_l1} + T_{pos} \quad (4-9)$$

where $T_{a-p(y)}$ is the time required to acquire the restricted signal on L1. Extending this to the dual frequency mode of operation, Eq. (4-5) is equally valid.

4.2 Limitations in existing dual frequency GNSS w.r.t TTFF

With the above understanding, this section presents the limitations of signals from a TTFF perspective in dual frequency services considering GPS and GLONASS.

4.2.1 Civilian signal

Figure 4-1 shows the current signals from a modern GPS satellite, which comprise L1, L2C, L5 civilian and L1/L2 P(Y) and L1/L2 M-code restricted signals. From a user perspective, $d(t)$ – (Eq. (2-1)) the NAV data transmitted on different frequencies effectively provide similar information (specifically primary parameters) of the satellite. For example, ephemeris and satellite clock corrections, which constitute primary parameters, are the same but broadcast differently based on optimization, coding (Figure 3-1, Figure 3-2) or the data rate as shown in Figure 4-4.

The above explanation is equally applicable to GLONASS, which supports data on both frequencies (Rosbach 2000). Rewriting Eq. (4-5) for GLONASS results in

$$TTFF_{opt_gl} = \min(T_{eph_l1}, T_{eph_l2}). \tag{4-10}$$

With the information that data available on both frequencies are identical, the optimal TTFF for GLONASS or in general for any dual frequency system with identical data can be shown as

$$TTFF_{opt_f1_f2} = T(eph_{f1}, eph_{f2})/2 \tag{4-11}$$

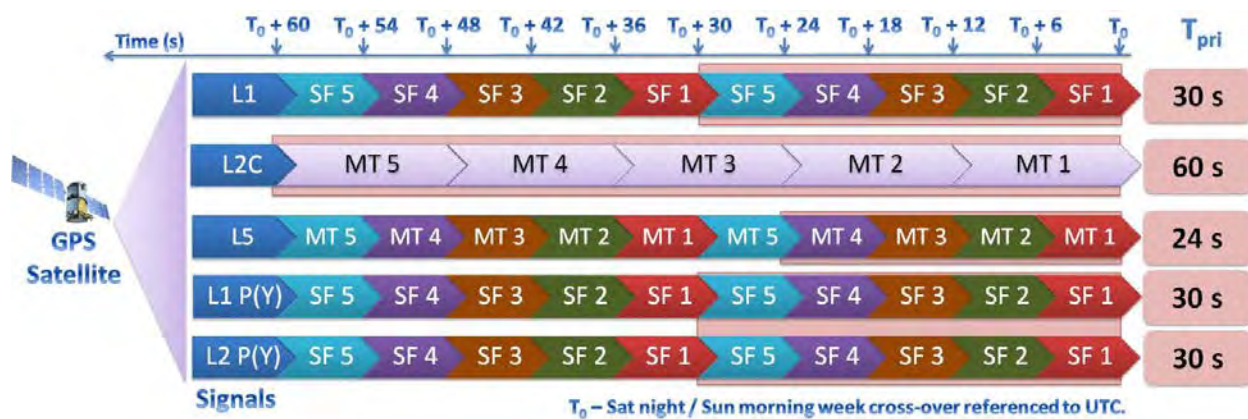


Figure 4-4: NAV data streaming on GPS L1 C/A, L5 and L2C and their transmission periods.

Extending, the above results are applicable to secondary parameters as well. Based on the analysis of datasheets available from receiver manufacturers and from the ICD of GPS and GLONASS, the time associated with primary and the secondary parameters in various combinations (dual frequency) are as shown in Table 4-2. In addition, Table 4-2 illustrates the analysis of Eq. (4-5). This research attempts to propose a signal design in IRNSS based on the signals derived in Chapter Three to overcome the above limitation.

Table 4-2: Summary of the achievable TTFF and secondary data collection in civilian dual frequency of operation for various combinations of existing operational systems, post bit synchronization.

Parameter	GPS- L1/L5 (s)	GPS-L1/L2 (s)	GPS-L5/L2 (s)	GLONASS-L1/L2 (s)
$T_{\text{eph}} / \text{TTF}$	24	30	24	30
T_{alm}	576	750	576	150
$T_{\text{iono utc}}$	96	750	96	150
T_{mt}	As required	-	As required	-

4.2.2 Restricted signal

In addition to three civilian signals, a GPS restricted receiver will have access to 4 additional signals - P(Y) code and M code on L1/L2 (GPS ICD 2010) as shown in Figure 4-1. Considering only the L1/L2 signal components, the signal is given by

$$\begin{aligned}
 Y(t) = & A_{L1}r_{L1}(t)d_{L1}(t) \cos(2\pi f_{L1}t) + A_{L1,P}r_{L1,P}(t)d_{L1,P}(t) \sin(2\pi f_{L1}t) \\
 & + A_{L2c}r_{L2c}(t)d_{L2c}(t) \cos(2\pi f_{L2}t) + A_{L2,P}r_{L2,P}(t)d_{L2,P}(t) \sin(2\pi f_{L2}t)
 \end{aligned}
 \tag{4-12}$$

Extending the explanation presented in civilian signals, two possible scenarios arise:

- First, with GPS transmitting NAV data on both the L1 and L2 signals, the argument presented under civilian signals is applicable to restricted signals as well:

$$TTF_{\text{opt_gps_res_l1_l2}} = T(\text{eph_f1}, \text{eph_f2})/2
 \tag{4-13}$$

- Second, with the analysis on datasheets of receivers supporting GPS restricted signals, the cold start TTFF is commensurate with the results shown in Table 4-2. In addition, there is no distinction w.r.t civilian or restricted signal achievable TTFF or on frequencies (for example, dual/triple). With Eq.(4-7) and results as tabulated in Table 4-2, it is assumed that in the cold start mode of receiver operation with SPS assistance, the TTFF of a restricted GPS L1/L2 receiver is

$$TTFF_{dual_res_sps_aid} = TTFF_{sps_dual} + T_{HOW_l1} \quad (4-14)$$

- SPS assisted signal acquisition necessarily needs to establish subframe synchronization following which HOW word is extracted. Subsequently, the NAV data is collected from restricted signals. Extending this, the optimal TTFF of restricted signals in *single frequency of operation* in GPS is given by

$$TTFF_{opt_gps_res_l1} = \min(T_{sps_l1_eph}, T_{res_l1_eph}). \quad (4-15)$$

A possible *diversity between the NAV data of SPS and restricted signals* can be exploited to achieve similar results as in Eq. (4-13).

Direct acquisition of restricted signal results in a similar TTFF as depicted in Eq. (4-9). However, the time required to acquire restricted signals is higher than that of SPS signals in cold start (assuming no time input) Eq. (2-18). In addition, the following limitations are prevalent from a system perspective *w.r.t TTFF*:

- In GLONASS, realizing the restricted signal correlator with the state of the art devices is still a difficult proposition. For example, with 10 bit code, 1023 correlators per channel constitute massive correlator architecture for GPS L1 C/A code, which reduces the signal acquisition time drastically. Extending this to GLONASS P-code, 5.11 M Chips * 6.566 correlators/channel are required to achieve similar performance (GLONASS-ICD 1998).

This, compounded with *dynamic environments*, presents a difficult proposition even with present day state of the art ASIC's.

- Second, the time information from the SPS signals of GLONASS is available only as a part of string-1, which repeats once in 30 s (GLONASS-ICD 1998). Dependence on this for assistance (for signal acquisition) delays the TTFF drastically Eq.(4-7). This and the previous point (complexity of correlator design) necessarily sets a constraint on the *time needed to be input to the receiver externally* for optimal signal acquisition, which may not be practical under all conditions (for example, restricted handheld devices as illustrated in Figure 1-1).
- Third, even with manual input, the time accuracy determines the acquisition of the signal. For example, if there is an offset of 100 ms and assuming 10000 correlators/channel, it translates to a large search range resulting in poor acquisition time (worst case may not detect the signal (with dynamics and signal dwell time of $1 / (5.11 \text{ MHz})$ – the chip duration) as well) and thus affects TTFF.
- Fourth, one argument for direct acquisition is in jamming environments where dependence on SPS may become critical. With a 10 dB (difference in restricted and SPS signal processing gain) advantage, the significant region where the SPS signal is vulnerable would effectively make the restricted signal non-usable (9x zone) as shown in the Figure 4-5.

In GPS based on cryptographic keys, the Anti-Spoofing (AS) feature is achieved (Kaplan & Hegarty 2006). One possibility is this key is dynamically changed based on some event/contents (time; spare/reserved bits) of the SPS NAV data signal (assisted mode). However, there is no literature mentioning this for GLONASS restricted signal. If this

were to be extended to GLONASS, with *direct acquisition and cold start mode* of receiver operation (for example, applications as illustrated in Figure 2-20) it might not be possible to acquire the signal (for example, the transition has occurred and the receiver has no knowledge). In addition, to transmit this information (possible change in key information) on a terrestrial network may not be always practical always (for example, application as shown in Figure 1-1). Thus the advantages stated (w.r.t AS feature and SPS assisted mode) overweigh the direct acquisition method.

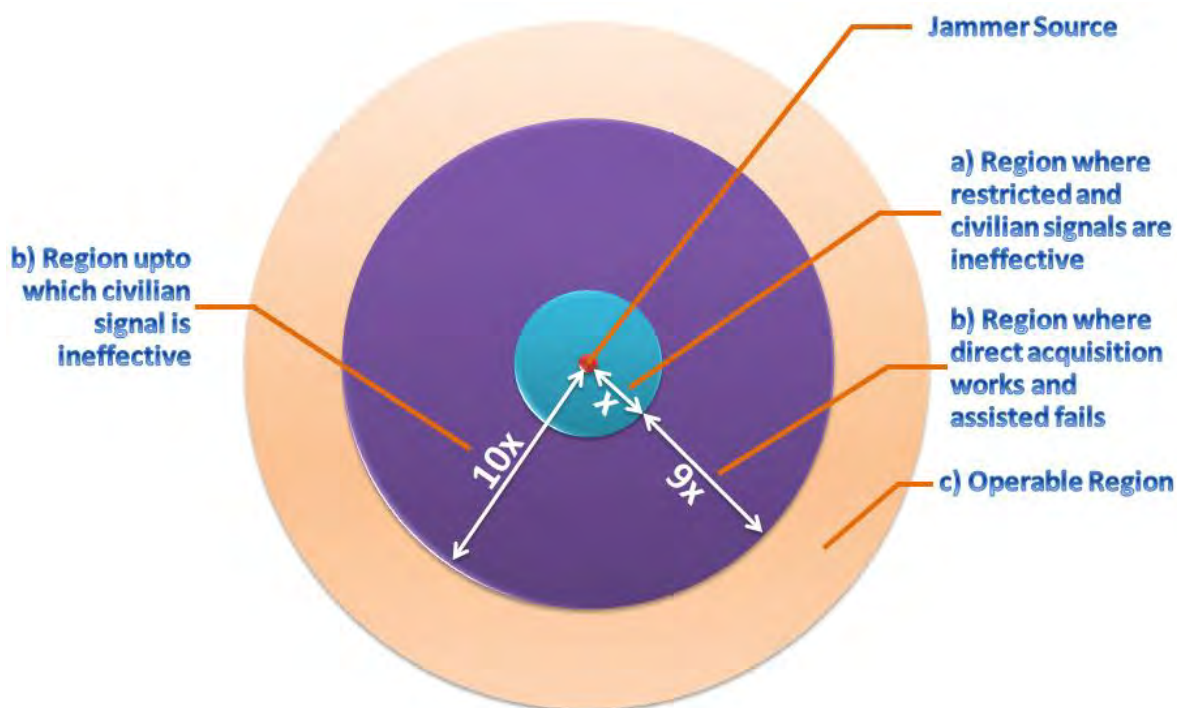


Figure 4-5: Bubble diagram depicting the region where a) restricted and civilian signals are ineffective b) civilian signal is ineffective c) operable region.

Given the limitations cited in Eq. (4-14) and Eq. (4-15) and summarized in Figure 4-6, a possible NAV data transmission for restricted signals is explored. Further, with the system level limitations cited above regarding the direct acquisition of GLONASS, this research restricts (w.r.t TTFF) the derivation/explanation/implementation to assisted mode (from satellite) of

restricted signal operation. The results obtained in assisted mode are generalized and presented for direct acquisition.

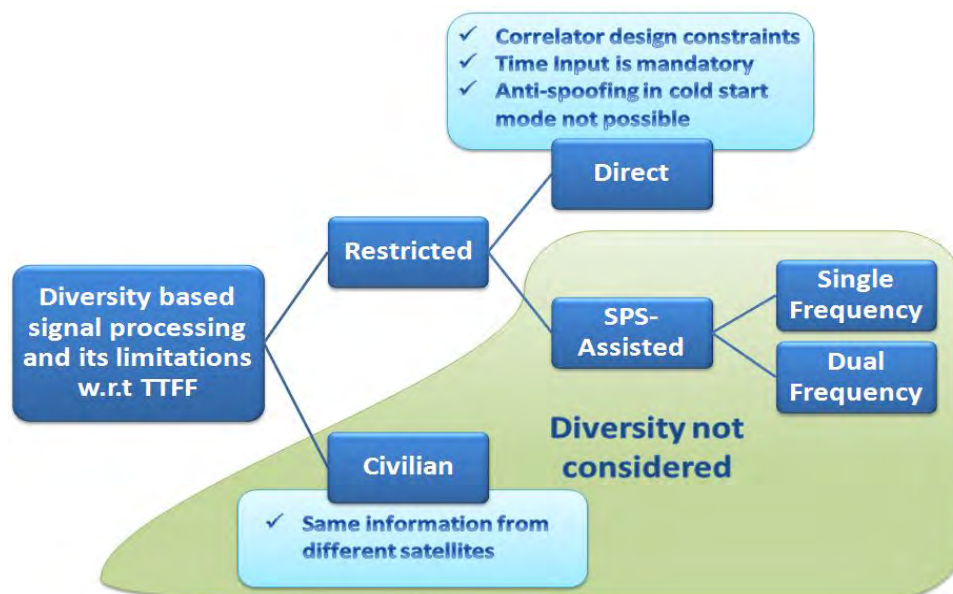


Figure 4-6: Summary of diversity based signal processing and its limitations w.r.t TTF.

4.3 Diversity based NAV data signal design derivation

This section derives the NAV data signal design in diverse modes of IRNSS receiver operation. As a first step, the necessary assumptions with which the proposed signals are derived are put forth.

4.3.1 Assumptions on IRNSS NAV data

Table 4-3 lists the assumptions made with necessary justifications/examples:

Table 4-3: List of assumptions with which the signals are derived in diversity mode for IRNSS.

Assumption	Description, Reasons/Examples, if any
IRNSS NAV data availability	With no information on NAV data of IRNSS, the signalling scheme shown in Figure 4-7 is assumed from a design perspective. This is <i>in line with GPS L1/ L2C and L1/L2 w.r.t restricted signal.</i>
Identical data	As mentioned in the GPS ICD ((IS-GPS-200E 2010), Page:

Assumption	Description, Reasons/Examples, if any
service/frequency	<p>11), the data is common to P(Y) and C/A codes on both L1 and L2. This assumption is retained for IRNSS and is explained for a few scenarios as follows:</p> <p>Prior to May 2000, the L1 C/A signals were intentionally dithered to degrade achievable accuracy. This was achieved by changing the clock and ephemeris parameters transmitted as a part of the NAV data (Parkinson & Spilker 1996). The user community was able to overcome this using DGNSS, where for a given region this error was estimated and radiated as a part of its corrections (RTCM 1994).</p> <p>In addition, the present day SBAS techniques would negate such intentional dithering. Any intentional dithering onboard a satellite is easily overcome with different user techniques. Thus, the NAV data (specifically: primary parameters) is assumed to be similar in SPS and restricted signals of IRNSS.</p> <p>This assumption is retained even in direct acquisition mode.</p>
Optimal NAV data on IRNSS	<p>GPS signals depicted in Figure 4-1 have evolved over nearly four decades. The recent signals (L5 and L2C) have specifically adapted optimized power, data/rate and new modulation techniques available at the time of the signal design commensurate (as explained in Chapter Two) with GNSS signal requirements. Barring the initial design of GPS, it has been a linear increment in each frequency augmented on the satellite constrained by backward compatibility with its predecessor signal. In addition, GPS L5 primary NAV data is mostly similar to GPS L1 (ICD-GPS-705 2002), Page: 40). However, in IRNSS the most optimal signal available during the initial formulation can be adapted specifically w.r.t NAV data and use the same on either services/frequency.</p>
Eliminated spare/reserved bits of GPS	<p>The proposed NAV data structure for single frequency IRNSS eliminated the spare and reserved bit fields from the GPS L1 C/A. The exact reasons for transmitting these bits are not available in the GPS ICD. However, if these bits are used in restricted receivers (for example, information of AS key being changed), <i>it is assumed that such bits are transmitted as a part of textual message in the IRNSS SPS signal and thus the TSF NAV data streaming (Figure 3-11) is not considered for this research.</i></p>
SPS data usage by restricted signals	<p>Fifth, extending point 3 (of this table), in assisted mode of restricted signal acquisition, the system data (all subframe information) from the <i>SPS path when available can be utilized by restricted signals</i> to improve its TTFF performance.</p>
Ranging codes in	<p>It is assumed that similar ranging codes for SPS and restricted</p>

Assumption	Description, Reasons/Examples, if any
SPS and restricted signals of IRNSS	signals on either frequency are similar. The advantage with this scheme is that the necessity of additional memory (for example, lookup-table in BPU containing L1-L2C mapping) required for collaborative acquisition of second from first is obviated.

With the above assumptions, the following section derives three schemes of NAV data signal design based on diversity: Code, Carrier and Hybrid. All three methods are applicable to restricted signals while carrier alone is applicable to civilians. Towards this, FSA and TSN methods are taken as a reference. Further, explanation and implementation is presented for FSA and the results are generalized to TSN method.

4.3.2 Code diversity

As shown in Figure 4-7, the restricted signal users on either service of IRNSS L5 will have access to the NAV data of SPS.

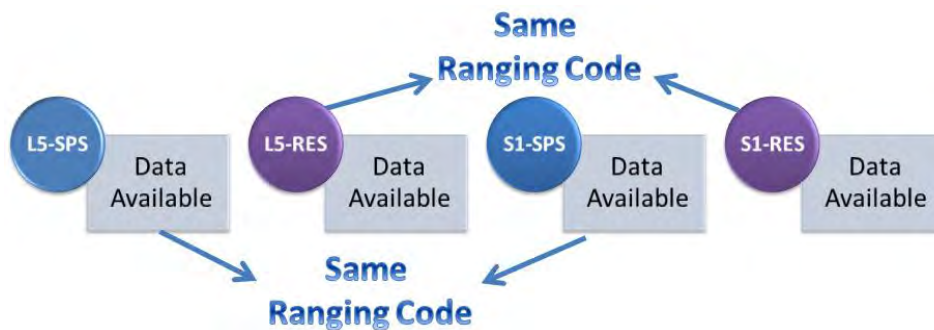


Figure 4-7: Assumption on IRNSS ranging codes and NAV data across frequencies/service.

The derivation is presented for L5, which can be generalized to S1. Extending Eq. (4-14) for IRNSS and applying the L1 C/A and P(Y) NAV data streaming (GPS ICD 2010) as shown in Figure 4-9a), we obtain

$$TTF_{opt_irnss_res_l5} = \min(TTF_{sps_l5}, TTF_{res_l5}). \quad (4-16)$$

Using Eq. (3-11), the optimal TTFFs achievable on SPS and restricted signals is given by

$$TTF_{opt_l5|sps\ or\ res} = \min_t \sum_n [SF_{n-enc}]_{sps\ or\ res} \quad (4-17)$$

Symbolically the subframe structuring on either services of L5 can be written as

$$|SF|_{sps_l5} = \sum_{i=1}^n SF_i \text{ and } |SF|_{res_l5} = \sum_{i=1}^n SF_i \quad (4-18)$$

where, $n = 4$ and 3 for the FSA and TSN methods, respectively. With the input that the data is similar and to optimize the data collection, the structuring is notionally altered as

$$|SF|_{sps_l5} = \sum_{i=1}^n SF_i \text{ and } |SF|_{res_l5} = \sum_{i=n}^1 SF_i. \quad (4-19)$$

Pictorially, Eq. (4-19) is as shown in Figure 4-8, which acts as a pointer to the data in Eq. (4-12), to result in a signal based on code diversity.



Figure 4-8: NAV data bits sourcing from subframe array on either service of IRNSS.

Processing the above signal effectively (from a minimum of four satellites) results in an optimal TTFF of a single frequency restricted receiver. In addition, the time required to collect the secondary data reduces by half.

One possible architecture to satisfy Eq. (4-19) is as shown in Figure 4-9b) where the subframes are straddled in opposite directions on either service. However, the transmission is not optimal from a system perspective, which is explained as follows: Assume the bit-synchronization on an SPS signal occurs at T_0 for a channel. After 6 s, the TOW is available and thus the time. With this, the restricted signal will be able to achieve system data (along with SPS) only after 24 s from T_0 . To counter this, the NAV data streaming as shown in Figure 4-9c) is adopted. With this arrangement, the system data (SF1 to SF4) from the satellite is transmitted in half the time compared to a single frequency system as shown in Figure 4-9a). This arrangement does not

affect the individual steaming of SPS or restricted signals. Effectively, the TTFF for IRNSS restricted signals in code diversity mode of operation is given by

$$TTFF_{code_irnss_n} = (T_{eph_sps_irnss_sf_n})/2 + T_{TOW} \quad (4-20)$$

where $TTFF_{code_irnss_n}$ is the TTFF achieved in code diversity with “n” subframes and $(T_{eph_sps_irnss_sf_n})$ is the time required to collect the ephemeris in a single frequency with “n” subframes.



Figure 4-9: Signal design based on code diversity a) similar to GPS L1 b) direct reversal scheme c) optimal transmission method as applied to FSA in IRNSS.

With this transmission, the TTFF of restricted signals is effectively reduced to 18 s as compared to 36 s for GPS L1 (Figure 4-9 a) in the code diversity mode of operation of IRNSS, a 50% improvement.

Extending this to direct restricted signal acquisition, it translates to 12 s TTFF that is 60% improvement with the entire data available from the constellation.

This signal design might assist restricted hand-held type receivers where single frequency of operation may be adequate for certain applications. As mentioned earlier, GPS L1 has the

provision to disable the data on L2 (Kaplan & Hegarty 2006)). In such a scenario, code diversity provides the most optimal TTFF for the restricted users.

4.3.3 Carrier diversity

The benefits derived from code diversity are applicable only to restricted users. With the data available on both civilian frequencies and extending the concept explained under code diversity results in carrier diversity based signal design for civilian and restricted users (Rao & Lachapelle 2012).

With reasoning similar to code diversity, the architecture shown in Figure 4-10 is deduced for carrier diversity. The entire system data on both the frequencies is available within 12 s and thus TTFF effectively reduces to

$$TTFF_{carr_irnss_sps_n} = (T_{eph_sps_irnss_sf_n})/2 \tag{4-21}$$

where $TTFF_{carr_irnss_sps_n}$ is the TTFF achieved in carrier diversity on SPS with “n” subframes.

The advantage with this transmission is that the civilian signal will be able to obtain the entire system data within 12 s as compared to 30 s in the case of GPS. In addition, compared to the code diversity, this method assists the restricted users to obtain the data within 12 s (assuming primary NAV data to be similar to SPS). Specifically, the TOW component of Eq. (4-20) is obviated. Similar results are applicable to the direct acquisition of restricted signals.

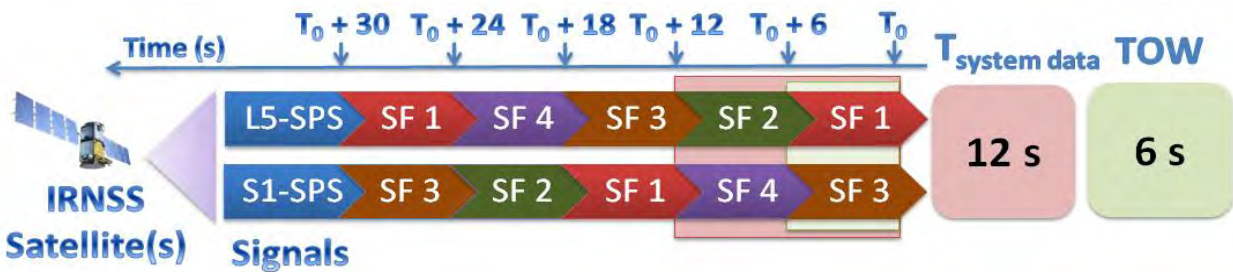


Figure 4-10: Signal design based on carrier diversity of SPS in IRNSS as applied to FSA.

4.3.4 Hybrid

Assuming data to be similar on either service, the results of civilian carrier diversity effectively applies to restricted signals as well. However, the system data from the satellite is not optimally transmitted with the dual frequency and service. To accomplish this, an equivalent alternate carrier diversity structure for restricted signals (w.r.t SPS) as shown in Figure 4-11 is considered. This and the carrier diversity of civilian signals effectively optimize the data transmitted from the satellites as shown in Figure 4-11.

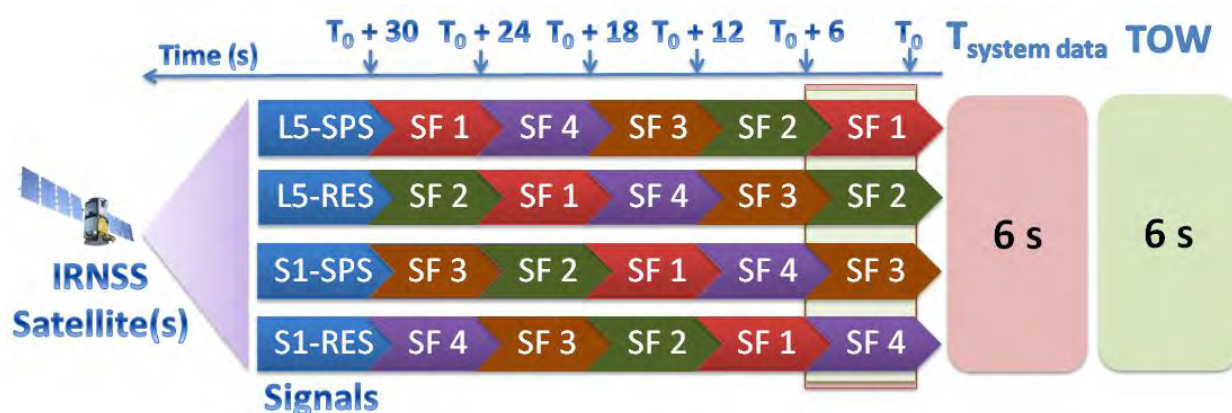


Figure 4-11: Signal design based on hybrid method in IRNSS as applied to FSA of NAV data streaming.

However with this optimal structuring, *gain either for the restricted users in assisted mode or the civilian user is not derived.* The scheme would assist the direct acquisition method drastically. The derivation was consistently applied to the FSA and achievable results presented w.r.t single frequency GPS L1/L2 signal transmission. Extending this to the TSN, TTFF reduces even further. The following section presents simulation approach with FSA and explains only the architectural changes necessary to accommodate the TSN method.

4.4 Signal simulation

To generate and test the proposed signals, the simulator as used in the previous chapter is considered. The necessary modifications required to generate the proposed signals in all three modes of operation are elaborated in detail in the following sub-sections.

4.4.1 Architecture

The firmware of the simulator is capable of supporting 45 channels. For this research, 28 channels are energized to generate the IRNSS signals in code, carrier and hybrid diversity modes.

As shown in Figure 4-12, the channel numbers 1 to 14 are dedicated to L5.

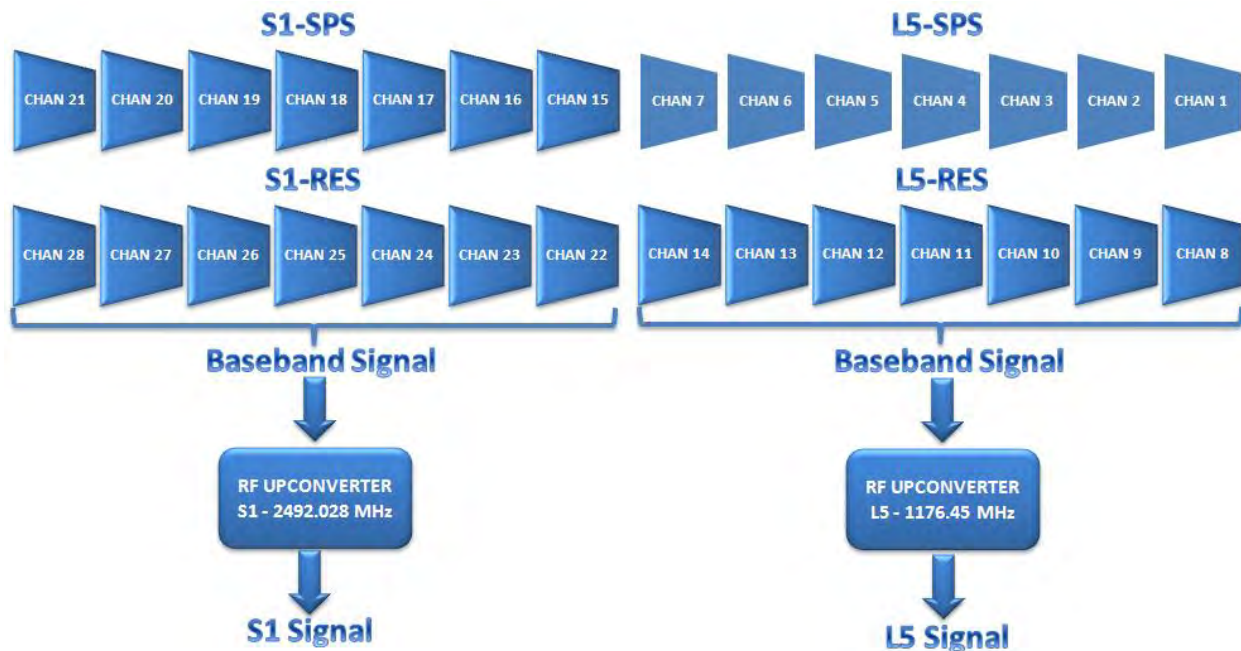


Figure 4-12: Signal simulation software design to generate the proposed diversity based IRNSS signals.

Seven are each dedicated to the SPS and restricted signals. Similar code assignments are applied on the S channels (15 to 28). Since the ICD and thus the codes of IRNSS are not available, GPS SPS 1 to 14 PRN are used for the simulation purpose of which 1-7 are dedicated to SPS and 8-14 are assigned to restricted signals. The individual channels generate the signal at 20 MHz IF,

which are up-converted (across channels) to respective L5 (1176.45 MHz) and S1 (2492.028 MHz) frequencies and combined. The simulation parameters are similar to those given in Table 3-6. To validate the three methods of signal simulation, independent versions of the simulator software are created.

4.4.2 Code diversity

The first component generated within the simulator hardware is the IF signal following Eq. (4-19) w.r.t NAV data. The resulting composite IF signal with a suitable mixer and filter generates the L5 RF signal, which is given by

$$y_{l5}(t) = \sum_{m=1}^7 (A_I (r_{m,l5}(t) \oplus d_{m,l5}(t)) * \cos \omega_{m,l5}t) + \sum_{m=8}^{14} (A_Q (r_{m,l5}(t) \oplus d_{m,l5}(t)) * \sin \omega_{m,l5}t) \quad (4-22)$$

where m is the channel number. The data in Eq. (4-22) is transmitted in accordance to the signalling method proposed in Figure 4-8 and Figure 4-9 c). Towards this, for each SPS and restricted signal, the data (subframe) are initialized as shown in Figure 4-13. At T_0 , the SPS path is initialized with the third subframe, and restricted signals with the first. The sequencing w.r.t time is as shown in Figure 4-13.

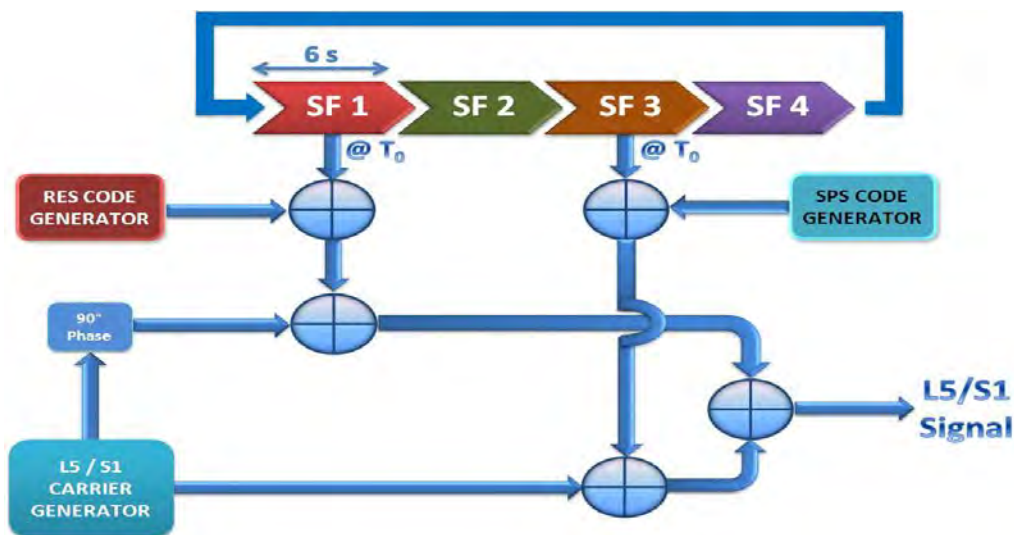


Figure 4-13: IRNSS NAV data signal generation to optimize TTFF based on code diversity.

Further, this data is modulo-2 added to the respective codes and BPSK modulated onto the carrier to generate a 20 MHz IF and then to obtain the requisite RF signal as represented in Eq. (4-22). A similar explanation is applicable to the S1 path channels.

4.4.3 Hybrid method

To test the functionalities of carrier and hybrid methods, one single version with hybrid architecture is designed as follows: The IF signals are simulated on L5 and S1 channels based on Eq. (4-20). Extending, similar quadrature components (restricted signals) are generated in the respective channels. The combined signals are translated with a suitable mixer and filter to obtain the composite RF signal given by

$$y_{hyb}(t) = \sum_{m=1}^7 \left(A_I \left(r_{m_{L5}}(t) \oplus d_{m_{L5}}(t) \right) * \cos \omega_{m_{L5}} t \right) + \sum_{m=15}^{21} \left(A_I \left(r_{m_{S1}}(t) \oplus d_{m_{S1}}(t) \right) * \cos \omega_{m_{S1}} t \right) + \sum_{m=8}^{14} \left(A_Q \left(r_{m_{L5}}(t) \oplus d_{m_{L5}}(t) \right) * \sin \omega_{m_{L5}} t \right) + \sum_{m=22}^{28} \left(A_Q \left(r_{m_{S1}}(t) \oplus d_{m_{S1}}(t) \right) * \sin \omega_{m_{S1}} t \right) \quad (4-23)$$

where, generically, m is the channel number and L5 & S1 represents individual signal components, respectively. The $d_m(t)$ on each quadrature component of L5 and S1 frequencies follows the sequencing shown in Figure 4-8 and Figure 4-11, respectively. The signal generation based on Eq. (4-23) is as shown in Figure 4-14. The in-phase components, which represent the civilian signal at T0, are set to Subframe 1 and Subframe 3 on L5/S1, respectively. Similarly, on the quadrature component that carries the data for the restricted signals, Subframe 2 and 4 are the initial states of L5/S1. On each of these arms, the data is swept cyclically as shown in Figure 4-14.

Individually, the carrier diversities are met on restricted and SPS paths. When these signals are combined and interpreted together, they represent the hybrid version as given in Eq.(4-23). The performance on individual frequencies is still maintained as in the single frequency version.

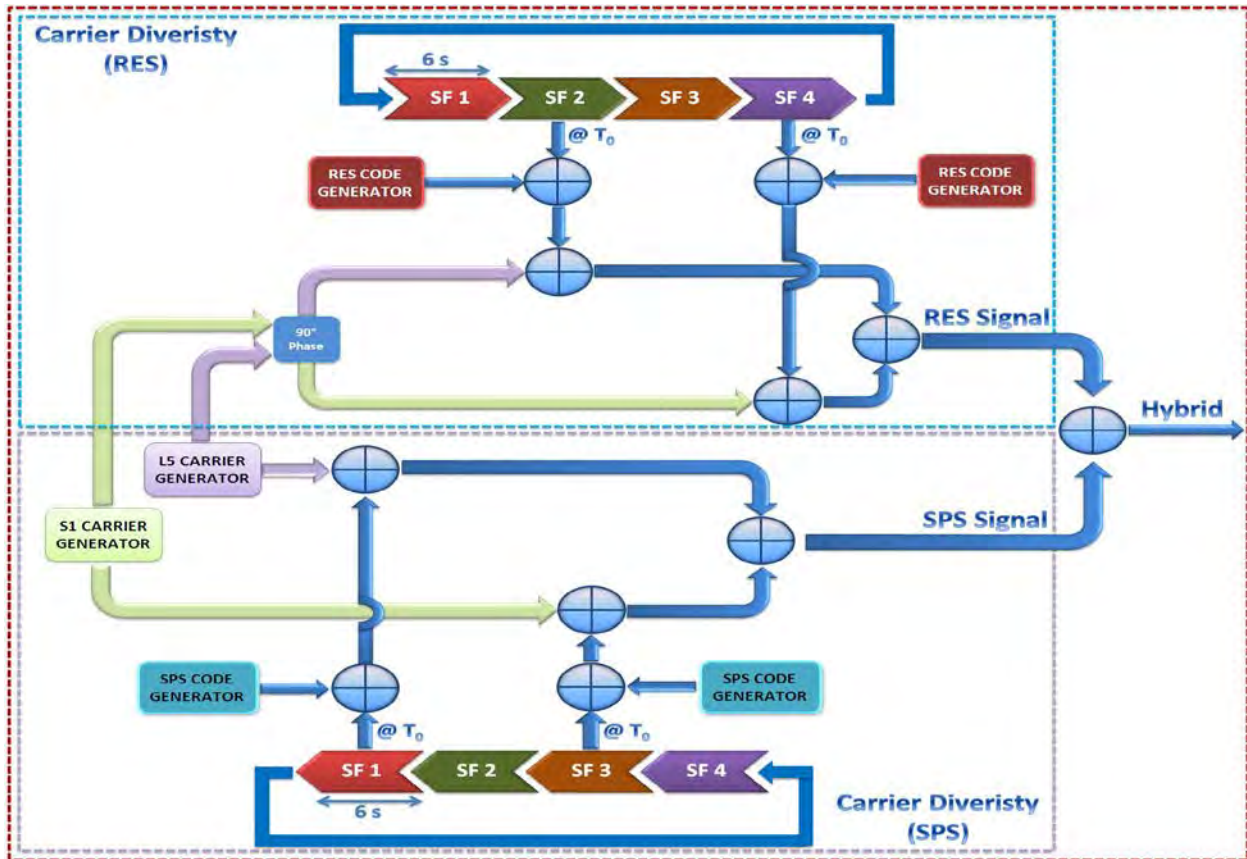


Figure 4-14: Carrier and hybrid methods of NAV data signal generation in IRNSS with a FSA.

4.4.4 Modifications for TSN

The derivation in the previous section was generic and is applicable to any “n” subframes/strings/pages of NAV data. In addition, the derivations were illustrated with a four-subframe example. Extending Eq. (4-21) with three-subframes results in 9 s TTFF, which is not an integer multiple of 6 s - the subframe period. This calls for an examination of methods to achieve this optimal result. At the outset, two possible architectures are possible as shown in Figure 4-15 and Figure 4-16. In the first architecture, the data bits are divided and grouped into sets of four on each frequency/service. Subsequently, the data is straddled. In the second architecture, post encoding with frame synch as reference, the data symbols are fragmented and

grouped into sets of four across subframes and transmitted. The signal structuring in either method ensures the optimal condition of Eq.(4-21) is achieved.

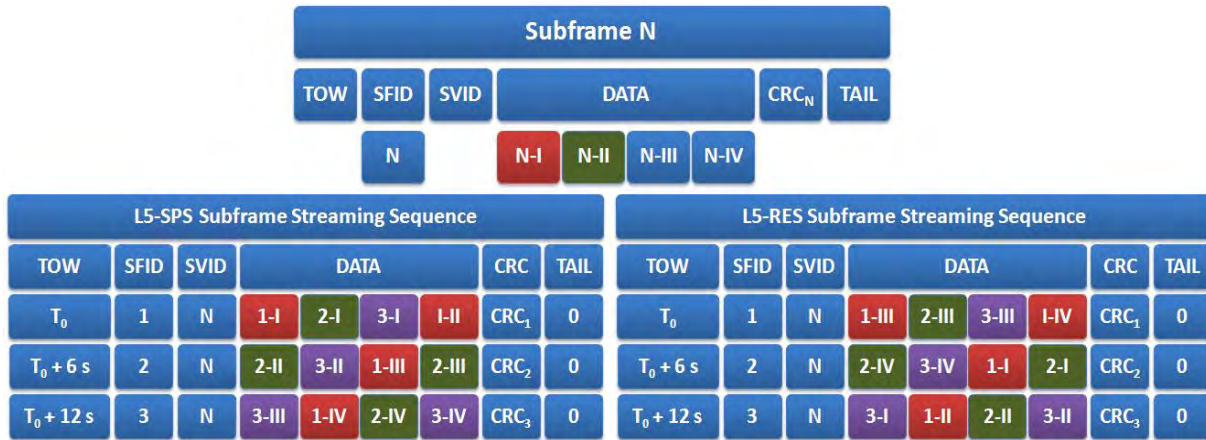


Figure 4-15: Architecture-1 with the NAV data bits are grouped into sets of four and straddled.

Based on Architecture 2, an algorithm for processing the TSN data structure in diverse modes is presented in Appendix E. The advantage of this architecture is in hybrid mode of operation (direct acquisition), where the data is usable within 4.5 s as opposed to 6 s in Architecture 1. This limitation arises due to the collection of CRC, which occurs once in 6 s.

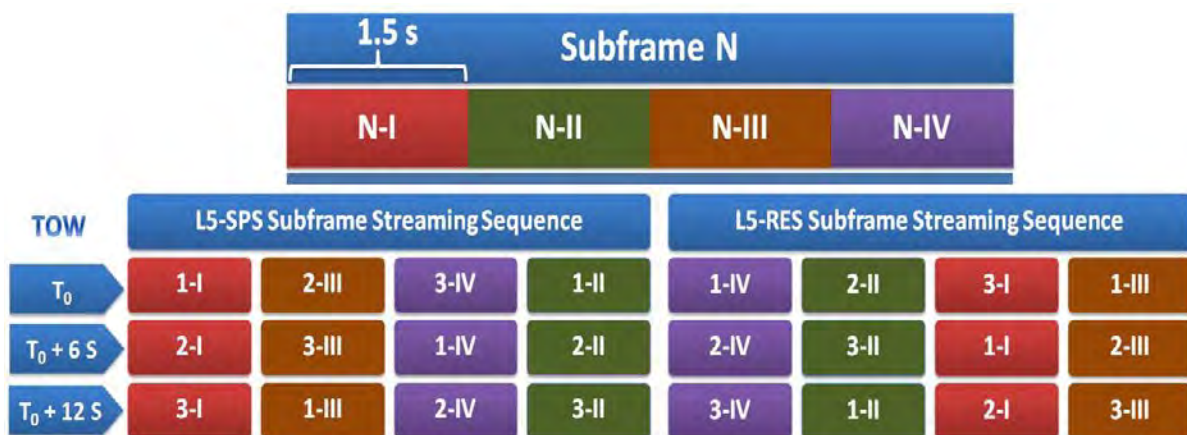


Figure 4-16: Architecture-2 with NAV data symbols grouped into sets of four and straddled.

4.5 Receiver software design

The GPSGL receiver used in the previous chapter is modified (software-wise) to account for the signal design of the proposed signal. This research uses two of the available three RF ports, with the third RF terminated. Figure 4-17 provides the architecture (hardware) of the receiver used for this research task. The following paragraph explains top-level modifications to the test apparatus of the previous chapter.

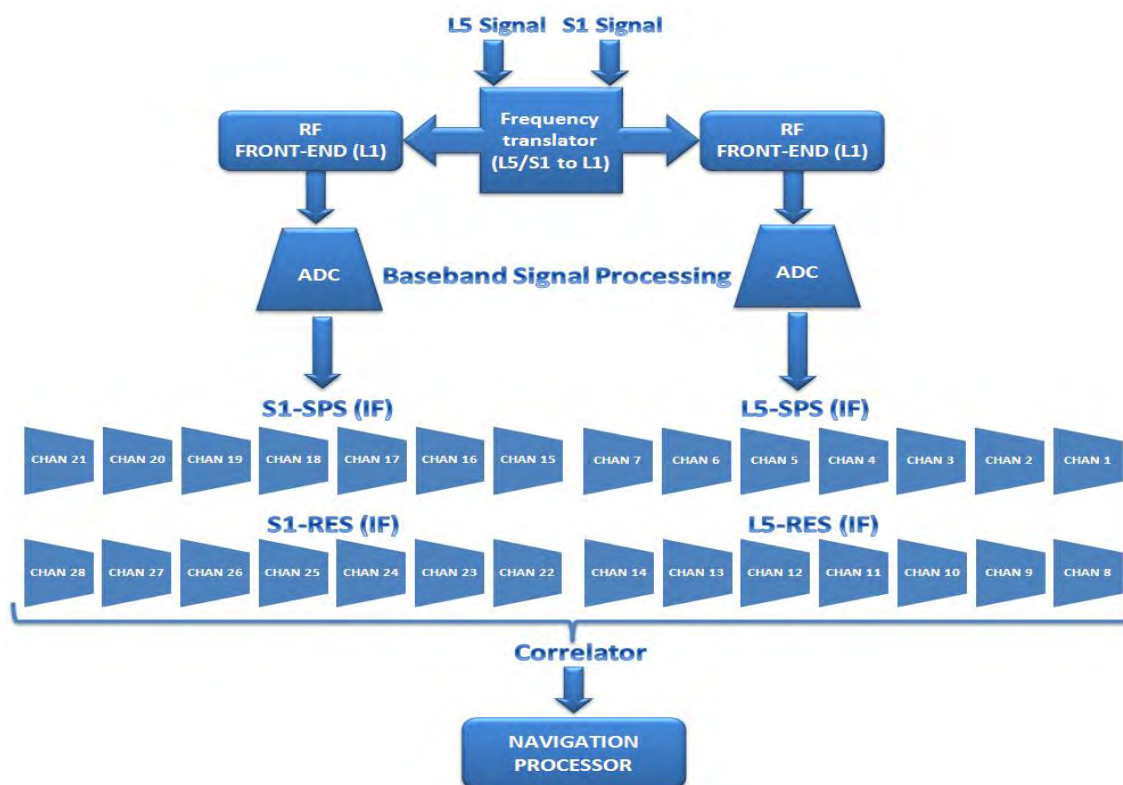


Figure 4-17: Top level details of the triple RF GPSGL receiver used for validation of the diversity results.

The top level hardware design details of the customized GPSGL receiver are as follows: The input IRNSS RF composite signal (S1 and L5) is fed to the RF translator, which is conditioned to two separate 1575.42 MHz frequencies. Subsequently, these signals are fed to separate GPS portions of the GPSGL hardware for further processing. The down-converted and digitized

signal is fed to the FPGA, where two separate 14-channel IRNSS correlator blocks are implemented, totalling 28 channels. Each block is dedicated to a particular frequency (L5 or S1) band. Of the 14 channels, seven are dedicated to the SPS and another seven to restricted signals. Following this, the DSP processes the correlation values from the FPGA leading to data-bit demodulation and user position computation. The receiver operations are commensurate with the signal flow/functions shown in Figure 4-2.

Figure 4-18, illustrates the signal flow post correlator (as explained in Chapter Two) leading to position computation with all three methods captured. To demonstrate the performance improvement, two versions (for all three methods) of the receiver software corresponding to code and hybrid methods of NAV data signal design are implemented. With necessary software modifications leading to data bit collection from either path, the following paragraph presents the top-level implementation details to achieve T_{eph} and T_{sec} improvements in the dual frequency mode of operation (Rao et al 2011).

To initiate the restricted signal detection, the following implementation steps need to be performed:

- The SPS channel is first acquired, the data bit collected and TOW extracted for each channel.
- For each subframe synched channel, the channel-time (TOW) is estimated.
- With channel-time as pointer (Figure 4-3), the restricted signal is detected with fine acquisition process as explained in Figure 4-2.

4.5.1 Code diversity

The previous chapter established the methodology of operations for single frequency civilian receivers, which is extendable to restricted assisted and direct signal acquisition (with time

input). The code diversity establishes the TTFF improvement of single frequency restricted signal operation in IRNSS relative to GPS. The top level receiver architecture to accomplish this is as follows:

The subframe received on the SPS channel is collected and stored based on the subframe-id. Following the TOW assistance, the corresponding restricted signal is acquired and data is collected concurrently on the SPS channels. Assuming the signal transmission shown in Figure 4-9c), the data is integrated and grouped. With Subframe 1 and 2 data, the ephemeris for a channel is available. With the ephemeris data from four satellites, the user position is estimated. Similarly, the secondary data is collected from Subframe 3 and 4.

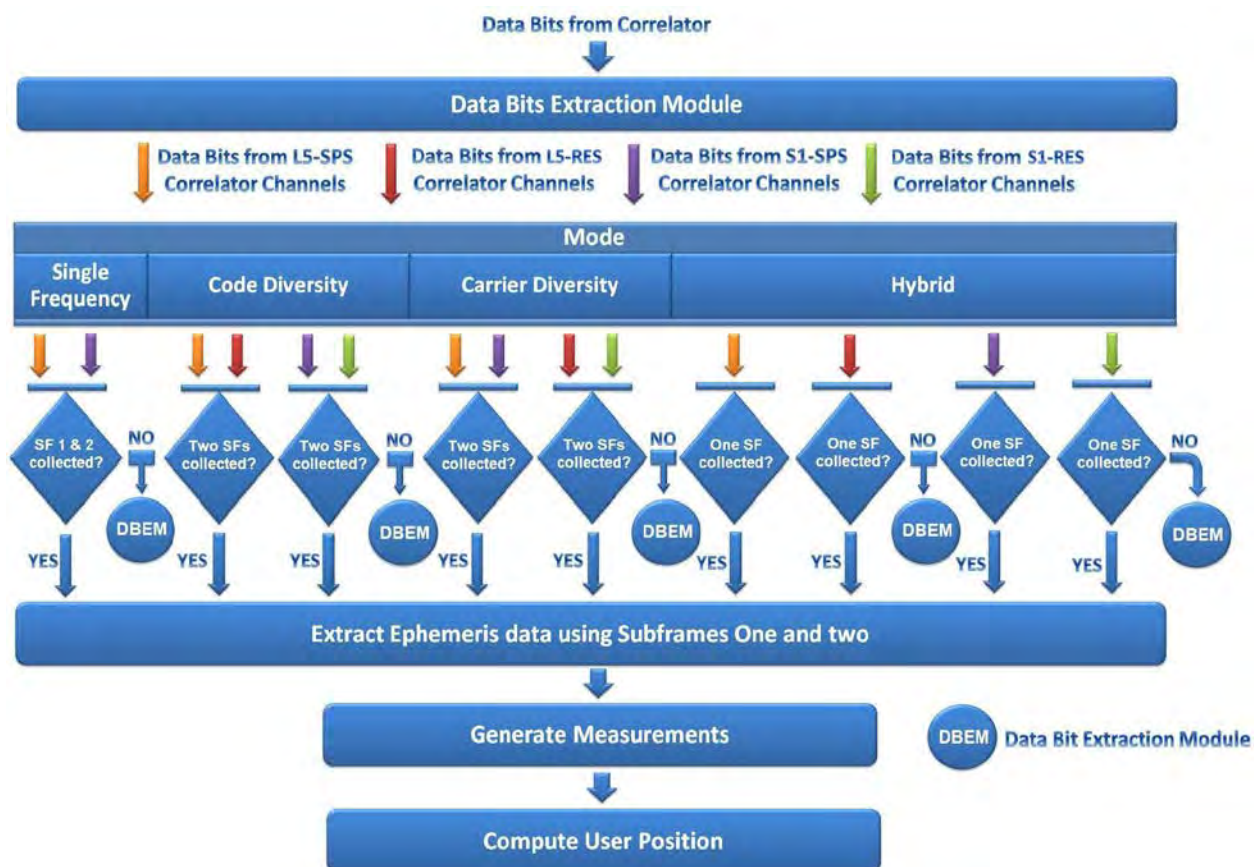


Figure 4-18: The software flowchart illustrating the proposed three diversity schemes for IRNSS.

The sequence of operations (timing diagram of data collection) commensurate with single frequency civilian (IRNSS) and that based on code diversity are shown in Figure 4-19 and Figure 4-20, respectively, and explained as follows: First, in the single frequency FSA, the data for a satellite/channel is obtained sequentially, stored and used based on the subframe-id. For code diversity the main difference is that the data collection on the second path (restricted signals/channels) starts post subframe synchronization of the corresponding SPS channel, as shown in Figure 4-20. Thus at $T_0 + 12$ s, the first subframe is available from restricted signals. In the following subframe period (at the end of $T_0 + 18$ s), complete data is available for the restricted service user as shown in Figure 4-20.

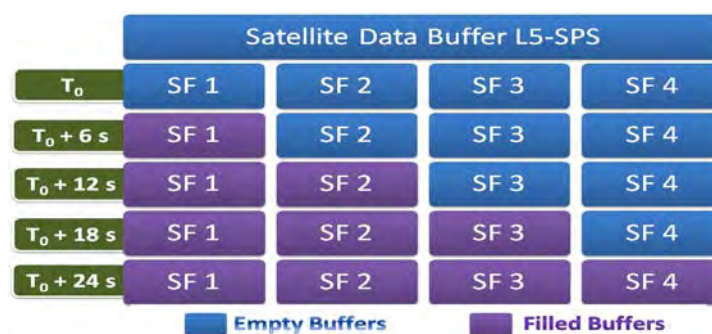


Figure 4-19: Timing diagram of NAV data collection with FSA in single frequency mode of IRNSS receiver operation.

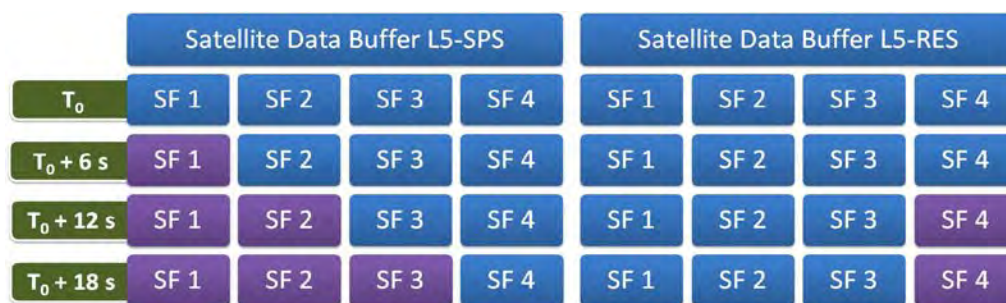


Figure 4-20: Timing diagram of code diversity based on NAV data collection with FSA in IRNSS.

The above results and explanation are equally applicable to the S1 path of IRNSS.

4.5.2 Hybrid scheme

A single version of software is realized to demonstrate the performance benefits derivable from carrier and hybrid method of NAV data signal transmission. First, the implementation based on diversities of each service is explained. With the data straddled and available on both frequencies, the data collection on the SPS is commensurate with the code diversity. The only difference is that in the post data bit detection, processing occurs on both channels on either frequency. Similar processing is applicable to restricted signals after the TOW word collection (channel-time) on their SPS channels. Figure 4-21 depicts the timing diagram commensurate for the civilian and restricted signals individually.

In the case of restricted receivers, post TOW word collection, when the data is collected from all the four paths independently, the complete system data of the IRNSS constellation is available in a receiver. The timing diagram for this implementation is shown in Figure 4-21.

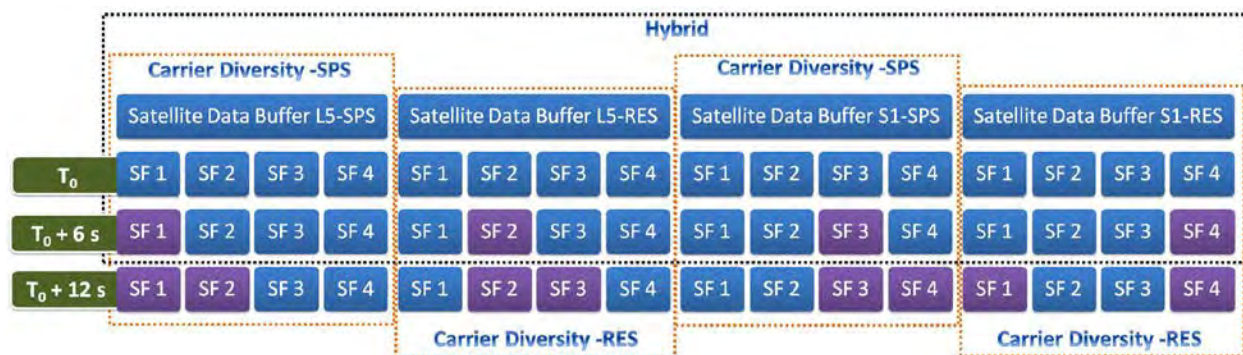


Figure 4-21: Timing diagram of carrier and hybrid method of NAV data collection with FSA in IRNSS.

To explain the benefits derivable for direct acquisition, a small change in the software is implemented. Subsequent to the bit synch of the SPS channel (which represents time availability), signal processing and subsequent data collection is enabled on all four paths (2 each of civilian/restricted).

Figure 4-21 depicts the timing diagrams w.r.t data collection typically in a receiver for carrier and hybrid methods. The highlight is for direct acquisition, the data buffers across channels at $T_0 + 6$ s results in complete system data.

4.6 Test methodology and performance analysis

To demonstrate the performance improvement of the proposed methods, the receiver and simulator are tested with the corresponding versions. The method used to assess the performance improvement is similar to the procedure described in the previous chapter. To profile and demonstrate the performance of assisted method of restricted signals, the following changes are performed.

4.6.1 Procedure

The receiver software for the channel post bit-synchronization is initiated with dedicated counters to profile the time required to collect the primary and secondary parameters. The results obtained from the FSA are presented in the following section. Finally, these results are analyzed and extended for the TSN data streaming.

4.6.2 Code diversity

To test the performance, only L5 signals are considered and channels 15-28 on the simulator are disabled. With the signal from the simulator and the corresponding receiver software, the TTFF (as expected) followed Eq. (4-20). The improvement is directly attributed to the FSA architecture and the data staggered on either service.

Figure 4-22 illustrates the improvement achieved in TTFF based on the diversity method. This technique results in both the TTFF and the entire system data being available within 18 s ($T_{\text{eph-cod}}$) in comparison with GPS L1's 36 and 192 s (assuming 7 GPS like NAV data (Figure 3-24)), an improvement of 50% in TTFF.

Extending the above result to the TSN method with TTFF of 15 s, 60% improvement is achieved compared to that achieved in GPS L1. In addition, the secondary data from all satellites are also obtained within 18 s, an improvement of 25% compared to the FSA.

4.6.3 Carrier diversity

For this mode of operation, the simulator and receiver are run in the hybrid method. The restricted signal channels (8-14 & 22-28) on the simulator are disabled for this test. With the signal, the receiver tracked and the counters used to profile T_{eph} and T_{sec} are logged for analysis.

Analysis of the logged data reveals an improvement in TTFF of 60% ($T_{eph-CAD}$) compared to existing GPS signals in dual frequency mode of operation as shown in Figure 4-22. This is attributed to the NAV data streaming and the reduced subframe count compared to GPS L1/L2 ($T_{eph-GPS}$). In addition, this method provides a TTFF comparable to that of TSF architecture and also the complete NAV data (secondary data) is available within 12 s. With the assumption that the primary NAV data of restricted signal is similar to that of civilian, its TTFF is also 12 s.

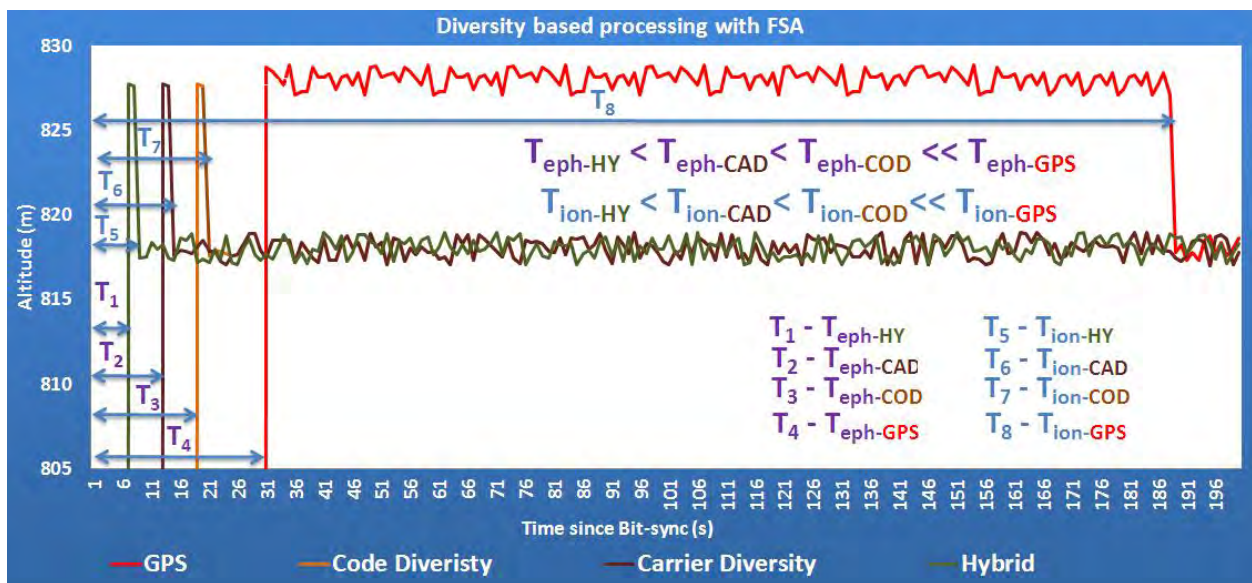


Figure 4-22: Altitude plot summarizing the improvements in proposed diverse methods for IRNSS.

Extending the above results to the TSN architecture, a TTFF improvement of 70% w.r.t GPS is achieved for civilian signals, which is the best till date from any system.

4.6.4 Hybrid scheme

To demonstrate the performance of the hybrid architecture and its merits, the simulator and receiver were first run in the hybrid mode with data from all the 28 channels enabled. First, the SPS assisted carrier diversity of restricted signals is tested. This results in a TTFF similar to that of carrier diversity with civilian signals.

Subsequently, the modified version with direct acquisition is tested. This results in $6\text{ s } T_{eph-HY}$ and T_{sec} values, best till date from any existing or proposed system, with a limitation/assumption of time input. Extending this to TSN, a *TTFF of 4.5 s in Hybrid mode of operation* is achievable.

4.7 Summary

This chapter presented the high level details required to adapt single frequency receivers for dual frequencies/service of operation. The TTFF characterisation for the dual frequency civilian and restricted signals was established. The limitations in the existing signal transmission assuming diverse mode of receiver operations were described. The merits/limitations in two modes of restricted signal acquisition were analysed. The assumptions with which the signals are derived were tabulated with justifications. Three new methods of NAV data signal transmission were designed. The necessary augmentations to the simulator architecture and the new receiver software developed were elaborated in detail. The results as summarized in Table 4-4 demonstrate improvements achievable compared to dual frequency GPS civilian receiver operation. With a 70% improvement in TTFF based on the TSN method, the results are best till

date. Similarly, Table 4-5 summarizes the results derivable from restricted signals in either mode of signal acquisition, which when compared with available datasheets, is the best till date.

Table 4-4: Summary of proposed methods compared to GPS L1/L2 (30 s) for civilian applications.

Diversity Mode of Operation	FSA Method (s)	TSN Method (s)
Carrier	12 60% improvement	9 70% improvement

Table 4-5: Summary of proposed methods compared to GPS L1/L2 (36 s) for restricted applications.

Mode of Operation	Assisted method of restricted signal acquisition		Direct method of restricted signal acquisition	
	FSA (s)	TSN (s)	FSA (s)	TSN (s)
Code	18 (50%)	15 (60%)	12 (66%)	9 (75%)
Carrier	12 (66%)	9 (75%)	12 (66%)	9 (75%)
Hybrid	12 (60%)	7.5 (80%)	6 (84%)	4.5 (87.5%)

(%) represents improvement w.r.t GPS L1-L2 mode of operation.

This chapter and the previous one deduced single frequency and diversity based signal designs. The following chapter derives the optimal TTFF and secondary NAV data signal design for civilian and restricted signals.

Chapter Five: CROSS CORRELATION DETECTION AND NAV DATA SIGNAL DESIGN FOR OPTIMAL TTFF IN IRNSS

With dual frequencies/services signal design, the best achievable TTFF results in different mode of receiver operations are as shown in Table 5-1.

Table 5-1: Representative datasheet of a receiver w.r.t TTFFs in single/dual frequency modes of receiver operation of IRNSS.

Service Frequency	TTFF (IRNSS)		Hot Start of GNSS using IRNSS (s)
	Civilian (s)	Restricted ⁺ (s)	
Single	18	15	?
Dual	9	9	

+ SPS-Assisted mode

Chapter Three highlighted that the basic impediment to achieving optimal TTFF values are secondary data. In the TSF architecture (Figure 3-11), this issue was completely dealt with to result in optimal TTFFs. However, the secondary data (almanac and textual messages) are essential for the *optimal performance of the system*. The objective of this research is to design an architecture that is optimal w.r.t TTFF (assuming diverse modes of receiver operation) and that yet support the secondary data.

With an objective to minimize secondary parameters, this research first explores its existing use. Following this, with necessary justifications, alternative approaches to derive the benefits of almanac are established, highlighting the need for cross correlation. A new method of Cross Correlation Detection (CCD) based on NAV data is derived. With this result (almanac eliminated), two new NAV data schemes with secondary data (textual messages only) are evolved. With these designs as pointers, two additional designs which are *optimal w.r.t TTFF performance* and yet support secondary data are derived (in all, four methods). With the

simulator and new receiver software, the results that are established are commensurate with this research goal.

5.1 Need for secondary data

The NAV data design in the FSA and TSN methods (Figure 3-8, Figure 3-9) supported the secondary NAV data. The optimal TTFF was established in TSN with almanac/textual messages alternated in the third subframe. The textual messages are user specific data, which is a recent inclusion in emerging systems ((ICD-GPS-705 2002), (IS-GPS-200E 2010)). With GPS/GLONASS L1 or GALILEO E1 this feature is not supported. However, these are available in their second or third frequencies. Since IRNSS supports only two frequencies, it is assumed that the textual messages will be present on *at least one frequency*. With this design input, the following section examines the use of the almanac and explores alternative methods to support its existing use and thus proposes to eliminate it from the NAV data.

Figure 5-1 presents the various use of the almanac, as explained in the following section.



Figure 5-1: Use of almanac in various receiver applications.

5.1.1 Visibility

As per Eq. (2-3), a GNSS receiver will need to search and detect satellites available. With the almanac, approximate user position and time the receiver will be able to predict the satellites that are visible and thus restrict the search only to those specific satellites (Rao et al 2011). This reduces the iterations necessary to search the entire constellation and effectively reduces TTFF.

With only seven satellites and always visible to the user in IRNSS, a channel can be dedicated to each satellite in receiver and thus obviate the need of an almanac from a visibility computation perspective. Assuming a global extension of IRNSS, the present day receiver technology easily supports 32 channels and thus eliminates the necessity of almanac from visibility estimation perspective.

5.1.2 Code phase and Doppler estimation

As explained in Chapter Two, the almanac assists the signal component (Doppler and code phase) search ranges to be minimized. This reduces the time required to acquire the signal and thus improves TTFF (Van Diggelen 2009).

With receiver categories as explained in Chapter Two (Figure 2-14), applications requiring fast TTFF necessarily will have a massive correlator architecture that can search all possible code-shifts in parallel. The advantage with this architecture is that acquisition time drastically reduces and thus obviates the need for the almanac. In addition, this argument is equally applicable to global extension (1K correlator/channel (massive correlator) * 32 (satellites), is easily realizable) of IRNSS.

5.1.3 Predictive Receiver Autonomous Integrity Monitoring (PRAIM)

RAIM is a method of detecting/isolating anomalous measurements and thus ensuring optimal navigation estimation (presented in Chapter Two). For aviation grade receivers, as a part of mission planning, the achievable reliability needs to be estimated prior to the flight. With the known trajectory, flight time and almanac, internal reliability (minimal detectable blunder on a measurement) estimates are determined (Petovello 2010). Based on this result, the external reliability (impact of the internal reliability if undetected on overall system performance) measure is estimated to access the dependence on GNSS measurements. This process where the

reliability is estimated prior to the flight without the need of any measurement is referred to as PRAIM.

The above process is a non-real time operation for which the data can be made available from external sources and not necessarily transmitted from the satellites. Thus, the almanac for this application and more so (geostationary/geosynchronous satellites are always visible over the Indian subcontinent and satellite positions w.r.t time can be maintained in a database) for IRNSS, is redundant.

5.1.4 Cross correlation

As explained in Chapter Two, the CDMA signals are extracted from a correlation process where a local replica of the satellite's ranging code is matched with the incoming signal. This process is possible based on two properties of the underlying ranging code: auto and cross correlation. The auto-correlation is a measure of the agreement of a code with a shifted replica of itself (Bao & Tsui 2004) and cross correlation is with that of another. The latter property enables the receivers to uniquely distinguish each satellite that are transmitted on the same frequency (Kaplan & Hegarty 2006).

The GPS L1 C/A received signal power is typically around -130 dBm (IS-GPS-200E 2010). For the 10-bit code used in it, the practically achievable cross correlation margin is about 22 dB (Parkinson & Spilker 1996). If the difference in the received absolute signal power exceeds this margin, cross correlation is potentially possible. Under this condition, the stronger signal effectively acts as a local spoofer (Nielsen et al 2011) on the weaker one and makes it ineffective for navigation estimation and *in turn may delay TTFF*. Several techniques have been proposed at the signal processing level (Glennon & Dempster 2005). With the need for highly reliable techniques for civil aviation applications, cross correlation detection based on NAV data as

obtained from the satellites is adopted. The technique relies on differencing measurements (pseudorange) with that of ranges estimated from the almanac. In order to minimize the secondary parameters and thus improve TTFF performance, it is important that an independent method of CCD based on NAV data be proposed, which eliminates this use of the almanac.

The following section explains in detail the cross correlation problem in a receiver, the existing range differencing method and highlights the limitations associated with it. Subsequently, two new methods of CCD are derived.

5.2 Cross correlation detection overview and the proposed methods

In a GNSS receiver, the correlation values are continuously compared against a threshold above which it is used for subsequent operations (for example, measurement validity and tracking limits are usually compared against a specific C/N_0 , based on the category of the receiver). Typically, this threshold is kept as low as possible to effectively obtain the satellite signal (Van Diggelen 2009). For a succinct explanation, two PRN's (1 & 2) of GPS are considered to be tracking, one with a higher signal strength w.r.t to the other. Under this scenario, PRN-1 is assumed at the possible lowest and the other at the extreme maximum permissible within the dynamic range of the receiver. If the absolute difference in the signal strength for this pair of satellites exceed the typical 22 dB margin, PRN-1 effectively will not be able to discriminate itself from PRN 2 and thus starts to falsely track it. With false lock and data continuously failing its integrity checks (for example, CRC or parity), the channel is reset and the processing attempted again. However, if the data passes the integrity tests, effectively PRN 1 will be tracking the data of the PRN 2 (Kaplan & Hegarty 2006). Figure 5-2 illustrates the effect of cross correlation in an open sky environment.

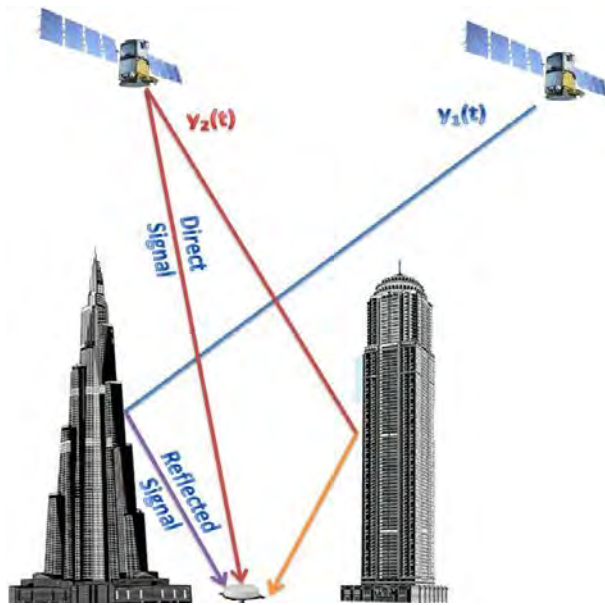


Figure 5-2: A typical scenario of cross correlation in outdoor application.

Extending (Eq. (2-1)), the individual signals as observed at the user antenna for the scenario depicted in Figure 5-2 is given by

$$y_1(t) = A_1 r_1(t) d_1(t) \cos(2\pi f_1 t) \quad (5-1)$$

$$y_2(t) = A_2 r_2(t) d_2(t) \cos(2\pi f_1 t) \quad (5-2)$$

The GNSS satellite antenna design ensures that the received signal from a user's local zenith or horizon are nearly the same. This is done to compensate the range variations (Bao & Tsui 2004). Thus, only from a local phenomenon as shown in Figure 5-2, A_1 and A_2 vary. If the differential power level for a satellite pair exceeds 22 dB , it results in cross correlation. Under such a scenario within the receiver, the correlation on $y_1(t)$ results in a false tracking of $y_2(t)$ and as a fallout,

$$d_2(t) = d_1(t). \quad (5-3)$$

To counter the above phenomenon, range differencing is adopted in civil aviation applications, as explained in the following section.

5.2.1 Range differencing

As a part of civil aviation receivers, CCD based on range differencing of measurements and that estimated from the almanac is performed. The methodology, illustrated in Figure 5-3, assumes that a recent and valid almanac is available within the receiver. Following measurements, pseudoranges in particular, the range to each satellite is estimated based on an approximate user position (which is obtained from external input or the last computed user position stored in the receiver's memory). The threshold value (for differencing) chosen is such that it accounts for the age of the almanac used for range estimation. If the difference is within the limits, the signal is valid. This method is unambiguous, specific to GNSS application and valid for all scenarios (DO-229D 2006).

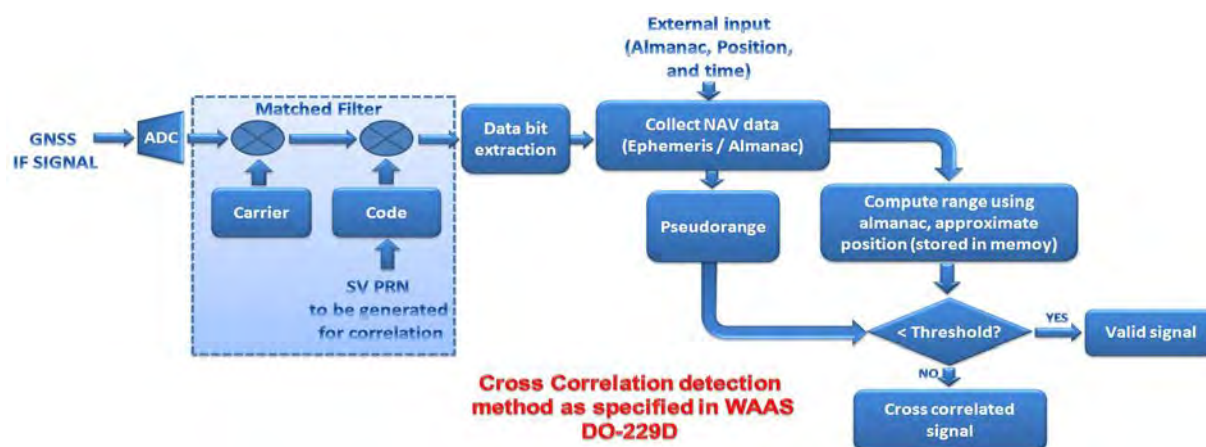


Figure 5-3: Existing cross correlation detection method based on range differencing in civil aviation GPS L1 C/A receivers.

With the objective of eliminating the almanac and yet achieve a similar CCD, the following section presents two methods based on the proposed IRNSS NAV data structure (Figure 3-4). It also explains how these methods can be adapted to existing and emerging GNSS systems.

First, with an experimental setup, the cross correlation effect and its detection based on the range differencing is established.

5.2.2 *Experimental analysis*

The GPSGL receiver used in the previous chapters is taken as reference hardware for this task. As mentioned in the previous chapter, the receiver does not have the provision to store any of the warm start parameters. The antenna position and the latest almanac are hard coded in the receiver software, with time alone estimated from the satellite signal. In addition, the flowchart shown in Figure 5-3 is implemented in the receiver. Specifically, the pseudorange measurements are compared with the range estimated using the latest almanac. This threshold, as per the civil aviation standards, is set to 200 km (DO-229D 2006). The receiver output is connected to a console, which had a GGVISION capable of displaying channel related parameters. Apart from several parameters displayed, specific to this research, pseudorange and Carrier to Noise (C/N_0) are profiled. An RF combiner's output drove the receiver antenna port. The inputs to the RF combiner are from a GPS antenna exposed to open sky and another from the simulator, as used in the previous chapter but with GPS simulation capability.

The simulator outputs the RF signal at -130 dBm on the front panel and for diagnostics, -70 dBm on the rear port. This test apparatus is shown in Figure 5-4a). The simulator is capable of generating twelve satellites and is input with the latest almanac, position (of the receiver antenna exposed to open sky) and the time at which the experiment is performed. However, for this activity only one channel is enabled. The signal from the rear panel is input to the RF combiner through suitable attenuators to ensure that it co-exists with the open sky signals but at a *relatively* high level. In addition, the single channel from the simulator is enabled with receiver estimating the position.

The receiver is powered-on with initial conditions as explained above. It then immediately acquired and tracked few channels and computed its position. Subsequently, the simulator signal

was enabled. This was acquired immediately by the receiver with a relatively high C/N_0 compared to the other channels. Since the simulation was not synchronized to GPS time, this channel was not used for positioning. Subsequently, one of the satellites acquired from open sky was observed to have a low C/N_0 and the pseudorange/satellite position was similar to the channel that tracked the simulator signal as shown in Figure 5-4b). As explained earlier, this is attributed to the cross correlation. With the range difference exceeding the threshold, a flag indicated CCD.

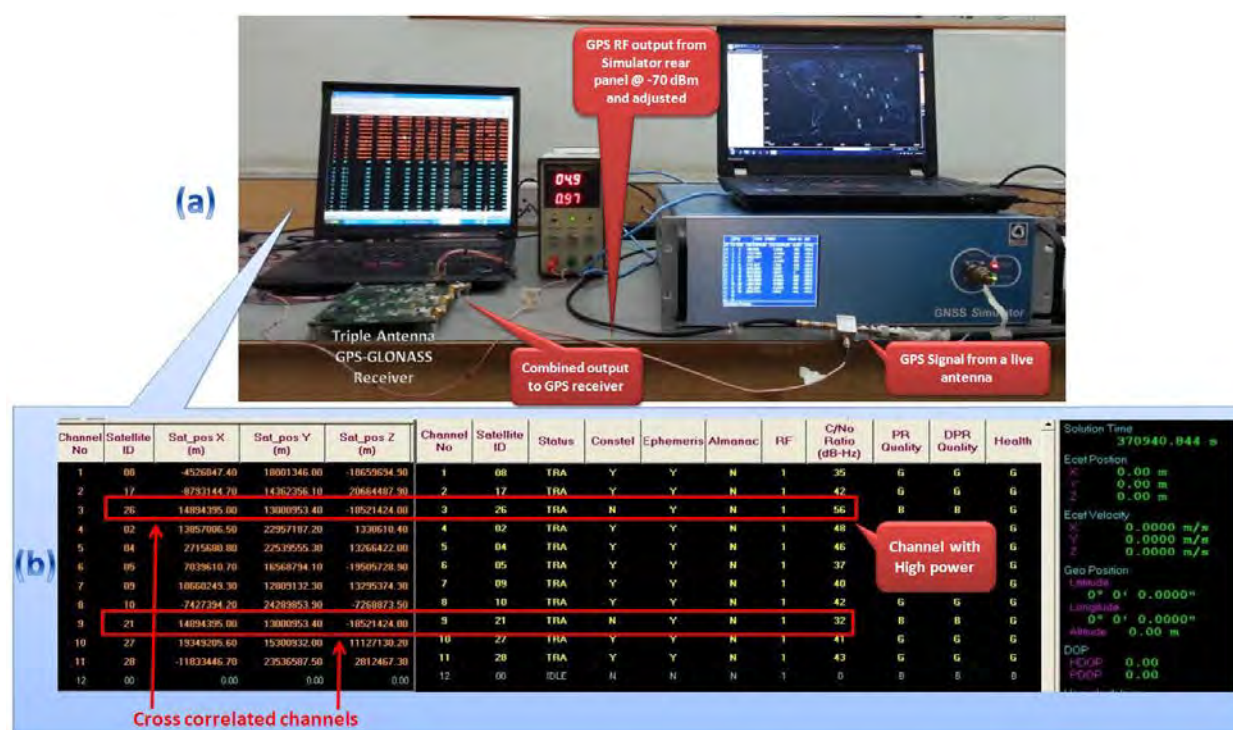


Figure 5-4: a). Test apparatus used to demonstrate cross correlation effects and detection based on existing methods b) the GGVISION snap-shot depicting the cross correlated channels.

5.2.3 Limitations

Aviation GNSS receivers fall under the category of open sky applications and the cross correlation effects are not as prevalent as indoors. In addition, the almanac, position and time, if

required, are input to the receiver from the Flight Management System (FMS) (DO-229D 2006). Thus, such a receiver is equipped with the latest (almanac) and relatively accurate information (time & position) either internally or through external assistance, which ensures that range differencing is always possible. However, some critical open sky applications (for example, applications shown in Figure 2-21) where similar effects are observed but are in cold start mode of receiver operation, the range differencing method is rendered ineffective. The following paragraph enumerates the limitations of range differencing in *cold start mode of receiver* operation:

1. A GPS receiver estimates time following which measurements to a minimum of four satellites provides an estimate of the user position. The by-product of this process is the estimation of the user clock bias. The accurate estimate of GPS time and pseudoranges are obtained when compensated by this bias. Subsequently, range differencing is possible (for example, initially (before position estimation) ranges can be off by 20 ms (6000 km, zenith to horizon satellites)). With positions and ranges corrected by the clock bias, range differencing is enabled. This implies that a minimum of 32 s (best case TTFF in GPS L1) is required from power on, after which this method is applicable.
2. In Chapter Two, it was highlighted that from the first subframe synched channel, the system time is estimated. However, in aviation grade receivers, the time is valid only after obtaining the information (TOW) from two satellites (DO-229D 2006). If one of these is a cross correlated signal, it would not be possible to detect until the cross correlation is detected (only after positioning). However, with data likely to be similar

- (Eq. (5-3)), time initialization occurs but the validation criterion (two satellite check) would be ineffective.
3. The existing method is only applicable with the availability of almanac. In addition, the age of almanac effectively determines its error contribution towards the range estimation. This sets a constraint that the almanac needs to be the most recent to obviate misleading information during the threshold comparison of a normal channel.
 4. With cross correlation, the channel is inadvertently blocked and not usable for positioning. In cold start mode of receiver operation, this channel is released only after position computation occurs. This delay may indirectly result in another satellite not being programmed, which may affect TTFF indirectly (for example, available satellites are more than the number of channels supported by the receiver).

5.2.4 Proposed cross correlation methods

The basic design constraints/assumptions in developing the methods are as follows:

- First, the detection shall occur in real time and is declared within a frame of NAV data.
- Second, it shall be applicable in cold start mode of receiver operation.

With the above constraints, the following two methods are proposed: first the CCD based on NAV data processing (CCD-NAV) and second based on satellite-id (CCD-SVID). The explanation is based on the proposed IRNSS NAV data processing, which can be extended to any GNSS system.

5.2.4.1 CCD-NAV

The IRNSS satellites are distributed as four geosynchronous (2 each in 2 planes) and three geostationary satellites (Rao et al 2011). As shown in Eq. (5-1), $d(t)$ represents the navigation data of a satellite, which will never be the same for any two satellites w.r.t. Keplerian and clock

parameters (bias (Af_0), drift (Af_1), rate of change of drift (Af_2)). As explained earlier, when the signal gets cross correlated and if the data *passes the integrity checks*, the NAV data of the weaker channel will be the same as that of the higher signal strength (Eq. (5-3)). With this input, the following algorithm is proposed (Rao & Lachapelle 2012):

- Extract the data post necessary integrity checks (Figure 3-19) and store it separately for the channel.
- Compare each channel data with that of the other. This calls for N-1 comparisons, where N is the number of subframe synched channels.
- If a match is observed, declare the channel with the lower C/N_0 as cross correlated.

The above scheme assumes that the *NAV data from the satellites are different*. If similar, it is attributed to a local phenomenon in cross-correlation. However, the above method is not *completely (still valid for ephemeris pages) applicable* to GPS/GLONASS L1. This is due to subframes 4 and 5 that are similar for all the satellites in GPS and strings 6 to 15 in GLONASS satellites, which constitutes the satellite almanac ((IS-GPS-200E 2010) (GLONASS-ICD 1998)).

With the proposed IRNSS NAV data (Figure 3-6, Figure 3-7), *secondary data are distinct across subframes*. This ensures the limitation as observed in GPS/GLONASS L1 w.r.t CCD, is not present in IRNSS. The design methodology is as shown in CCD-NAV part of Figure 5-5.

5.2.4.2 CCD-SVID

In the proposed IRNSS NAV data, each page has a unique satellite id, unlike GPS L1. This was primarily used to assist staggering messages across satellites as a part of a secondary NAV data set. However, it is taken as an advantage to detect the cross correlation as follows: A closer examination of the matched filter shows that the PRN used to generate the local replica of the

ranging code is programmed typically to FPGA from DSP (explained in Chapter Two). Post detection of a satellite signal, extraction and *validation of the NAV data* is performed. Subsequently, the extraction of the PRN id (from NAV data) and comparison with the programmed id (FPGA) ensures the validity of the signal w.r.t cross correlation. The opposite (mismatch in ID) is a cross correlated signal.

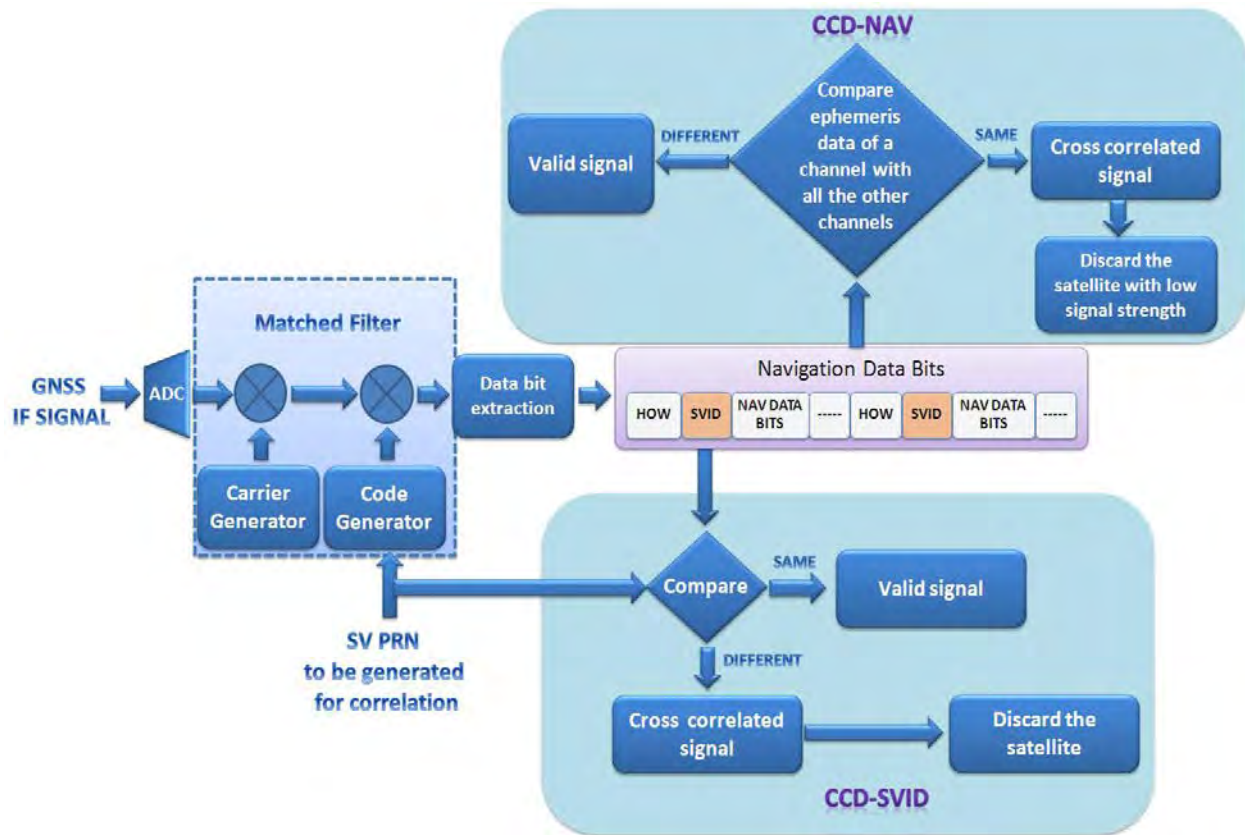


Figure 5-5: Proposed cross correlation methods based on NAV data processing in IRNSS.

This technique when combined with the CCD-NAV ensures that integrity w.r.t cross correlation is guaranteed for any signal that has passed the data level checks.

The relative merits of the proposed schemes are as follows:

- Provides instantaneous detection and ensures that when the data is presented, integrity w.r.t cross correlation is assured.

- Does not depend on any receiver parameters or external input. The detection occurs prior to measurement formulation and thus ensures that the system time even with single satellite is guaranteed for cross correlation.
- However, from an implementation perspective, CCD-NAV has to perform $(n-1)$ comparisons where n is the number of tracking and subframe synced channels.

The above methods unambiguously detect cross correlation (on the proposed IRNSS NAV data) and thus obviate the dependence on the almanac from satellites for any real-time applications. With this input, the following section attempts to design a NAV data signal to meet this research objective.

5.3 Combinational design for optimal TTFF

With inputs derived from single and dual frequency signal designs (Chapter Three and Chapter Four), this section presents several combinational architectures and explores/proposes the most optimal signal design for IRNSS in the dual frequency mode of receiver operation. The objective is to achieve the best TTFF and yet obtain the secondary data (restricted to textual messages).

The following constraints/assumptions are imposed on the signal design process:

- The ionosphere and UTC parameters necessarily need to be transmitted to facilitate corrections for single frequency user and parameters to align the IRNSS time to UTC respectively.
- SPS and restricted data/rates are identical.
- The single frequency of receiver operation should not be affected.
- In FSA (Figure 3-8), a complete frame was dedicated to almanac. Based on the results from the previous section, dropping the almanac frame reduces it to TSN with only

textual messages (Figure 3-9). Thus for further analysis/design, TSN and TSF (Figure 3-11) NAV data structures are considered as inputs.

The proposed methods follow a sequence centered on the service of operation supported, which are combined or service specific, with the ultimate objective of reducing the time required to transmit primary NAV data. The basis for this design is Eq. (3-14) and Eq. (3-15).

5.3.1 Combined mode 1

As a first step, a conservative approach of dropping the secondary data on a frequency of either service is proposed. The design rationale is as follows:

- The TSF method is adopted for optimal TTFF.
- The secondary data is derived from the TSN NAV data design.

Based on the above criterion, the signal transmission method shown in Figure 5-6 is deduced.

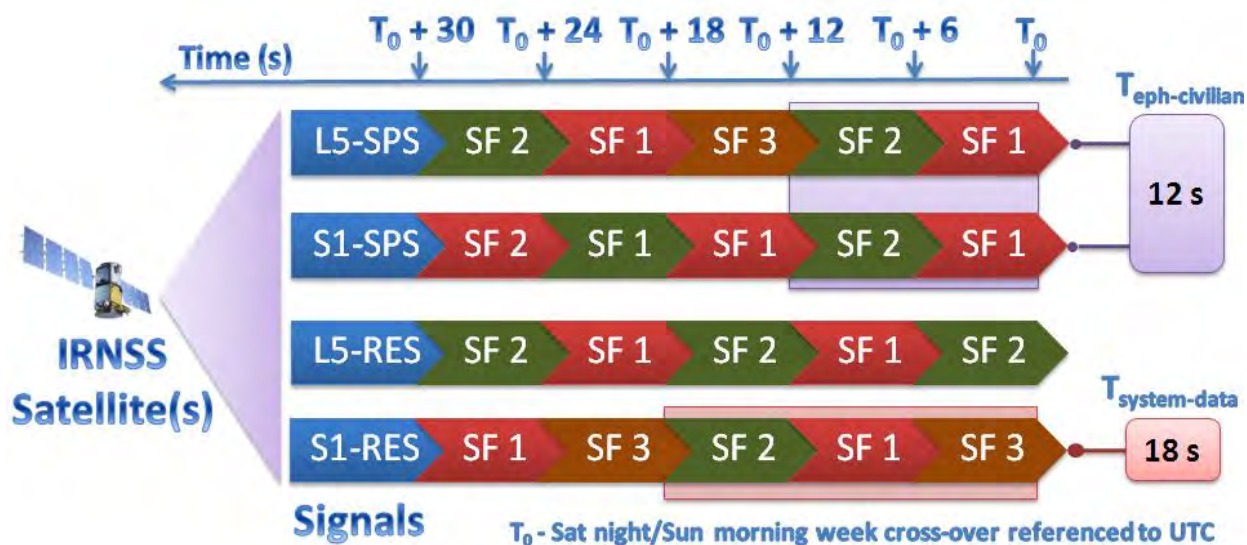


Figure 5-6: NAV data signal design in combined mode 1 of IRNSS.

The salient features of this design are as given in Table 5-2.

Table 5-2: Summary of NAV data signal design in combined mode 1 of IRNSS.

Mode of Operation	SPS [s]	Restricted [s]	Description
Single	12	12	The transmission of the primary parameters is optimal from the S1 path for a SPS user. For restricted users, in code diversity mode of operation (Figure 4-9c)) an optimal TTFF results from the S1 path with the data assistance from SPS. In either case, the secondary data is available within 18 s.
Dual	12	12	The data from the S1 path results in a SPS/restricted receiver to achieve the best TTFF in this mode of operation.

5.3.2 Combined mode 2

To improve the TTFF of the restricted service, this approach drops the secondary data completely on both frequencies and employs the TSF method (Figure 3-11) of NAV transmission. On the SPS paths, TSN (Figure 3-9) and TSF architectures are adopted on the SPS L5 and S1, respectively. The design rationale is as follows:

- The restricted signals shall be able to achieve the TTFF within a subframe period after TOW collection.
- SPS signals will be able to obtain the optimal TTFF from one frequency and achieve the secondary data through the other.

Based on the above, the architecture shown in Figure 5-7 is derived.

The salient features of this architecture are:

- The restricted signals which adopt the TSF architecture shall transmit the data as shown in Figure 5-8 on the L5 path and the counter component of this on the S1 path (Figure

3-11). A noteworthy change in the design is that the slotting of the textual message is reversed in Figure 5-8 w.r.t Figure 3-11. However, a direct reversal results in DOP being relatively high at $(T_0 + 72)$ s {the textual (MT-3) data transmitted from both the frequencies of the restricted service (Figure 3-11)}, similar to the condition explained in Figure 3-12. To overcome this, at $(T_0 + 72)$ s on L5, MT3 is transmitted on SV3 to ensure that a dual frequency receiver obtains the primary data from all the satellites and thus obviates the DOP problem. This sequence repeats itself every 144 s.

- The secondary data for the restricted services is available from the SPS path.
- The SPS NAV data design on either frequency is similar to the combined model.

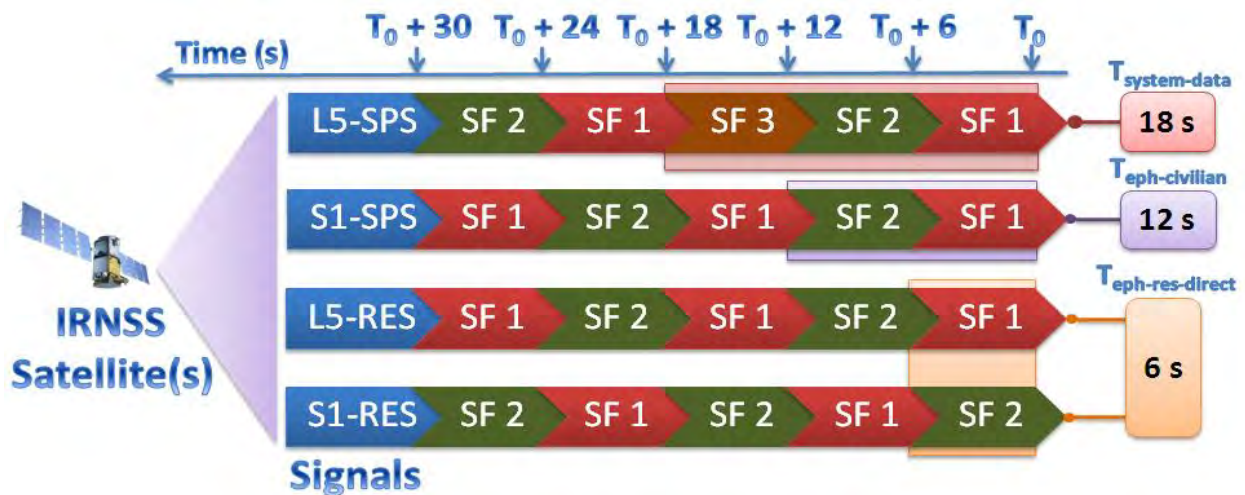


Figure 5-7: NAV data signal design in combined mode 2 of operation in IRNSS.

The explanation in Table 5-2 is equally applicable to this method with the following additional points in dual restricted mode of operation:

- The TTFF in direct acquisition method is achieved in 6 s and *exclusively from restricted service*.

- The results obtained from combined mode 1 and 2 correspond to architectures whose relative performance w.r.t existing GNSS (in dual frequency) is better but still not comparable to Table 5-1

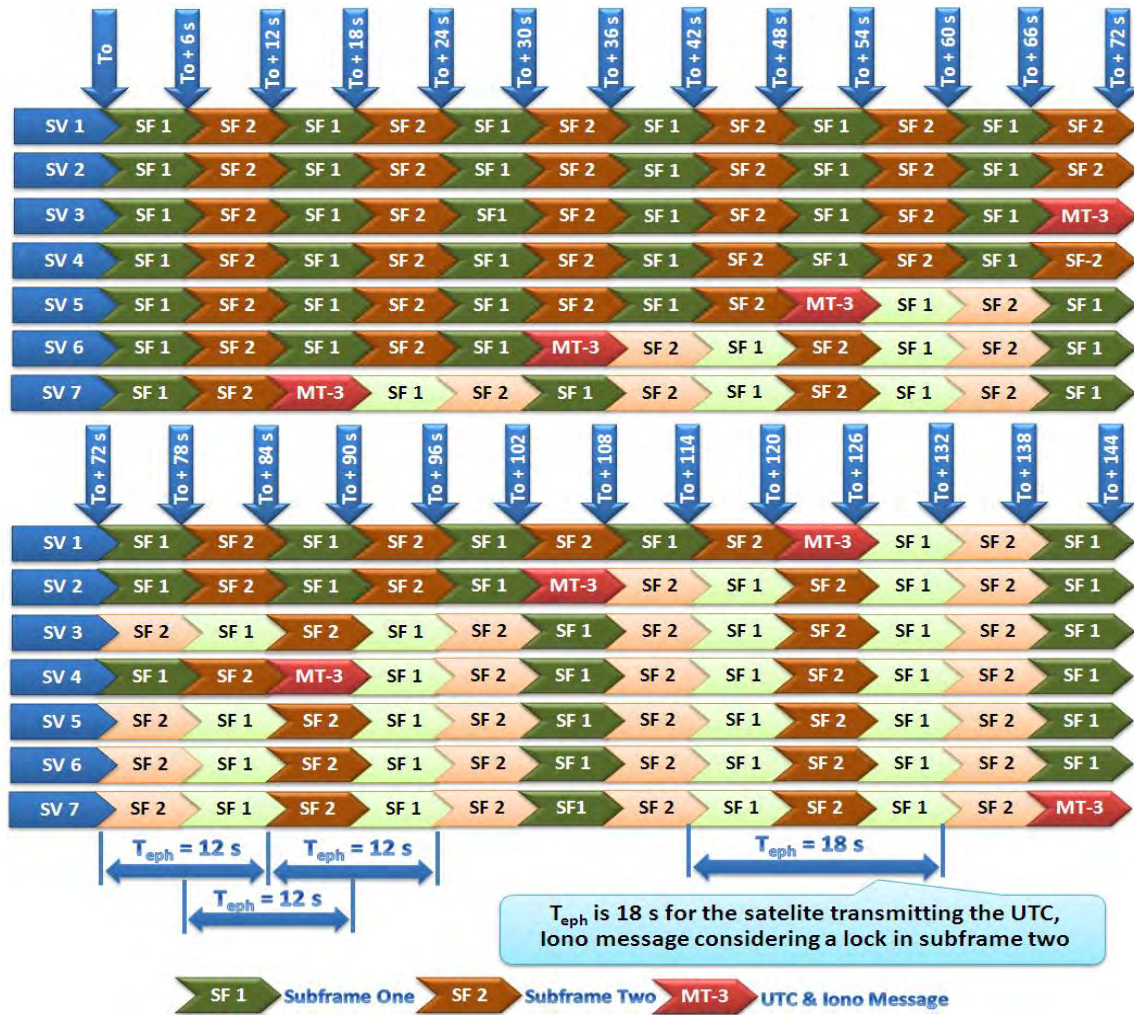


Figure 5-8: Proposed TSF method of NAV data transmission on L5 path of restricted service of IRNSS in combined mode 2 (sequencing of MT3 changed w.r.t Figure 3-11 and assuming it to be supported on S1 to resolve DOP).

With the design merits (messages slotting in either frequency of restricted service) presented in combined mode 2, the following section explores how to derive the most optimal NAV data design for SPS and restricted services.

5.3.3 *Optimal civilian mode (OCM)*

Extending the concepts derived in combined mode 2 to SPS signals and considering that secondary data (textual messages) are transmitted on it, results in TSF architectures on both services/frequencies with necessary design modifications as follows:

- The MT-3 message in Figure 3-11, is replaced by MT (n, m) as shown in Figure 5-11, where n is the message types supported (Table 3-5) and m can vary from 1 to 14, which signifies specific transmission slots in either frequency. Slots 1 to 7 correspond to 1- 7 satellite id in L5 and 8-14 to that of 1-7 of S1 respectively.
- With Figure 3-11 as a reference, message slotting as shown in Figure 5-9 is adopted on either services. As with the combined mode 2, the sequencing of the messages obviates DOP issues.
- Sequencing of textual messages similar to SPS is adopted in restricted services as well.
- The message slotting shown in Figure 5-9 is generic w.r.t a particular message transmission. One possible approach is that the UTC/IONO message be transmitted alternatively on either frequency to ensure that single frequency users obtain the ionosphere corrections faster.
- Following the above design constraints, the architecture shown in Figure 5-10 is designed. For simplicity, the MT message (Figure 3-11) is indicated as SF 1 and SF 2 in Figure 5-10 with SF1 / SF2 carrying the MT message corresponding to its respective slot is as shown in Figure 5-9. The OCM method enhances the *primary NAV data transmission* and thus facilitates faster TTF in a receiver supporting diverse modes of operation. The signal design methodology followed in OCM (Figure 5-10) is explained as follows:

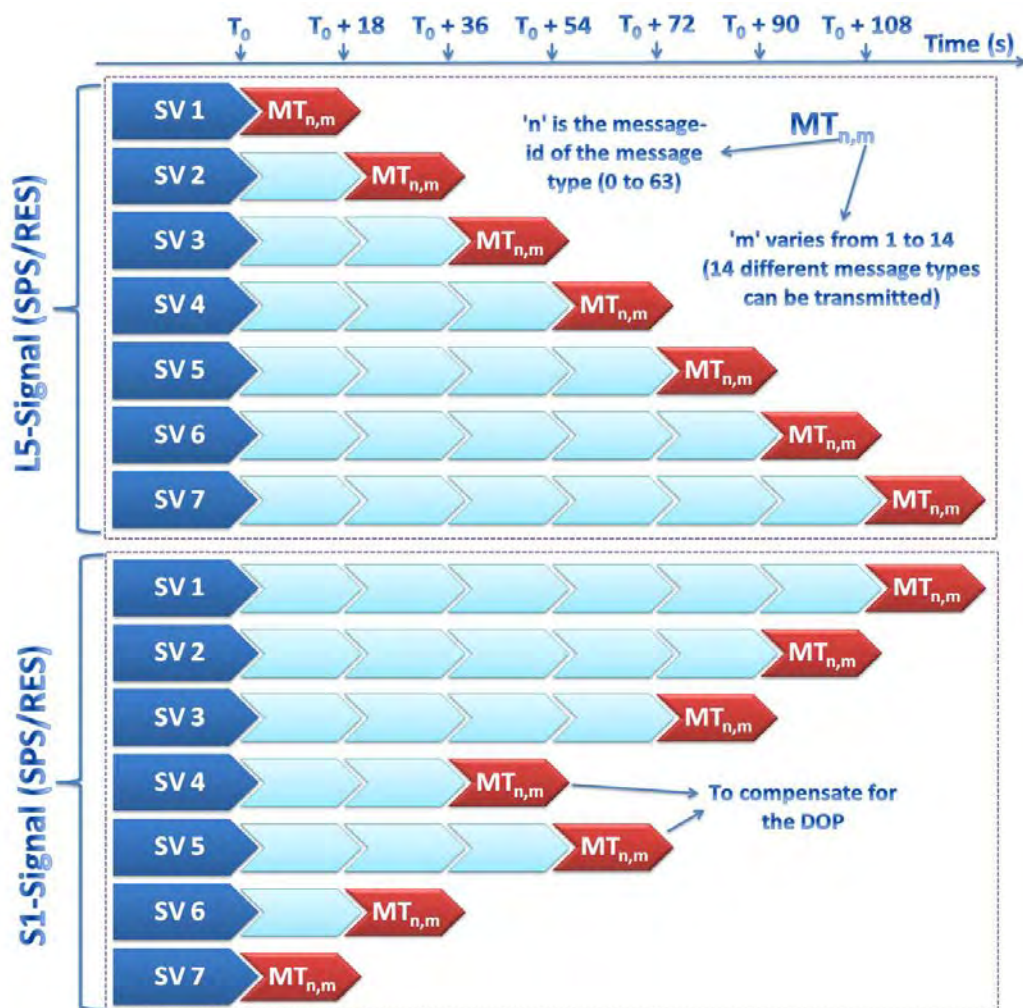


Figure 5-9: Timing diagram illustrating the transmission slots of various messages in either frequencies of the SPS/RES service in IRNSS OCM method of NAV data design.

- The NAV data symbols are staggered and transmitted from the satellite. The staggering of a subframe is accomplished as shown in Figure 5-10 b). The objective of this approach is to ensure that 1200 symbols (2 subframe effective data) are transmitted in 6 s from either service/frequency. For example, at T_0 , the SPS channels on either frequency are initialized with SF 1 and SF 2 first portion of their subframes respectively. The complement portions of these subframes are assigned to the restricted service on either of

their frequencies. For $T_0 + 3$ to $T_0 + 6$ s, the above sequence is reversed across service and frequencies.

- On either frequency of both services, the NAV data is transmitted as shown in Figure 5-10a) where the carrier diversity of SPS and restricted services are met individually.
- The receiver operation in a single frequency mode is unaffected by this method of NAV data signal transmission.

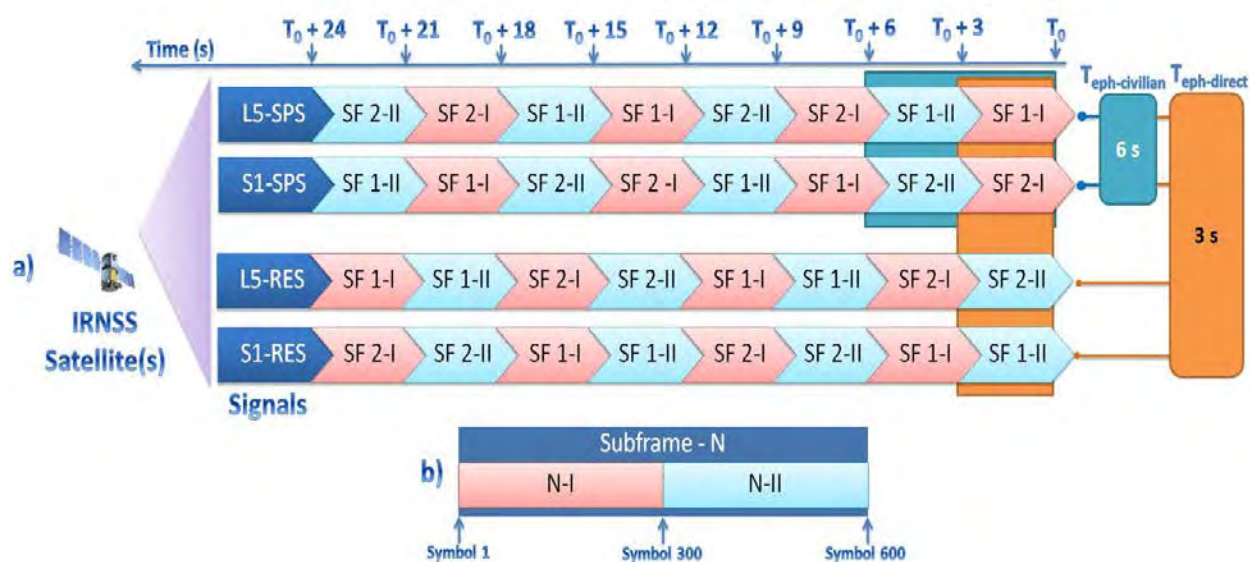


Figure 5-10: OCM of NAV data signal design in IRNSS.

Table 5-3 presents the merits of this architecture w.r.t various parameters across frequencies and services. The results depicted clearly indicate a performance improvement in all categories in comparison with Table 5-1.

The advantage with this design is that in real-time (directly from satellites), the receivers cold start TTFF performance is equal to the HOT start performance (data stored in receiver's memory) of GPS or the AGPS ephemeris assistance. In addition, if IRNSS were to be extended globally, this architecture would still be applicable (for example, adopting Table 3-4 and

interpreting set 1 to 4 contents as MT (n, m)) thus making this approach the most optimal w.r.t TTFF and data rate or power being commensurate with that of existing operational GNSS systems. Further, this design is generic and can be used in any emerging dual frequency GNSS system.

Table 5-3: OCM of NAV data signal design in IRNSS.

Mode of Operation	SPS [s]	Restricted [s]	Description
Single	12	12	The transmission of the primary parameters is optimal from either the L5 or S1 path for a SPS user, which is the TTFF of restricted user also.
Dual	6	6	The data from the L5/S1 paths effectively enable the SPS receiver to achieve the most optimal TTFF. With TOW, the restricted service enters into measurement mode (Chapter Four) and provides instantaneous positioning (with NAV data from SPS path). <i>The direct acquisition results in reception of primary parameters within 3 s, ensuring the best TTFF.</i>

5.3.4 Optimal restricted mode (ORM)

All the methods till now have assumed similar data/rate on the restricted and SPS signals. With the results achieved from OCM, *from an operational perspective the TTFF achievable on a restricted service* should be better or equal to that of the SPS. This section presents a signal design where it assumes that the data on a restricted service is different from the SPS signal.

Towards this, the following assumptions/design constraints are made:

- The acquisition of the signal is SPS assisted (restricted only to obtaining time for restricted signal acquisition).

- From Eq.(4-7), the first impediment in achieving a fast TTFF for a restricted user is the time taken to collect TOW information, which takes a minimum of 6 s in the proposed IRNSS signal design (Figure 3-4). As a design constraint in the diverse mode of receiver operation, reduction of this component is set as a design objective.
- The slotting of the subframes on either services/frequencies is as shown in Figure 5-9.

With the above constraints, the architecture shown in Figure 5-11a) is derived, whose salient features are as follows:

- The NAV data (subframes) on either frequency are identical (SF1/SF1) (unlike OCM, where it is SF1/SF2 straddled). However, the data contents within are straddled on one frequency of SPS to ensure that TOW is available within 3 s. This is accomplished by splitting the subframe of S1 SPS path as shown in Figure 5-11b).
- The subframes are straddled on either frequencies of the restricted service (assuming different data w.r.t SPS) and thus ensures a TTFF of 9 s (including 3 s for TOW collection) as listed in Table 5-4.

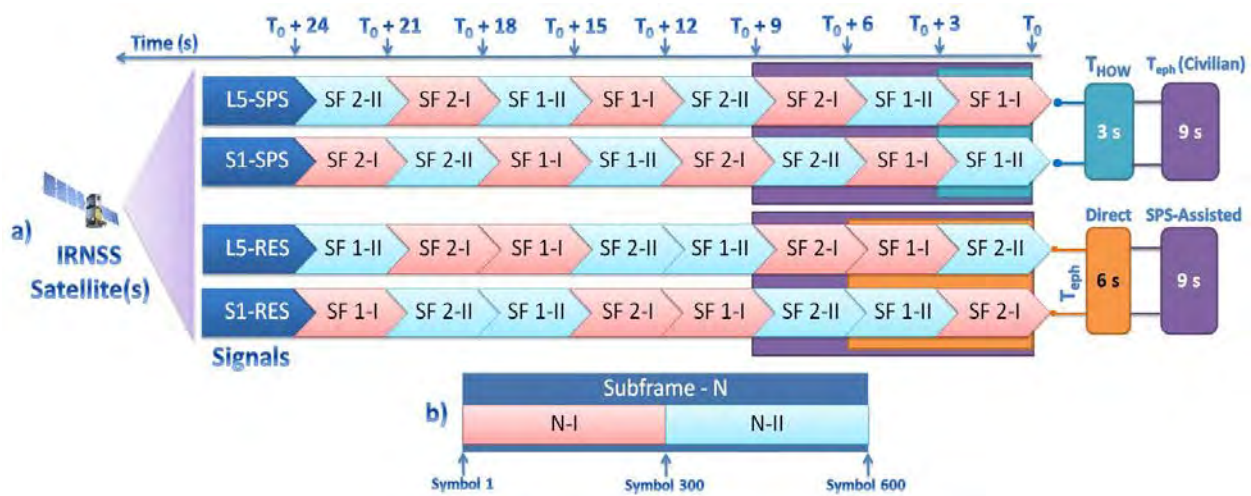


Figure 5-11: ORM of NAV data signal design in IRNSS.

Table 5-4: Summary of ORM of NAV data signal design in IRNSS.

Mode of Operation	SPS [s]	Restricted [s]	Description/Remarks
Single	12	18	The transmission of the primary parameters is identical and thus TTFF from either L5 or S1 remains the same. With data being different, the code diversity is not applicable and thus with SPS assistance, the TTFF follows Eq. 4-7 for restricted users in single frequency mode.
Dual	9	9	In the civilian mode of operation, the data from L5 and S1 when processed effectively results in a TTFF of 9 s. With HOW available in 3 s (straddling of the SPS subframes), the TTFF of the restricted <i>users in SPS assisted mode with different data is 9 s, which is the best from SPS assisted and different data architecture.</i>

The advantage with this method is that if the data rate of the restricted signal is increased to enable the faster transmission of the primary parameters, this technique will assist the TOW collection faster (from SPS channels).

The signal generation and receiver design philosophies are similar to that explained in the previous chapter for combined mode 1 and 2. However, the optimal design architectures presented in this chapter is a new component and thus the top level signal generation and the commensurate receiver designs are presented in the following sections.

5.4 Components of test apparatus

This section presents the top-level architecture of the new software modules developed for the simulator and receiver. The reference hardware for either is as used in the previous chapter.

5.4.1 Signal generation

The base software used for simulation follows Equation 4-23. The data component ($d(t)$) corresponding to it is generated by using the software as depicted in Figure 5-12 (OCM) and Figure 5-13 (ORM). At a top level, the TOW determines the generation of the subframe content in either mode of operation. Based on the method adopted, the grouping of data is done into sets of NAV data symbols. The operations specific to each method is explained as follows:

In OCM, the grouping is done commensurate with Figure 5-10 and is as shown in Figure 5-12.

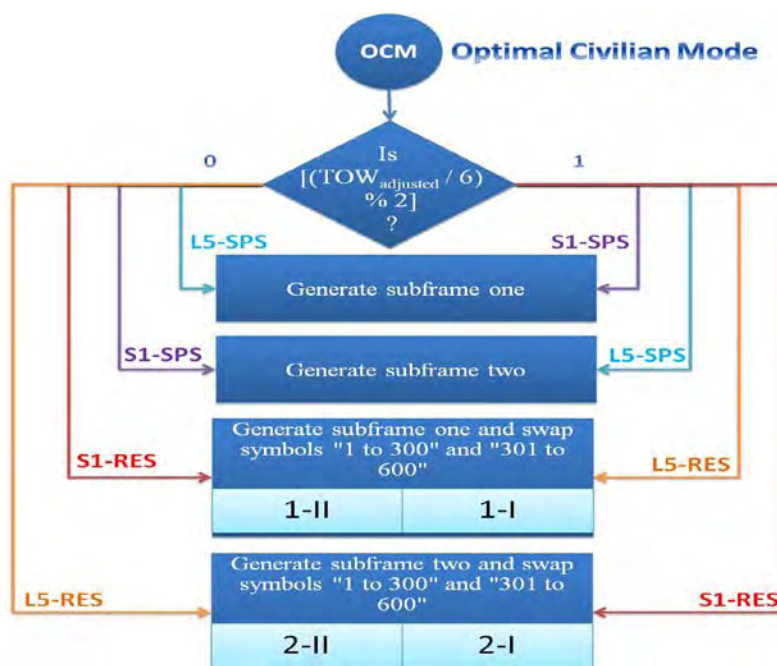


Figure 5-12: Signal generation methodology to derive the proposed OCM signals in IRNSS.

The details are as follows: T_0 (Saturday night/Sunday morning) is reference for the signal generation. For any arbitrary TOW, the signal generation starts from the next closest multiple of subframe period to it (for example, if $TOW = 15$, the next closest subframe period is 18 and the signal generation corresponding to it occurs). For this TOW, the subframe data across SPS channels follows as shown in Figure 5-12. For odd subframe ($[\text{quotient of adjusted } TOW/6] \% 2 = 1$), the subframe data across SPS channels follows as shown in Figure 5-12.

2), the data is loaded as shown on the right side of Figure 5-12. Similarly, for even subframes, the data is filled as on the left side of Figure 5-12. For the restricted channels, the data contents of SPS (L5/S1) are swapped, grouped and loaded into the buffer of the restricted service as (S1/L5) as shown in Figure 5-10.

Explanations of OCM holds good for ORM as well with the difference that the data for the SPS channels are split, swapped and arranged into four sets. For the restricted channels, from these four sets, data are grouped into two sets as shown in Figure 5-13.

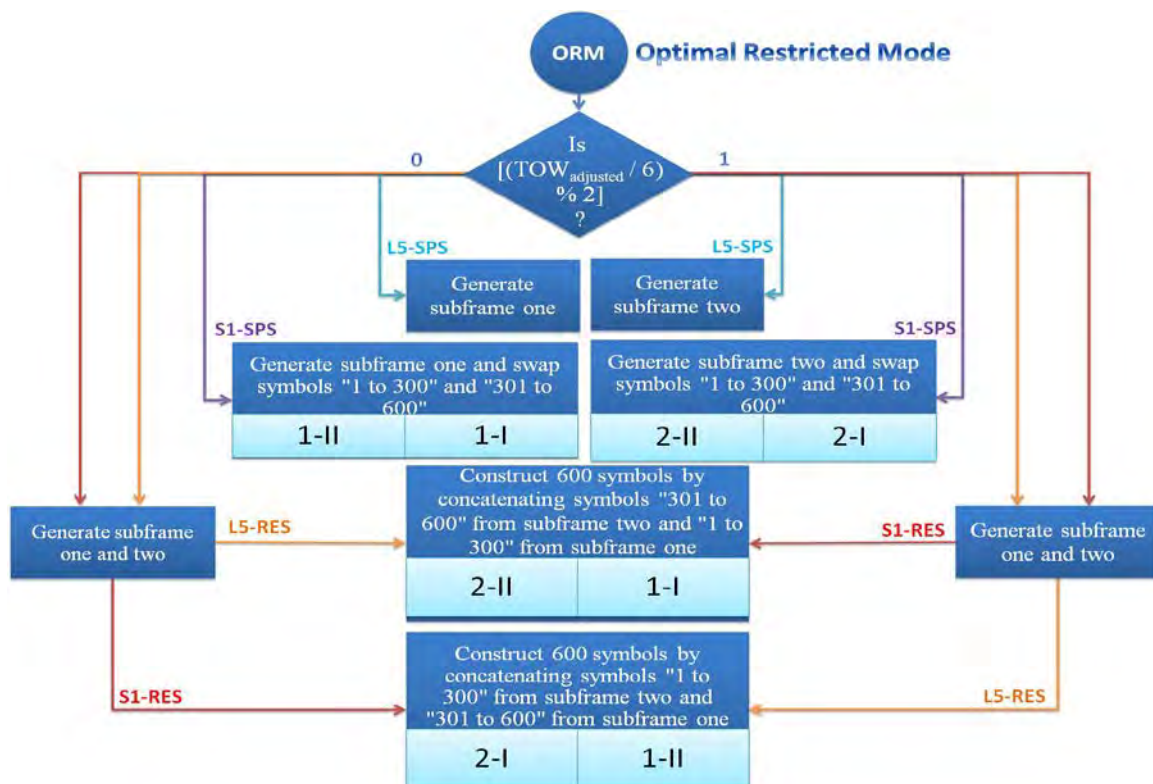


Figure 5-13: Signal generation methodology to derive the proposed ORM signals in IRNSS.

5.4.2 Receiver algorithm design

To derive the benefits of the proposed signal, with Figure 4-18 as reference, the processing shown in Figure 5-14 is adopted. The algorithm assumes that the contents are available from the

correlators from all four paths (SPS/RES L5/S1). The processing on the individual channels is as shown in Figure 5-14. To derive the benefits, in accordance to the OCM/ORM methods of signal transmission, satellite wise data processing is performed after 300 symbols are collected.

As shown in Figure 5-14, the second synch pattern search (across frequency/service) ensures optimal processing and facilitates easy extraction of straddled data across frequencies/services to generate the NAV data. Subsequent to this, the operations in Figure 4-18 are performed w.r.t measurements and positioning.

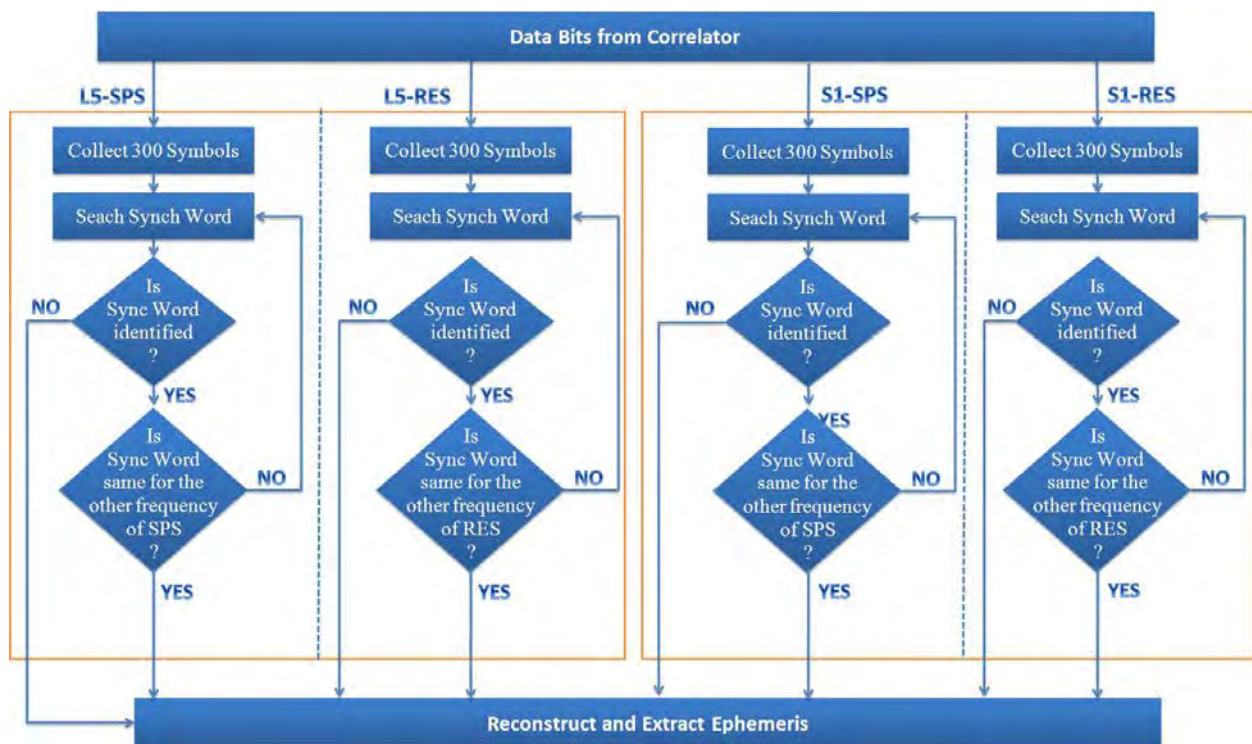


Figure 5-14: High level receiver design to derive the benefits of OCM and ORM of NAV data signal design in IRNSS.

5.5 Test methodology and performance analysis

5.5.1 Cross correlation

To validate the performance of the proposed cross correlations schemes, the test setup as shown in Figure 5-4 is adopted with the following changes: instead of the RF signal from open sky, the

simulator input was directly fed to the receiver port. The signal strength on each channel of the simulator can be varied from -20 to 20 dB about an absolute power setting in the range of -110 to -150 dBm, which was effectively used to simulate a cross correlation effect. At the start of the simulation, the power on one channel was kept relatively high compared to the other channels and was disabled. Two versions of the simulator software were used: IRNSS with NAV data similar to GPS L1 (Chapter Three) and carrier diversity (Chapter Four). The receiver software used in Chapter Three was modified to incorporate the logics of the range differencing (Figure 5-3). With the input from the simulator (the high power and two other channels disabled initially), the receiver computed a position within 24 s. Subsequently the channel configured for high power and two other channels was enabled. This channel acquired and in addition, cross correlation on another channel was observed. However, it took 192 s (post bit synch of first channel) to collect the almanac after which the range differencing method was invoked. With the almanac, the receiver declared the cross correlated channel. The trial was conducted on different satellite ids (power level on simulator varied) with the result shown in Figure 5-15.

To demonstrate the performance of the proposed versions, corresponding receiver software was generated: The first was with NAV data based comparison and the second with SVID based cross correlation detection. An integrity flag was used and logged from the bit-synchronization of a channel.

The simulator was changed for carrier diversity version as in Chapter Four (Figure 4-10). The setup was similar to that of the previous trial w.r.t the simulator. The receiver was run with two versions independently - one with NAV data processing and the other based on SVID. Unlike range differencing, only two satellites were used one with high and low signal strength settings respectively on the simulator. The results from both versions demonstrated that with the NAV

data collection/SVID identification, the CCD was identified within 6 s of tracking as shown in Figure 5-15.

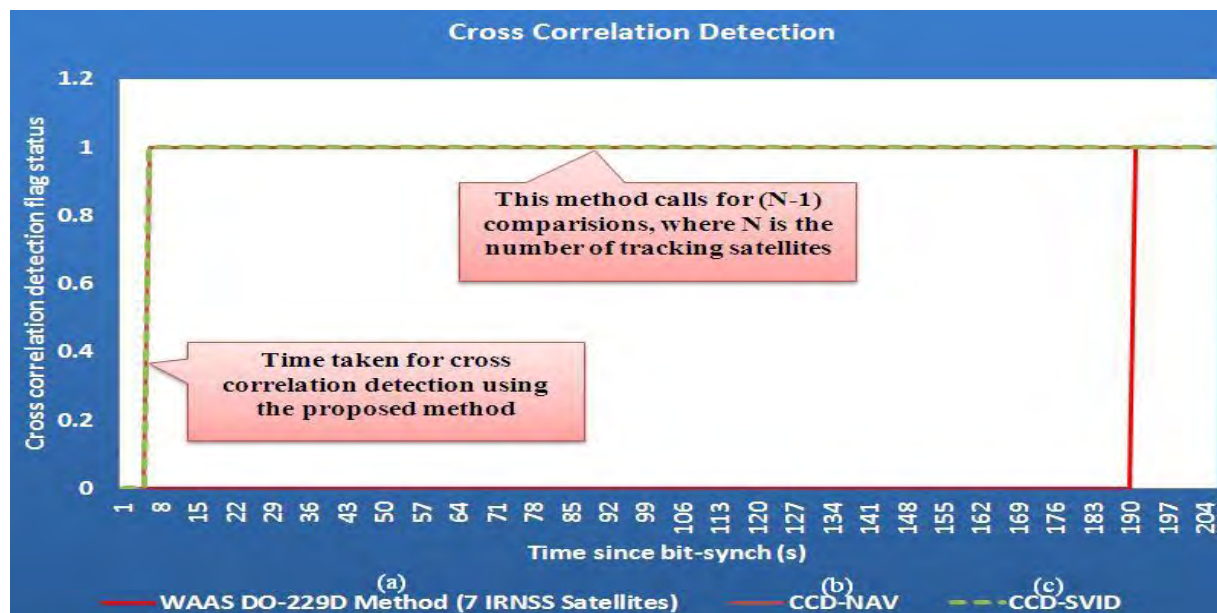


Figure 5-15: Time taken to detect cross correlation with various methods a) range differencing as in GPS L1, b) proposed NAV data processing, c) proposed satellite id method.

Both versions demonstrated similar detection performance as shown in Figure 5-15, which is relatively better than the existing GPS L1 method and are best till date.

The proposed NAV data processing is applicable to GPS and GLONASS L1 (partially). This is based on the input that ephemeris frames are different and thus the NAV data processing is applicable unambiguously (SVID is not present in GPS/GLONASS L1 NAV data). In addition, similar scenario arises when almanac/textual messages are transmitted in the emerging GNSS (for example, L2C, L5 and GALILEO E1). By adopting the SVID detection, the partial limitation is completely resolved in the emerging systems. *Thus the proposed methods (in combination) can become defacto standard for civil aviation applications and in general.*

5.5.2 TTF

To validate the performance of the OCM and ORM methods, the simulator and receiver hardware used in the previous chapter with the modified versions of the software developed are used. The results presented only depict the T_{eph} component and the ionosphere is dropped. This is under the assumption that the receivers are operating in dual frequency mode and thus, with measurements, will be able to estimate directly the ionosphere effect.

With the simulator and the receiver software in OCM/ORM configurations, the receiver data was logged in GGVISION to profile the T_{eph} component. Three runs were conducted to establish the results in different configurations as follows:

- First, to profile SPS only mode of operation
- Second, restricted direct (hybrid, only in OCM)
- Finally, restricted direct (ORM).

The results shown in Figure 5-16 are commensurate with Table 5-3 and Table 5-4.

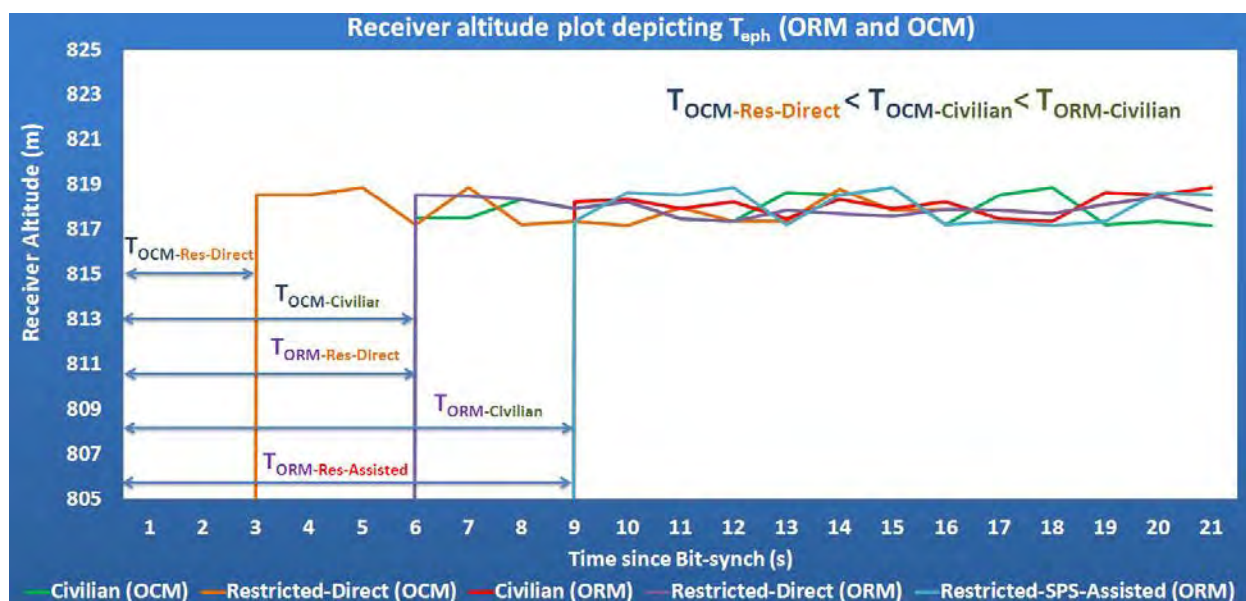


Figure 5-16: Altitude plot illustrating the TTF performance with the OCM/ORM method of NAV data signal design.

In lines with Table 5-3, the OCM method was able to output the position within 6 s post bit synchronization in dual frequency mode of operation, which is attributed to the structuring of the NAV data. Second, when all the channels were effectively processed together (*bit synch of SPS channels implies time estimate is available for direct acquisition of restricted signals*), the TTFF was 3 s in direct acquisition mode. Finally, in the ORM method, with assistance from TOW, TTFF was 9 s, which is attributed to the data being different on SPS and restricted service.

5.6 Summary

With optimization of primary NAV data transmission as the main criterion, this chapter established the basic constraint in achieving enhanced TTFF values in dual frequency systems. Following this, the current use of the almanac as a part of receiver operations was highlighted. With an experimental setup, the effectiveness/limitations in the existing method of cross correlation detection in civilian applications were presented. With the objective of eliminating the almanac as part of the NAV data, two new methods of cross correlation were derived. It was shown that these methods are capable of detecting cross correlation instantaneously and without any assistance. Further, various architectures based on different combinations of NAV data structures were deduced. It was shown that a 6 s positioning was possible for civilian receivers in dual frequency mode of operation. In addition, for SPS assisted acquisition with different data (w.r.t SPS), it was shown that 9 s positioning is possible for the restricted service. With a simulator and a receiver combination commensurate with the proposed design, the TTFF improvement was demonstrated. The following chapter establishes the third frequency of operation for IRNSS and proposes methods to reduce the TTFF even further for the restricted service.

Chapter Six: THIRD FREQUENCY AND REAL TIME HOT/SNAP START OF GNSS/IRNSS

The existing, emerging and proposed GNSS systems have at least three frequencies supporting civilian operations. Multiple frequencies provide greater flexibility w.r.t signal design and a medium to meet various user requirements (for example, sensitivity, multipath, TTFF). In addition, most of these GNSS constellations support SBAS, which offers an added advantage in providing corrections to the measurements derived from GNSS. Specific to this research, Chapter Three and Chapter Four highlighted the limitations associated in LOS TTFF and the dependence on terrestrial link in existing and emerging GNSS systems for critical applications.

IRNSS, a dual frequency/service, is in the initial stages of signal design and research primarily to explore the benefits derivable from a regional perspective will minimize the *future backward compatibility* issues presented in Chapter One. Thus, the goal of this chapter is as follows:

- To develop an engineering synergy between IRNSS and SBAS and thus propose a third frequency of operation for IRNSS.
- Employ the derived third frequency to propose a real-time hot start of GNSS.
- To present architectures towards real time snap start of IRNSS restricted users directly from satellites.

The organization of this chapter is as follows: first, a brief overview on multi-frequency GNSS systems is provided highlighting the challenges (system level) involved during the initial formulation of a signal. Following this, a brief overview of IRNSS/GAGAN space and control segment is presented. Later, the third frequency of operation in IRNSS is derived with detailed analysis. Based on this, three engineering propositions involving IRNSS and GAGAN are presented *highlighting the drastic cost reductions* achievable. With the third frequency, a hot

start method of GNSS is derived, which encompasses the *future SBAS of IRNSS*. With a detailed simulation setup and new receiver architecture, experimental results are presented. Finally, from the results/methods of the hot start architecture, a SNAP start for restricted services is derived and with analyses, the achievable results presented.

6.1 Overview of multi-frequency GNSS system

The GPS and the GLONASS program started in the mid-seventies where the system designers were confronted with system level problems in selecting the most optimal signal specifications (for example, frequency, power and data rate) (Parkinson & Spilker 1996). No other system was operating and the design was relatively simpler. The success of these programs and the independence sought by some countries for their strategic applications has resulted in the emergence of new GNSS systems (for example, GALILEO, COMPASS, IRNSS). The following sub-sections briefly present the existing and proposed multi-frequency GNSS systems from a SiS perspective and explains key components specific to this research.

6.1.1 Existing/proposed GNSS systems

Figure 6-1 ((IS-GPS-200E 2010), (Galileo 2008), (GLONASS-ICD 1998)) depicts the various signals supported by GNSS systems. As explained in Chapter One, each of these has evolved to cater to specific user requirements. For example, L2C specifically addresses the indoors and L5, civil aviation applications.

Two points noteworthy in Figure 6-1 and relevant to this research are highlighted and explained in the following paragraph:

- Pilot signal: In Chapter Two it was mentioned that to improve sensitivity, longer integration of the signal needs to be performed and one of the methods of achieving this

is by aiding the receiver with data bits. With this, longer coherent integration is possible (Borio 2008) to enhance achievable signal strength. The underlying process is by aiding whereby the receiver can wipe off the data component and thus be able to continuously integrate the signal (ranging code) for a longer duration and derive the requisite benefits. Alternatively, high sensitivity requirements are met if a synchronous signal originates without data from the satellites. This is realized in emerging systems by employing the pilot signals (*ranging code only*) which are in phase quadrature with its (*data + ranging code*) signal. From Figure 6-1 it is evident that *three such signals* that effectively serve the high sensitivity applications are available from GPS satellites (L1C in near future).

- Signal power: Figure 6-1 clearly illustrates that *11 signals originate* from GPS satellites whose power levels vary from -157 to -166 dBW. Though the constellation is not complete (w.r.t L2C, L5) these signals are transmitted from at least one of the satellites (at present 9 L2C, 2 L5, L1C yet to be beamed (NAVSTAR GPS 2012)).

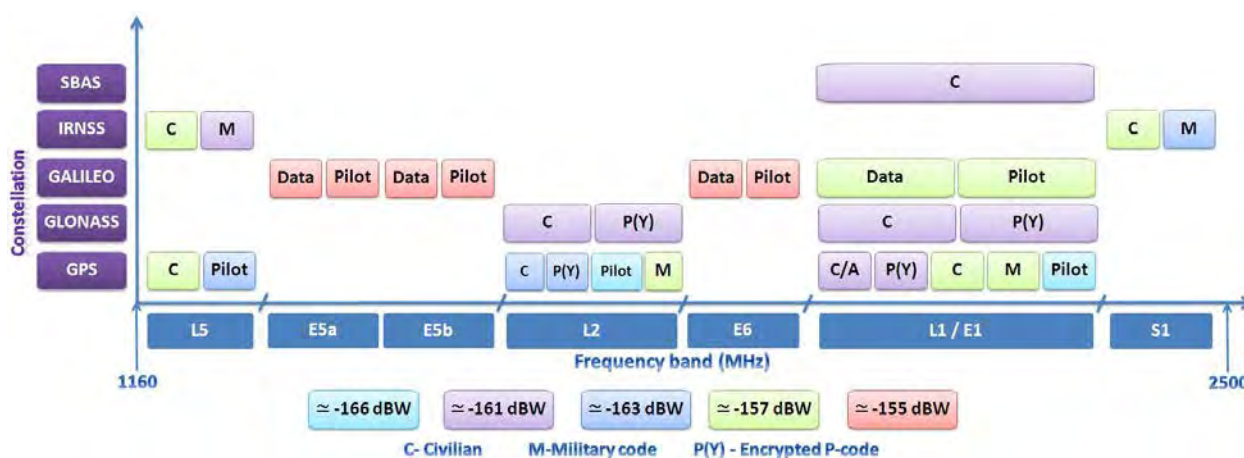


Figure 6-1: Existing and proposed GNSS systems and their frequencies/minimum assured power levels (IRNSS power levels assumed).

6.1.2 SBAS

Figure 6-1 presents the SBAS supported in the L1 band, which are primarily used to assist the GNSS with integrity and corrections messages over a particular region, the need for which is explained as:

1. In GPS L1 C/A code, primary NAV data changes (typically) once in 2 hours. If an anomalous event occurs onboard the satellite, its communication is delayed till the next NAV data upload. Receivers used for safety of life applications (for example, aviation applications) require the integrity information to be available very fast and directly from the satellites.
2. The aviation grade GNSS receiver supports the following phases of operation (typically) – oceanic, remote area and domestic en route, terminal and approach, with the accuracy demands of last being very high (DO-229D 2006). The main error contributor is the measurement of the ionosphere, which for a single frequency user is available as modelled terms in NAV data. The model being an approximation, its performance is not uniform across the globe (Parkinson & Spilker 1996). This residual error in measurement affects the navigation solution. Although this error is not a major concern for the oceanic phase, it is a critical requirement of the terminal phase.

To address the above two key requirements of the civil aviation sector and in general, SBAS was introduced in early part of the last decade. The signals transmitted from SBAS are in the same band as *GPS L1* and thus only the software needs to be modified to account for its benefits. The data contains correction/status messages of the GNSS satellites. The correction messages are similar to the Radio Technical Commission for Maritime applications (RTCM) DGPS (RTCM

1994) corrections and the health status indicates the usability of a particular satellite in the navigation solution.

In addition to meeting the aviation requirements, general single frequency (for example, GPS L1 only) users (non-carrier phase positioning) can obtain DGNSS equivalent corrections without having to depend on additional hardware (for example, modem to obtain DGNSS). This derived benefit is being exploited extensively in map matching applications (Burnell and Flerkevitch 2012).

6.1.3 System level challenges

When a new system or a signal is to be added to an existing system, the system designers are confronted with challenges some within and others, across the systems. This section highlights a few of these issues.

6.1.3.1 Interoperability

When the GPS/GLONASS signal design was formulated, there were no other GNSS signal and thus a major design issue of coexistence was obviated (Kaplan & Hegarty 2006). However, for the subsequent systems if the signal transmission were intended to occur in this band, the system designers had the challenge of evolving techniques and demonstrate seamless mutual coexistence. For example, BOC (1, 1) for GALILEO had to ensure that the same center frequency as GPS L1 C/A is used and yet that both signals be processed independently (Betz 1999). Thus if a new system (for example, IRNSS) is proposed, it is imperative that this issue is handled collaboratively at the signal design level.

6.1.3.2 Backward compatibility

When the signal design is formulated, care needs to be exercised to ensure that the most optimal design considering requirements of various user segments be drafted (Stewardship project 2004). Post deployment, with a need to augment a new signal, the first design constraint is the compatibility that needs to be established with existing signals of the same system. For example, GPS L5 when proposed had to demonstrate that it could seamlessly co-exist with L1 and L2C.

6.1.3.3 Frequency Filing

With the interoperability issues resolved, the next major step is filing for the usage of the frequency spectrum. Typically, this is a lengthy process, post approval of which only the signals are transmitted onboard a satellite. This process ensures that the signals radiated are in the designated band and the regulatory bodies' (Singh et al 2008) approval signifying its seamless co-existence with the existing signals.

6.2 Indian navigation systems

Indian space programs are conceptualized, designed, developed and deployed by the Indian Space Research Organization (ISRO). From a navigation perspective, the augmentation and independent regional system have been drafted by ISRO in the last decade, an initiative towards regional independence in GNSS. The following sub-sections explain at a top level the sub-system components of GAGAN and IRNSS and presents limitation (potential engineering optimization) from a regional perspective.

6.2.1 GAGAN

The void SBAS foot-print between the EGNOS (Europe) and MSAS (Japan) is established by GAGAN. The need and the contribution of SBAS were described in the previous section. This

section presents the control and space segment components which makes it operational, specifically GAGAN.

The GPS satellites visible over the Indian subcontinent are continuously tracked at several monitoring stations, as explained in Chapter Two. The stations are equipped with state of the art reference (survey grade) receivers that provide precise estimates of pseudoranges, carrier phase measurements and time information based on dual frequency. The stations will also have the antenna located at a surveyed location. In addition, these receivers provide estimates of satellite related anomalies (SQM as explained in Chapter Two), if any. With these inputs and traits, measurements are formulated. Further, the integrity stations are spread across the Indian land mass (to obtain the ionosphere data for modelling), which relay the data to the master control station located in Bangalore. Based on the collated data from various stations, the messages are generated as per SiS requirements of SBAS (DO-229D 2006). These structured messages are uplinked in C-band to the GAGAN satellites as shown in Figure 6-2 a) ((GAGAN Architecture 2012), (Ganeshan 2012)).

GAGAN will have three geostationary satellites when fully operational with the signal footprint spanning over the Indian subcontinent (Kibe & Gowrishankar 2008) .

Points which are noteworthy of this signal are (used later in this research):

- transmitted in L1 band at 1575.42 MHz
- transmitted at -160 dBW, similar to GPS L1 C/A
- codes used are from the GPS L1 C/A family
- basic data rate is 250 Hz
- rate $\frac{1}{2}$ 7 bit Viterbi encoding is employed on data bits and thus effective symbol rate is 500 sps.

- GPS receiver accuracies achievable over the Indian land mass with this signal will be similar to that achieved over the US with or without WAAS.

From the above points, it is clear that the signal (data) is transmitted five times higher than the GPS L1 C/A (IS-GPS-200E 2010) but its power has not been increased. This can be attributed to the following reasons:

- First, to achieve similar performance as L1 C/A (w.r.t measurement accuracies), 12 dB additional power is required. This will act as *in-band jammer* and lift the noise floor of the GPS L1 channels (Parkinson & Spilker 1996).
- Second, to accommodate the above requirement, the absolute power required would be -148 dBW, which *violates the guidelines for space based signal transmission* (Singh et al 2008). Thus, with -160 dBW the ranging measurement performed on SBAS will be relatively inferior to GPS L1 (Parkinson & Spilker 1996). This not being a system objective, SBAS focusses on providing integrity messages and can effectively be interpreted as a *data channel*.

6.2.2 IRNSS

As a second initiative in the space based navigation, IRNSS is ISRO's second contribution with an objective to provide independent regional navigation to cover its territorial footprint and slightly beyond. The system is expected to be operational by end of 2015 (Bhaskaranarayana 2008). The system of space and control segment for IRNSS is as shown in Figure 6-2b) (IRNSS Architecture 2012). The top level details of the control and space segments are as follows:

Similar to the GAGAN control segment, IRNSS Range Integrity Monitoring Stations (IRIMS) will be deployed at several places spread across Indian subcontinent. These stations will be equipped with high end receivers which will provide all relevant information (explained in

Chapter Two under receiver categories) about the satellites. With the signal transmission from the first satellite, these receivers will perform measurements and collect the NAV data. The data will be relayed to the master control station located in Bangalore. Based on this data, batch (typically) processing is performed to generate the Keplerian parameters of all the satellites, the clock correction terms and the secondary NAV data information. Unlike GAGAN, this is a complex activity, which determines the overall system accuracy (User Equivalent Range Error (UERE) (Rao et al 2011). The data generated is uplinked to IRNSS satellites.

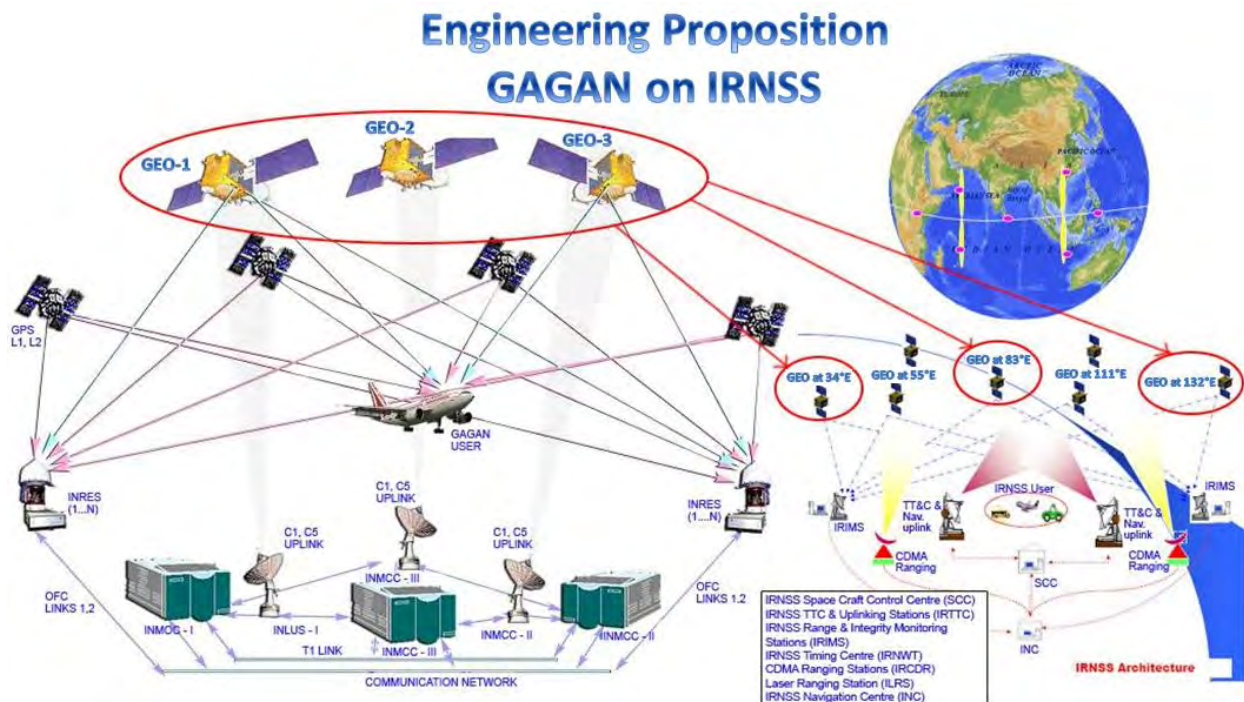


Figure 6-2: Control and space segment architectures of a) GAGAN b) IRNSS.

The space segment will have in all seven satellites, four in geostationary and three in geosynchronous orbits (Bhaskaranarayana 2008). Some features about IRNSS signals available from open sources are:

- The IRNSS L5 and S1 will transmit signals for civilian/restricted operations (Kibe & Gowrishankar 2008).
- In all there will be seven satellites, three in geostationary and four in geosynchronous orbit as shown in Figure 6-2b).

6.2.3 Optimization

From a regional perspective, it is clear from Figure 6-3 that there will be six payloads on six geostationary (3 each of IRNSS and GAGAN) satellites serving the navigation needs centered over the Indian subcontinent in the near future. From a system perspective, an obvious *engineering optimization* w.r.t the number of satellites is evident from Figure 6-3, *constrained by the individual specifications of each system*. Optimization w.r.t reduction in the number of satellites as the objective, the following section *proposes to reduce the satellite count, yet meet the IRNSS and GAGAN functionalities and finally deduce a simple third frequency option for IRNSS*.

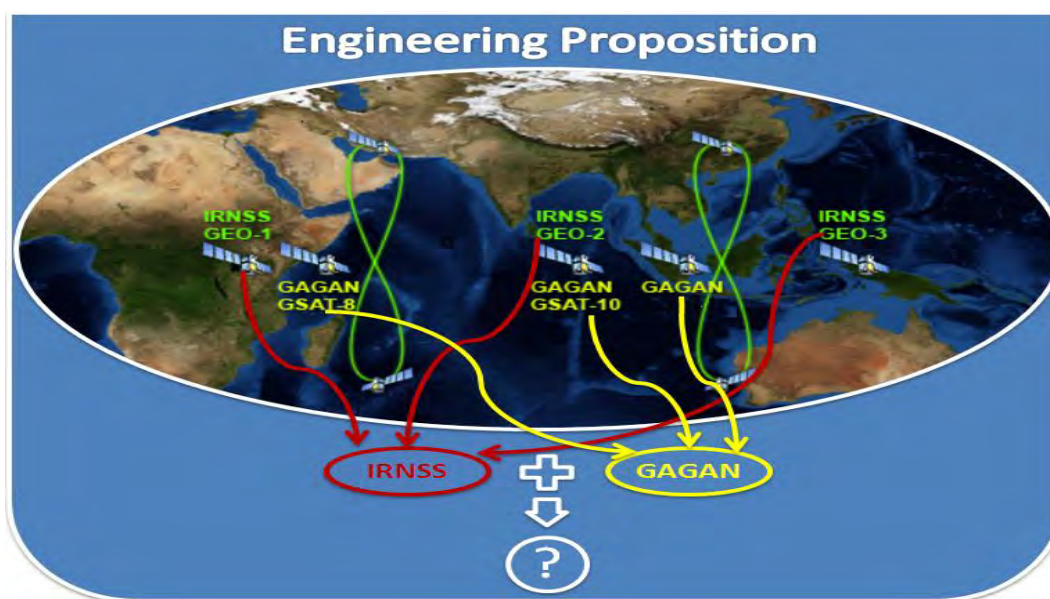


Figure 6-3: GAGAN (GEO-3 position assumed) and IRNSS geostationary satellites.

6.3 Proposed third frequency in IRNSS

To begin with, the assumptions made towards the optimization are presented in Table 6-1. These assumptions are for the signals (GAGAN, IRNSS, and (GAGAN+IRNSS) w.r.t GNSS) over the Indian subcontinent.

Table 6-1: Assumptions towards the engineering optimization proposition.

Parameter	Description, Reasons/Examples
Backward compatibility	<p>Two of the GAGAN satellites are already launched and deployed. GSAT-8 and GSAT-10 are in final and initial stages of testing.</p> <p>IRNSS is yet to be launched. It is assumed that there are no backward compatibility issues from a user perspective.</p> <p>This is largely valid as IRNSS and SBAS address different objectives with SBAS primarily not meant for ranging. Thus compatibility issues between IRNSS and GAGAN are not applicable as was with GPS L5 (L2C and L1 C/A signals being present)</p>
Interoperability	<p>This is explained as IRNSS/GAGAN (intra) and across GNSS (inter) systems:</p> <p>First, given that the projects have been conceived and are in the development stage, it is assumed that the signal levels do not pose a <i>mutual</i> problem. This is largely acceptable as the diversity that exists between GAGAN (L1) and IRNSS (L5/S1) consists of operating in different frequency bands. Further, it is comparable to WAAS and GPS L5 over the north American continent.</p> <p>Second, given that the GAGAN (deployed) and IRNSS are largely in the developmental stage, it is assumed that all the necessary studies w.r.t these signals co-existing with other GNSS in the coverage region (Indian subcontinent) for mutual co-existence have been carried out.</p>
Frequency filing	<p>The first GAGAN satellite is transmitting the signal and uses the codes/frequencies as supported by SBAS (DO-229D 2006)</p> <p>In addition SBAS is a coordinated effort across GNSS bodies. Both these points assume/obviate the frequency filing proposition.</p>

Parameter	Description, Reasons/Examples
	For IRNSS, which is in the development stage, it is assumed that the codes/frequencies have been filed and approved by the International governing bodies (Singh et al 2008).

The space initiatives of GAGAN and IRNSS are undertaken by ISRO and thus are fully under its control. As can be seen from Figure 6-3, the geostationary satellites are present as a part of both IRNSS and GAGAN systems. The following design rationale is adopted and explored at length in the ensuing sections with the emergence of a third frequency:

“With IRNSS signals onboard GAGAN satellites, three signals in L5, L1 and S1 bands will be radiated by GAGAN satellites. Further, this (L1) is generalized to the IRNSS geosynchronous satellites as the third frequency, which is used for improving GNSS TTFF in LOS applications”.

The following sections *analyze* in detail the merits of the above design statement and present (in later sections) the methodology to accomplish it. The *analysis* is performed under the following headings:

- Availability and accuracy: to access the performance of the integrated system (IRNSS + GAGAN) in comparison with IRNSS and GAGAN standalone architectures.
- Interoperability: access the issue from an intra and inter system perspective.
- Implementation: to access whether the proposed integrated system is realizable. Towards this, necessary assumptions/parallels from Figure 6-1 have been adopted / derived.
- Expandability to geosynchronous: to access the inclusion of this frequency in geosynchronous satellites of IRNSS and thus result in the *third frequency*.
- Advantages of this architecture: access the potential benefits which this system might offer to either the IRNSS or GAGAN program.

6.3.1 Availability and accuracy

Several documents to date have been published that explain in detail the merits of a combined GNSS architecture from a user perspective (for example, GPS+GLONASS+GALILEO (O'Keefe 2001) & IRNSS+GPS+GLONASS, (Rao et al 2011)). However, for the design proposition put forth, an analysis needs to be performed *within the systems (optimization w.r.t satellites)* and presents the availability/accuracies achievable. Towards this, three formulations are investigated - IRNSS on GAGAN, GAGAN on IRNSS and IRNSS with GAGAN. Table 6-2 presents the locations of IRNSS and GAGAN used as a part of simulations.

Table 6-2: Summary of the IRNSS and GAGAN locations considered for simulations.

Constellation	Description	
	Geostationary Satellites	Geosynchronous Satellites
Current IRNSS	34°, 83° and 132° east	55°, 111° east
GAGAN	55°, 83° and 111° (assumed) east	-----
Proposed IRNSS	55°, 83° and 111° (assumed) east	55°, 111° east

6.3.1.1 IRNSS on GAGAN

Figure 6-4 and Figure s6-5 provide the IRNSS standalone visibility/PDOP (accuracy with an assumed UERE) performance (Rao et al 2011) in comparison with the proposed IRNSS constellation. It is evident that there is a *significant improvement* with the proposed integrated system in availability and thus DOP performance as compared to IRNSS standalone.

The detailed analysis from assumption to improvements is explained (sequentially) as follows:

1. The reason for assuming *111° east* for the third GAGAN (Table 6-2) is to have a common overlapped foot-print with its existing satellites and thus facilitate redundancy (satellite failure) from a system perspective. Second, MSAS is relatively close to this

assumed location and thus system (GAGAN+MSAS overlap) level redundancy is also inadvertently met.

2. The availability with the proposed IRNSS constellation is as shown in Figure 6-4. The result is an improved (*wider common footprint along with current IRNSS geosynchronous (Figure 6-2) as opposed to its current IRNSS*) resulting in DOP improvement as shown in Figure 6-5. The relative improvement (reasons) is as explained as follows:

- The availability with existing IRNSS is as shown in Figure 6-4 and, in the area “a” all seven satellites are visible. Outside this polygon on either sides (longitudinally), visibility to satellites 34° and 132° east is lost on either side and thus availability drops to six satellites.
- In contrast, with the proposed IRNSS constellation, this area “b” Figure 6-4 is wider due to the close spacing of the geostationary satellites 55° and 111° east, which results in a wider coverage area along with the geosynchronous satellites. Thus the significant improvement in availability area, which from a regional perspective is *greatly desirable*.

3. The IRNSS objective is independent positioning and thus as a system objective it is imperative to maximize the coverage area where independent positioning can be established. A close examination of Figure 6-4 reveals the following: Availability west of line “c” remains the same and is less than 4. Thus the effective region of operation (independently) is east of this line for either configuration. The reason for this is that in either configuration visibility to the geostationary satellite (83° east) is lost, which is the common to both configuration. A similar phenomenon exist on the right side of the “a”

and “b” polygons. However a marginal (in-significant) area where the current IRNSS is better than the proposed one.

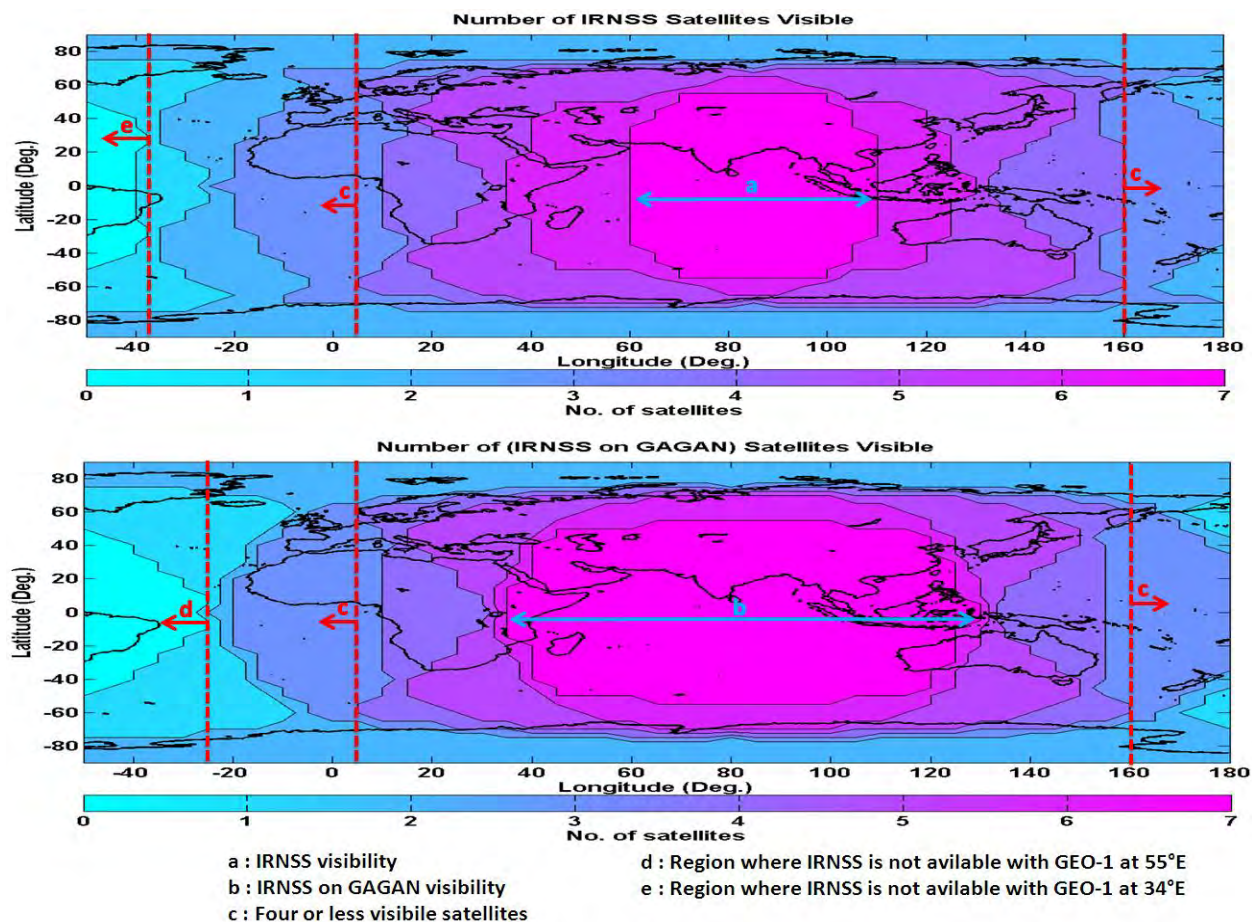


Figure 6-4: Satellite availability with current IRNSS and proposed IRNSS constellation.

4. One possible reason for having the current IRNSS geostationary satellites at 34° and 132° east could be for extended coverage of IRNSS system. The merit of this argument is highlighted in Figure 6-4 and explained as:

- To the west of line “d” and “e”, the visibility is completely lost in both the proposed and existing IRNSS. This is attributed to the visibility from the geostationary satellites at 55° and 34° east respectively. Though visibility is established for an

extended range of about 15° with the current IRNSS constellation, it does not assist with independent positioning. A similar condition exist on the right side of the “a” and “b” polygons.

- In addition, the analysis for locations 90° and 100° east is as presented in Appendix G. From the results (Figure 6-4 and Appendix G) any *available* geostationary location (in the region on 90° and 111° east) with IRNSS signals will enhance the *IRNSS regional operation as compared to the current IRNSS constellation*.

5. This architecture does not have any impact on GAGAN w.r.t its availability as its locations are the same in either configuration.

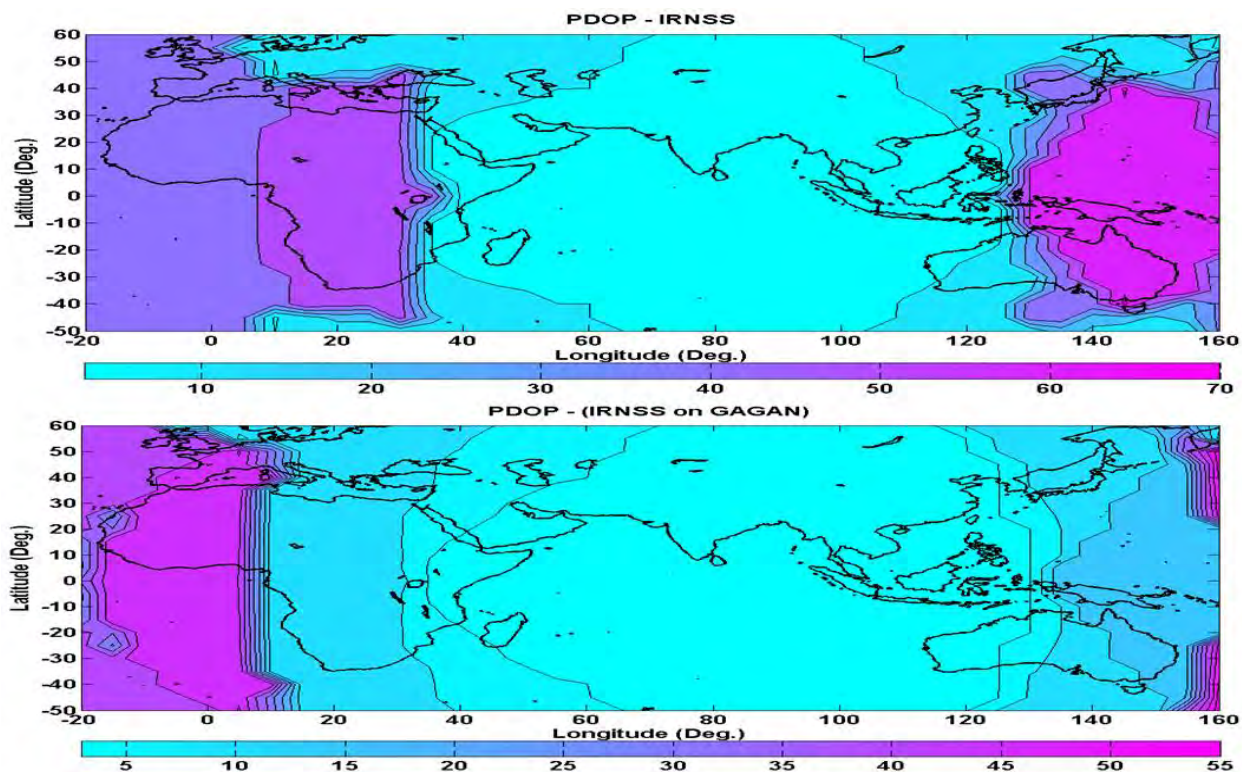


Figure 6-5: PDOP with current IRNSS and proposed IRNSS constellation.

Thus from an availability and accuracy (Figure 6-5(only available region is considered)) perspective, the proposed integrated architecture is *more beneficial from a regional perspective*.

6.3.1.2 GAGAN on IRNSS GEO

This architecture implies that the GAGAN signal will be transmitted from the IRNSS geostationary satellites located at 34° and 132° east of IRNSS along with the third one at 83° (Rao & Lachapelle 2012). This architecture will result in availability and DOP of IRNSS as shown in Figure 6-4 and Figure 6-5, respectively. However from a GAGAN's perspective, the coverage area is reduced. This is implicitly deduced from the availability plot of IRNSS on GAGAN (Figure 6-4). Thus in a relative context, GAGAN on IRNSS reduces its effective coverage area and is not a desirable proposition.

6.3.1.3 IRNSS with GAGAN GEO

This scenario is where both systems co-exist and GAGAN satellites transmit IRNSS signals. The availability and in turn the DOP are minimal with the increased satellites as shown in Figure 6-6. Though this architecture is desirable (for example, from a redundancy perspective), it is not an optimal solution from regional scenario.

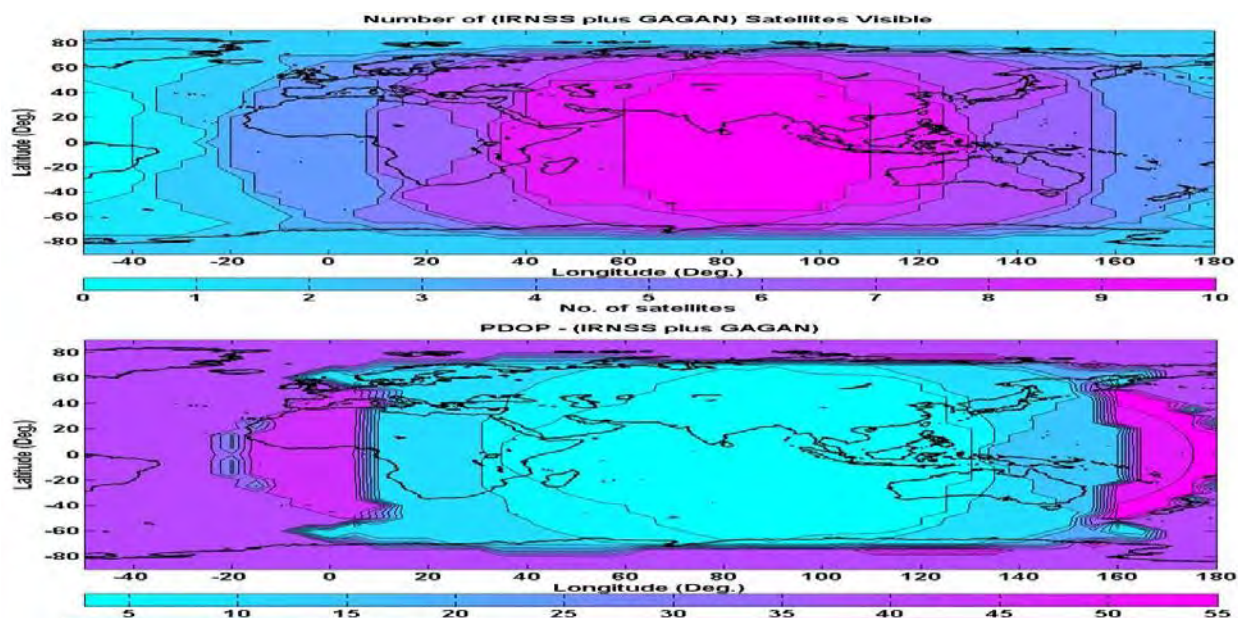


Figure 6-6: Availability and PDOP with IRNSS and GAGAN.

From the analysis of the three configurations, IRNSS on GAGAN is optimal from availability and DOP, which will only be considered for further analysis.

6.3.2 Implementation issues

This section presents the implementation aspects that need to be carried out to augment this proposed architecture onboard the GAGAN satellites with adequacies successfully presented in the previous section w.r.t availability and accuracy. With no information available on the power levels of IRNSS signals, the assumptions as listed in Table 6-3 are made on the signals originating from IRNSS/GAGAN satellites.

Table 6-3: Assumed power levels onboard proposed IRNSS+GAGAN configuration.

Frequency of operation	L5 (dBW)	S1 (dBW)	L1 (SBAS/ geosynchronous) (dBW)
Service Mode			
SPS	-157	-157	-160
Restricted	-160	-163	-

Figure 6-1 presented the power levels onboard various GNSS satellites. Specifically, with GPS as reference, the listings in Table 6-4 are explained as:

- The L5 and S1 SPS power levels follow L5 and L1C of GPS respectively.
- The restricted signals are assumed to be radiated at similar levels as that of GPS P(Y) L1/L2 signals.
- SBAS signals follow the existing GPS L1 C/A signal.

Thus from a power management perspective, the assumed levels are commensurate with existing levels of GPS and thus are implementable. *Further, these are only five signals as opposed to 11 signals originating from GPS satellites.* With the above, it is clearly evident that the IRNSS

signals can be carried by GAGAN geostationary satellites, which eliminates the three IRNSS geostationary satellites.

6.3.3 Interoperability

Table 6-1 listed the assumptions on backward compatibility, interoperability and frequency filing, which are equally applicable to this integrated architecture as well. Of the three, interoperability is the only issue, which may need further investigation and explained as follows: IRNSS on GEO from a spectrum perspective is merely a re-distribution and thus does not affect the signal flux (in the Indian subcontinent region it would otherwise have originated from GAGAN and IRNSS satellites independently) or receiver performance (in comparison with distributed IRNSS and GAGAN architectures). Similarly, the inter system performance remains similar to that with independent signals.

6.3.4 Expandability

The engineering proposition of having IRNSS on GAGAN ensures mapping of the geostationary satellites and in turn L1 signal being beamed along with L5/S1. However, the geosynchronous satellite signals were not mapped for L1 transmission. Table 6-4 presents assumptions made towards this.

Table 6-4: Assumptions made towards transmitting L1 signal on geosynchronous satellites of IRNSS.

Parameter	Description, Reasons/Examples
<p>Signal transmission on geosynchronous satellites of IRNSS at L1 with -160 dBW, SBAS ranging codes and 250 Hz data</p>	<p>GAGAN, an approved program, transmits in the L1 band centered on GPS. With this, if the geosynchronous satellites of IRNSS also radiate on L1 with an SBAS structure, its increase in in-band power can be appreciated with the following practical examples:</p> <p>Worst case, an increase of four GPS satellites in the region over Indian subcontinent. This is analogous to a receiver visibility variation over a given region in GPS only mode. Typically, the</p>

Parameter	Description, Reasons/Examples
	<p>satellites availability varies from 8 to 12 over the Indian subcontinent (Rao et al 2011) in a given day. Thus, this increase in 4 satellites can be interpreted as 12+ satellites always in the L1 band, which is largely acceptable.</p> <p>Second, QZSS (apart from two MSAS satellites) will have a total of three satellites when completely operational (Glennon 2011). These satellites, which radiate signals similar to GPS, are used for regional augmentation purpose with GPS L1 and their power levels are comparable with those of GPS L1 C/A at around -160 dBW. With the assumption of L1 on four geosynchronous satellites of IRNSS (one additional in comparison with QZSS) the GPS L1 receiver performance will be similar to that with QZSS over Japan.</p> <p>Thus with the above two examples, L1 signal transmission on geosynchronous satellites is largely acceptable.</p>
Data channel	<p>It was mentioned earlier that there is a pilot signal on three frequencies supporting high sensitivity applications in GPS (Figure 6-1). Alternatively, to support high sensitivity requirements, three sources (L2C, L5 & L1C (in future)) originate from the same GPS satellites. Similarly in GALILEO, four such signals exist. There are none to address the issue of LOS TTFF.</p> <p>SBAS, which is a data channel (also supports ranging codes) does not have any message dedicated w.r.t primary NAV data of the constellation which it supports.</p> <p>This research proposes/assumes to have a data only channel transmitting primary NAV data messages, with SBAS SiS characteristics. This is adopted as a part of the geosynchronous IRNSS satellites.</p>

With the above necessary assumptions/justifications, the third frequency onboard the four geosynchronous satellites of IRNSS is adopted. This is primarily restricted only as a data channel and not for ranging purpose.

6.3.5 Advantages

The merits of IRNSS on GAGAN are explained as follows:

6.3.5.1 SBAS & high dynamics

As mentioned in the earlier section, with the success of GPS and the need for correction/integrity, the SBAS program emerged. A similar proposition might arise in future for IRNSS. With few additional messages exclusively for IRNSS, GAGAN can be modified to account for the IRNSS's SBAS corrections as well. Though with textual data (for example, TSF architecture (Figure 3-11)), some of these SBAS messages for IRNSS can be supported and, due to the inherent data rate limitations (50 Hz) and the need for some of the messages to be fast (for example, fast correction messages of SBAS), dedicated medium is required. This can be easily handled by additional messages onboard GAGAN (for example, GLONASS SBAS messages transmitted in EGNOS in addition to GPS (EGNOS 2011)).

As explained in Chapter Two, high user dynamics require wider Doppler search ranges. This coupled with high data rates (500 sps) puts a constraint (sensitivity) w.r.t SBAS acquisition in standalone mode (for example, no estimates of position, velocity, almanac or time). With the integrated proposal, IRNSS satellites when tracked in L5/S1 can directly assist L1 (SBAS) and thus improve performance drastically w.r.t acquisition in high dynamics.

6.3.5.2 Satellite count

An obvious advantage with this approach is that GAGAN satellites with IRNSS frequencies eliminate three IRNSS geostationary satellites. Unlike GAGAN, IRNSS are dedicated navigational satellites. Assuming a *pessimistic estimate of 100 million USD/satellite including launch, a significant reduction in the cost is achieved (300 million USD in all) with the proposed integrated architecture*. At the same time, the specifications of both systems are effectively met.

6.3.5.3 Control segment

A synergized network can be established to effectively have a common control and monitoring station for both IRNSS and GAGAN ensuring all system parameters are obtained as required by *individual systems and collated at a common master control station*. With this, *the operational overheads are drastically reduced* resulting in the architecture shown in Figure 6-7.



Figure 6-7: Proposed integrated IRNSS+GAGAN architecture.

6.3.5.4 Third frequency on IRNSS

With the geosynchronous satellites always visible over Indian subcontinent, the third frequency (L1) can be used for safety of life applications as in GALILEO E6 (Galileo 2008). With the advantage that these satellites carry the L5/S1 signals and assuming collaborative tracking (Borio 2008), the data rate can effectively be increased to 1 KHz on these channels without increasing power. *This proposal is commensurate with the ORM (previous chapter) assumption of high data rate for the restricted signals.*

6.4 Proposed fast start of GNSS using IRNSS

The previous sections derived the third frequency which can be effectively used as a data channel. The four geosynchronous satellites can effectively be used for any user specific needs. This research explores the possibilities of using this bandwidth to improve TTFF. The following proposal is put forth using these satellites over the Indian subcontinent along with IRNSS in dual frequencies of operation: Real-time HOT start of GNSS (GPS/GLONASS). Analysis of this method to enhance the TTFF of IRNSS restricted users is presented later.

6.4.1 Real-time hot start of GNSS

In Chapter Two under receiver operating modes, it was mentioned that receivers can enter a fast positioning mode with the primary NAV data stored in them or through external aiding (for example, AGPS in ephemeris assistance mode). With the proposal of having a data channel onboard geosynchronous satellites primarily to assist fast TTFF and a background of the OCM method (Figure 5-10), this research proposes real time hot start of GNSS. The details of the design steps are as explained in Table 6-5 w.r.t GPS, which holds for GLONASS as well.

Table 6-5: Methodology to accomplish real time hot start of GNSS using the geosynchronous satellites of IRNSS.

Parameter	Description
Objective	To achieve real time positioning of GPS in 6-8 s with the data as transmitted from the geosynchronous satellites of IRNSS.
Assumptions	<ol style="list-style-type: none"> 1. Monitoring stations collect the primary NAV data and relay it to the master control station. 2. Receivers do not have any data stored as a part of their internal memories. 3. GPS+SBAS receivers can accommodate <i>four</i> additional SBAS channels. 4. Receivers are equipped with algorithms/architectures with fast acquisition of GPS satellites (for example, automobile grade receivers with fast TTFF architecture)
Signal Design	Monitoring stations: <ol style="list-style-type: none"> 1. The stations collecting the GPS data for GAGAN will

Parameter	Description
	<p>also collect the primary NAV data and relay it to the master control station.</p> <p>Master Control Station:</p> <ol style="list-style-type: none"> 1. It will collate data from all the stations and create a table of visible satellites primarily over the Indian subcontinent. 2. Only the healthy ephemeris data is uploaded to the geosynchronous satellites as per the sequence described in Appendix F. <p>Geosynchronous Satellites:</p> <ol style="list-style-type: none"> 1. The satellites after encoding transmit this data at 500 sps.

6.5 Test Methodology

This research proposed two components: the IRNSS signals onboard GAGAN satellites and the geosynchronous satellites transmitting in the L1 band. The former, from a signal generation perspective, is no different in comparison with the signal generation presented in Chapter Four. Based on the latter, hot start of GNSS is proposed. This section presents the signal generation methodology to demonstrate the TTFF performance of GNSS using IRNSS geosynchronous satellite signals.

6.5.1 Signal generation

As explained in Chapter Four, the simulator hardware can support 45 channels. To the 28 channels supporting IRNSS (SPS/RES L5/S1), 4 channels supporting geosynchronous satellites (at 500 sps for SBAS) were added. With the requirement that these channels need to operate in the L1 band, the composite IF was translated to the L1 frequency. The following paragraph explains the hardware configuration of the simulator. For the geosynchronous satellite channels, the reserved satellite id's 33-36 of GPS were used.

With respect to the explanations presented in Chapter Three, on the simulator hardware, three additional points noteworthy from the signal generation for this research are presented:

- First, the simulator hardware is capable of accepting an external clock as a reference input. This input overrides the internal clock and acts as a source to derive all its signal components.
- Second, the simulator is capable of accepting 1 PPS external trigger input. Typically, this is used to start a simulation in synch with an external application. For example, Hardware in the Loop (HIL) simulations for GNSS+INS integration where the simulator needs to generate the signals in real time commensurate with a common trajectory input (user state vectors) to it and the INS simulator.
- Third, the simulator is capable of accepting the NAV data for simulation purpose.

The above mentioned features are used for generating the signals for this research, as shown in Figure 6-8 b).

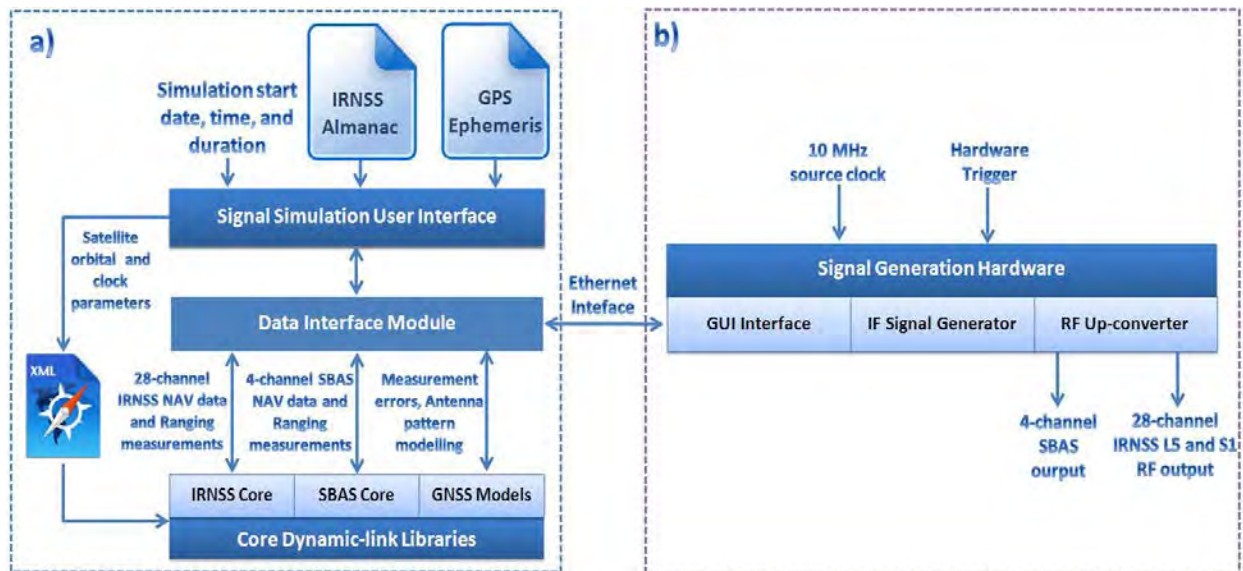


Figure 6-8: Methodology to generate the proposed L1 signals onboard channels of IRNSS geosynchronous satellites.

The software components used in Chapter Four are reused with the addition of four geosynchronous satellite channels. The operations performed on these channels are as follows:

Data from an external receiver/file is input to the simulator's port, which for this research is ephemeris data of GNSS structured as shown in Appendix F. This data (encoded) along with ranging measurements is transmitted to the hardware section as shown in Figure 6-8 a). The major difference is the data rate of these four geosynchronous satellite channels is 500 Hz as opposed to 100 Hz (encoded) IRNSS/GPS/GLONASS. Finally, the hardware section generates the L1 signal for the geosynchronous satellite channels

6.5.2 Receiver algorithm design

Chapter Two and Chapter Four presented the signal processing performed within a receiver w.r.t single and dual frequency of operation. The noteworthy point in dual frequency processing was the aiding from one frequency to the other. Figure 6-9 presents the generic architecture with the OCM/ORM (Figure 5-10, Figure 5-11) method of positioning in an IRNSS receiver. The following section explains the method to achieve hot start of GNSS. The explanation is presented for GPS, which is equally applicable to GLONASS (whose results are presented later).

The restricted channels are not used for this research and the resources were utilized for the geosynchronous satellites with reserved GPS ranging codes. The first four channels of S1 RS were effectively used to simulate geosynchronous satellites (Figure 4-17). As explained in Chapter Five, the GPSGL receiver has three independent RF ports. The port terminated in Chapter Five was used for this simulation and was dedicated to GPS signal reception. The IRNSS receiver operating in OCM mode tracks and acquires the signals. With bit synchronization, the estimates are directly programmed onto the L1 channels to enable fine acquisition and tracking. Following this state, the data from the L1 channels are acquired and demodulated. The data effectively contains the ephemeris of the GPS satellites. With position

from the OCM method, time and the data from the IRNSS L1 path, the GPS section (third RF port) of the receiver software is operational and enters into the snap start mode of operation.

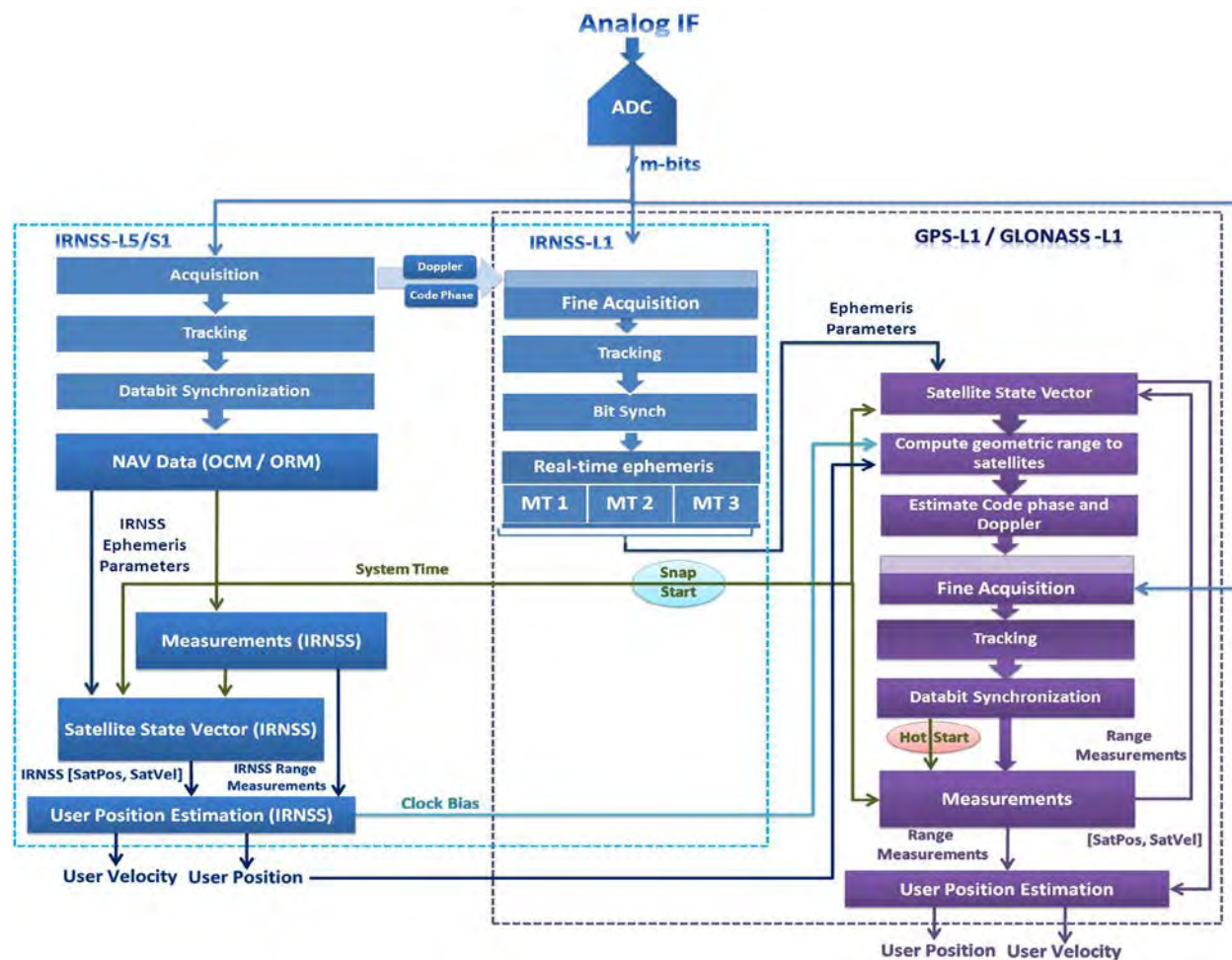


Figure 6-9: Receiver architecture to achieve HOT start of GPS/GLONASS in real time using the third frequency on geosynchronous satellites.

In an alternate method, without the OCM channels, the GPS channels are enabled post geosynchronous satellite acquisition. Subsequent to bit/subframe synchronization of the GPS channels and with the NAV data from geosynchronous satellites, position estimation of the GPS section is enabled. *This approach does not depend on IRNSS channels and with additional four SBAS channels (on GPS+SBAS receiver), the NAV data of visible satellites are obtained.*

6.5.3 Test Apparatus

The previous section explained the individual components of the test apparatus, as detailed in the block schematic shown in Figure 6-10. The details of the diagram are as follows:

A GPS antenna was exposed to open sky conditions. The output from this antenna through a splitter was taken to a GPSGL reference receiver and GPS clock (GPSCLK). The GPSGL receiver acquired and tracked all the satellites and output ephemeris data along with other receiver parameters. This output was taken to the simulator in real-time for the generation of NAV data on the geosynchronous satellites. The ephemeris data of satellites whose health field read all zeros (indicating healthy, (IS-GPS-200E 2010)) were only transmitted, to ensure the bandwidth was optimized.

GPSCLK is a rubidium based timing unit housing a GPS receiver and provides high accuracy measurements. The second output from the antenna splitter was connected to this receiver inside the GPSCLK unit. The main function of this receiver was to generate precise measurements in position constrained mode to output accurate 1 PPS. The Rb in standalone mode generates 1 PPS, which initially is not referenced. With 1PPS from the receiver and adequate averaging, the Rb oscillator was reset. Subsequently, 1 PPS from Rb was in phase lock with GPS time. In addition, a phase locked 10 MHz is also output from the unit. This 10 MHz is connected to the simulator's external 10 MHz input port as explained earlier. The GPSCLK has a provision to output the 1 PPS for any programmed instant, which is connected to the simulator's hardware trigger input.

Thus the simulator was configured to take the data in real-time and store it as a part of its memory prior to the start of the simulation.

The GPSGL receiver (modified) has three RF ports. Two of these inputs were from translated L5/S1 to L1. The other port was from a combiner whose inputs were from the simulator and the other from live antenna as shown in Figure 6-10.

6.5.4 Method

The sequence of steps followed for the simulation is as follows:

- The GPSCLK was powered on at T_0 and allowed to warm up (specifically Rb). The 1 PPS trigger was programmed for $T_0 + 30$ minutes from power-on.
- The GPSGL reference receiver was powered on at the same time as the GPSCLK. It acquired, tracked and collected the NAV data, which was in turn relayed to the simulator unit.
- The simulator was also powered on around T_0 and the simulation start time was set to $T_0 + 30$ minutes, commensurate with the trigger instant set on the GPSCLK. However, the data from the reference receiver was collected on the PC's RS232 port and stored.
- The GPSGL modified receiver was powered on at around T_0 . With no RF input, the receiver was in search mode. A small modification was applied to the GPS channels to enable them to enter acquisition only after one of IRNSS SPS channels (IRNSS L5/S1) had acquired. This ensured a reference to estimate hot start performance.

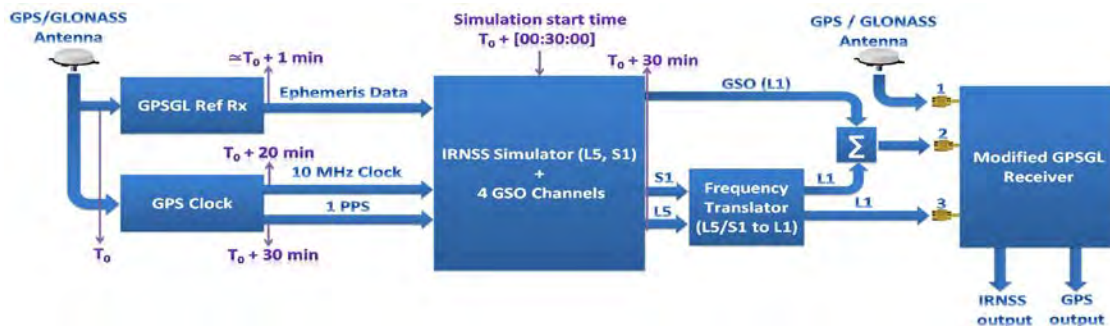


Figure 6-10: Block schematic detailing the test apparatus used for the simulation.

- The phase locked 10 MHz was output at around $T_0 + 20$ minutes from the GPSCLK to the simulator. The 1 PPS was output at $T_0 + 30$ minutes to the simulator enabling the RF generation. The first seven channels on S1/L5 simulate the IRNSS constellation w.r.t SPS. The first four channels of RS were modified on the (S1) port and dedicated for geosynchronous satellites. The simulations (position set in the simulator) corresponded to the GPS/GLONASS antenna exposed to clear sky.
- With the 1 PPS, the IRNSS simulation signals were generated in phase locked condition with that of GPS, and the receiver was able to acquire the data on the L5 and S1 channels. With the OCM method and in post bit-synchronization, the GPSGL modified receiver was able to estimate position within 6 s. With this, the estimates were programmed to the GPS L1 channels, which acquired, tracked and were used for positioning in 2 - 3 s.

The commensurate test apparatus w.r.t Figure 6-10 is shown in Figure 6-11.

6.5.5 Mapping test apparatus to proposed IRNSS

The test apparatus presented architecture to meet the underlying objectives set in Table 6-5. Table 6-6 explains the mapping of the architecture to the integrated IRNSS and GAGAN control station.

Table 6-6: Mapping of test apparatus to the system segments of IRNSS.

Segments of IRNSS and GAGAN system	Test Apparatus
The monitoring stations spread across India collate the GPS measurements / NAV data and relay these to the master control station.	This is analogous to the GPSGL Ref Rx, which collects the NAV data and relays it to the simulator.
The Master control station maintains the system time information and continuously compares and corrects with the UTC. In addition, the time synchronization of all the	The simulator set at $T_0 + 30$ minutes initiates the process for all the satellites and thus simulation of all the signals within the simulator (channels) occur at the

satellites is established by using the NAV data transmitted terms Af_0 , Af_1 and Af_2 (the clock terms). This is estimated and uploaded by the control station (Misra & Enge 2001).	same time. In addition, the 1 PPS derived from the GPSCCLK ensures that the data is synchronous with GPS/UTC.
Satellites L5/S1 and geosynchronous L1 satellite simulation.	The simulator effectively simulates the three frequency components of all seven IRNSS satellites.

6.6 Analysis

The above tests were conducted several times and the worst case result is plotted in Figure 6-12.

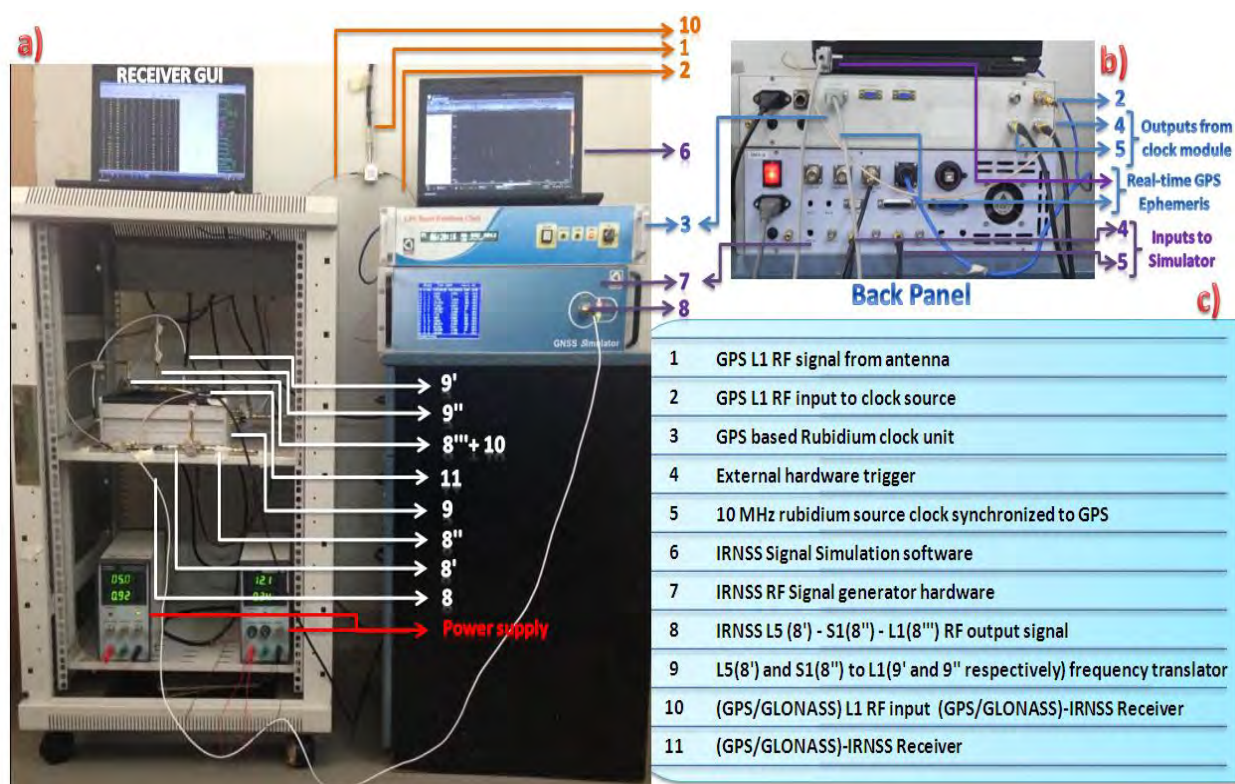


Figure 6-11: a). Test apparatus used to simulate GNSS Hot start performance with IRNSS b) rear panel connects of the simulator c) various subsystems used as a part of test setup.

The analysis is as follows: The GPS ephemeris data is collected from the L1 path of IRNSS. With 480 bits (Appendix F), it takes 3 subframes with 500 sps. With a geosynchronous satellite transmitting GPS ephemeris once every 3 s, it takes 9 s to transmit 12 (typically) visible GPS

satellites ephemeris data as shown in Figure 6-13. However, if the initial lock on the geosynchronous satellite occurs on the second subframe of the first set, it will take an additional 3 s (12 s in all). The first position of GPS was with relatively high PDOP (in some runs). After an additional 3 s, data was obtained from four additional satellites (eight in all), which resulted in a reduced (better) PDOP. For either method with or without OCM, the TTFF performance was similar and the results along with the OCM method of IRNSS are as shown in Figure 6-12.

The problem seen with GPS was not observed with GLONASS (340 NAV data bits first four strings as opposed to 480 bits in GLONASS). This effectively reduces three subframe/satellite (Figure 6-13) to two. The data was communicated within 6 s (worst case) for eight satellites. With OCM position, the GLONASS entered into measurement mode and was able to provide the position within 8 s from the instant of geosynchronous satellite bit synchronization as shown in Figure 6-12.

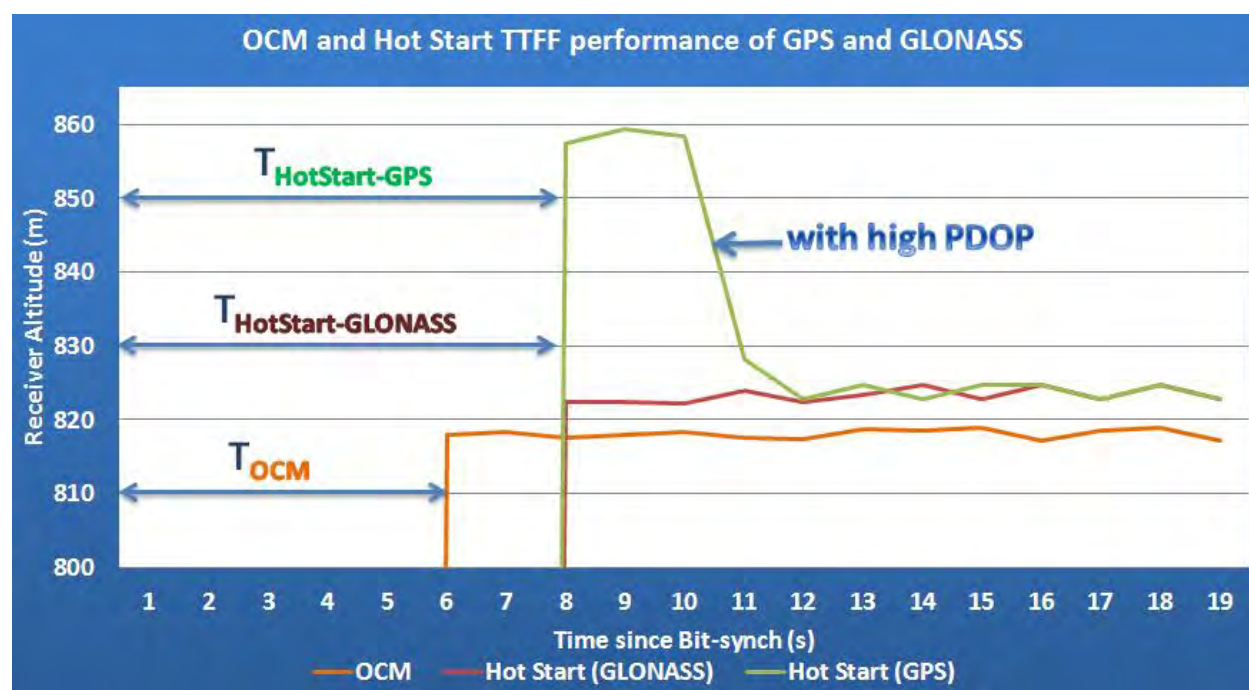


Figure 6-12: Fast TTFF test results for IRNSS and GPS in Hot start mode of operation.

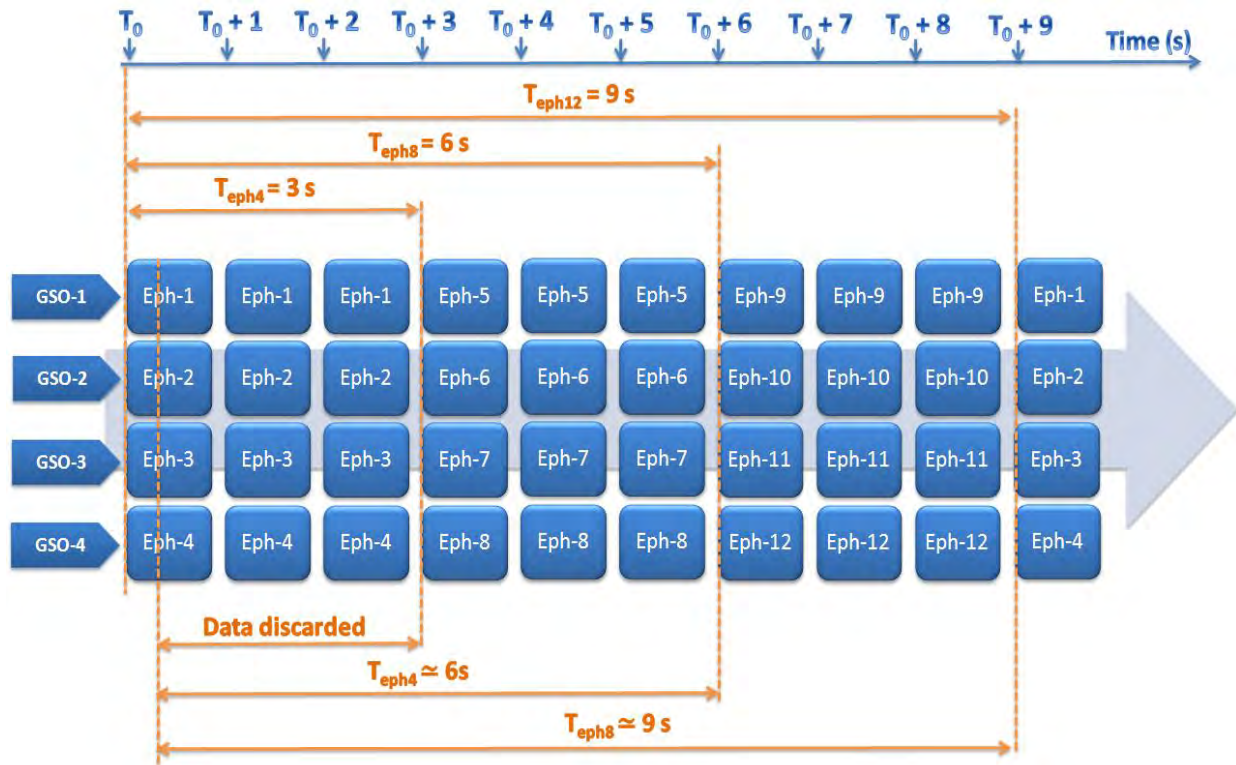


Figure 6-13: Time taken to transmit NAV data of GPS satellites on geosynchronous satellites.

The method and the results provide pointers to further analysis highlighted as follows:

- Instead of transmitting GPS, if we were to transmit IRNSS primary NAV data on the L1 channels, the results would not have been any better than the OCM method. This is again attributed to the NAV data in the Keplerian format, which requires a minimum of 480 bits.
- Second, if the NAV data of IRNSS were sent as absolute state vectors as in GLONASS, it would still have taken 5 s (worst case) to estimate the position.

The inference that can be deduced from the above analysis is that from a system perspective, the OCM method (Figure 5-10) is optimal and any further improvement calls for the data rate to be enhanced.

6.7 Real time snap start architectures in IRNSS

The HOT start analysis presented shows that any further improvement in IRNSS's TTFF can only be achieved with an increase in data rate. With an inherent limitation in the simulator (greater than 500 sps, simulation was not supported), this section extends the results of previous sections and presents two approaches with the necessary analysis to optimize the TTFF of the IRNSS restricted service. This assumes the following:

- A dedicated frequency is available only to restricted users of IRNSS with data at 1 KHz and signal strength of -157 dBW in line with the GALIEO E6b channel (Figure 6-1).
- The above signal is present only on the geostationary satellites of IRNSS.
- To reduce the bandwidth of the data exchanged, the IRNSS parameters are transmitted as absolute state vectors as in GLONASS on this channel.

6.7.1 ORM method based fast TTFF

With the time information available within 3 s employing the OMR method (Figure 5-11) in IRNSS (from the instant of tracking the SPS channels) as a pointer, the respective P(Y) code and the 1 KHz channel are locked. The ephemeris data is available within 1 s (Appendix F) from the 1 KHz channel and based on the measurements from P(Y) (post fine acquisition and bit synchronization), the position is estimated. The result is a TTFF of 4-5 s (3 s for time and 1-2 s for measurements/ephemeris data/positioning) for the restricted service.

This formulation assumes SPS-assistance to obtain TOW, independent of proposed L1 channel and requires an encrypted data channel.

6.7.2 Time from L1 channel of IRNSS

Assuming the proposed third frequency (L1) (IRNSS on GAGAN and the third frequency on IRNSS geosynchronous satellites) on all the satellites, the time information is available from it,

within 1 s of its tracking (Appendix F). The time information is used as a pointer to acquire the P(Y) code and the 1 KHz data channel. With this method the TTFF will be around 3-4 s for restricted users (1 s for fine acquisition of the L1 channel, 1 s for fine acquisition of P(Y) and 1 KHz channel, and 1-2 s to obtain the ephemeris data / measurement / position estimation).

Alternatively, an assumption on the availability of time was implicitly done in OCM in restricted direct acquisition (Figure 5-16). With this input (time from L1 channel of IRNSS in 1 s), the results shown in Figure 5-16 are achievable, which translates to 4 s positioning on the restricted service (1 s for L1 and 3 s for data collection). With this approach, the 1 KHz channel is obviated and yet restricted and civilian positions are obtained in 4 and 6 s respectively, post bit synchronization. *This is the most optimal architecture where, for the restricted service, one obtains the TTFF faster than SPS users and without needing the assumed 1 KHz signal. However, this approach assumes the L1 channel is available on all IRNSS satellites.*

6.8 Summary

The components derived from this chapter are presented pictorially in Figure 6-14.

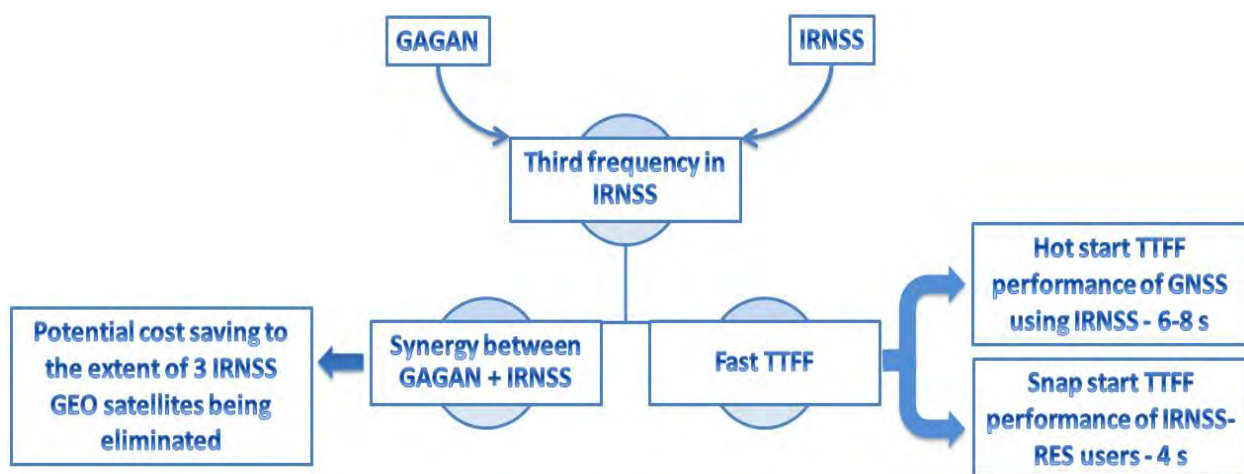


Figure 6-14: Summary of chapter contribution.

To summarize, this research derived three major components. First, a synergy between IRNSS and GAGAN was established, resulting in the third frequency of operation restricted to data channel. In addition, a new proposal of having IRNSS on GAGAN satellites was put forth. This architecture demonstrated two major improvements: First, the positioning of the satellites was optimal w.r.t availability when compared to the existing IRNSS constellation. Second, with the IRNSS signals beamed from GAGAN satellites, effectively three IRNSS satellites are eliminated, having a major cost implication. Following this, with necessary assumption third channel in L1 of geosynchronous satellites was presented. Using this as a data channel, hot start TTFF of existing GNSS was demonstrated. Finally, two additional architectures to obtain the most optimal TTFF of IRNSS in restricted service mode were presented with necessary assumptions/benefits.

Chapter Seven: CONCLUSIONS AND RECOMMENDATIONS

This chapter presents the conclusion of the thesis where several signal design strategies for IRNSS to enhance receiver TTFF performance directly from the satellites were proposed. In addition, recommendations for possible future work to enhance/optimize TTFF performance further are made.

7.1 Conclusions

A summary of the research outcomes are presented in Figure 7-1. Based on the results and analysis presented in the previous chapters, this section lists the conclusions as follows.

7.1.1 *Single frequency signal design*

1. Existing GPS L1 C/A single frequency receivers were experimentally characterized and the major components affecting their TTFF in modern receivers, especially in critical applications, were deduced. In addition, the need for faster secondary NAV data transmission from satellites was established.
2. A new technique of optimal secondary NAV data transmission in the IRNSS was established. With this method, a drastic improvement of 87% (w.r.t GPS L1) in secondary data collection was demonstrated.
3. A four subframe method of NAV data transmission was proposed. It was shown that a 20% improvement in IRNSS TTFF w.r.t GPS L1 and the complete system data (across satellites) is available within 24 s.
4. With the four-subframe method as a reference and constraining its content, an optimal architecture in three-subframe normal was derived. It was shown that the primary NAV data transmission was reduced by 40% w.r.t GPS L1 and hence in the TTFF improvement.

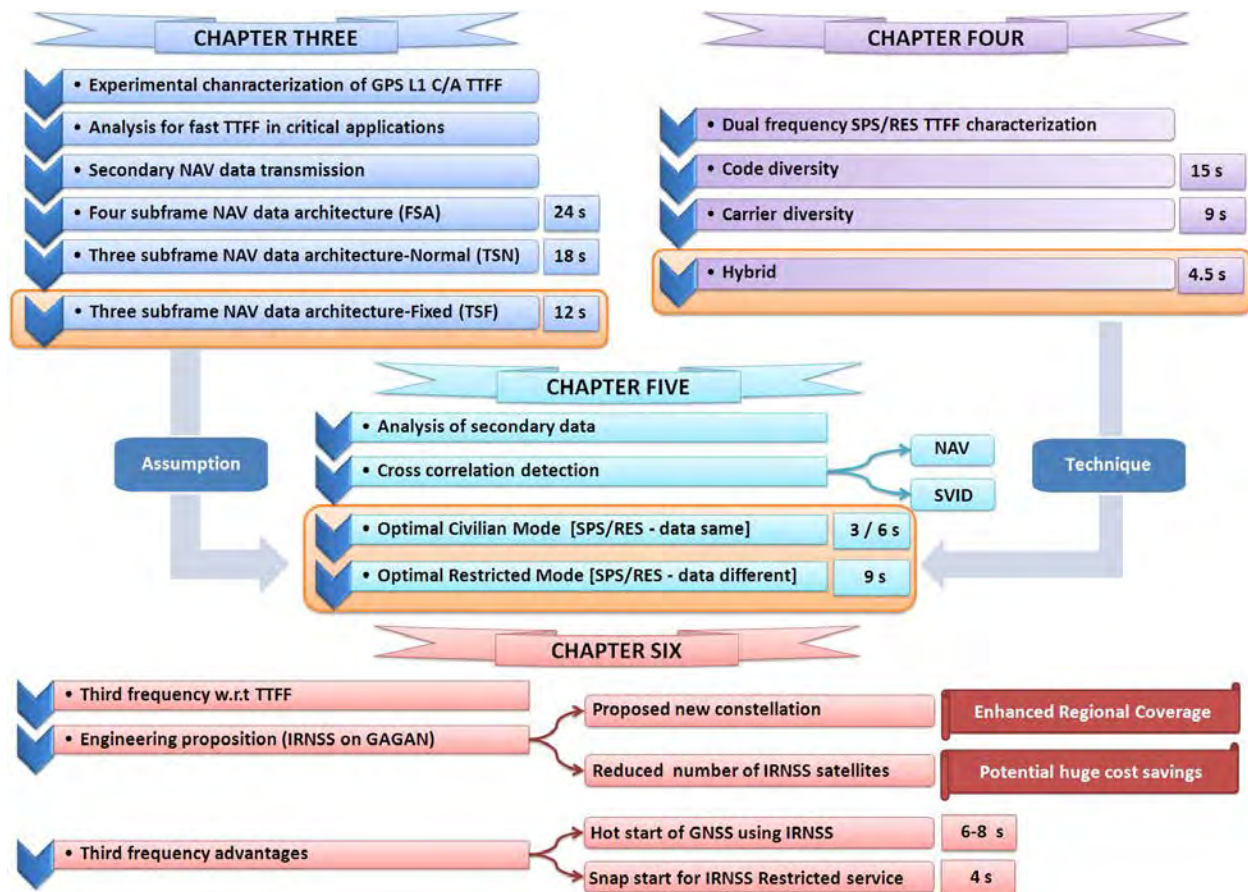


Figure 7-1: Summary of contributions/conclusions of the research.

- A novel three-subframe fixed method of *optimal* NAV data transmission was proposed for IRNSS. It was demonstrated that this scheme resulted in best (60% improvement w.r.t GPS L1) TTFF from any *single frequency* operational / emerging GNSS system.
- In addition, it was shown that all above methods are equally applicable from a global perspective.

7.1.2 Diversity based signal design

- The TTFF values achievable with existing operational dual frequency civilian and restricted signals were characterized and their limitations were presented. A detailed analysis of acquisition of restricted signals was described from an operational perspective, leading to TTFF.

2. A novel code diversity scheme was proposed for the single frequency assisted mode of IRNSS restricted signal acquisition. A 60% improvement in TTFF was shown, including complete secondary NAV data collection w.r.t GPS L1 C/A and P(Y) signals.
3. A new method based on carrier diversity for civilian signals of IRNSS was derived. A 70% improvement in TTFF was shown compared to various combinations of GPS civilian frequencies in dual mode of operation.
4. Based on code and carrier diversities, hybrid architecture was derived exclusively for restricted users. It was shown that a major improvement of 85 % in TTFF w.r.t GPS L1 is achievable assuming a direct method of restricted signal acquisition.

7.1.3 Optimized signal design

1. It was shown that in order to achieve the most optimal TTFF, the main impediment is the secondary data. Further, with necessary assumptions, the need for cross correlation detection based on NAV data was established to obviate almanac from secondary data and thus enhance the TTFF.
2. Two novel methods of cross correlation detections based on NAV data were proposed, wherein the cross correlation detection is instantaneous. In addition, it was shown that these methods are applicable to existing and emerging GNSS systems.
3. Four combined architectures were presented to enhance the TTFF in frequency/service mode of operation, with necessary assumptions. One of these methods (OCM) demonstrated 80% improvement in TTFF (6 s) in dual frequency mode of SPS operation w.r.t GPS.

7.1.4 Triple frequency IRNSS system

1. The fundamental activities prior to designing a new signal onboard a GNSS system were presented and highlighted for the Indian satellite navigation system. The limitations in the existing proposed IRNSS in conjunction with GAGAN was enumerated.
2. It was shown that an engineering synergy between IRNSS and GAGAN is possible, which effectively resulted in a third frequency proposal for IRNSS.
3. By using the IRNSS frequencies on the GAGAN geostationary satellites, it was shown that the relative availability of IRNSS would improve drastically. With IRNSS on GAGAN, *three of the proposed seven satellites could be eliminated* and yet achieve the individual objectives of IRNSS and GAGAN. The IRNSS and GAGAN control segments could be integrated as a consequence, *resulting in phenomenal cost savings*.
4. A data channel (primarily not meant for ranging) based on the third frequency on geosynchronous satellites of IRNSS was proposed. It was demonstrated that HOT start of GPS was possible over the Indian subcontinent without any assistance to receivers. In addition, this architecture would not warrant any hardware change in existing GPS receivers.
5. With fast TTFF values being one of the important specifications of critical applications, the real time SNAP start of restricted receivers was theoretically derived, without dependence on external networks or assistance.

Chapter Two presented a representative datasheet that can effectively become a future component of any receiver's datasheet. Alternatively, this research proposed a signal design for IRNSS over the Indian subcontinent exclusively for TTFF (*not disturbing other parameters*), which would make an IRNSS receiver datasheet a unique component, as shown in Table 7-1.

Table 7-1: Potential IRNSS receiver datasheet w.r.t TTFF in open sky conditions using proposed signals (post bit synchronization).

TTFF (IRNSS)			
Service Frequency	Civilian (s)	Restricted ⁺ (s)	
	Single	12	12
Dual	6	6	9
Third Frequency (Regional)	Snap start of IRNSS-RES (s)	Hot start TTFF of GNSS using IRNSS (s)	
	4	6-8	

+ SPS-Assisted mode Different data on SPS / RES Similar data on SPS / RES

With the result of the signal specifications listed (w.r.t TTFF) in Table 7-1, the limitations cited in the applications discussed in Chapter One and Chapter Two (Figure 2-19 and Figure 2-21) are easily overcome, meeting all other signal requirements as in existing and emerging GNSS systems and making *IRNSS - the world's first system to achieve fast TTFF directly from satellites without increasing data rate or onboard power, if the signal structure proposed herein were adopted.*

7.2 Recommendations

The research work assumed similar data rate/power as that of the existing operational systems and demonstrated the TTFF improvements achievable. This ensured the reference (for example, GPS/GLONASS L1/L2) w.r.t few signal parameters (for example, data rate and power) are established, parallels (w.r.t results) could be easily drawn and further, system level

implementation issues (for example, interoperability or realization (power) on board the satellite) would be obviated. Table 7-2 enumerates the work that could be carried out in future to further enhance/optimize TTFF performance.

Table 7-2: Possible future activities to enhance the TTFF performance.

Parameter	Possible futuristic work
Navigation data	<p>This work established Keplerian parameters as a part of ephemeris data. The reason to adopt this was the NAV data uploads to the satellite need to happen very frequently if absolute state vectors are used as a part of primary NAV data (for example, GLONASS transmits absolute state vectors updates every 30 minutes as opposed to GPS L1 C/A's 2 hours).</p> <p>Further studies and work could be carried out to optimize/process algorithms generating NAV data that are valid for a longer duration as for Keplerian parameters. The advantage of this approach is 340 NAV data bits are adequate to represent the primary NAV data (first five strings of GLONASS) as opposed to 480 bits (two subframes for current proposal).</p> <p>Adopting the techniques presented in this thesis with the stringed structure (assuming ephemeris is valid for two hours) would result in 1/3 reduction of the results presented in Table 7-2.</p>
Data Rate and Power	<p>This research assumed a data rate of 50 Hz similar to GPS/GLONASS L1 and power of -157 dBW similar to L5/L1 C for civilian and -160 dBW for restricted signals (for example, L1 P(Y)). GALILEO signals have assured transmission levels of -155 dBW. This additional power can enhance the data rate and thus the TTFF (though it might impact other features).</p> <p>Studies and analyses on the impacts of increased data rates w.r.t other parameters could be explored.</p>
Packet size	<p>The size of the data packet has 24 CRC and six tail bits. In all, 120 bits are transmitted for four subframes. To minimize this, two subframe architectures, one for primary and the other for secondary data could be explored, with a marginal increase in the CRC bit requirements. Effectively, 50% of these bits could be minimized.</p>
Additional frequency for restricted operations onboard IRNSS satellites to	<p>This research assumed a frequency for the restricted users of IRNSS for the most optimal TTFF performance. Further studies could be performed in the following areas:</p> <ul style="list-style-type: none"> • Choice of frequency: preferably close to either existing

Parameter	Possible futuristic work
transmit data/power	<p>frequencies (L5/S1) and thus minimize the receiver antenna design complexities.</p> <ul style="list-style-type: none"> • Maximum power and thus data that can be supported on it.
Navigation message of SBAS for a collaborative approach to enhance TTFF	<p>This research proposed that through geosynchronous satellites of IRNSS as a data channel, TTFF performance of GPS is achievable in 6 s in real time without any assistance (assuming a signal level of -160 dBW), and thus co-exist with GPS L1.</p> <p>With a likely possibility of each region (across globe) having two/three SBAS and assuming an increase in power level by 3 dB, data rate can be increased to 1 KHz from the existing 500 Hz. This additional bandwidth can be used for the TTFF from a constellation (say GPS L1) within 6 s for LOS applications, which obviates the need for any assistance in outdoor applications.</p> <p>Towards this, a framework structure could be explored and a collaborative approach across all satellite navigation bodies could be established to ensure that for a given constellation of civilian service (for example, GPS L1) the SBAS satellites transmit the NAV data as a part of its message and thus facilitate TTFF enhancements.</p>

References

- Analog Devices (2012), <http://www.analog.com/en/processors-dsp/products/index.html#>, last accessed December 10, 2012
- Arknava (2008) *A-133 GPS Active Antenna*, Arknava International Inc.
- Assisted GPS (2010), last accessed September 20, 2012
- Balaei, A. T. and D. M. Akos (2011) "Cross Correlation Impacts and Observations in GNSS Receivers," in *Navigation*, Vol. 58, pp. 323-333
- Bao, J. and Y. Tsui (2004) *Fundamentals of Global Positioning System Receivers: A Software Approach*, Wiley Series
- Betz, J.W. (1999) "The Offset Carrier Modulation for GPS Modernization," in *Proceedings of the Proceedings of ION National Technical Meeting*, , San Diego, CA
- Bhaskaranarayana (2008) *Indian IRNSS & GAGAN*
- Borio, D. and G. Lachapelle (2009) *A non-coherent architecture for GNSS digital tracking loops*, *Annals of Telecommunications*, pp. 601-614
- Borio, D. (2008) *A Statistical Theory for GNSS Signal Acquisition*, *Doctoral Thesis*, Doctoral Thesis, Dipartimento di Elettronica, Politecnico di Torino
- Borio, D. (2008) *A Statistical Theory for GNSS Signal Acquisition*, *Doctoral Thesis*, Dipartimento di Elettronica
- Borio (2010) *GNSS Receiver Design*, ENGO0638, University of Calgary, PLAN Group
- Burnell and Flerkevitch (2012) *Value of SBAS to Positioning in Emerging Applications*, http://www.gisdevelopment.net/application/Miscellaneous/mi08_154.htm
- CommSync II (2010), last accessed September 20, 2012
- CSR (2011) *InstantFix Extended Ephemeris (EE) and SUPL A-GNSS*, last accessed September 14, 2012
- Deshpande, S. and M.E. Cannon (2004) "Interference Effects on the GPS Signal Acquisition," in *Proceedings of the ION NTM-2004*, , San Diego, Institute of Navigation, pp. 1026-1036
- Dixon, R.C. (2004) *Spread Spectrum Systems: CDMA Design and Capabilities*, Wiley John, pp. 640
- DO-229D (2006) *Minimum Operational Performance Standards for GPS / WAAS System Airborne Equipment*, Sc-159

Doberstein, D. (2012) "Sliding Correlators, Delay Based Discriminators, Processing Gain and their Application in a GPS Receiver,"

Anon. (2010)
Dynetics, <http://www.dynetics.com/pdf/High%20Dynamic%20GPS%20Receiver%20Module.pdf>, last accessed September 20, 2010

EGNOS TRAN (2003) *The use of AIS as a local augmentation system for EGNOS in a maritime environment*, Datasheet EGNOS Tran 2003

EGNOS (2011) *EGNOS Safety of Life Service Definition Document*

Erlandson, R.J., T. Kim, and A.J. Van Dierendonck (2004) "Pulsed RFI Effects on Aviation Operations Using GPS L5," in *Proceedings of the Proceedings of the 2004 National Technical Meeting of The Institute of Navigation*, , San Diego, CA, The Institute of Navigation, pp. 1063-1076

Fastraxgps (2012), <http://www.fastraxgps.com/products/gpsmodules/300series/it310/>, last accessed November 20, 2012

Fontana, R.D., W. Cheung, and T. Stansell (2001) "The Mordernized L2 Civil Signal - Leaping forward in 21st Century," *GPS World*, September

GAGAN Architecture (2012), <http://www.defence.pk/forums/indian-defence/223371-gagan.html>, last accessed September 19, 2012

Galileo (2008) *Galileo Open Service Signal In Space Interface Control Document, OS SIS ICD, Draft I*, European Space Agency / European GNSS Supervisory Authority, <http://www.gsa.europa.eu/go/galileo/os-sis-icd>

Ganeshan, A.S. (2012) "GAGAN: Status and Update," in *Coordinates*, September 2012

Gerein , N., A. Manz, G. Pinelli, G. Franzoni, and A. Zin (2007) "Galileo Receiver Chain – The NonPRS Ground Reference Receiver," in *Proceedings of the ION GNSS 2007*, , Fort Worth, TX , The Institute of Navigation

Glennon, E.P. and A.G. Dempster (2005) "A Novel GPS Cross Correlation Mitigation Technique," in *Proceedings of the Proceedings of the 18th International Technical Meeting of the Satellite Division of The Institute of Navigation (ION GNSS 2005)*, , Long Beach, CA, pp. 190-199

Glennon, E. (2011) "QZSS Research at UNSW," in *Proceedings of the International Global Navigation Satellite Systems Society, IGNSS Symposium 2011*, , Sydney

GLONASS-ICD (1998) *GLONASS Interface Control Document, Version 4.0*, Moscow

- GR-10 (2012), <http://www.robotshop.com/eu/20-channel-sr-92-gps-engine-board-antenna-2.html>, last accessed December 13, 2012
- Greene, B. (2006) "Wireless Cellular Communications and Next Generation GPS," *Next Generation GPS Forum*, U S Dept. of Commerce
- Halamek, J., I. Viscor, and M. Kasal (2001) *Dynamic Range and Acquisiton System*, Measurement Science Review
- Haykin, S. (2001) *Communication Systems*, ohn Wiley & Sons, Inc., New York
- Hein, G., M. Anghileri, M. Paonni, J.A.A. Rodriwuez, and B. Eissfeller (2010) "Ready to navigate, A Methodology to estimation of Time To First Fix," *Inside GNSS*, March/April
- ICD-GPS-705 (2002) *Navstar GPS Space Segment / User Segment L5 Interfaces, Interface Control Document*
- Ipatov, V.P. and B.V. Shebshayevich (2010) "GLONASS CDMA Some Proposals on signal formats for future GNSS Air Interface," *InsideGNSS*, July-August
- IRNSS Architecture (2012) *IRNSS and GAGAN Explained*, http://trishul-trident.blogspot.in/2011_05_01_archive.html, last accessed September 9, 2012
- IS-GPS-200E (2010) *Navstar GPS Space Segment/Navigation User Interfaces, Interface Specification*
- Jakab, A.J. (2001) *Quality Monitoring of GPS Signals*, MSc Thesis , Department of Department of Geomatics Engineering, University of Calgary, UGCE Report No. 20149
- Jansen (2012) *Barriers to Mixed-Signal Technology Growth in Space*
- Jasper (2010) *NF (Noise Figure)*
- Kaplan, E.D. and C. Hegarty (2006) *Understanding GPS Priciples and Applications*, Artech House
- Kay, S.M. (1998) *Fundamentals of statistical Signal Processing*, Prentice Hall Inc.
- Kennedy, G. (1999) *Electronic Communication Systems*, Tata Magraw Hill
- Kibe, S. and D. Gowrishankar (2008) *APRSAF-15: Space for Sustainable Development*
- Kopp (1996) *GPS Aided Guided Munitions - Parts I-V*, last accessed December 13, 2012
- Lachapelle, G. (2010) *Advanced GNSS Theory and Application, ENG0625 Course Notes Department of Geomatics Engineering, University of Calgary, Alberta, Canada*

- Launching in Underwater (2012), <http://openwalls.com/image?id=10864>, last accessed November 10, 2012
- Li, B. (2005) *A Cost Effective Synchronization system for multi sensor integration*, University of New South Wales
- Lyons, R. G. (2004) *Understanding Digital Signal Processing*, Prentice Hall
- Magnavox-WM101 (2012), <http://www.underhill.ca/history/time-line/1980>, last accessed September 20, 2012
- Martin-Yug (2009) *Argos Platform Transmitter Terminal MT105AM with RTC and GPS options*, Revision 3.1
- Melbourne, W.G., T.P. Yunck, W.I. Bertiger, and B.H. Haines (1993) "Davis Scientific Applications of GPS On Low Earth Orbits," *J Geophy Res*
- Misra, P. and P. Enge (2001) *Global Positioning System: Signals, Measurements and Performance*, Ganga-Jamuna Press Lincoln, USA
- Navika (2012), <http://navika-electronics.com/Navika-300.html>, last accessed December 14, 2012
- NAVSTAR GPS (2012), <http://www.gps.gov/>
- Nayak, R. A. and J. K. Ray (2008) "Architecture of an FAA Certified TSO-C145c Precision Approach Receiver," in *Proceedings of the ION GNSS-2008*, , Savannah, GA, Institute of Navigation
- Nielsen, J., A. Broumandan, and G. Lachapelle (2011) "GNSS Spoofing Detection for Single Antenna Handheld Receivers," in *Navigation*, Vol. 58, Issue 4, pp. 335-344
- O'Keefe, K. (2001) "Availability and Reliability Advantages of GPS/Galileo Integration," in *Proceedings of the ION GPS-2001*, , Salt Lake City, Contract Report Prepared for Canadian Space Agency
- Pany, T. (2011) *Navigation Signal Processing for GNSS Softwares*, Artech House
- Parkinson, B.W. and J.J. Spilker (1996) *Global Positioning System: Theory and Applications*, American Institute of Aeronautics and Astronautics Inc, Cambridge, Massachusetts
- Petovello, M. (2010) "GNSS Solutions: GLONASS inter frequency biases and ambiguity resolution," *InsideGNSS*
- Phoenix (2012), <http://www.weblab.dlr.de/rbrt/GpsNav/Phoenix/Phoenix.html>, last accessed September 19., 2012
- PocketGPSWorld (2012), <http://www.pocketgpsworld.com/>, last accessed November 20, 2012

Predator Drone (2012) *Predator Firing Missile*, <http://notthemsmidotcom.wordpress.com/2012/09/29/america-in-yemen/predator-firing-missile4/>, last accessed November 10, 2012

Rao, V. G. and G. Lachapelle (2012) "New Method of Cross Correlation Detection in IRNSS and Civil Aviation Receivers," in *Proceedings of the NAVCOM-2012, Pearl Jubilee International Conference, Navigation & Communication*,

Rao, V. G. and G. Lachapelle (2012) "Proposed Dual Frequency Signal Design for Optimal TTFF in IRNSS," in *Proceedings of the NAVCOM-2012, Pearl Jubilee International Conference, Navigation & Communication*,

Rao, V. G. and G. Lachapelle (2012) "Proposed Third Frequency of Operation for IRNSS and its Advantages," in *Proceedings of the NAVCOM-2012, Pearl Jubilee International Conference, Navigation & Communication*, , pp. 4

Rao, V. G., R. Deviprasad, and S. Vishwanath (2006) "GPS Receiver with Soft Correlator Approach for LEO Orbits," in *Proceedings of the ION GNSS 2006*, , Dallas, Institute of Navigation

Rao, V. G., G. Lachapelle, and S. B. Pappu (2011) "Proposed Code and Carrier Dimension Dependent Signal Design for Optimal TTFF in IRNSS," in *Proceedings of the GNSS Signals 2011 Workshop, ENAC*, , Toulouse

Rao, V. G., G. Lachapelle, and S. B. Pappu (2012) "Proposed NAV Data Signal Design for Optimal TTFF in a Single Frequency IRNSS Receiver," in *Proceedings of the GNSS-2012*, , Nashville, TN, The Institute of Navigation

Rao, V. G., G. Lachapelle, and M. Sashidharan (2011) "Proposed LOS Signal Design for IRNSS to Reduce TTFF in a Single Frequency Receiver," in *Proceedings of the GNSS Signals 2011 Workshop*, , Toulouse

Rao, V. G., G. Lachapelle, and M. Sashidharan (2011) "Proposed LOS Signal Design for IRNSS to Reduce TTFF in a Single Frequency Receiver," in *Proceedings of the GNSS Signals 2011 Workshop*, , Toulouse

Rao, V. G., G. Lachapelle, and S.B. Vijaykumar (2011) "Analysis of IRNSS over Indian Sub-continent," in *Proceedings of the International Technical Meeting*, , San Diego, The Institute of Navigation, pp. 13

Ray, J. K. and M.E. Cannon (2000) "Synergy Between GPS Code, Carrier and SNR Multipath Errors," in *AIAA Journal of Guidance, Control and Dynamics*, Vol. 24, pp. 54-63

Ray, J. K. and K.V. Kalligudd (2001) "Development and Test Results of a Cost Effective Inverse DGPS System," in *Proceedings of the ION GPS-2001*, , Salt Lake City, Institute of Navigation, pp. 2618-2626

Ray, J. K. and R. A. Nayak (2008) "Offline, Online and On-target FD/FDE Test Results for Approach Phases in an Aviation Receiver," in *Proceedings of the ION GNSS-2008*, , Savannah, GA

Ray, J. K., M.E. Cannon, and P. Fenton (1998) "Mitigation of Static Carrier Phase Multipath Effects Using Multiple Closely-Spaced Antennas," in *Proceedings of the ION GPS-98*, , pp. 1025-1034

Ray, J. K., M.E. Cannon, and P. Fenton (2000) "Mitigation of Carrier Phase Multipath Effects Using Multiple Closely-Spaced Antennas," in *NAVIGATION: Journal of the Institute of Navigation*, Vol. 46, pp. 193-201

Ray, J. K., D. S.M., R. A. Nayak, and C. E.M. (2006) "GNSS Radio," *GPS World*, Vol.17, No.5, pp. 54-59

Rosbach, U. (2000) *Positioning and Navigation Using the Russian Satellite System GLONASS*

RTCM (1994) *RTCM Recommended Standards for Differential NAVSTAR GPS Service*, RTCM Special Committee

Ryan, S. and G. Lachapelle (1999) "Augmentation of DGNSS With Dynamic Constraints For Marine Navigation," in *Proceedings of the ION GPS99*, , Nashville

Salychev, O., V.V. Voronov, M.E. Cannon, R. A. Nayak, and G. Lachapelle (2000) "Attitude determination with GPS-Aided Inertial Navigation System," in *Proceedings of the ION IAIN World Congress Meeting*, , San Diego CA, pp. 705-711

Satyanarayana, S., D. Borio, and G. Lachapelle (2011) "A Non-coherent Block Processing Architecture for Standalone GNSS Weak Signal Tracking," in *Proceedings of the Proceedings of GNSS11*, , Portland, OR, The Institute of Navigation, pp. 9

Satyanarayana, (2011) *GNSS Channel Characterization and Enhanced Weak Signal Detection*, University of Calgary

Shivaramaiah, N.C. (2004) *A Fast Acquisition Hardware GPS Correlator*, Master's Thesis, Center for Electronics Design & Technology, IISc

Singh, A.K., A.K. Sisodia, and V. Garg (2008) "Modulation Designs For Indian Regional Navigation Satellite Systems," in *International Aeronautical Federation*

SkyTraq (2012), <http://www.skytraq.com.tw/>, last accessed November 20, 2012

Stewardship Project (2004) *GPS-L1 Civil Signal Modernization*, The Interagency GPS Executive Board

Tippenhauer, N. O., C. Pöpper, K. B. Rasmussen, and S. Capkun (2011) "On the Requirements for Successful GPS Spoofing Attacks,"

Triumph (2012), <http://www.javad.com/>, last accessed September 15, 2012

Van Dierendonck, A.J. (1994) "Understanding GPS Receiver Terminology: A Tutorial on What Those Words Mean," in *Proceedings of the International Symposium on Kinematic Systems in Geodesy, Geomatics, and Navigation*, , Banff, Canada, Univeristy of Calgary

Van Diggelen, F. (2009) *A-GPS: Assisted GPS, GNSS and SBAS*, Artech House

Veggeberg, K. (2010) *Advanced Wireless Architecture for Synchronizing dynamic measurements with GPS Technology*, National Instruments

Vijaykumar, S.B. and V. G. Rao (2007) "Innovative approach to overcome GPS signal masking during attitude manoeuvres," in *Proceedings of the ION GNSS-2007*, , Dallas, Institute of Navigation

Vimala, N. C.S., H. M.S., V. M.S., and M.R. Shenoy (2000) "Accord's Next generation High Performance GPS/WAAS Receiver Based on Soft-CorrelatorTM," in *Proceedings of the ION GPS-2000*, , Salt Lake City, pp. 329-336

Vucetic and Yuan (2010) "Turbo codes: Principles and Applications : Explaining Interleaving," ,

Woodcock, G. and G. Girard (2008) *Embedded LNA Antenna*, Jaybeam Wireless Technical Review Notes

Xilinx (2012), <http://www.xilinx.com/>, last accessed December 13, 2012

APPENDIX A: NAV DATA STRUCTURE FOR FOUR SUBFRAME

In this appendix, additional information related to the structuring of NAV data bits within each frame is presented. The meaning and definitions of the data bits follow GPS L1/L5 ((IS-GPS-200E 2010), (ICD-GPS-705 2002)) and suitably modified for the proposed IRNSS NAV data (Figure 3-4). The grouping is done based on the proposed subframe structure (Figure A1) and in four subframes.

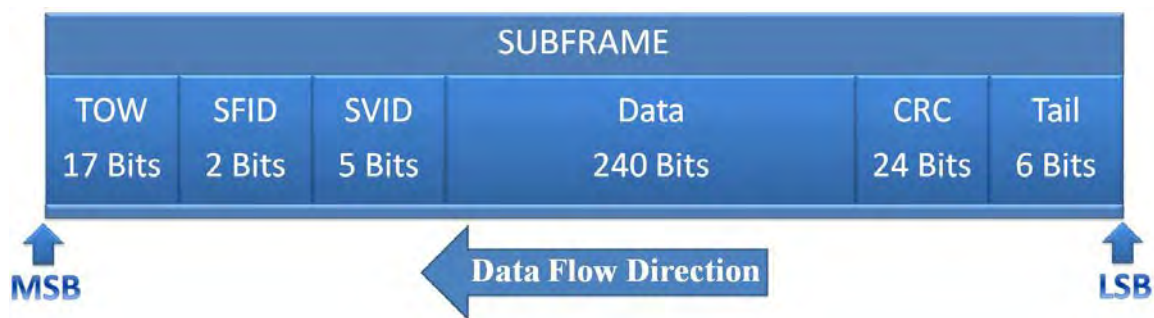


Figure A1: Subframe data structure for primary navigation parameters.

The two-bit definition of the subframe id is as shown in Table A1.

Table A1: Subframe ID description of IRNSS signals in four-subframe architecture.

Subframe ID	Description
00	Subframe One
01	Subframe Two
10	Subframe Three
11	Subframe Four

Following this, the details of primary parameters are presented and followed by the secondary NAV data details.

A.1. Primary navigation parameters

The bitwise lists of subframe 1 and 2 are as given in Table A2 and Table A3, respectively. The major optimization w.r.t GPS L1 are the removal of the telemetry word, health information is

single bit information as opposed to six bits. All the reserved and the spare bits listed in GPS L1 have been removed to enhance the TTFF. If any of these bits carry information that is relevant but not mentioned in GPS ICD, such bits are assumed to be transmitted as a part of textual messages.

Table A2: Subframe-1 parameter list for proposed IRNSS signals.

Parameter	Description	No of bits	Scaling factor	Bit location
Z-count	Time of week / Subframe Duration	17	1	0-16
SFID	Subframe ID - 00	2	1	17-18
SVID	Satellite PRN-ID of the transmitting satellite	5	1	19-23
AutoNAV	Bit-field indicating AutoNAV mode	1	1	24
WN	Week Number	10	1	25-34
T_{gd}	Group Delay	8	2^{-31}	35-42
T_{oc}	Clock data reference time of week	16	2^4	43-58
Af_2	SV Clock Drift Rate Correction Coefficient	8	2^{-55}	59-66
Af_1	SV Clock Drift Correction Coefficient	16	2^{-43}	67-82
Af_0	SV clock bias correction coefficient	22	2^{-31}	83-104
C_{rs}	Amplitude of Sine harmonic correction to the orbit radius	16	2^{-5}	105-120
C_{is}	Amplitude of Sine harmonic correction to the Angle of inclination	16	2^{-29}	121-136
C_{us}	Amplitude of Sine harmonic correction to the Argument of Latitude	16	2^{-29}	137-152
M_0	Mean Anomaly at reference time	32	2^{-31}	153-184
e	Eccentricity	32	2^{-33}	185-216
\sqrt{A}	Square root of semi major axis	32	2^{-19}	217-248
URA	User Range Accuracy	4	1	249-252
L5-Health	SV health information	1	1	253
S1-Health	SV health information	1	1	254
L1-Health	SV health information	1	1	255
IODC	Issue of Data Clock	8	1	256-263
CRC	Cyclic Redundancy Check code	24	1	264-287
Tail	Tail bits: 000000	6	1	288-293

Table A3: Subframe-2 parameters list as a part of proposed IRNSS signals.

Parameter	Description	No of bits	Scaling factor	Bit location
Z-count	Time of week / Subframe Duration	17	1	0-16
SFID	Subframe ID - 01	2	1	17-18
SVID	Satellite PRN-ID of the transmitting satellite	5	1	19-23
AutoNAV	Bit-field indicating AutoNAV mode	1	1	24
T_{oe}	Reference Time of Ephemeris	16	2^4	25-40
Ω_0	Longitude of ascending node of the orbit plane at reference time	32	2^{-31}	41-72
I_0	Inclination Angle of the orbit plane at reference time	32	2^{-31}	73-104
ω	Argument of perigee	32	2^{-31}	105-136
Ω_{dot}	Rate of right Ascension	24	2^{-43}	137-160
I_{dot}	Rate of inclination angle	14	2^{-43}	161-174
Δn	Mean motion difference from the computed value	16	2^{-43}	175-190
C_{ic}	Amplitude of Cosine harmonic correction term to the angle of inclination	16	2^{-29}	191-206
C_{uc}	Amplitude of Cosine harmonic correction term to the argument of Latitude	16	2^{-29}	207-222
C_{rc}	Amplitude of Cosine harmonic correction term to the orbit radius	16	2^{-5}	223-238
ISC-L5	Group delay differential correction terms	8	1	239-246
ISC-S1		8	1	247-254
IODE	Issue of Data Ephemeris	8	1	255-262
Spare	Spare bits	1	1	263
CRC	Cyclic Redundancy Check code	24	1	264-287
Tail	Tail bits : 000000	6	1	288-293

A.2. Secondary navigation parameters

The secondary NAV data are transmitted in subframe 3 and 4 as shown in Figure A2. Subframe 3 is dedicated to almanac transmission and subframe 4 carries messages. The first six bits of the NAV data in 4 are reserved to identify the message type, whose description is as given in Table A4.

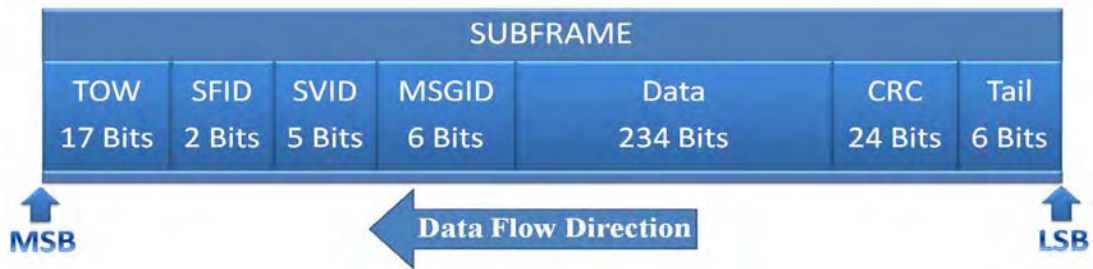


Figure A2: Subframe data structure for message transmission in subframe 4 of IRNSS.

Table A4: Message ID description for proposed IRNSS secondary messages.

Message Type	Description
00	Reserved
01	Almanac-IONO
02	Almanac-UTC
03	Iono-UTC
04 – 63	Any User Data

In addition, subframe 3 contains Ionosphere correction coefficients and UTC parameters, whose definitions are as in Table A5 and Table A6, respectively.

Table A5: Almanac-Iono / Message Type 1 field descriptions.

Parameter	Description	No of bits	Scaling factor	Bit location
Z-count	Time of week / Subframe Duration	17	1	0-16
SFID	Subframe ID - 10	2	1	17-18
SVID	Satellite PRN-ID of the transmitting satellite	5	1	19-23
MSGID	Message ID – 000011	6	1	24-29
SVID	SVID of the Almanac parameters	5	1	30-34
WN _a	Almanac Reference Week	8	1	35-42
E	Eccentricity	11	2 ⁻¹⁶	43-53
t _{oa}	Time of Applicability	8	2 ¹²	54-61
δ _i	Correction to the inclination angle	11	2 ⁻¹⁴	62-72
Ω ₀	Longitude of ascending node of the orbit plane at reference time	16	2 ⁻¹⁵	73-88
√A	Square root of semi major axis	17	2 ⁻⁴	89-106
Ω _{dot}	Rate of right Ascension	11	2 ⁻³³	107-117
ω	Argument of perigee	16	2 ⁻¹⁵	118-133
M ₀	Mean anomaly at reference time	16	2 ⁻¹⁵	134-149
Af ₀	SV clock bias correction coefficient	11	2 ⁻²⁰	150-160
Af ₁	SV Clock Drift Correction Coefficient	11	2 ⁻³⁷	161-171
L5-Health	SV Health	1	1	172
S1-Health	SV Health	1	1	173
L1-Health	SV Health	1	1	174
α ₀	Ionospheric correction parameters	8	2 ⁻³⁰	175-182
α ₁		8	2 ⁻²⁷	183-190
α ₂		8	2 ⁻²⁴	191-198
α ₃		8	2 ⁻²⁴	199-206
β ₀		8	2 ¹¹	207-214
β ₁		8	2 ¹⁴	215-222
β ₂		8	2 ¹⁶	223-230
β ₃		8	2 ¹⁶	231-238
A ₁	Drift co-efficient of IRNSS-time scale relative to UTC time scale	24	2 ⁻⁵⁰	239-262
Spare	Spare bits	3	1	263-265
CRC	Cyclic Redundancy Check code	24	1	264-287
Tail	Tail bits: 000000	6	1	288-293

Table A6: Almanac- UTC/ Message type 2 field descriptions.

Parameter	Description	No of bits	Scaling factor	Bit location
Z-count	Time of week / Subframe Duration	17	1	0-16
SFID	Subframe ID	2	1	17-18
SVID	Satellite PRN-ID of the transmitting satellite	5	1	19-23
MSGID	Message ID – 000010	6	1	24-29
SVID	SVID of the Almanac parameters	5	1	30-34
WN _a	Almanac Reference Week	8	1	35-42
e	Eccentricity	11	2 ⁻¹⁶	43-53
t _{oa}	Time of Applicability	8	2 ¹²	54-61
δ _i	Correction to the inclination angle	11	2 ⁻¹⁴	62-72
Ω ₀	Longitude of ascending node of the orbit plane at reference time	16	2 ⁻¹⁵	73-88
√A	Square root of semi major axis	17	2 ⁻⁴	89-105
Ω _{dot}	Rate of right Ascension	11	2 ⁻³³	106-116
ω	Argument of perigee	16	2 ⁻¹⁵	117-132
M ₀	Mean anomaly at reference time	16	2 ⁻¹⁵	133-148
Af ₀	SV clock bias correction coefficient	11	2 ⁻²⁰	149-159
Af ₁	SV Clock Drift Correction Coefficient	11	2 ⁻³⁷	160-170
L5-Health	SV Health	1	1	171
S1-Health	SV Health	1	1	172
L1-Health	SV Health	1	1	173
A ₀	Bias co-efficient of IRNSS-time scale relative to UTC time scale	32	2 ⁻³⁰	174-205
Δt _{LS}	Current or past leap second count	8	1	206-213
t _{ot}	Time data reference time of week	16	2 ⁴	214-229
WN _{ot}	Time data reference week number	8	1	230-237
WN _{LSF}	Week number of leap second adjustment	8	1	238-245
DN	Leap second reference day number	4	1	246-249
Δt _{LSF}	Current or future leap second count	8	1	250-257
Spare	Spare bits	6	1	258-263
CRC	Cyclic Redundancy Check code	24	1	264-287
Tail	Tail bits: 000000	6	1	288-293

Subframe 4 consists of user defined messages types (Table A7), retained here as dummy frames.

Table A7: User defined message types to be transmitted as a part of subframe 4.

Parameter	Description	No of bits	Scaling factor	Bit location
Z-count	Time of week / Subframe Duration	17	1	0-16
SFID	Subframe ID	2	1	17-18
SVID	Satellite PRN-ID of the transmitting satellite	5	1	19-23
MSGID	Message ID	6	1	24-29
Dummy	User-defined parameters	234	-	30-263
CRC	Cyclic Redundancy Check code	24	1	264-287
Tail	Tail bits: 000000	6	1	288-293

APPENDIX B: NAV DATA STRUCTURE FOR THREE SUBFRAME NORMAL

This appendix presents the definitions of parameters of the TSN method. The subframe ID description for the proposed TSN is shown in Table B1. The first two subframes are as specified in Table A2 and Table A3, respectively. The third subframe transmits the data as messages. The id definitions for the different types of message are given in Table B1.

Table B1: Subframe ID description of IRNSS signals in TSN.

Subframe ID	Description
00	Subframe One
01	Subframe Two
10	Subframe Three
11	Not Applicable

B.1. Secondary navigation parameters

The almanac is included as a message type and is transmitted in subframe 3. Towards this, message type-1 and message type-2 of the FSA is used. To facilitate transmission of UTC and Ionosphere terms along with the messages, message type-3 as enumerated in Table B2 is used.

Table B2: UTC-Iono Message / Message Type 3 field descriptions.

Parameter	Description	No of bits	Scaling factor	Bit location
Z-count	Time of week / Subframe Duration	17	1	0-16
SFID	Subframe ID	2	1	17-18
SVID	Satellite PRN-ID of the transmitting satellite	5	1	19-23
MSGID	Message ID – 000011	6	1	24-29
α_0	Ionospheric correction parameters	8	2^{-30}	30-37
α_1		8	2^{-27}	38-45
α_2		8	2^{-24}	46-53
α_3		8	2^{-24}	54-61
β_0		8	2^{11}	62-69
β_1		8	2^{14}	70-77
β_2		8	2^{16}	78-85
β_3		8	2^{16}	86-93
A_0		Bias co-efficient of IRNSS-time scale relative to UTC time scale	32	2^{-35}
A_1	Drift co-efficient of IRNSS-time scale relative to UTC time scale	24	2^{-51}	126-149
Δt_{LS}	Current or past leap second count	8	1	150-157
t_{ot}	Time data reference time of week	16	2^4	158-173
WN_{ot}	Time data reference week number	8	1	174-181
WN_{LSF}	Week number of leap second adjustment	8	1	182-189
DN	Leap second reference day number	4	1	190-193
Δt_{LSF}	Current or future leap second	8	1	194-201
ISC-L5	Group delay differential parameters	8	2^{-31}	202-209
ISC-S1	Group delay differential parameters	8	2^{-31}	210-217
ISC-L1	Group delay differential parameters	8	2^{-31}	218-215
L5 health	SV Health	1	1	226
S1 health	SV Health	1	1	227
L1 health	SV Health	1	1	228
Spare*	Spare bits	35	1	229-263
CRC	Cyclic Redundancy Check code	24	1	264-287
Tail	Tail bits: 000000	6	1	288-293

* Used for GPS-L1 almanac health in test suite 1 of Chapter Three.

APPENDIX C: NAV DATA STRUCTURE FOR THREE-SUBFRAME FIXED ARCHITECTURE

The definitions for the TSF architectures are presented in this appendix with the subframe definitions as given in Table C1. Subframe 1 and 2 remain same as in the TSN method. However, for subframe 3, message Type-3 as explained in Appendix B is transmitted.

Table C1: Subframe ID definitions for TSF structure.

Subframe ID	Description	Contents
00	Subframe One	Ephemeris -1 (Table A2)
01	Subframe Two	Ephemeris-2 (Table A3)
10	Subframe Three	UTC-Iono (Table B2)
11	Not Applicable	----

APPENDIX D: PDOP VARIATION WITH A SATELLITE EXCLUSION IN TSF METHOD

This appendix presents the PDOP variation as a function of one satellite being dropped in the IRNSS. As explained in Chapter 3, this scenario arises due to the transmission of the textual message (MT-3, UTC/IONO message) as a part of one satellite's NAV data. This condition prevails for 6 s for a satellite (among 7 satellites) and is applicable only with the first power-on (position). With the receiver in continuous lock and even with ephemeris change (typically once in 2 hours), this issue (PDOP) will not be observed, which is attributed to the validity of ephemeris for 4 hours and thus the previous ephemeris can be used for the first 18 s of the satellite on which the textual data is transmitted. The existing IRNSS constellation was considered for the generation of these plots. Figure D1, Figure D2, and Figure D3 illustrate the variation with single satellite being dropped.

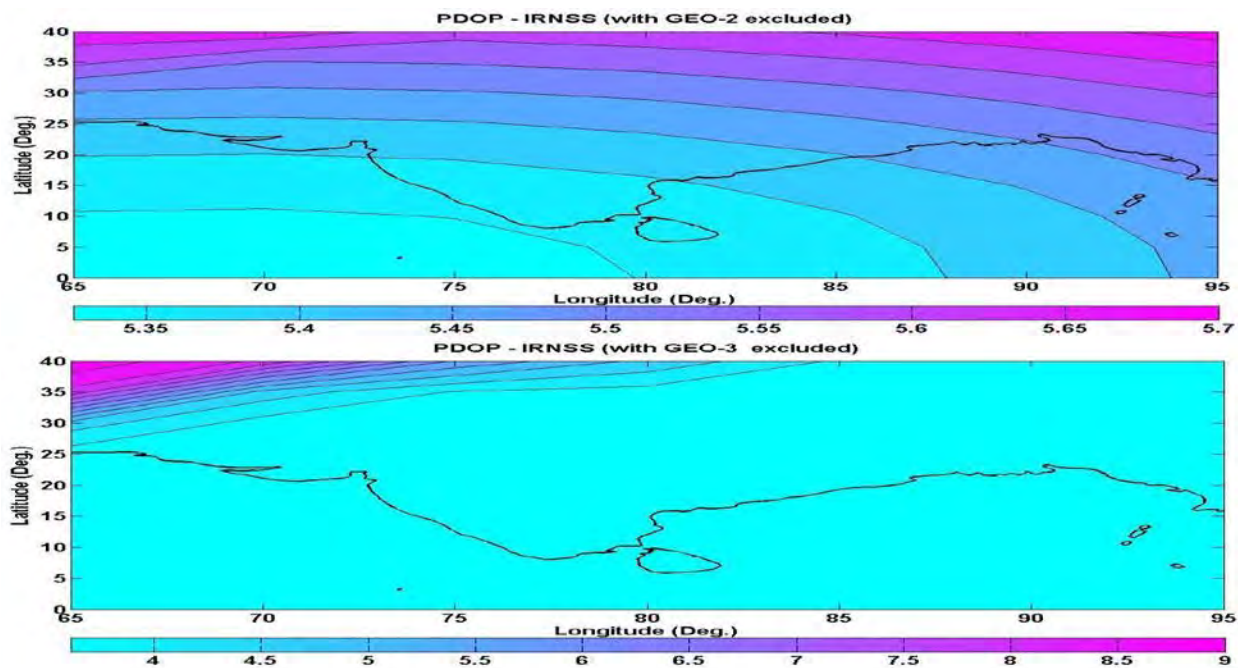


Figure D1: Variation in PDOP considering the GEO-2 and GEO-3 exclusion in IRNSS.

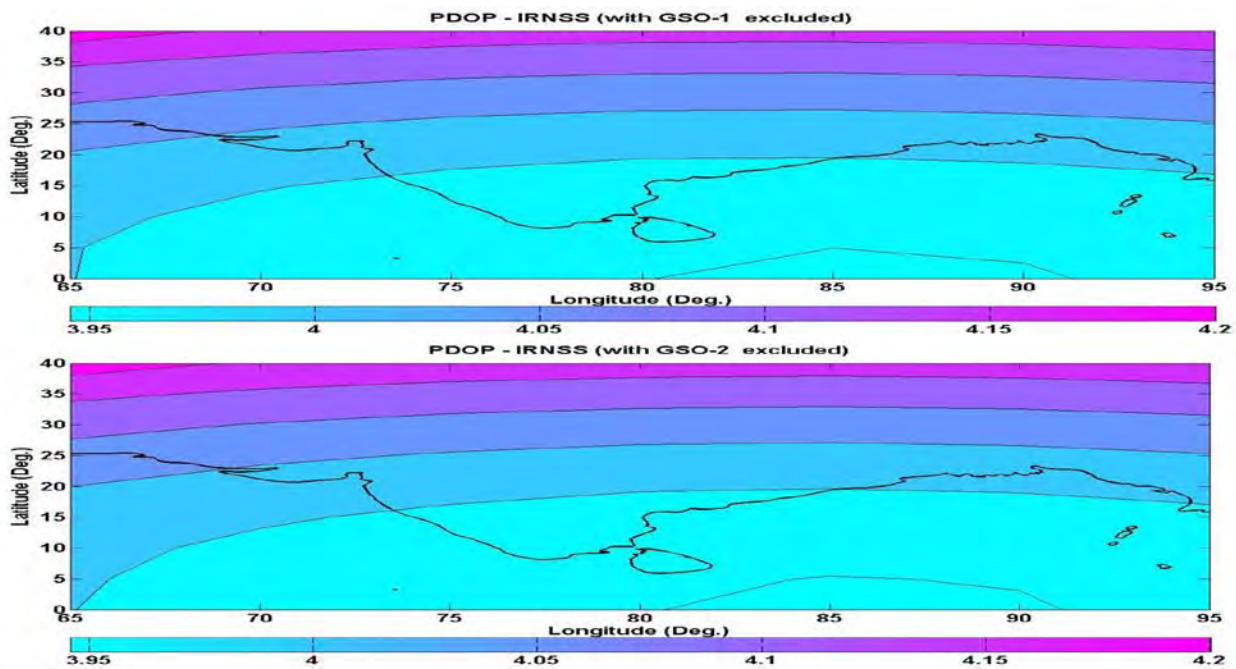


Figure D2: Variation in PDOP considering the GSO-1 and GSO-2 exclusion in IRNSS.

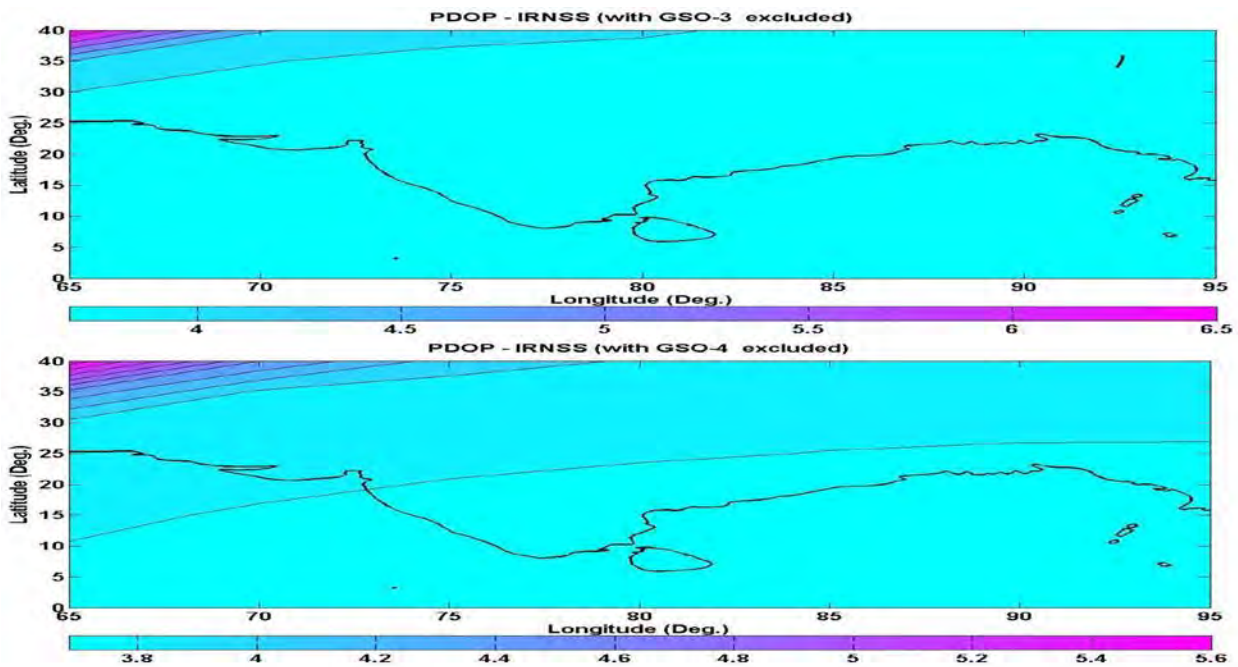


Figure D3: Variation in PDOP considering the GSO-3 and GSO-4 exclusion in IRNSS.

APPENDIX E: ALGORITHM FOR THREE-SUBFRAME ARCHITECTURE

This appendix presents the implementation details of subframe synchronization with TSN processing for all three modes of receiver operation in code, carrier and hybrid architectures. The validation of this algorithm has been performed based on the initial data bit synchronization on each bit starting from 1 to 588 (synch pattern excluded) and straddled across frames/frequency/service. The simulator used as part of this research can generate the data in virtual mode without RF being generated. Utilizing this feature, the data sets were collected for validation purpose.

E.1. Code Diversity

The data structure is as specified in Chapter Four. All three subframes are obtained by collecting 900 symbols from SPS channels and RES channels of corresponding SVs. The 900 symbols from SPS and RES of corresponding SVs are read from the simulator data set and are concatenated to form 1800 symbols. Sync patterns are searched from an array of 1800 symbols and their positions are stored in another array. Separation between two successive sync patterns should be 600 symbols. There is a possibility of having a maximum of three Sync patterns. If the receiver locks in between sync patterns, the number of sync patterns obtained is two.

E.1.1. Half Data Block Collection (HDBC)

If the receiver locks in between 150-symbol blocks, depending upon the number of 150 symbol blocks collected (count) before the first sync position, the following four cases are possible.

Case 1: When the number of 150 symbol blocks collected before the first sync position is three.

Consider the example as shown in Table E1. The 900 symbols from two channels are concatenated. There are three 150-symbol blocks before the first sync position. Parts of block 1' and 1'''' are concatenated. Then the rearrangement of the three subframes is done as explained.

Table E1: Received 1800 symbols in HDDB-case 1.

Channels 1 to 7							Channels 8 to 14									
	1'	2''	3'''	1''	2'	3''	1'''		1'''	2''	3'	1''	2'''	3''	1'	

If the start bit is between TOWs (13 to 90), the TOW value of 3' is copied to that of 1' after decoding. If the start bit is between 91 and 138, a part of the CRC of subframe 1 is divided into two parts. Each part is received for different TOWs. Thus the CRC has to be reconstructed. If the start bit is between 139 and 150, the receiver locks in between tail symbols. Tail bits will not be zeros when decoded. This is because two parts of the tail bits were encoded with different TOW values.

Case 2: When the number of 150-symbol blocks collected before the first sync position is two.

Consider the example shown in Table E2. The 900 symbols from two channels are concatenated. There are two blocks before first sync position. Parts of block 2''' and 2'' are concatenated. The subsequent rearrangement of the three subframes is done as explained. The TOW and CRC reconstruction for the start bits 151 to 300 is not required.

Table E2: Received 1800 symbols in HDDB-case 2.

Channels 1 to 7							Channels 8 to 14									
	2'''	3'''	1''	2'	3''	1'''	2''		2''	3'	1''	2'''	3''	1'	2'''	

Case 3: When the number of 150-symbol blocks collected before first sync position is 1.

Consider the example as shown in Table E3. The 900 symbols from two channels are concatenated. There is one 150-symbol block before the first sync position. Parts of block 3''' and 3' are concatenated. Then the rearrangement of the three subframes is done as explained.

Table E3: Received 1800 symbols in HDBC-case 3.

Channels 1 to 7							Channels 8 to 14										
	3''''	1''	2'	3'''	1''''	2''	3'			3'	1''''	2''''	3''	1'	2'''	3''''	

If the start bit is between TOWs (bit location 313 to 390), the TOW value of 2' is reduced by 6 and copied to the TOW of 3' after decoding. If the start bit is between 391 and 438, part of the CRC of subframe 3 is divided into two parts. Each part is received for different TOW values. Thus the CRC has to be reconstructed. If the start bit is between 439 and 450, receiver locks in between tail symbols. Tail bits will not be zeros when decoded. This is because two parts of the tail bits were encoded with different TOW values.

Case 4: When the number of 150-symbol block collected before the first sync position is 0.

Consider the example shown in Table E4. The 900 symbols from two channels are concatenated. There is no block before the first sync position. Parts of block 1'' and 1'''' are concatenated. Then the rearrangement of three subframes is done as explained. The TOW and CRC reconstruction for the start bits 451 to 600 is not required.

Table E4: Received 1800 symbols in HDBC-case 4.

Channels 1 to 7							Channels 8 to 14										
	1''	2'	3'''	1''''	2''	3'	1''''			1''''	2''''	3''	1'	2'''	3''''	1''	

E.1.2. Full Data Block Collection (FDBC)

This case is obtained when start bit is at the start of the block (1, 151, 301 and 451). Consider an example as shown in Table E5. The 900 symbols from two channels are concatenated and rearrangement is done as explained.

Table E5: Received 1800 symbols in FDBC.

Channels 1 to 7						Channels 8 to 14					
1''	2'	3'''	1''''	2''	3'	1'''	2''''	3''	1'	2'''	3''''

E.1.3. Rearrangement

The 600 symbols from sync position 1, position 2, and position 3 are stored in buffer 1, buffer 2, and buffer 3, respectively. Consider the example as shown in Table E6.

- Step 1: Append last 150 bits to the 151th position of respective buffers.
- Step 2: Copy 150 symbols from the 301st position of buffer 1, buffer 2 and buffer 3 to the 301st position of buffer 2, buffer 3 and buffer 1, respectively.
- Step 3: Copy 150 symbols from the 451st position of buffer 1, buffer 2 and buffer 3 to the 451th position of buffer 3, buffer 1 and buffer 2, respectively.

After rearranging the contents of these three buffers, the data is decoded and extracted depending on SFID.

Table E6: Contents of three buffers.

Initial	Buffer 1	3'	1'''	2''''	3''
	Buffer 2	1'	2'''	3''''	1''
	Buffer 3	2'	3'''	1''''	2''
Step 1	Buffer 1	3'	3''	1'''	2''''
	Buffer 2	1'	1''	2'''	3''''
	Buffer 3	2'	2''	3'''	1''''
Step 2	Buffer 1	3'	3''	3'''	2''''
	Buffer 2	1'	1''	1'''	3''''
	Buffer 3	2'	2''	2'''	1''''
Step 3	Buffer 1	3'	3''	3'''	3''''
	Buffer 2	1'	1''	1'''	1''''
	Buffer 3	2'	2''	2'''	2''''

E.2. Carrier Diversity/Hybrid

The proposed data structure is shown in Figure E1.

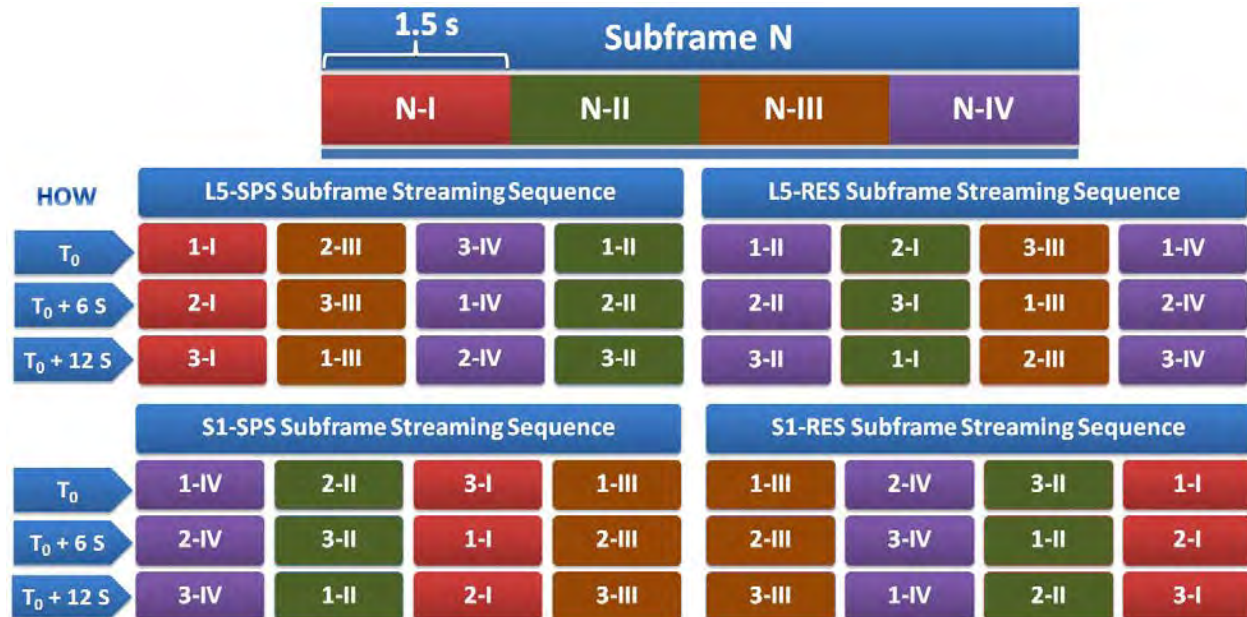


Figure E1: Proposed three-subframe data structure carrier diversity or hybrid architecture in IRNSS.

All three subframes are obtained by collecting 450 symbols from SPS and RS of two frequencies (L5 and S1) of corresponding SVs. In 4.5 s all three subframes data is available within the receiver. Hence the TTFF can be reduced. There are 28 channels in the receiver; channels 1 to 14 correspond to L5 and channels 15 to 28 correspond to S1. The first even channels of L5 and S1 correspond to seven SVs with SPS. The next seven channels correspond to the same seven SVs with RS.

The 450 symbols from SPS and RS of L5 and S1 of corresponding SVs are read from the simulator data. They are concatenated to form 1800 symbols. Sync patterns are searched from an array of 1800 symbols and their positions are stored in an array. The separation between two

successive sync patterns should be 600 symbols. The maximum sync pattern available will be three. If the receiver locks in between sync patterns, the number of sync patterns obtained is two.

E.2.1. HDBC

If receiver locks in between 150-symbol blocks, depending upon the number of 150-symbol blocks collected (i.e. count) before the first sync position, four cases are possible.

Case 1: When the number of 150-symbol blocks collected before the first sync position is three.

Consider the example shown in Table E7. The 450 symbols from four channels are concatenated.

There are three 150-symbol blocks before the first sync position. Parts of block 1', 1'', 1''' and 1'''' are concatenated. Then the rearrangement of the three subframes is done as explained.

TOW and CRC reconstruction for start bit 1 to 150 is not required.

Table E7: Received 1800 symbols in HDBC-case 1.

Channels 1 to 7					Channels 8 to 14					
	1'	2'''	3''''	1''		1''	2'	3'''	1''''	
Channels 15 to 21					Channels 22 to 28					
	1''''	2''	3'	1'''		1'''	2''''	3''	1'	

Case 2: When the number of 150-symbol blocks collected before the first sync position is two

Consider the example shown in Table E8. The 450 symbols from four channels are concatenated.

There are two blocks before the first sync position. Parts of block 2''', 2', 2'' and 2'''' are concatenated. Then the rearrangement of the three subframes is done as explained.

Table E8: Received 1800 symbols in HDBC-case 2.

Channels 1 to 7					Channels 8 to 14					
	2'''	3''''	1''	2'		2'	3'''	1''''	2''	
Channels 15 to 21					Channels 22 to 28					
	2''	3'	1'''	2''''		2''''	3''	1'	2'''	

If the start bit is between TOWs (163 to 240), a TOW value of 3' is copied to that of 2' after decoding. If the start bit is between 241 and 288, part of the CRC of subframe 2 is divided into two parts. Each part is been received for different TOWs. Thus the CRC has to be reconstructed. If the start bit is between 289 and 300, the receiver locks between tail symbols. Tail bits will not be zeros when decoded. This is because two parts of the tail bits were encoded with different TOW values.

Case 3: When the number of 150-symbol blocks collected before the first sync position is one.

Consider the example shown in Table E9. The 450 symbols from four channels are concatenated. There is one 150-symbol block before the first sync position. Parts of block 3'', 3''' block, 3'''' and 3' are concatenated. Then the rearrangement of the three subframes is done as explained.

Table E9: Received 1800 symbols in HDBC-case 3.

Channels 1 to 7					Channels 8 to 14				
	3''''	1''	2'	3'''		3'''	1''''	2''	3'
Channels 15 to 21					Channels 22 to 28				
	3'	1'''	2''''	3''		3''	1'	2'''	3''''

If the start bit is between TOWs (313 to 346), a TOW value of 1' is copied to that of 3' after decoding. If the start bit is between 391 and 438, part of the CRC of subframe 3 is divided into two parts. Each part is received for different TOWs. Thus the CRC has to be reconstructed. If the start bit is between 438 and 450, the receiver locks between tail symbols. The tail bits will not be zeros when decoded. This is because two parts of the tail bits were encoded with different TOW values.

Case 4: When the number of 150 symbol blocks collected before the first sync position is zero.

Consider the example shown in Table E10. The 450 symbols from four channels are concatenated. There is no block before the first sync position.

Table E10: Received 1800 symbols in HDBC-case 4.

Channels 1 to 7					Channels 8 to 14				
1''	2'	3'''	1''''		1''''	2''	3'	1'''	
Channels 15 to 21					Channels 22 to 28				
1'''	2''''	3''	1'		1'	2'''	3''''	1''	

Parts of block 1', 1''', 1'' and 1'''' are concatenated. Then the rearrangement of three subframes is done as explained. If the start bit is in between TOWs (463 to 540), a TOW value of 2' is reduced by 6 and copied to that of 1' after decoding. If the start bit is between 541 and 588, part of the CRC of subframe 1 is divided into two parts. Each part is received for different TOWs. Thus the CRC has to be reconstructed. If the start bit is between 589 and 600, the receiver locks in between tail symbols. Tail bits will not be zeros when decoded. This is because two parts of the tail bits were encoded with different TOW values.

E.2.2. FDBC

This case is obtained when the start bit is at the start of the block (1, 151, 301 and 451). Consider the example shown in Table E11. The 450 symbols from four channels are concatenated and rearrangement is done as explained.

Table E11: Received 1800 symbols.

Channels 1 to 7			Channels 8 to 14			Channels 15 to 21			Channels 22 to 28		
1'	2'''	3''''	1''	2'	3'''	1''''	2''	3'	1'''	2''''	3''

E.2.3. Rearrangement

The 600 symbols from sync position 1, position 2, and position 3 are stored in buffer 1, buffer 2, and buffer 3, respectively. Consider the example shown in Table E12.

- Step 1: Append last 150 bits to the 151th position of respective buffers.
- Step 2: Copy 150 symbols from the 301th position of buffer 1, buffer 2 and buffer 3 to 301th position of buffer 2, buffer 3 and buffer 1, respectively.
- Step 3: Copy 150 symbols from the 451st position of buffer 1, buffer 2 and buffer 3 to the 451st position of buffer 3, buffer 1 and buffer 2, respectively.

After rearranging the contents of these three buffers, decoding is done and the data is extracted depending on SFID.

Table E12: Content of three buffers.

Initial	Buffer 1	3'	1''''	2''''	3''
	Buffer 2	1'	2''''	3''''	1''
	Buffer 3	2'	3''''	1''''	2''
Step 1	Buffer 1	3'	3''	1''''	2''''
	Buffer 2	1'	1''	2''''	3''''
	Buffer 3	2'	2''	3''''	1''''
Step 2	Buffer 1	3'	3''	3''''	2''''
	Buffer 2	1'	1''	1''''	3''''
	Buffer 3	2'	2''	2''''	1''''
Step 3	Buffer 1	3'	3''	3''''	3''''
	Buffer 2	1'	1''	1''''	1''''
	Buffer 3	2'	2''	2''''	2''''

E.3. Summary

The Figure E2 shows the summary of the initial bit synchronization and the subsequent operations that need to be performed in different modes of receiver operation.

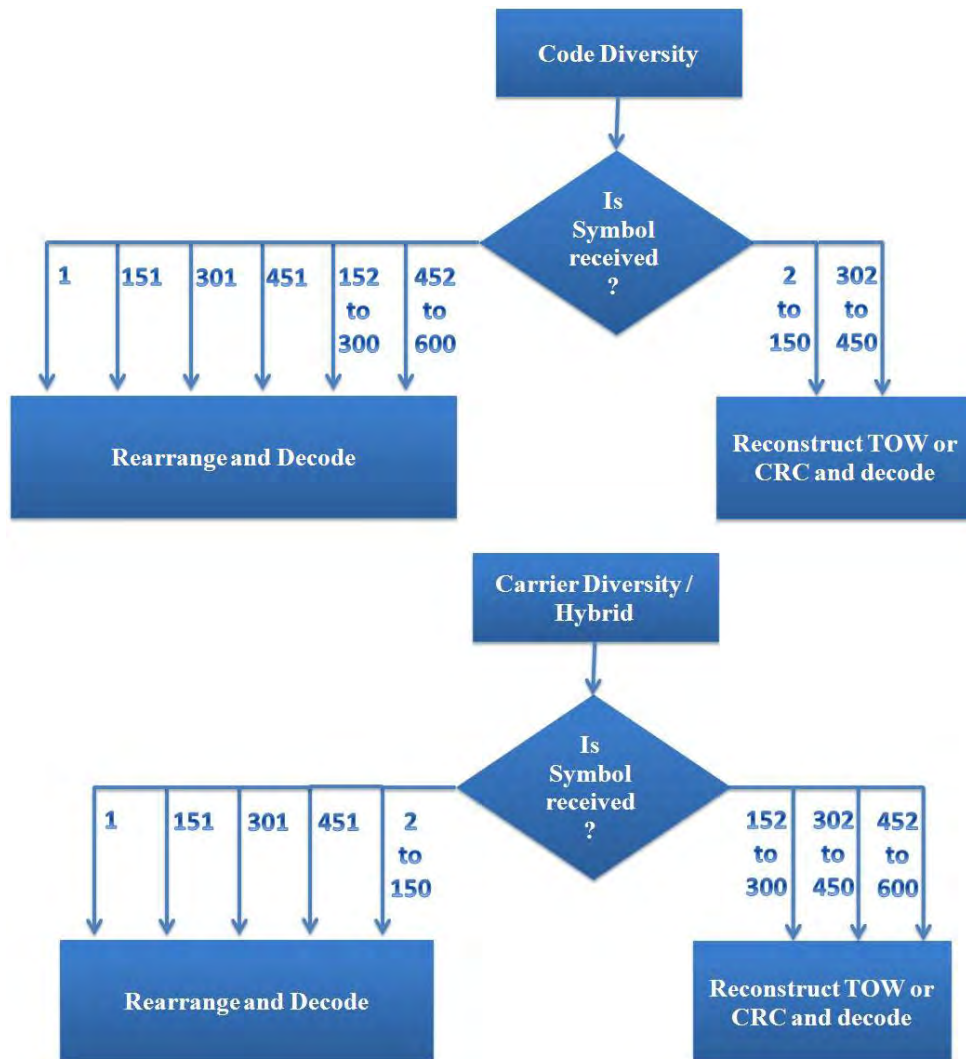


Figure E2: Initial bit synchronization and data reconstruction mechanism.

APPENDIX F: NAV DATA SIGNAL DESIGN FOR HOT START OF GNSS

This appendix describes the NAV data transmission methodology as a part of the proposed third frequency in IRNSS discussed in Chapter Six. Thus the SBAS (GAGAN) NAV data structure has been adopted to transmit the primary NAV data of GPS/GLONASS satellites. The following two assumptions have been made during this formulation: First, to reuse the research software, the synch pattern (preamble)/tail bits are retained, which is not present in SBAS. Second, the NAV data of only those satellites that are healthy (ephemeris health bits all zeros in GPS) are transmitted from the third frequency. Third, the definitions and the number of bits are as in the GPS ICD 2010 (for example, the primary NAV data parameters). The resultant message structure is as shown in Table F1.

Table F1: NAV data structure proposed for transmission on the third frequency of IRNSS geosynchronous satellites.

Parameter	Description	Number of Bits
Z-Count	Time of Week / Subframe duration	17
SW	Subframe seed word (This reads from 0 to 5) the values in between of Z-count commensurate with the L5/S1 channel	3
SVID	Satellite PRN-ID of the transmitting satellite	5
MSGID	Message ID	6
SVID_GPS	SVID of the GPS	5
Data	Data	178
CRC	Cyclic Redundancy Code	24
Tail	Tail bits: 000000	6
TOTAL		244

There are 244 bits in each subframe, which is then encoded to get 488 symbols. These are then appended with 12 bit sync pattern to get 500 symbols in accordance with the SBAS NAV data structure.

The above structure is equally valid for GLONASS with the DATA set filled from the first 4 strings of GLONASS (GLONASS ICD 1998). Further, subframe 1 contains string 1 & 2 data information and subframe 2, the 3rd, 4th and 5th string, respectively. In the case of GLONASS, subframe 3 is not present; SVID corresponds to the frequency id (satellite) which is visible and mapped from -7 to 6.

APPENDIX G: PERFORMANCE WITH THE THIRD GEO AT 90°E AND 100°E

This appendix presents the availability and accuracy results with the proposed IRNSS constellation discussed in Chapter 6 and assuming two extreme points at 90° and 100° E (Figure G1 and Figure G2). This exercise is performed due to lack of information about the location of the third GAGAN satellite. From the plots, it is evident that the availability is better than the existing IRNSS GEO locations and associated PDOP.

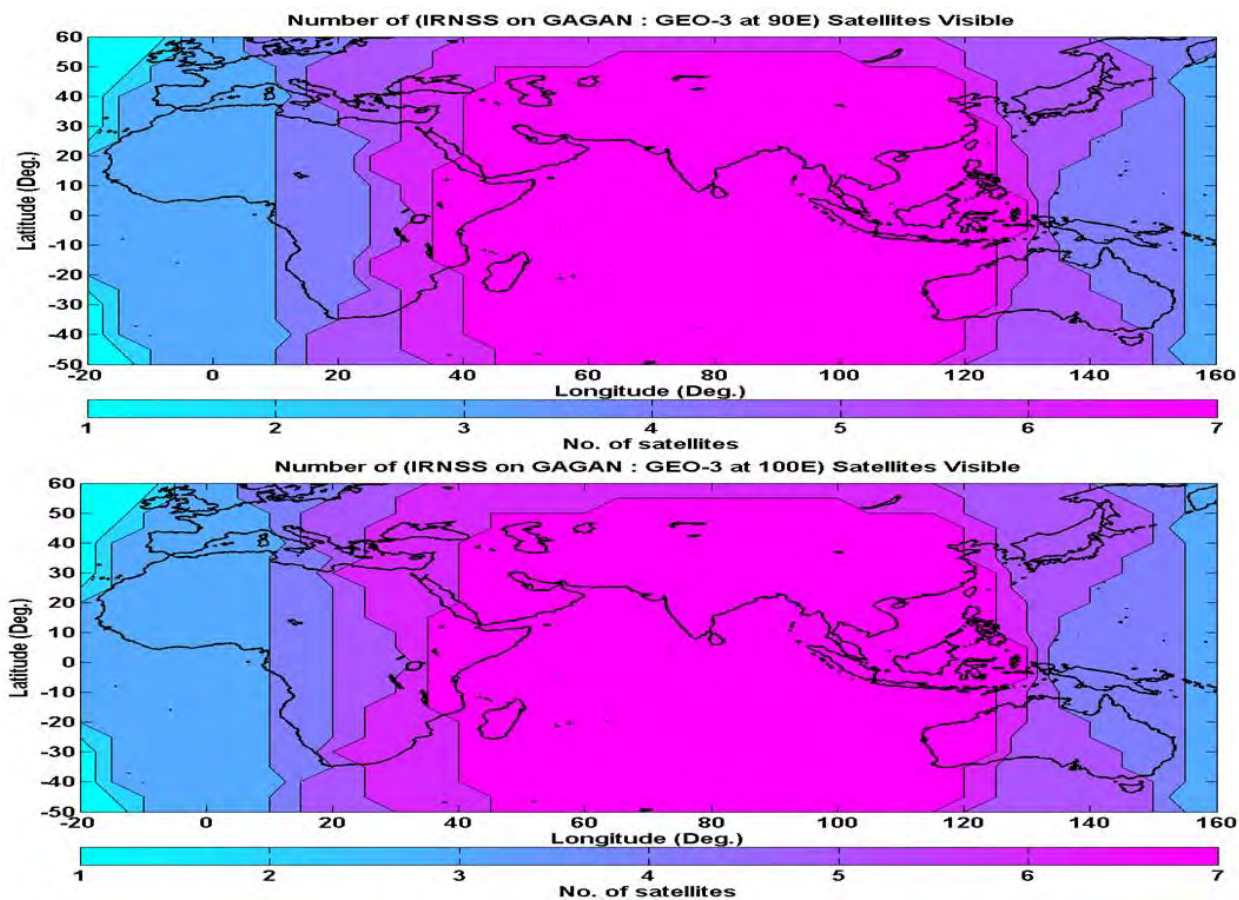


Figure G1: Visibility plots for the third GEO at 90°E and 100°E.

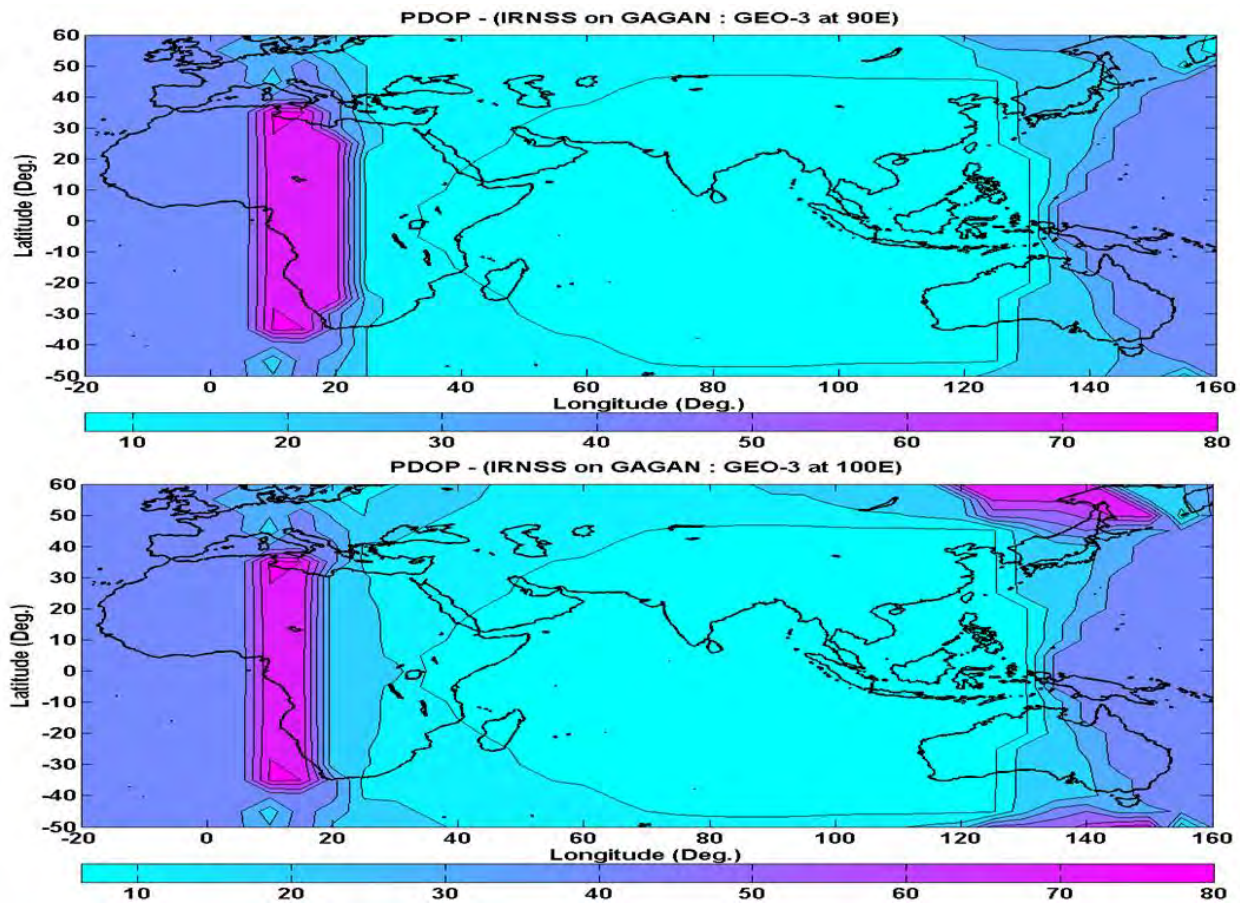


Figure G2: PDOP plots for the third GEO at 90°E and 100°E.